Properties of GABAergic Inhibition in the Medial Prefrontal Cortex

Tanja Herlt

A thesis submitted to the University College London for the degree of Doctor of Philosophy

January 2016

Department of Neuroscience, Physiology and Pharmacology
University College London
Gower Street,
London
WC1E 6BT

Declaration

I, Tanja Herlt, confirm that the work presented in this thesis is my own. Where information has been derived from other sources, I confirm that this has been indicated in the thesis.

Abstract

Gamma-aminobutyric acid type A receptors ($GABA_ARs$) are the main inhibitory neurotransmitter receptors in the central nervous system. As such, they play a pivotal role in synchronising neuronal network activity in the brain and their dysregulation has been implicated in numerous neuropsychiatric diseases such as depression, anxiety and schizophrenia. $GABA_ARs$ are ligand-gated heteropentamers and can be modulated either directly or indirectly by a number of therapeutically-relevant compounds, such as the benzodiazepines, or by endogenous neuromodulators, such as the neurotransmitters dopamine and serotonin, and by neurosteroids. While much is known about the function of $GABA_ARs$, their modulation and interaction with neuromodulators and other neurotransmitter systems are less well understood. In particular, their role in the prefrontal cortex (PFC), a brain area strongly involved in motivation and planning, which is often negatively affected in neuropsychiatric disease, remains to be elucidated.

The aims of this research project were to characterise synaptic and tonic inhibition in the PFC, explore dopaminergic and neurosteroid modulation of GABA inhibition and to examine effects on neuronal excitability. We focused on α2 subunit-containing $GABA_ARs$ because of their role in anxiety and preferred subcellular localisation at the axon initial segment (AIS), an area that is critical for regulating neuronal spike output.

Contrary to previous findings, we could not detect an effect of dopamine D4 receptor activation on GABA inhibition. However, using a mouse model expressing neurosteroid-insensitive $GABA_AR$ α2 subunits, we found evidence for a significant differential involvement of this subunit and neurosteroid modulation in GABAergic synaptic inhibition between various layers of the PFC. We discovered that alterations in phasic GABA-mediated inhibition had no significant effects on pyramidal cell excitability, whilst increasing tonic inhibition reduced cell firing. Overall, this study demonstrates that tonic GABA inhibition has a more important role to play in regulating cortical network function than previously thought.

Acknowledgements

I am truly thankful for everyone who has helped me throughout my PhD, both personally and professionally. I would especially like to thank Prof. Trevor Smart for allowing me to work on this project and for always offering helpful advice, encouragement and a positive attitude even in the face of the most puzzling results. This project was funded by the Wellcome Trust and would not have been possible without the support of my PhD committee members, David Attwell, Sarah-Jayne Blakemore, Patricia Salinas and Alasdair Gibb.

I also owe many thanks to past and present members of the Smart Lab for making this such a great place to work in. I had good times both in- and outside the lab with you. I could not imagine the past 4 years without your lunch-time banter or our legendary Christmas parties. I want to thank Phil and Damian in particular, my “guardian angels”, who were always taking the time to offer me a helping hand and providing new angles and insights when I thought I had reached a dead-end.

Of course all of this would have never been possible without my family. Words cannot describe how truly grateful I am to have such a loving and supportive family, whom I can always count on, no matter the distance. I would also like to thank all my friends, in particular the scientists and runners, for enriching my life outside of the PhD.

Finally, thank you Alex for being by my side, for being supportive, understanding, loving and patient, and for sharing all those happy, sad, confusing, delighting, frustrating, exhilarating moments with me. I could not wish for a better man to share my life with.

Table of Contents

List of Tables

List of Figures

List of Abbreviations

ABBREVIATION	DISAMBIGUATION
(m)PFC	(medial) prefrontal cortex
(s)IPSC	(spontaneous) inhibitory postsynaptic current
3α-HSD	3α-hydroxysteroid dehydrogenase
5-HT	5-hydroxy tryptamine (serotonin)
5-HT_{2C}R	Serotonin 2C receptor
5α-DHDOC	5 -dihydrodeoxycorticosterone
5α-DHPROG	5α-dihydroprogesterone
ACC	Anterior cingulate cortex
aCSF	Artificial cerebrospinal fluid
AIS	Axon initial segment
AFxxx	Alexa Fluor xxx
Allopregnanolone	3α,5α-THPROG / 5α-pregnan-3α-ol-20-one
ANOVA	Analysis of variance
AP	Action potential
AP2	Clathrin-adaptor protein 2
APV	(2R)-amino-5-phosphonovaleric acid
ASPA	Animals (Scientific Procedures) Act
BCA	Bicinchoninic acid
Bic	Bicuculline
BLA	Basolateral amygdala
BSA	Bovine serum albumin
CA1	Cornu ammonis area 1
CAML	Calcium-modulating cyclophilin ligand
cAMP	Cyclic adenosine monophosphate
CB	Calbindin
CBP	Calcium binding protein
CCK	Cholecystokinin
CGC	Cerebellar granule cell
C_M	Membrane capacitance
CNQX	6-cyano-7-nitroquinoxaline-2,3-dione
CNS	Central nervous system
CR	Calretinin

ABBREVIATION	DISAMBIGUATION
DA	Dopamine
DG	Dentate gyrus
DGGC	Dentate gyrus granule cell
DIV	Days in vitro
dlPFC	Dorsolateral prefrontal cortex
dmPFC	Dorsomedial PFC
DMSO	Dimethyl sulfoxide
Dx	Dopamine receptor type x
EGTA	Ethylene glycol tetraacetic acid
EPSP	Excitatory postsynaptic potential
FS	Fast spiking
$GABA_AR$	Gamma-aminobutyric acid type A receptor
GABARAP	17 kDa $GABA_AR$ associated protein
GAD67	Glutamate decarboxylase 67
GAT1	GABA transporter 1
GIRK	G-protein coupled inwardly rectifying K^+-channel
GODZ	Golgi-specific DHHC zinc finger protein
GPCR	G-protein coupled receptor
HAP-1	huntingtin-associated protein 1
HEPES	4-(2-hydroxyethyl)-1-piperazineethanesulfonic acid
Het / $\alpha2^{Q/M}$	Heterozygous
Hom / $\alpha2^{M/M}$	Homozygous mutant
HRP	Horseradish peroxidase
ICC	Immunocytochemistry
IEI	Inter-event-interval
IL	Infralimbic cortex
IPSC	Inhibitory post-synaptic current
KA	Kynurenic acid
KIF5	Kinesin superfamily motor protein 5
MAP2	Microtubule-associated protein 2
MRK-016	3-(1,1-Dimethylethyl)-7-(5-methyl-3-isoxazolyl)-2-[(1-methyl-1H-1,2,4-triazol-5-yl)methoxy]-pyrazolo[1,5-d][1,2,4]triazine
mRNA	Messenger ribonucleic acid
NA	Numerical aperture
NAcc	Nucleus accumbens
NGS	Normal goat serum

ABBREVIATION	DISAMBIGUATION
NKCC1	Na^+-K^+-2Cl^--cotransporter
NMDA	N-methyl-D-aspartate
NPY	Neuropeptide Y
PB	Pentobarbitone
PBS	Phosphate-buffered saline
PC	Pyramidal cell
PCR	Polymerase chain reaction
PD	Postnatal day
PDL	Poly-D-lysine
PFA	Paraformaldehyde
PL	Prelimbic cortex
PLC	Phospholipase C
PLIC1	protein that links integrin-associated protein with the cytoskeleton-1
PMSF	Phenylmethylsulfonyl fluoride
PP(1α or 2A)	Protein phosphatase (1α or 2A)
Pregnanolone	3α,5β-THPROG / 5β-pregnan-3α-ol-20-one
PRIP	phospholipase C-related catalytically inactive protein
PSP	Post-synaptic potential
PV	Parvalbumin
Pxx (e.g. P28)	Postnatal day xx
R_A	Access resistance
R_{in}	Input resistance
RIPA	Radio-immunoprecipitation assay
RMP	Resting membrane potential
RMS	Root mean square
RPM	Rotations per minute
RT	Room temperature
SD	Standard deviation
SDS	Sodium dodecyl sulphate
SEM	Standard error of the mean
SN	Substantia nigra
SOM	Somatostatin
THDOC	Allo-tetrahydro-deoxy-corticosterone (3α,21-dihydroxy-5α-pregnan-20-one)
THIP / gaboxadol	4,5,6,7-Tetrahydroisoxazolo[5,4-c]pyridin-3-ol hydrochloride
TSPO	Translocator protein 18 kDa
TTX	Tetrodotoxin
VIP	Vasoactive intestinal peptide
V_m	Membrane potential
vmPFC	ventromedial PFC
VTA	Ventral tegmental area
WB	Western blot
Wt / $\alpha2^{WT}$	Wildtype

1 Introduction

1.1 GABAergic inhibition in the brain

Inhibitory neurotransmission is vitally important for regulating neuronal excitability and information processing in the central nervous system (CNS). The main mediators of inhibition in the brain include γ-aminobutyric acid (GABA) receptors, which can be distinguished into two principal types: type A and type B. Type A GABA receptors ($GABA_ARs$) are members of the Cys-loop containing ligand-gated family of ion channels and conduct Cl^- and bicarbonate and are now known as the pentameric ligand-gated ion channel family (Moss and Smart, 2001; Sieghart, 1995; Sivilotti and Nistri, 1991; Smart and Paoletti, 2012). Type B GABA receptors ($GABA_BRs$), on the other hand, are G-protein coupled receptors (GPCRs). They are mainly found presynaptically, where they couple to Ca^{2+} channels, while postsynaptic $GABA_BRs$ mostly couple to inwardly-rectifying K^+ channels or adenylyl cyclase via G proteins (Bettler, 2004). Activation of presynaptic $GABA_BRs$ can thus mediate inhibition by a presynaptic decrease in neurotransmitter release or by hyperpolarising the postsynaptic membrane (for reviews on $GABA_BRs$, see Bowery, 1993; Chalifoux and Carter, 2011). A third type, $GABA_CRs$, are sometimes distinguished. They are a group of homomeric ionotropic GABARs, comprising combinations of ρ subunit isoforms and are highly expressed in the retina (Lukasiewicz et al., 2004), though now considered to be a subgroup of the $GABA_AR$.

While all types of GABA receptors play an important role in the CNS, $GABA_ARs$ are responsible for fast synaptic inhibition in the brain. Since maintaining the delicate balance between excitation and inhibition is crucial for normal function of the brain and often negatively affected in psychiatric disease (Möhler, 2006a, 2012; Rudolph and Möhler, 2014), $GABA_ARs$ are the focus of this thesis.

1.1.1 Structure and function of $GABA_A$ receptors

$GABA_ARs$ are ion-conducting channels forming a heteropentamer (Figure 1.1) which surrounds a central pore (Moss and Smart, 2001; Smart and Paoletti, 2012). Each subunit contains a large N-terminal domain, which contains the agonist binding site, and four

transmembrane-spanning domains (TM1-4, see Figure 1.1) with a large intracellular domain between TM3 and TM4 (Möhler, 2006b; Moss and Smart, 2001). The M2 domains of each subunit are thought to form the lining of the pore, while the intracellular M3-M4 loop is thought to be a substrate for phosphorylation by protein kinases and involved in receptor targeting and clustering (Kittler and Moss, 2003; Möhler, 2006b; Moss and Smart, 2001; Smart, 1997).

There are 19 known subunits (six α, three β, three γ, three ρ, as well as δ, ε, π and θ), which can be combined to form receptors of varying physiological and pharmacological properties (Farrant and Nusser, 2005; Tretter, 2008). Typically, two α and two β subunits are assembled together with one γ subunit to form a functional $GABA_AR$ (Figure 1.1) that is usually found at inhibitory synapses, whereas receptors substituting the γ subunit for a δ subunit are commonly extrasynaptic (reviewed in Moss and Smart, 2001; Sieghart and Sperk, 2002; Smart and Paoletti, 2012). However, there are exceptions to these

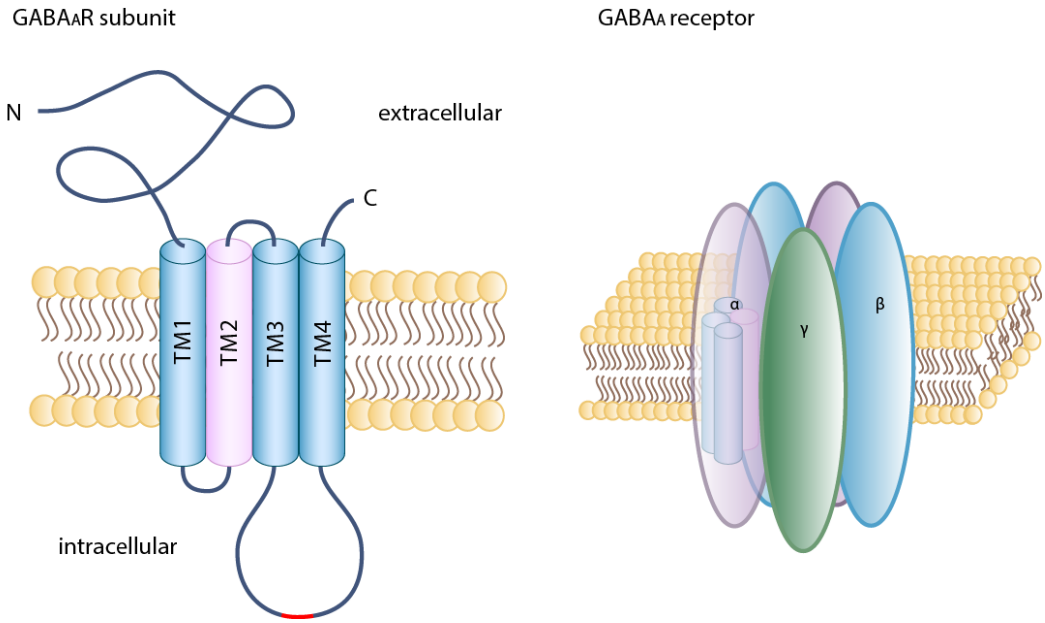

Figure 1.1: Structure of the $GABA_AR$ and its subunits
Schematic model of a typical $GABA_AR$ subunit structure (left) and their alignment in the pentameric structure of a $GABA_AR$ (right). $GABA_AR$ subunits typically consist of 4 transmembrane spanning domains (TM1-4) with a long extracellular N- and a short extracellular C-terminal domain (see text). The intracellular loop between TM3 and TM4 is thought to mediate receptor-protein interactions (see text). The amino acid sequence interacting with gephyrin on $GABA_AR$ α subunits is coloured in red (Tretter et al., 2012). TM2, shown in pink, lines the channel-pore, as demonstrated in the model on the right. The most common $GABA_AR$ heteropentamers consist of two α-, two β- and one γ subunit (see text). Modified figure from Tretter et al. (2012).

'rules', as $\alpha_1\beta\gamma$-$GABA_A$Rs have also been found outside the synapse (Nusser et al., 1998; Thomas et al., 2005) and, in fact, up to 60% of α1, α2 and β3 subunit labelling in hippocampal CA1 pyramidal cells has been postulated to be extrasynaptic (Kasugai et al., 2010). Furthermore, αβ-$GABA_A$Rs (i.e. without a γ- or δ subunit) have also been observed (Brickley et al., 1999; Mortensen and Smart, 2006).

Whilst, in theory, the number of different subunits would allow for a multitude of different $GABA_A$R combinations, even when taking into account preferred subunit associations, studies have shown less than 20 native receptor combinations to commonly occur *in vivo*, the most prevalent of which are α1β2/3γ2, α2β3γ2, α3β3γ2 (Fritschy and Möhler, 1995; Möhler, 2006b; Olsen and Sieghart, 2009; Sieghart and Sperk, 2002; Whiting et al., 1995).

$GABA_A$R isoforms

The structural and physiological diversity of $GABA_A$Rs is paralleled by receptor isoform expression patterns varying with brain area, cell type and even subcellular location (Fritschy and Möhler, 1995; Laurie et al., 1992a; Mody and Pearce, 2004; Pirker et al., 2000; Sieghart and Sperk, 2002). Furthermore, receptor composition undergoes changes during early postnatal development (Hutcheon et al., 2000; Kobayashi et al., 2008; Laurie et al., 1992b) and throughout the oestrous cycle (Maguire et al., 2005). For example, while α1-containing $GABA_A$R (α1- $GABA_A$R) expression is abundant throughout the brain, α5 subunits, which preferably co-assemble with β3 and γ2 subunits, are largely found in the hippocampus, where they comprise up to 20% of all diazepam-sensitive $GABA_A$Rs (Fritschy and Möhler, 1995; Möhler, 2006b; Sieghart and Sperk, 2002). By comparison, α6 subunits are exclusively expressed in the granule cell layer of the cerebellum (Nusser et al., 1996a). Furthermore, $GABA_A$R isoforms can be localised to specific subcellular compartments. δ-$GABA_A$R, for example, are exclusively found at extrasynaptic sites, whereas the incorporation of a γ subunit is necessary, although not an absolute determinant, for synaptic localisation (Nusser et al., 1998; Wei et al., 2003). In addition, $GABA_A$R isoforms may be specifically localised to synaptic sites in a manner that is dependent on the type of presynaptic neuron (Figure 1.2). For example, on

hippocampal pyramidal neurons, α2-$GABA_A$Rs are mainly found at synapses innervated by Chandelier cells (Nusser et al., 1996b), while interneurons expressing the calcium binding protein (CBP) cholecystokinin (CCK) preferentially contact synapses enriched in α2- and α5-$GABA_A$Rs, and α1-$GABA_A$Rs are mainly found in synapses with basket cells expressing the CBP parvalbumin (PV) (Ali and Thomson, 2008; Klausberger et al., 2002; Nyíri et al., 2001; Thomson et al., 2000). Furthermore, somatic or perisomatic synapses mainly contain α1- or α2/3-$GABA_A$Rs, while α5-$GABA_A$Rs are found predominantly on distal dendrites (Ali and Thomson, 2008; Fritschy and Mohler, 1995; Sperk et al., 1997) and α2-$GABA_A$Rs are enriched at the axon initial segment (AIS) (Nusser et al., 1996b).

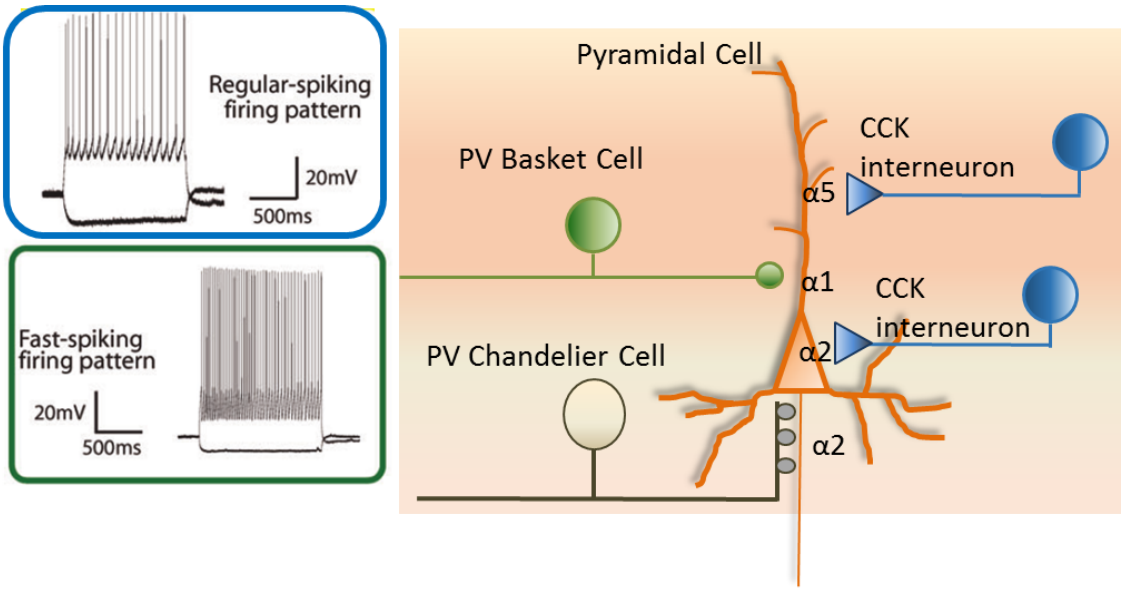

Figure 1.2: $GABA_A$R-subtype specific interneuron innervation at pyramidal cell membrane subcompartments

Schematic drawing of a pyramidal cell and its innervation pattern by different types of interneurons. PV-positive Chandelier cells innervate α2-$GABA_A$R-enriched AIS, while PV-positive basket cells preferentially contact α1-$GABA_A$Rs in the perisomatic region. CCK-positive interneurons contact α5-$GABA_A$Rs on distal dendrites as well as perisomatic α2-$GABA_A$Rs (see text). As will be explored in more depth in section 1.4.2, CCK interneurons typically show a regular-spiking firing pattern (blue box), while PV-positive interneurons exhibit a fast-spiking firing pattern (green box; adapted from Armstrong and Soltesz, 2011).

$GABA_AR$ pharmacology

The different $GABA_AR$ isoforms also possess varying pharmacological profiles. Presence of the γ subunit, for example, is required to convey sensitivity to benzodiazepines, a class of psychoactive drugs widely used to treat anxiety and other disorders (Möhler et al., 2000; Sieghart, 1995). γ2-$GABA_ARs$ are the most sensitive, while γ1 and γ3 show reduced sensitivity to benzodiazepines. In addition, pharmacological properties of $GABA_ARs$ are influenced to a large extent by the α subunit, which forms part of the binding site for the neurotransmitter GABA (β-α interface) as well other well-known allosteric modulators, such as the benzodiazepines (α-γ interface; binding sites will be explored in more detail in section 1.2)(Möhler, 2006b; Sieghart, 1995). For example, the affinity for GABA is most strongly affected by the α subunit isoform, with α3 subunits showing the highest sensitivity and α6 the lowest (Farrant and Nusser, 2005; Mortensen et al., 2011; Picton and Fisher, 2007). Furthermore, α1 is thought to mediate the sedative effects of benzodiazepines (McKernan et al., 2000; Rudolph et al., 1999), while α2 and α3 mediate their anxiolytic and antihyperalgesic properties (Crestani et al., 2001; Dias et al., 2005; Löw et al., 2000; Zeilhofer et al., 2009). Likewise, the development of tolerance to benzodiazepines seems to be dependent on the activity of both α1 and α5-containing $GABA_ARs$ (van Rijnsoever et al., 2004). The action of other allosteric ligands such as barbiturates, ethanol, anaesthetics and neuroactive steroids are thought to be mediated via binding-pockets in the transmembrane region. These lie either within α- or β subunits or in an α/β-inter subunit transmembrane pocket, and can therefore also be differentially affected by the subunit isoform (Olsen and Sieghart, 2008, 2009).

Furthermore, $GABA_AR$ composition influences biophysical receptor properties, varying in particular with the α subunit incorporated into the receptor (for a review, see Farrant and Nusser, 2005). These properties comprise the affinity for an agonist, as well as the efficacy of the agonist in gating the receptor channel. The subunit composition also affects the kinetic profile of receptor currents, such as the rise time, the decay time upon receptor inactivation and also the desensitisation rate of the receptor (i.e. a non-conducting state in the continued presence of the agonist binding) (Farrant and Nusser,

2005). For example, in response to fast applications of high concentrations of GABA, α1-$GABA_A$Rs exhibit 2 to 10 times faster decay kinetics compared to α2-$GABA_A$Rs, whilst rise times are twice as fast in α2-$GABA_A$Rs (Dixon et al., 2014; Lavoie et al., 1997; McClellan and Twyman, 1999) and activation, desensitisation and deactivation of α3-$GABA_A$Rs are 2 to 4 times slower compared to α1-$GABA_A$Rs (Gingrich et al., 1995).

Different α subunit isoforms can also be linked to specific functions. For example, deficits in, or inhibition of, α5-$GABA_A$Rs have been shown to improve cognition and enhance performance in hippocampal-dependent memory tasks (Chambers et al., 2004; Crestani et al., 2002). Given their high expression in midbrain dopaminergic neurons (Fritschy and Möhler, 1995; Pirker et al., 2000), α3-$GABA_A$Rs are thought to be the main $GABA_A$R isoform exerting inhibitory control over the dopaminergic system. Evidence for this are the sensorimotor deficits observed in α3-knockout mice, which can be rescued by administration of haloperidol, a dopamine D2-specific antagonist (Yee et al., 2005).

Tonic vs phasic inhibition

There are two main forms of inhibitory conductance mediated by $GABA_A$Rs: tonic and phasic inhibition (for a review, see Farrant and Nusser, 2005). $GABA_A$Rs which mediate phasic inhibition are synaptically located and deliver rapid changes in membrane conductance in response to synaptic neurotransmitter release. Synaptic $GABA_A$Rs are thus exposed to transiently high quantal GABA concentrations. These receptors usually contain the γ subunit and, compared to $GABA_A$R containing the δ subunit, possess a lower affinity for GABA (e.g. an EC_{50} of 2.6 - 11 μM for γ- vs 0.2 – 0.5 μM for δ-$GABA_A$Rs (Brown et al., 2002; Mortensen et al., 2011; Saxena and Macdonald, 1996)), as well as faster receptor activation (0.46 ± 0.04 ms for γ- vs. 2.4 ± 0.27 ms for δ-$GABA_A$Rs) and slower deactivation (193 ± 31 ms for γ- vs. 79.7 ± 7.3 ms for δ-$GABA_A$Rs (Haas and Macdonald, 1999)).

Conversely, tonic inhibition is mediated by extrasynaptic receptors, which are activated by low, ambient GABA levels and result in a persistent “tonic” conductance. The main receptor isoforms mediating tonic inhibition are α5βγ and α4/6βδ-$GABA_A$Rs (Farrant and Nusser, 2005). α4/6βδ-$GABA_A$Rs possess the highest affinity for GABA (i.e. the

lowest EC_{50} value, see above) (Brown et al., 2002; Feng and Macdonald, 2004) but a much slower receptor activation and desensitisation (Brown et al., 2002; Haas and Macdonald, 1999). They provide an underlying inhibitory tone, which is revealed by a change in the holding current in the presence of $GABA_AR$ blockers (Brickley et al., 1996; Kaneda et al., 1995). The source of GABA activating these extrasynaptic receptors is thought to result from "spillover" generated from activation of neighbouring synapses as well as ambient levels of GABA in the extracellular space (Farrant and Nusser, 2005). GABA transporters play a key role in resulting ambient GABA levels since, in addition to removing GABA from the extracellular space, the transport of GABA can be reversed, dependent upon membrane potential and transmembrane gradient for the substrates (GABA, Na^+, Cl^-) (Bertram et al., 2011; Farrant and Nusser, 2005; Richerson, 2004; Semyanov et al., 2004). In the cerebellum, the anion channel Bestrophin 1 is thought to be responsible for tonic GABA release from glial cells (Lee et al., 2010).

On a functional level, $GABA_ARs$ containing the α5 subunit regulate pyramidal excitability in the *cornu ammonis* area 1 (CA1) of the hippocampus (Caraiscos et al., 2004; Semyanov et al., 2004) as well as in layer V somatosensory cortex (Yamada et al., 2007). $GABA_ARs$ containing the δ subunit, on the other hand, mediate tonic inhibition in cerebellar granule cells (CGCs), denate gyrus granule cells (DGGs), pyramidal cells (PCs) in layer II/III neocortex, thalamic relay neurons and medium spiny neurons of the striatum, as examples (Brickley and Mody, 2012; Drasbek and Jensen, 2006; Salin and Prince, 1996; Stell et al., 2003).

Phasic and tonic inhibition are thought to have different physiological roles, which will be explored more thoroughly in chapter 5. Briefly, while phasic inhibition is thought to mediate transient changes in excitability and thus shape the neuronal firing pattern as well as generate rhythmic network activity, tonic inhibition is thought to set the basic threshold for firing as well as affecting the neuronal gain (for a review, see Farrant and Nusser, 2005).

Physiological role of $GABA_AR$ channel gating

The physiological consequences of $GABA_AR$ channel opening can be manifold, depending largely on the electrochemical gradient of ions conducted by $GABA_ARs$ and the receptor's particular subcellular location. $GABA_AR$ activation increases the membrane conductance for Cl^- and, to a lesser extent, HCO_3^- (Bormann et al., 1987; Kaila, 1994), which usually leads to an influx of Cl^- and transient hyperpolarisation of the postsynaptic membrane. However, the direction of ion flow (and, therefore, the effect on the membrane potential (V_m)) depends on the relationship between the Cl^- equilibrium potential (E_{Cl}, which is determined by the distribution of Cl^- across the membrane and its Cl^- permeability) and the resting membrane potential (Figure 1.3). This is regulated by a number of Cl^- transporters and varies with cell-type, subcellular location and development. Usually, the K^+-Cl^--cotransporter, KCC2, maintains a chloride equilibrium potential more negative than RMP (Figure 1.4; Payne et al., 2003)„ e.g. -76 to -81 mV compared to an RMP of -74 mV in crayfish stretch receptor neurons (Kaila et al., 1992). Early in development, however, GABA transmission is thought to be excitatory due to the expression of the sodium- and potassium-coupled cotransporter, NKCC1 (Payne et al., 2003), which leads to an E_{Cl} depolarised compared to the RMP (e.g. an E_{Cl} of −38 ± 4 mV in immature primary cerebellar neurons (Succol et al., 2012)), causing a relative efflux of Cl^- (Figure 1.4).

Early in postnatal development, the expression of chloride transporters changes to the adult form, the chloride-extruding potassium-chloride co-transporter KCC2 (Payne et al., 2003; Rivera et al., 2005), thus shifting E_{Cl} to a more negative potential than the RMP, leading to Cl^--influx and hyperpolarisation upon receptor activation. But even in the mature brain, $GABA_A$ may still exert depolarising effects in some cases (Chavas and Marty, 2003; Gulledge and Stuart, 2003; Stein and Nicoll, 2003). An interesting example of this involves a subtype of GABAergic interneurons, the Chandelier cells, whose axo-axonic connections at the AIS may be depolarising under certain conditions (Woodruff et al., 2009, 2010, 2011). The reversal potential of pyramidal neuron inhibitory postsynaptic currents (IPSCs) elicited by Chandelier cells in layer II/III somatosensory

cortex, for example, was shown to be more depolarised (–51.1 ± 5.4 mV) compared to the RMP (–72 ± 2 mV) (Szabadics et al., 2006).

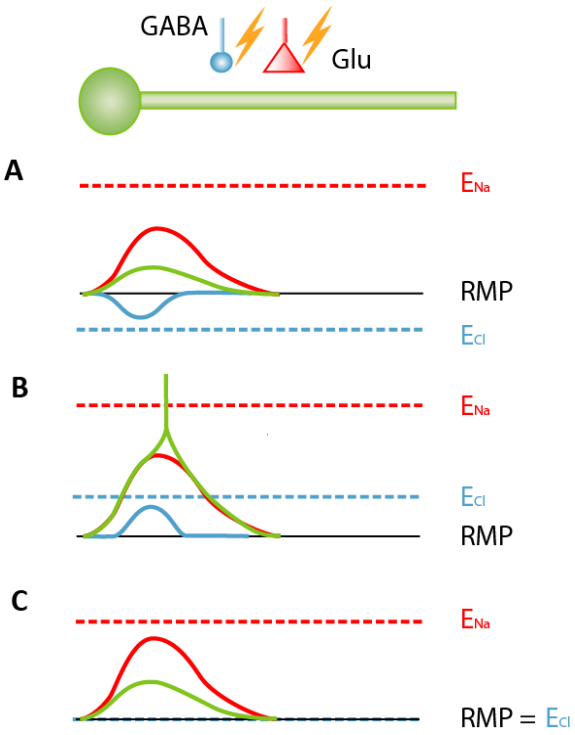

Figure 1.3: Different effects of $GABA_AR$ receptor activation on postsynaptic membrane potential depends on the chloride reversal potential

Figure demonstrating the resulting post-synaptic potential (PSP, green) from a concurrent GABAergic PSPs (blue) and a glutamatergic excitatory PSP (EPSP, red). **A**. In most mature neurons, E_{Cl} (blue dotted line) is more negative than the RMP (black line), while E_{Na} (red dotted line), the main conductance of glutamate receptors, lies more positive than the RMP. Opening of $GABA_ARs$ will therefore lead to an influx of Cl^- and a hyperpolarising IPSP (blue line), while opening of glutamate receptors leads to an influx of Na^+ and a depolarising EPSP (red line). The sum of coincident glutamatergic and GABAergic inputs in this scenario will be a slightly reduced EPSP (green line) possibly falling below threshold for spike generation. **B.** In immature neurons and some mature neurons, E_{Cl} can rest more depolarised than the RMP, leading to a depolarising GABAergic PSP. The sum of parallel glutamatergic and GABAergic inputs in this scenario will be more depolarising than a glutamatergic input alone and may elicit an action potential, if the threshold for action potential generation is crossed. **C.** In some cases, E_{Cl} may lie very close to, or at the RMP, causing no significant net ion flow upon $GABA_AR$ opening. However, a simultaneous glutamatergic input may still be reduced due to an overall increase in conductance, causing shunting inhibition (see text).

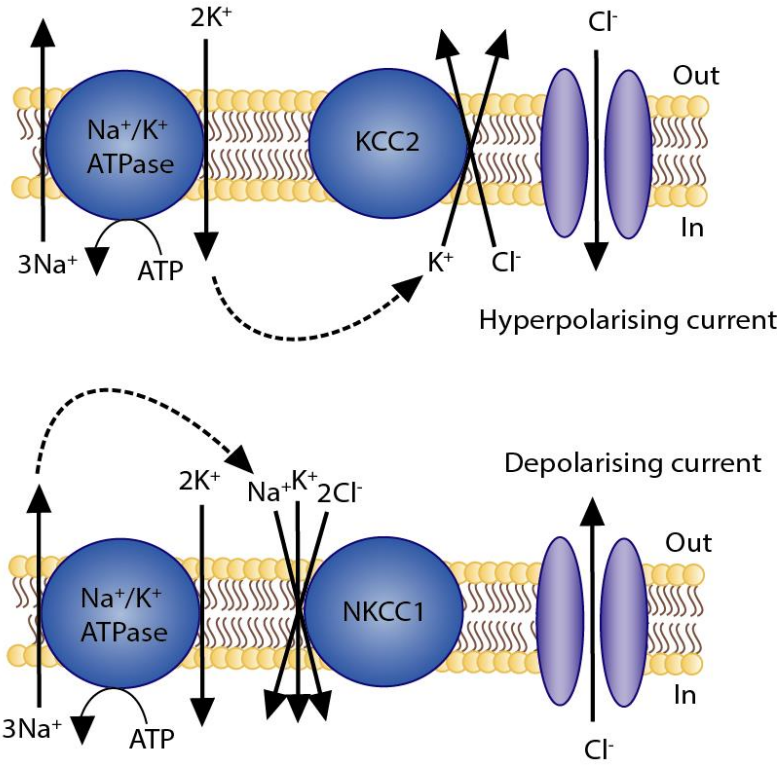

Figure 1.4: Chloride transporters determine the direction of chloride flow through $GABA_A$Rs
Schematic models demonstrating the effect of different chloride transporters on the direction of chloride flow across the membrane. Na^+/K^+ ATPases maintain the distribution of sodium and potassium across the membrane by concomitantly extruding sodium and importing potassium against their concentration gradients via the hydrolysis of ATP. This transporter is essential in maintaining the RMP in the presence of leak currents and during intense action potential activity and is thought to be one of the most energy-consuming processes in the brain (Howarth et al., 2012). Most adult neurons express the K^+/Cl^-cotransporter KCC2, which exports K^+ along, and Cl^- against their concentration gradients, creating a chloride reversal potential more negative than the RMP, which leads to a hyperpolarising Cl^- current upon opening of $GABA_A$Rs. In immature neurons, however, the $Na^+/K^+/Cl^-$cotransporter NKCC1 imports Na^+ and Cl^- along and K^+ against their concentration gradients, creating a chloride reversal potential more positive than the RMP, which leads to a depolarising Cl^- current upon opening of $GABA_A$Rs. Figure adapted from Payne and colleagues (2003).

Often, however, E_{Cl} and RMP lie very close together (around -70 mV), in which case $GABA_A$R opening has no effect major effect on V_m. The net effect on cellular excitability in this case may still be inhibitory, though (Gulledge and Stuart, 2003; Staley and Mody, 1992). This can be explained by the concomitant increase in membrane conductance upon channel opening, which attenuates voltage changes across the membrane. This phenomenon is called shunting inhibition and its physiological role will be explored in more detail in chapter 5.

1.1.2 Modulation of $GABA_AR$s

Varying effects of $GABA_AR$ channel opening

GABAergic transmission can be modulated pre- or postsynaptically. The pattern and strength of GABAergic inputs onto a cell depend on the magnitude and the rate with which GABA, in the synaptic cleft, occupies and dissociates from receptor binding sites. One important factor which dictates this is the quantity and frequency of presynaptic GABA release, which is largely modulated through activity of the presynaptic neuron and leads to the release of one to several transmitter vesicles (Rudolph et al., 2015). To some extent, transmitter release, however, is action potential-independent and is usually the result of spontaneous vesicle fusion with the presynaptic membrane (Ropert et al., 1990). Uptake of GABA through transporters is another factor changing ambient GABA levels (Richerson and Wu, 2003). GABA transporters can undergo subcellular redistribution (both laterally within the cell membrane and vertically through changes in their cell surface expression) and functional modulation by protein kinases and phosphatases (Corey et al., 1994; Quick et al., 2004; Scimemi, 2014).

Trafficking, clustering and post-translational modification

At the postsynaptic level, the profile of GABAergic inhibition can be modulated by a number of different processes affecting receptor composition, subcellular localisation and pharmacological properties. $GABA_AR$s display rapid lateral diffusion between cellular compartments on the cell surface, or can be trafficked from intracellular compartments to the cell surface, and vice versa (see Figure 1.5; Comenencia-Ortiz et al., 2014; Jacob et al., 2008; Luscher et al., 2011; Muir et al., 2010; Smith et al., 2012; Thomas et al., 2005). Interaction of the intracellular loops of specific subunits with a host of regulatory proteins is crucial for $GABA_AR$ trafficking and targeting, and these interactions can be modulated by post-translational modifications (Arancibia-Cárcamo and Kittler, 2009; Comenencia-Ortiz et al., 2014; Kittler et al., 2005; Luscher et al., 2011).

Palmitoylation of the γ subunit by the Golgi-specific DHHC zinc finger protein (GODZ) is thought to play an important role in receptor trafficking within the secretory pathway and normal assembly of $GABA_AR$ at the synapse (Fang et al., 2006; Keller et al., 2004).

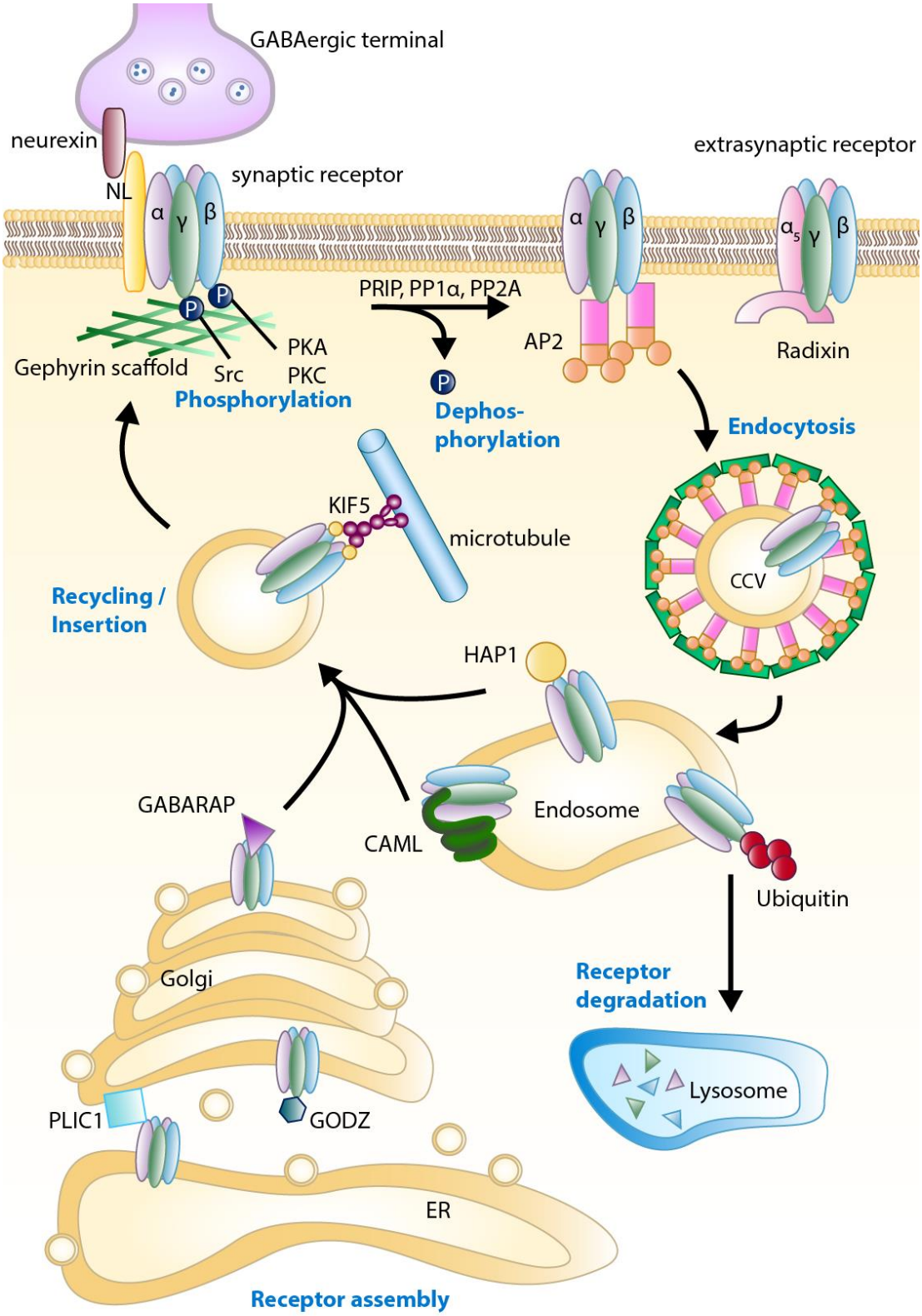
GABAergic terminal
neurexin
NL
synaptic receptor
α
γ
β
extrasynaptic receptor
α
γ
β
α5
γ
β
PRIP, PP1α, PP2A
P
P
P
PKA
PKC
Src
Gephyrin scaffold
Phosphorylation
Dephos-
phorylation
AP2
Radixin
Endocytosis
KIF5
microtubule
CCV
Recycling /
Insertion
HAP1
GABARAP
CAML
Endosome
Ubiquitin
Golgi
Receptor
degradation
Lysosome
PLIC1
GODZ
ER
Receptor assembly

Figure 1.5: $GABA_AR$ trafficking and localisation are regulated by an array of interacting proteins
Cell surface clustering of synaptic and extrasynaptic $GABA_ARs$ as well as their dynamic transport to and from the cell membrane is regulated by the differential interaction of the receptor subunits with membrane-bound or intracellular proteins, such as scaffolding proteins and kinases (see main text). Gephyrin, radixin, neurexin and neuroligins (NL) are responsible for surface clustering. The interaction between these proteins and $GABA_AR$ is modulated by phosphorylation via protein kinase A (PKA), PKC and Src, or dephosphorylation by protein phosphatases (PP) such as phospholipase C-related catalytically inactive protein (PRIP), PP1α and PP2A. Interaction with AP2 facilitates endocytosis and ubiquitinylation targets the receptor for degradation. Interaction with HAP1, CAML, the protein that links integrin-associated protein with the cytoskeleton-1 (PLIC1), GODZ, GABARAP and KIF5, however, mediate recycling via endosomes or delivery to the surface from the endoplasmatic-reticulum (ER) and Golgi apparatus (figure has been modified from Arancibia-Cárcamo and Kittler, 2009; Jacob et al., 2008; Luscher et al., 2011).

Dephosphorylation of β or γ subunits facilitates their interaction with the clathrin-adaptor protein 2 (AP2) and clathrin-mediated endocytosis, thus allowing dynamic removal from the membrane (Kittler et al., 2000, 2005; Figure 1.5). Ubiquitynation of the γ subunit tags receptors for lysosomal degradation (Arancibia-Cárcamo et al., 2009), while interaction of γ2 subunits with calcium-modulating cyclophilin ligand (CAML) aids in receptor recycling to the membrane (Yuan et al., 2008). Receptor recycling is also favoured by interaction of β subunits with huntingtin-associated protein 1 (HAP-1)(Kittler et al., 2004) via a complex with the kinesin superfamily motor protein 5 (KIF5) and microtubule directed vesicular transport (Twelvetrees et al., 2010; Figure 1.5). Another important protein involved in $GABA_AR$ surface delivery is the 17 kDa $GABA_AR$ associated protein (GABARAP), a microtubule-binding protein which co-localises with $GABA_ARs$ in the Golgi compartment and interacts with the γ subunit to regulate receptor trafficking (Kittler and Moss, 2001; Wang et al., 1999).

On the other hand, interactions with intracellular scaffolding proteins can change inhibitory properties by clustering of $GABA_ARs$ to particular membrane sites. (Renner et al., 2012; Tretter et al., 2012; Vithlani et al., 2011). The γ subunit and its interaction with the scaffolding protein gephyrin is thought to be of particular importance to $GABA_AR$ anchoring at synaptic sites (Tretter et al., 2012). The presence of a γ2 subunit is considered the main determining factor for synaptic localisation and clustering of

$GABA_AR$s, since ablation of γ2 results in concomitant downregulation of gephyrin and reduction in miniature-(m)IPSC frequency (Essrich et al., 1998). Yet, synaptic targeting of $GABA_AR$s is not solely dependent upon the γ subunit, since overexpression of α6 subunits (Wisden et al., 2002) or the incorporation of α5 subunits can override γ2-mediated synaptic targeting (Brünig et al., 2002; Crestani et al., 2002) and synaptic IPSCs can still be detected in mice lacking the γ2 subunit (Kerti-Szigeti et al., 2014). It has been suggested, that while the γ subunit undoubtedly plays a significant role in anchoring $GABA_AR$s, it does not mediate targeted receptor trafficking to the synapse (Tretter et al., 2012). Instead, the α subunit was postulated for this role. Variations in receptor isoform targeting beyond localisation at synaptic or extrasynaptic sites seem to rely on the isoform of the α subunit (evidenced by synapse-specific localisation of α subunits, as detailed in section 1.1.1 and Figure 1.2) and direct interactions of gephyrin with α1,2 and 3 subunits have since been proven (Mukherjee et al., 2011; Tretter et al., 2008, 2011). Despite an earlier study which failed to show a direct interaction between gephyrin and $GABA_AR$ β subunits (Meyer et al., 1995), more recent research also suggests a role for a phosphorylation-dependent interaction between gephyrin and β3 subunits in mediating chemically induced inhibitory long-term potentiation (Petrini et al., 2014).

Specific interactions between the presynaptic and postsynaptic site may aid in both, receptor targeting to specific synapses and in the guided formation of synapses (Fuchs et al., 2013; Thomson and Jovanovic, 2010). The mechanisms that govern this distinction remain unknown, however, complexes between postsynaptic neuroligins, in particular neuroligin 2, which is specific for GABAergic synapses (Graf et al., 2004), and presynaptic neurexins, are thought to play a vital role in synapse formation (Craig and Kang, 2007; Kang et al., 2008; Figure 1.5). Neurexins may even regulate GABAergic transmission through interacting with postsynaptic receptors (Zhang et al., 2010). There is also interesting evidence from a recent study documenting the propensity of $GABA_AR$s to initiate synapse formation. In this study, a co-culture system of neurons and human embryonic kidney (HEK) cells expressing α1β2γ2-$GABA_AR$s was used, and showed the formation of active synaptic contacts between the two cell types (Fuchs et al., 2013).

Mechanisms governing the cell surface clustering of extrasynaptic $GABA_AR$s are less well understood, however, the actin-binding protein radixin has been identified as an essential component in the extrasynaptic clustering of α5-$GABA_AR$s (Loebrich et al., 2006; Figure 1.5).

Modulation of $GABA_AR$s by protein kinases and phosphatases

Beyond trafficking and receptor localisation, phosphorylation of $GABA_AR$s can have wide-ranging implications for receptor properties. The effect can vary with the identity of the kinase or phosphatase involved, which target specific amino acid sequences and $GABA_AR$ subunits (see reviews Arancibia-Cárcamo and Kittler, 2009; Brandon et al., 2002; Kittler and Moss, 2003; Smart, 1997). Studies using recombinant receptors have revealed key residues within the intracellular loop between M3 and M4 of β1-3 and γ2 subunits as substrates for a range of different kinases, such as PKC, PKA and the receptor tyrosine-kinase Src (Brandon et al., 2002). An example demonstrating the subunit specificity of protein kinase action is the observation that PKA negatively regulates β1-$GABA_AR$s, but enhances the GABA-response in receptors containing the β3 subunit (McDonald et al., 1998). Phosphorylation by PKC is generally thought to reduce $GABA_AR$ function and PKC has been shown to bind to β3-$GABA_AR$s, providing a basal level of phosphorylation (Brandon et al., 2000). PKC phosphorylation at β3-$GABA_AR$s can also disrupt their interaction with AP2 and therefore stabilise the receptor at the synapse (Kittler et al., 2005; Smith et al., 2012). Interestingly, a similar function is fulfilled by tyrosine kinases at γ2-$GABA_AR$s (Kittler et al., 2008). Changes in intracellular Ca^{2+}-levels also play a role in regulating $GABA_AR$ function via various Ca^{2+}-dependent kinases and phosphatases. For example, activation of N-methyl-D-aspartate (NMDA) receptors can affect $GABA_AR$ lateral mobility via calcineurin mediated dephosphorylation of the γ2 subunit (Muir et al., 2010).

1.2 Pharmacological modulation of $GABA_AR$s

In addition to their native agonist, GABA, a wide array of pharmacological compounds modulate $GABA_AR$s at distinct sites (Figure 1.6), some of which commonly find clinical

use, such as barbiturates, benzodiazepines and anaesthetics (Korpi et al., 2002; Sieghart, 1995). Here, only a brief introduction is given to some of the most studied allosteric modulators. The role of allosteric modulators on $GABA_A$Rs have recently been reviewed in-depth by Sieghart (2015).

Barbiturates, amongst them pentobarbitone, are positive allosteric modulators of the $GABA_A$R, which are anxiolytic and hypnotic. Depending on their concentration, they can act either as allosteric modulators, potentiating the action of GABA, as direct activators of channel gating or, at very high concentrations, as channel blockers (Thompson et al., 1996). At concentrations <50 µM, barbiturates allosterically increase the GABA response by increasing the average channel opening time, without affecting the channel conductance or opening frequency (Akk and Steinbach, 2000; Sieghart, 1995). Their binding site has been postulated to lie within the transmembrane region of the α/β- and γ/β-interface (Chiara et al., 2013) (Figure 1.6).

Benzodiazepines, such as lorazepam, flunitrazepam and diazepam, act as allosteric modulators and do not gate the receptor directly. They have superseded barbiturates in clinical use due to their lower risk of overdose (Smith and Rudolph, 2012). They bind at the α/γ-interface and potentiate the response to GABA by increasing the frequency of receptor opening (Sigel and Buhr, 1997). The affinity of $GABA_A$R isoforms for benzodiazepines is dependent on their subunit composition. For example, binding of benzodiazepines relies on the presence of a γ subunit, and the absence of α4 and α6 subunits (Pritchett et al., 1989; Wieland et al., 1992). Introducing a histidine to arginine point mutation at position 101 (H101R) in the benzodiazepine binding-site of α-$GABA_A$Rs has been shown to ablate benzodiazepine binding without affecting receptor function and has been a vital tool in studying receptor pharmacology (Crestani et al., 2001; Löw et al., 2000; Rudolph et al., 1999). In addition to pharmacological compounds, there is also evidence for endogenous ligands at the benzodiazepine binding site, so-called endozepines, such as the 10 kDa peptide diazepam-binding inhibitor, which has been shown to potentiate GABAergic transmission in the thalamic reticular nucleus (Christian et al., 2013; Farzampour et al., 2015).

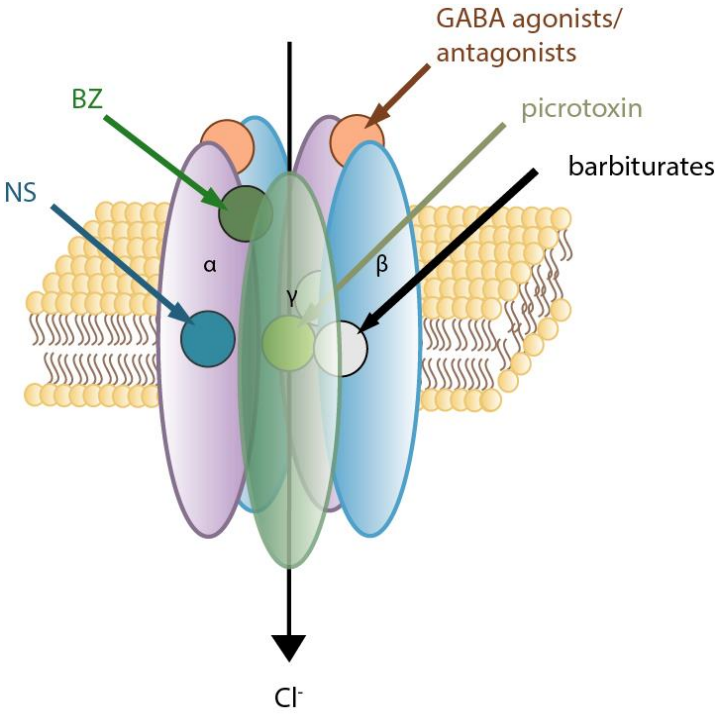

Figure 1.6: Binding sites of specific molecules at the $GABA_AR$
$GABA_ARs$ possess several distinct binding sites for different pharmacological compounds (see text). GABA and other orthosteric agonists and antagonists, such as muscimol or bicuculline, respectively, bind at the β/α-interface in the extracellular domain. Benzodiazepines (BZ) act as allosteric modulators at the α/γ-interface. Barbiturates are thought to bind in the transmembrane spanning part of the β/γ-interface, while neurosteroids (NS) can either allosterically modulate $GABA_ARs$ through a binding site in the transmembrane region of the α subunit, or directly gate channel opening via another site near the agonist binding site at high concentrations (>1 µM).

Other modulators of $GABA_ARs$ are convulsants such as picrotoxin, which non-competitively blocks $GABA_ARs$ by binding in or close to the channel pore (Korpi et al., 2002; Figure 1.6). Non-selective compounds competing for the GABA binding site at $GABA_ARs$ are the agonist muscimol and the competitive antagonist bicuculline, which are commonly used as experimental tools in studying $GABA_AR$ function (Korpi et al., 2002). To target specific receptor isoforms, selective compounds have been developed, such as the δ-$GABA_AR$-selective agonist, 4,5,6,7-Tetrahydroisoxazolo[5,4-c]pyridin-3-ol hydrochloride (THIP) (Krogsgaard-Larsen et al., 2004) or the α5-$GABA_AR$-selective inverse agonists, 3-(1,1-Dimethylethyl)-7-(5-methyl-3-isoxazolyl)-2-[(1-methyl-1H-

1,2,4-triazol-5-yl)methoxy]-pyrazolo[1,5-d][1,2,4]triazine (MRK-016) and L-655,708 (Chambers et al., 2004; Quirk et al., 1996).

Contrary to most of the compounds discussed above, neurosteroids are synthesised *de novo* in the brain and play an important role in modulating GABAergic function. Given their important role in psychiatric disorders, their physiology will be explored in more detail below.

1.2.1 Neurosteroid physiology

Neurosteroids are allosteric modulators at $GABA_ARs$, enhancing GABAergic transmission by increasing the probability of channel opening at low nM concentrations (<100 nM)(Callachan et al., 1987; Chisari et al., 2010a) or at higher concentrations, directly gating the channel pore in a GABA-mimetic fashion, through a site independent from the GABA binding site (Hosie et al., 2006; Lambert et al., 1990). At high doses, neurosteroids can act as anaesthetics, whereas lower doses produce anxiolytic and analgesic effects (Belelli and Lambert, 2005; Lambert et al., 2009; Mitchell et al., 2008; Poisbeau et al., 2005; Wang, 2011). Furthermore, neurosteroids can enhance GABAergic transmission by increasing IPSC frequency. This presynaptic effect of neurosteroids is mediated by changes in presynaptic Ca^{2+}-permeability following activation of presynaptic $GABA_ARs$ (Haage et al., 2002; Poisbeau et al., 1997). Whilst there are reports of sulphated neurosteroid derivatives, which possess an inhibitory action at $GABA_ARs$ (Hosie et al., 2007; Paul and Purdy, 1992), these will not be discussed within the scope of this thesis.

Amongst the endogenously synthesised positive allosteric steroids are the progesterone derivatives, 5α-pregnan-3α-ol-20-one (3α,5α-THPROG or allopregnanolone) and 5β-pregnan-3α-ol-20-one (3α,5β-THPROG) and the deoxycorticosterone metabolite, 5α-pregnan-3α,21-diol-20-one (THDOC) (Belelli and Lambert, 2005; Lambert et al., 2009; Mitchell et al., 2008; Wang, 2011).

An important discovery in the characterisation of neurosteroids was that neurosteroids in the brain are not only derived from endocrine glands such as the adrenals and ovaries (Paul and Purdy, 1992; Purdy et al., 1991), but can be synthesised *de novo* by certain types of neurons as well as glial cells, and be secreted in a paracrine fashion to modulate GABAergic inhibition in the brain (Agís-Balboa et al., 2006; Melcangi et al., 2001; Mellon and Vaudry, 2001).

Neurosteroids are involved in physiological as well as pathophysiological processes (Mitchell et al., 2008). Concomitant with their role in physiological as well as pathophysiological processes, neurosteroid levels in the brain undergo highly dynamic changes, fluctuating with stress hormone levels, the ovarian cycle, and development (Paul and Purdy, 1992; Purdy et al., 1991). At the hypothalamic-pituitary-adrenal (HPA) axis, neurosteroids are part of the stress response (Mody and Maguire, 2011; Purdy et al., 1991; Sarkar et al., 2011; Skilbeck et al., 2010). Levels of both allopregnanolone and THDOC are increased in response to acute stress. However, chronic stress has been shown to reduce neurosteroid levels at rest, while leading to a stronger increase in allopregnanolone levels in response to acute stress (Serra et al., 2000). In addition, repeated stress exposure can have adverse effects, such as memory impairment (Lupien et al., 2005). This may in part be mediated by long-term changes to the GABAergic system, since downregulation of $GABA_A$Rs has been observed to occur in response to chronic neurosteroid exposure (Barnes, 1996). Conversely, upregulation of δ-$GABA_A$R in response to increases in stress- and sex hormones has been shown to be mediated by neurosteroid metabolites in hippocampal dentate gyrus granule cells (DGGCs) (Maguire and Mody, 2007). These findings are just some examples for the wide-ranging stress-induced changes in brain neurosteroid levels that may significantly contribute to psychiatric disorders (Gunn et al., 2015; Mody and Maguire, 2011; Skilbeck et al., 2010).

Neurosteroid levels also change in pregnancy. Allopregnanolone, the neurosteroid metabolite of progesterone, reaches its highest physiological levels during the later stages of pregnancy (Corpéchot et al., 1997), and plays an important role in parturition (for a review, see Brunton et al., 2014). The onset of parturition is regulated by oxytocin-

releasing magnocellular neurons in the supra-optical and paraventricular nuclei. The release of oxytocin is sensitive to stressors, such as the interleukins, levels of which increase in relation to an immune challenge. To prevent premature parturition, oxytocin neurons are quiescent during the later stages of pregnancy, presumably via an increase in GABAergic inhibition through raised levels of allopregnanolone (Brunton and Russell, 2008). Shortly before birth, a sudden reduction in allopregnanolone synthesis has been suggested to promote oxytocin release and facilitate parturition (Brunton et al., 2014).
On a pathophysiological level, neurosteroids have been implicated in mental disorders such as anxiety and depression (Eser et al., 2008), mood changes related to the menstrual cycle (Wang, 2011) and puberty (Shen et al., 2007), neurodegenerative disorders such as Alzheimer's disease (Luchetti et al., 2011; Marx et al., 2006), as well as different forms of epilepsy (Biagini et al., 2010; Reddy and Rogawski, 2012). Abnormal levels of neurosteroids have been found in a variety of pathophysiological conditions, including schizophrenia and various forms of depression (Lambert et al., 2009). They can be influenced by drugs such as alcohol, shown by an increase in allopregnanolone in response to acute ethanol administration (Kumar et al., 2004; Sanna et al., 2004), and antidepressants, as evidenced by decreases in THDOC in fluoxetine-treated depressed patients (Ströhle et al., 2000).

Mutagenesis studies suggest two discrete binding sites of neurosteroids at $GABA_A$Rs: within the transmembrane domains of the α subunit (allosteric modulation; Figure 1.6) and at the β-α-interface (direct activation)(Hosie et al., 2006, 2009). At the allosteric site, binding of neurosteroids alters the kinetics of $GABA_A$R ion channel gating, prolonging the decay time of IPSCs. The strength of the effect depends on the brain area and neuronal subtype, due to differential expression of neurosteroid synthetic enzymes, and it varies with the activity of local kinases and phosphatases as well as the subunit composition of $GABA_A$R isoforms (Adams et al., 2014; Belelli and Lambert, 2005; Belelli et al., 2002; Lambert et al., 2009). While only subtle differences exist between $GABA_A$Rs incorporating isoforms of α, β and γ subunits, neurosteroids have profound effects on extrasynaptic tonic inhibition (Belelli and Lambert, 2005). They are particularly effective at enhancing GABA mediated tonic conductance at δ-$GABA_A$Rs (Belelli et al., 2002;

Brown et al., 2002), since GABA only acts as a partial agonist at these receptors compared to THIP (a super agonist) (Bianchi and Macdonald, 2003). Sensitivity to neurosteroids can be dynamically regulated by receptor phosphorylation (Adams et al., 2015; Comenencia-Ortiz et al., 2014). For example, in addition to the aforementioned drop in neurosteroid synthesis around parturition, the neurosteroid sensitivity of $GABA_AR$s has also been shown to reduce drastically, which has been linked to PKC activation (Koksma et al., 2003). In the hippocampus, on the other hand, phosphorylation by PKC has been shown to increase neurosteroid sensitivity of $GABA_AR$-mediated IPSCs (Harney et al., 2003).

Adding to the heterogeneity of neurosteroid responses is the differential distribution of enzymes for the neurosteroid synthetic pathways in the brain (see Figure 1.7; Melcangi et al., 2001; Mellon and Vaudry, 2001; Do Rego et al., 2009). The enzyme 5α-reductase metabolises progesterone to 5α-dihydroprogesterone (5α-DHPROG), a precursor of allopregnanolone, and also deoxycorticosterone into 5 –dihydro-deoxycorticosterone (5α-DHDOC), the precursor for THDOC (for a review, see Do Rego et al., 2009). There are two isoforms of 5α-reductase enzymes, Type I and II. Type I is the more abundant variant and Type II can be hormonally regulated (Torres and Ortega, 2003). Conversion of the precursors into the bioactive neurosteroids is catalysed by the enzyme 3α-hydroxysteroid dehydrogenase (3α-HSD). This enzyme works in both directions, and the preferred direction depends on the enzyme isoform. Membrane-bound 3α-HSD converts allopregnanolone into its inactive form, while cytosolic 3α-HSD converts the precursor to the active form.

The components of the neurosteroid biosynthesis pathway are highly expressed in PCs of various brain regions, amongst them the prefrontal cortex (PFC) (Castelli et al., 2013; Grobin et al., 2003; Gunn et al., 2015; Figure 1.7), suggesting the capability of this cell type to synthesise neurosteroids *de novo* to act in a paracrine or autocrine manner. However, the translocator protein 18 kDa (TSPO), another component of the neurosteroid biosynthesis pathway, which provides the rate-limiting step in neurosteroid synthesis preceding 5α-reductase and 3α-HSD (Rupprecht et al., 2010), is

more strongly expressed in glial cells (Gunn et al., 2015). This implies an involvement of this cell type in endogenous neurosteroid synthesis.

In summary, endogenous neurosteroids can exert strong modulatory effects over GABAergic function in a wide array of physiological and pathophysiological processes. They are distributed throughout the brain, and their levels, as well as efficacy at $GABA_ARs$, can be dynamically modulated. Their anxiolytic and analgesic properties place them alongside benzodiazepines as potential therapeutic compounds. Elucidating their normal function as well as dysregulation in disease are important ongoing areas of research. The role of neurosteroids in the PFC is of particular interest for the present thesis, given the involvement of both neurosteroids and the PFC in psychiatric disease (see section 1.4) and the dearth of knowledge on neurosteroid function in the PFC so far.

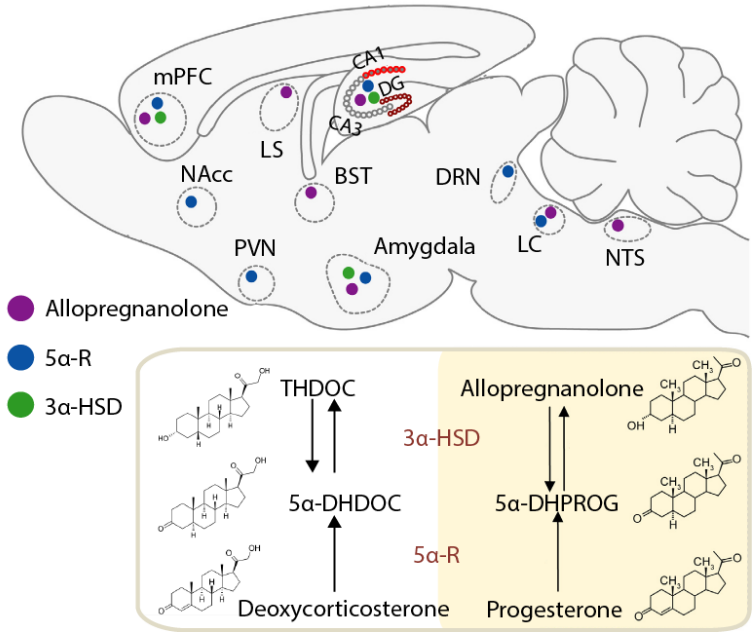

Figure 1.7: Neurosteroid biosynthesis pathways and the distribution of key enzymes in the brain

Sagittal brain section showing the expression pattern of neurosteroid synthesising enzymes 5α-reductase (5α-R) and 3α-HSD, as well as the neurosteroid allopregnanolone (coloured dots). The box (bottom) shows the molecular structure and biosynthesis pathways for THDOC and allopregnanolone (see main text). PVN – paraventricular nucleus; LS – lateral septum; BST –bed nucleus of the solitary tract; DRN – dorsal raphe nucleus; LC – locus coeruleus; DG – dentate gyrus; NAcc – nucleus accumbens; NTS – nucleus of the solitary tract. Figure adapted from Gunn and colleagues (2015).

1.3 GABAergic inhibition in psychiatric disease

Given the central role of $GABA_A$Rs in mediating inhibition, it is unsurprising that abnormal GABAergic function can have dramatic psychological consequences. Even small disruptions to the very delicate balance between inhibition and excitation necessary for normal function of the nervous system can result in a range of neuropsychiatric conditions, amongst them schizophrenia, anxiety, depression and addiction (Benes and Berretta, 2001; Beneyto et al., 2011; Möhler, 2006a, 2012; Nakazawa et al., 2012; Rudolph and Möhler, 2014; Volk and Lewis, 2005). In line with their varying pharmacological profiles and expression patterns in the brain, different $GABA_A$R subtypes have been linked to different mental illnesses. Several behavioural studies using heterozygous γ2 subunit knockout mice ($\gamma2^{+/-}$) showed an anxiogenic phenotype in comparison to wild-type littermates, highlighting the involvement of the GABAergic system in anxiety (Smith and Rudolph, 2012). However, since γ2 subunits are expressed in the majority of $GABA_A$Rs, these experiments were limited in their identification of $GABA_A$R subtypes relevant for specific psychiatric disease. Studies involving pharmacological as well as genetic manipulations revealed an important role for the α subunit (Smith and Rudolph, 2012). For example, $GABA_A$Rs containing α2/3 subunits have been studied as potential treatment targets for anxiety disorders and depression (Möhler, 2012). This was prompted by behavioural studies using knock-in mouse models carrying the aforementioned H101R point mutation in specific $GABA_A$R α subunits, rendering those receptors insensitive to diazepam. These studies showed that anxiolytic effects of benzodiazepines are mediated via α2/3 subunits (Dias et al., 2005; Löw et al., 2000). Moreover, in support of a role for α2/3-$GABA_A$Rs in anxiety and depression are studies showing the anxiolytic effects of L-838,417, an α2/3/5 subunit-selective allosteric agonist (McKernan et al., 2000), and studies demonstrating depression-like behaviour of knockout mouse models for α2 and α3 subunits (Fiorelli et al., 2008; Vollenweider et al., 2011). Likewise, rodent studies have provided promising results for anxiolytic effects of eszopiclone, a hypnotic selective for α2/3 and, to a lesser extent, α1-$GABA_A$Rs (Nutt and Stahl, 2010). Additionally, human trials have shown a synergistic antidepressant effect between eszopiclone with serotonin reuptake inhibitors (SSRIs) but not with zolpidem (an α1 subunit specific agonist) (Fava et al.,

2011a, 2011b). These results underline the therapeutic potential of targeting of α2/3-$GABA_A$Rs for the treatment of anxiety and depression.

Further evidence points to a dysregulation of α2-$GABA_A$Rs within the fear-response pathways in the pathophysiology of anxiety disorders. Gating of the fear response is strongly regulated by GABAergic inhibition in the amygdala, which is driven by the PFC (Ehrlich et al., 2009). Interestingly, GABAergic interneurons in the central amygdala largely act through α2-$GABA_A$Rs. A reduction in the level of control of the medial PFC (mPFC) over the amygdala is thought to be a common mechanism underlying both depression and anxiety disorders (Möhler, 2012).

The α2 subunit is also highly expressed in brain regions involved in learning and reward (Pirker et al., 2000; Sieghart and Sperk, 2002), and, as such, has been implicated in addiction to alcohol and drugs of abuse (Dixon et al., 2008; Engin et al., 2012; Kareken et al., 2010; Morris et al., 2008). For example, a recent human post-mortem study comparing mRNA levels of different $GABA_A$R subunits between control subjects and alcoholics found a significant reduction in the expression of α2 subunits in the central amygdala (Jin et al., 2014). Moreover, polymorphisms of the α2 subunit encoding gene have been linked to higher risks of developing alcohol dependence, including a response to alcohol and alcohol cues and severity of withdrawal symptoms as well as a predictor of treatment outcomes (Engin et al., 2012).

A role for tonic inhibition in the pathophysiology of neuropsychiatric disorders

$GABA_A$Rs mediating tonic inhibition have also received a significant amount of attention in searching for links between $GABA_A$R subtypes and psychiatric disease. Dysregulation of tonic inhibition has been linked to sleep disorders, susceptibility to stress-related disorders (e.g. depression), epilepsy and schizophrenia, whilst the potentiation of δ-$GABA_A$Rs is thought to be involved in the intoxicating effects of alcohol (reviewed in Brickley and Mody, 2012). THIP, which at low concentrations is a selective δ-$GABA_A$R agonist, also promotes non-REM sleep (Faulhaber et al., 1997). Since extrasynaptic $GABA_A$Rs containing the δ subunit are highly expressed in the thalamus, they are

thought to be involved in modulating cortico-thalamic network oscillations important for the perceptive state and non-REM sleep (Wafford and Ebert, 2006). Animal studies using δ-/- knockout mice, for example, have also found a potential role for $GABA_A$ receptors containing this subunit in postpartum depression and anxiety (Maguire and Mody, 2008).

An increasing amount of evidence is accruing suggesting that GABAergic dysregulation is a potential underlying cause of cognitive deficits in schizophrenia (Benes and Berretta, 2001; Beneyto et al., 2011; Curley and Lewis, 2012; Lewis, 2011; Nakazawa et al., 2012; Stan and Lewis, 2012; Volk and Lewis, 2005). Many studies find alterations in GABAergic markers in patients with schizophrenia, as well as laminar alterations in subunit expression of $GABA_A$Rs and changes in GABAergic interneurons (see below).

Levels of the GABA-synthesising enzyme, glutamate decarboxylase (GAD67), as well as the GABA membrane transporter, (GAT1), which is responsible for GABA reuptake in neurons, are reduced in a subset of interneurons in the PFC of schizophrenic patients (reviewed in Volk and Lewis, 2005). The affected interneurons were mainly PV-expressing interneurons, in particular Chandelier cells, which strongly innervate the AIS (Somogyi, 1977) and, therefore, are in an ideal location to modulate neuronal output (Cobb et al., 1995). A deficit in Chandelier cell input may underlie the observed deficits in γ-oscillations in schizophrenic patients (Lewis, 2011). This may have interesting ramifications for GABAergic inhibition at the AIS and its role in schizophrenia (Lewis, 2011). As mentioned previously, the AIS is enriched in α2-$GABA_A$Rs, which, while only comprising 15% of all neuronal $GABA_A$Rs (Fritschy and Möhler, 1995), are found in > 95% of inhibitory synapses at the AIS (Nusser et al., 1996b; Nyíri et al., 2001), and may, therefore, be of particular importance to the modulation of PC output. Interestingly, α2 subunit immunoreactivity at the AIS of schizophrenic subjects was significantly increased compared to control subjects (Volk et al., 2002). This may represent a compensatory upregulation of α2 subunits in response to a decrease in inhibitory input from Chandelier cells onto the AIS (Volk and Lewis, 2005).

In summary, GABAergic inhibition plays a significant role in regulating network activity in the brain and its dysregulation is thought to underlie a range of pathological conditions. A better understanding of the underlying mechanisms governing GABAergic inhibition and their specific alterations in disease is important for the development of novel treatments. In particular, elucidating the role of GABAergic inhibition in the PFC, a brain area which is often negatively affected in psychiatric disease, remains an ongoing challenge.

1.4 Structure and function of the prefrontal cortex

The PFC plays a significant role in executive function, which Funahashi defined as *"a product of the coordinated operation of various processes to accomplish a particular goal in a flexible manner"* (Funahashi, 2001). This comprises cognitive processes such as working memory, task flexibility and planning, which show deficits in studies involving PFC lesions (Elliott, 2003). Working memory, i.e. the ability to maintain or recall information for a short period of time to regulate behaviour and emotional responses, is the most characterised function of the PFC, and is thought to be diminished in schizophrenia (Goldman-Rakic, 1995, 1996, 1999; Kesner and Churchwell, 2011). The PFC promotes goal-directed behaviour and planning by exacting top-down control over processing of aversive and appetitive stimuli from the external and internal environment (Aron et al., 2014; Buschman and Miller, 2007). It assesses errors in expectations and adjusts them accordingly, in order to flexibly modulate behavioural responses to a changing environment (Lee and Seo, 2007). Given the broad spectrum of PFC functions, it is not surprising that it has been linked to an array of psychiatric conditions. For example, cognitive deficits in schizophrenia have been linked to altered network oscillations in the PFC (Arnsten et al., 2012; Volk and Lewis, 2005) and human brain imaging studies have found altered PFC control of the limbic system plays a central role in addictive behaviours (Goldstein and Volkow, 2002, 2011). Underlining this is the particular vulnerability of the PFC to acute and chronic exposure to stress, the effects of which can trigger extensive changes in prefrontal neurochemistry and even cytoarchitecture, increasing the chance for the development of psychiatric diseases such as depression, anxiety and schizophrenia (Arnsten, 2009, 2011).

Since different functions of the PFC are linked to different subregions (Kesner and Churchwell, 2011), the cellular and regional composition of the PFC will be explored further, with a focus on the mPFC (see below).

1.4.1 Connectivity of prefrontal subregions

The PFC receives afferents from other cortical as well as subcortical regions (Figure 1.8 A; Table 1.1) and in turn sends efferents across the brain (Figure 1.9; Table 1.2) to regions such as the basolateral amygdala (BLA), a region important for emotional stimuli, and the ventral tegmental area (VTA), which is involved in the reward circuitry of the brain and is the origin of the main dopaminergic afferents to the cortex (Gabbott et al., 2005; Hoover and Vertes, 2007). The PFC is therefore thought to be responsible for top down control of emotional responses and motivational behaviour. In certain circumstances, such as chronic exposure to stress, however, cortical control can be compromised, which can lead to inappropriate behavioural responses and, in the long term, to an array of mental disorders (for a review, see Arnsten, 2009).

The PFC denotes the frontal regions of the cortex, anterior to the corpus callosum (Bregma + 4.5 to + 2). It can be approximately subdivided into medial (m; further subdivided into dorsal (d) and ventral (v) areas) and orbital PFC (further subdivided into ventral, lateral (l), dorsolateral (dl) and ventrolateral (vl) areas) (Heidbreder and Groenewegen, 2003; Uylings et al., 2003). The dorsolateral PFC (dlPFC) is connected to sensorimotor areas of the cortex and is important for regulating attention, thought and behaviour (Goldman-Rakic, 2011). In humans and primates, the mPFC can be further divided into ventromedial PFC (vmPFC) and dorsomedial PFC (dmPFC). The vmPFC is connected to subcortical structures such as the amygdala, nucleus accumbens (NAcc) and hypothalamus and is generally thought to regulate emotional responses (Price et al., 1996), while the dmPFC is thought to assess errors (Modirrousta and Fellows, 2008).

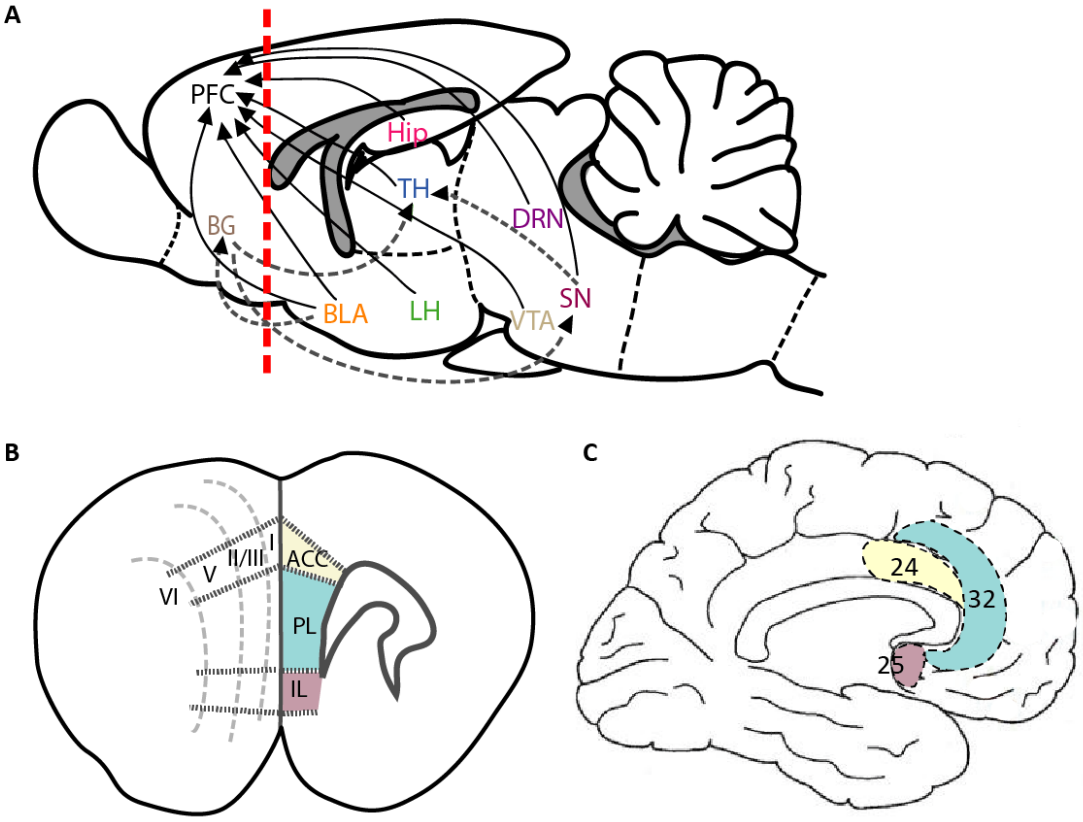

Figure 1.8: Afferents onto the mPFC originate from many central brain regions
A. Parasagittal section of the rat brain displaying afferents to the PFC from other cortical and subcortical areas. Dashed lines represent indirect afferents from or via the basal ganglia (BG; minus the substantia nigra (SN), which is separately labelled in this schematic model). The red dotted line marks the approximate location of the coronal slice below **(B)**, which shows the mPFC subregions and indicates their laminar structure. ACC – anterior cingulate cortex; PL – prelimbic cortex; IL – infralimbic cortex. **C.** Lateral view (top) and parasagittal section (bottom) of the human brain. Brodman's areas 24, 32 and 25, which correlate to rat mPFC ACC, PL and IL, respectively, are indicated. LH – lateral hypothalamus; BLA – basolateral amygdala; VTA – Ventral tegmental area; DRN – dorsal raphe nucleus; TH – thalamus; Hip – hippocampus.

	mPFC area			
Layer	**Anterior cingulate cortex**	**Prelimbic cortex**	**Infralimbic cortex**	
I	SN (Uylings et al 2003)			TH**; Hip (Little and Carter, 2012)
II	SN (Uylings et al 2003)	Hip$^{\#}$, TH (Parent 2010); BLA (Orozco-Cabal et al 2006)	BLA (Orozco-Cabal et al 2006)	TH***; BLA; Hip (Little and Carter, 2012)
III	SN (Uylings et al 2003)	Hip$^{\#}$, TH (Parent 2010);		TH***; Hip (Little and Carter, 2012)
V	VTA (Uylings et al 2003)	Hip$^{\#\#\#}$; BLA (Orozco-Cabal et al 2006)	BLA (Orozco-Cabal et al 2006)	
VI	VTA (Uylings et al 2003)	Hip$^{\#\#\#}$		
	TH^{+++}; Hip^{++}; VTA^{+++}; BLA^{++}; LH^{++};DRN^{+++}; SN^{+}	Hip^{+++}; TH^{+++}; BLA^{+++}; LH^{+}; VTA^{+++}; SN^{+}; DRN^{+++}	Hip^{+++}; TH^{+++}; BLA^{+++};LH^{+}; VTA^{++}; DRN^{+++}; SN^{+}	

Table 1.1: Subregional and laminar distribution of mPFC afferents
The table shows a summary of the literature on subregional and laminar distribution of some of the afferents in the mPFC. Most studies used retrograde tracers, wherein a region of interest is injected with the tracer, which spreads to the presynaptic neuron, labelling monosynaptic connections. Where applicable, an approximate quantification of the strength of retrograde tracer, i.e. the number of afferents, is represented by the number of signs following the brain region (one – weak labelling; two – medium; three – strong labelling). The different signs represent the respective studies referenced. +(Hoover and Vertes, 2007); * (Little and Carter, 2012); #(Parent et al., 2010). Where no information on the strength of innervation was given, no sign is used and the respective study is named in parentheses (Little and Carter, 2012; Orozco-Cabal et al., 2006; Parent et al., 2010; Uylings et al., 2003). Information on laminar afferent distribution, which lacked subregional distinction, is summarized at the end of the rows, while information on subregional distribution without laminar distinction is summarised at the base of the columns. DS – dorsal striatum; LH – lateral hypothalamus; BLA – basolateral amygdala; VTA – Ventral tegmental area; VS – ventral striatum; DRN – dorsal raphe nucleus; TH – thalamus.

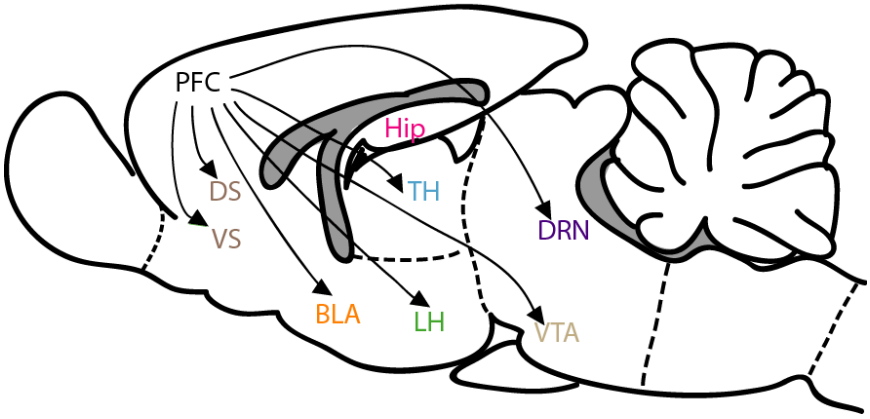

Figure 1.9: Brain regions targeted by PFC efferents
Parasagittal model of the rat brain displaying efferents from the PFC to other cortical and subcortical areas. See Table 1.1 for disambiguations.

	mPFC area		
Layer	**Anterior cingulate cortex**	**Prelimbic cortex**	**Infralimbic cortex**
II	DS*; LH*; BLA*	VS**; DS*; LH*;BLA*	VS*; DS*; LH*; BLA**
III	DS*; LH*	VS*; DS*; LH*;	VS*; LH*; BLA*
V	VS*; VTA*; DS***; LH***; BLA*; DRN**	VS***; VTA**; DS**; LH***; BLA*; DRN***	VS*; VTA**; DS*; LH***; BLA**; DRN*
VI	TH***; DS**; LH**	TH*** ; VS*; DS*; LH**	TH*** ; VS*; DS*; LH**

Table 1.2: Subregional distribution of mPFC efferents
Table showing subregional and laminar distribution of efferents in the mPFC as described by Gabbott et al., 2005. Asterisks indicate the relative strength of anterograde tracer labelling found by Gabbott and colleagues for the respective areas. * - weak labelling; ** - medium; *** - strong labelling. Layer I generally showed marginal or no labelling and was therefore omitted. For clarification of abbreviations, see Table 1.1.

The rodent PFC, while no doubt less complex in structure than the primate or human PFC, is nevertheless capable of exerting similar executive functions and, together with their versatility in a wide range of experimental applications, rodents are an indispensable tool in dissecting structure-function relationships in the PFC (Kesner and

Churchwell, 2011; Uylings et al., 2003). The rodent mPFC can be subdivided into anterior cingulate cortex (ACC), prelimbic cortex (PL) and infralimbic cortex (IL), based on functional and anatomical differences (Heidbreder and Groenewegen, 2003; Figure 1.8 B). These regions are functional correlates to areas of the human PFC (Brodman's areas 24, 32, 25, respectively, see Figure 1.8 C) and are linked to disorders such as schizophrenia, depression and drug abuse (Heidbreder and Groenewegen, 2003; Kesner and Churchwell, 2011; Riga et al., 2014) .

While it is beyond the scope of this thesis to give a full account of the hitherto uncovered local cortical pathways as well as existing cortical afferents and efferents with other brain regions, the central findings will be summarised here (see Figure 1.8 & Figure 1.9; Table 1.1 & Table 1.2 and refer to reviews Gabbott et al., 2005; Hoover and Vertes, 2007; Riga et al., 2014; Shepherd, 2009; Uylings et al., 2003).

Afferents and efferent projections of the mPFC

Cytoarchitecturally, six cellular layers can be distinguished in the PFC. Layer I, supragranular layers II-III, and a granular layer IV separating the supragranular layers from the infragranular layers V and VI. The rodent PFC varies from the primate PFC in the lack of a granular layer IV, however, layers II/III are visually distinguishable from layers V/VI by a dark thalamocortical fibre tract band in deep layer III (Dembrow and Johnston, 2014; Shepherd, 2009). This has functional consequences for signal processing, since in granular cortex, layer IV comprises the main input station, while most long-ranging efferents originate from layers V/VI. In the rodent mPFC, both inner and outer layers receive cortical and subcortical afferents and send efferents to limbic structures (see Figure 1.8 & Figure 1.9, Table 1.1 & Table 1.2 and review Riga et al., 2014). However, the interconnectivity may be laminar- and subregion specific in some cases. Outputs from the cortex to the thalamus, for example, usually originate from deep layer VI (Table 1.2), while thalamic inputs into the mPFC are mainly received by layer III (Heidbreder and Groenewegen, 2003; Shepherd, 2009; Table 1.1). Dopaminergic innervation of the mPFC is strongest in the PL, as evidenced by neuroanatomical as well as neurochemical studies (Heidbreder and Groenewegen, 2003). Axons from the SN

terminate in the superficial layers of the ACC (Table 1.1), while dopaminergic axons originating from the VTA terminate in deeper layers of the PL and IL. Furthermore, levels of dopamine are higher in PL and IL areas compared to ACC, while levels of dopamine transporter are higher in the ACC, overall suggesting higher concentration of extracellular dopamine in the more ventral mPFC regions (Heidbreder and Groenewegen, 2003). Serotonergic inputs from the raphe nuclei mostly innervate the PL and IL areas of the mPFC, and show differential laminar distribution, with a preference for the outer cortical layers. The hippocampus and the amygdala preferentially innervate the PL and IL areas (Table 1.1). However, the amygdala also innervates the ACC, albeit to a lesser extent, and while connections from the hippocampus to the mPFC are unilateral, amygdala-PFC connectivity is bidirectional (Heidbreder and Groenewegen, 2003). Connections between the mPFC and the striatum (i.e. the NAcc and the caudate-putamen) are strictly topographically organised, following a dorso-ventral pattern as well as laminar differentiation (Table 1.2). The ventral PL and IL of the mPFC project to the shell of the NAcc, while the dorsal Acc projects to the core of the NAcc and the caudate-putamen. At the same time, the superficial layers of the mPFC project to different areas within the caudate-putamen and NAcc core (matrix compartment) compared to the deeper layers (patch compartment)(Heidbreder and Groenewegen, 2003).

These are just a few examples of the vast and intricate networks that the mPFC forms just a part of, and serve to underline its important role in orchestrating normal brain function.

1.4.2 Cytoarchitecture of the mPFC and cortical networks

The mPFC is mainly composed of excitatory PCs (80-90%) and inhibitory GABAergic interneurons (10-20%), which can be further distinguished according to morphological, functional and biophysical properties (Riga et al., 2014). The cells responsible for the main excitatory output, the PCs, are strongly interconnected to form local networks and project to both cortical as well as subcortical structures. Their concerted activity is tightly regulated by a number of different types of interneurons, which specifically

innervate different subcellular compartments of PCs to regulate their activity (Palmer et al., 2012; see Figure 1.2). Interneurons, most of which are GABAergic form local connections, although recent research has identified long-range GABAergic projections from the PFC onto the NAcc (Lee et al., 2014a). They exert strong control over pyramidal cell firing and are a crucial component in generating neuronal network oscillations, a feature thought to be vital for information processing (Klausberger et al., 2003; Kvitsiani et al., 2013; Mann and Paulsen, 2007; Whittington and Traub, 2003; Yee et al., 2005). Interneurons possess remarkable morphological diversity in contrast to PCs and are more excitable, as evidenced by faster action potential firing frequency and faster excitatory synaptic current kinetics (for a review, see Möhler, 2006b).

Both types of neurons can be further subdivided based on morphological and electrophysiological properties as well as their laminar localisation and connectivity (see below). These subtypes have been shown to be differentially affected by neuromodulators such as dopamine and serotonin (Béïque et al., 2007; Dembrow and Johnston, 2014) which highlights the complexity and flexibility underlying cortical network function.

Pyramidal cells - complexity and diversity

Several classes of cortical PCs have been defined, which possess unique electrophysiological properties and laminar distribution (van Aerde and Feldmeyer, 2015; Dégenètais et al., 2002; Kawaguchi, 1993; Wang et al., 2006). Kawaguchi and colleagues (1993) were amongst the earlier authors who characterised different types of PCs. They defined two types of PCs in layer V of the rat PFC based on somatic size and input resistance (Kawaguchi, 1993). Small, high input resistance cells showed a similar laminar distribution to larger, small input resistance cells, but they varied in their dendritic morphology. While both cell types extended dendritic branches in layer I and layer V, only the smaller cells also received input from layer II/III. In a later study, Lee and colleagues (2014) identified two PC subpopulations in layer V of the PFC, type A and type B, which are differentially innervated by presynaptic interneurons. Type A, consisting of thick-tufted, sub-cortical projecting PCs with a strong a hyperpolarisation-

activated inward current (I_h) that may act as a pacemaker for spontaneous interneuron activity (Maccaferri and McBain, 1996)), and type B, which are thin-tufted, project to the callosum and do not possess I_h. One observation of this study was that type A PCs were preferentially innervated by PV-positive, but not somatostatin (SOM)-expressing interneurons, providing stronger feed-forward inhibition on this type of PC (Lee et al., 2014b).

Further studies have shown that particularly in the mPFC, different types of layer V PCs form reciprocal connections and specific subnetworks (Wang et al., 2006). This study found interconnections between PCs with accommodating spike patterns to form depressing synapses with one another, while another subpopulation with non-accommodating discharge pattern formed facilitating synapses. These results show that the complex modulation of cortical microcircuit behaviour extends beyond the diversity of inputs from interneurons.

Recently, van Aerde and colleagues (2015) conducted a thorough electrophysiological study in rat mPFC, discovering more than 10 different types of PCs with distinct morphologies, laminar distributions and firing properties (see Figure 1.10; van Aerde and Feldmeyer, 2015). This study found two classes of PCs in layer V: broad-tufted, regular spiking PCs and slender-tufted, accommodating PCs. PCs in layer II exhibited the widest apical dendritic field. They showed a variety of responses to current injections, from regular-spiking to accommodating, lacking a voltage sag in response to hyperpolarising current injections, with a high rheobase and more negative resting membrane potential (Figure 1.10). Layer III PCs generally extended an apical dendrite to layer one, where it bifurcated, and showed a variety of electrophysiological responses, but was the only region with cells exhibiting burst-firing in response to depolarising current injections (Figure 1.10). Layer VI PCs, although mostly uniform in displaying a regular spiking pattern, comprised the most morphologically diverse group of neurons, many of them exhibiting long apical dendrites extending up to layer I.

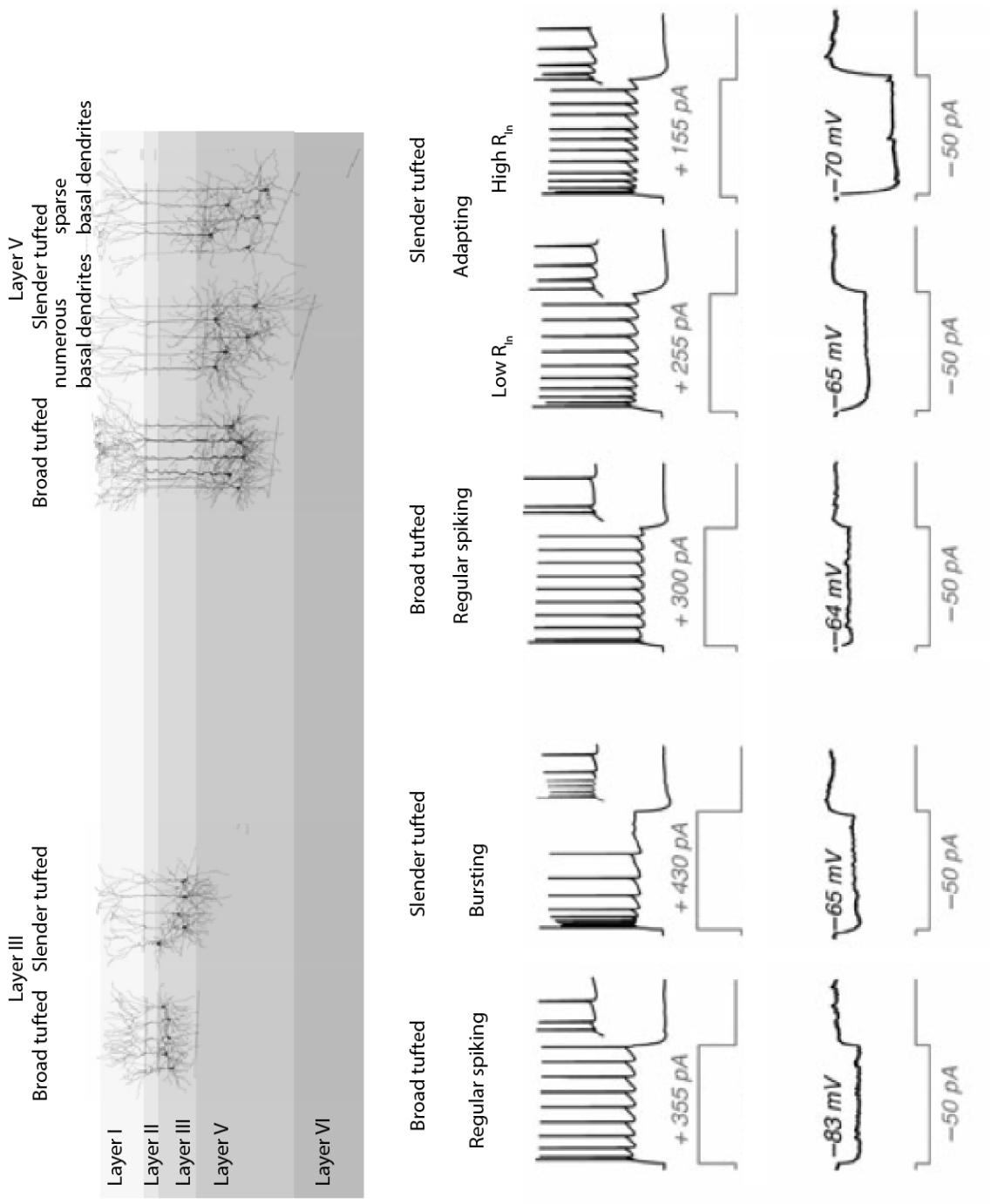

Figure 1.10: Diversity of cortical pyramidal cells

Figure adapted from van Aerde and Feldmeyer (2015), showing an overview of some of the diverse morphologies and electrophysiological firing properties of PCs in different layers of the rat mPFC. Top panel, reconstructions of the different morphological subtypes identified are shown and their laminar origin indicated. Electrophysiological properties of the respective PC subtypes are presented in the bottom panels: Action potential firing patterns in response to a current injection (grey line) are shown. The insets show a magnification of the first few spikes. The bottom row shows the voltage response to a hyperpolarising current of -50 mV and the RMP is indicated.

In summary, these studies show a surprising diversity in cortical PCs, which further adds to the complexity of cortical networks and poses additional challenges for studying this brain region.

Diverse morphology and biochemical markers of cortical interneurons

Cortical interneurons are mostly GABAergic and are generally characterised by aspiny dendrites and by a restriction in their axonal extensions, which are usually vertically limited to their own cortical column or laterally limited within their layer (Markram et al., 2004). More than ten different types of interneurons can be distinguished in the neocortex, based on dendritic and axonic morphology, their expression of biochemical markers, as well as their electrophysiological properties and synaptic connectivity with specific PC membrane sub-compartments (Markram et al., 2004).

As opposed to the fairly uniform morphology of PCs, interneurons come in a range of shapes and sizes (Figure 1.11). Morphologically, they can be categorised into basket cells (further divided into large, small and nest basket cells), Chandelier cells, Martinotti cells, double-bouquet cells, bipolar cells, bitufted cells, neurogliaform cells and Cajal-Retzius cells (Druga, 2009; Markram et al., 2004). Basket cells are large, multipolar, and are the most prominent inhibitory interneurons, representing about half of the GABAergic interneuron population. Their name stems from the appearance of their axon-terminals, which form basket-like structures around the soma and proximal dendrites of the target neuron, which can be other interneurons or PCs. Chandelier cells, on the other hand, can be multipolar or bi-tufted and innervate the AIS of PCs only. Their name is derived from the characteristic structure of their axon terminals, which branch and form vertical rows of axonal boutons along the postsynaptic membrane similar to candles in a chandelier (Druga, 2009; Markram et al., 2004).

Another distinguishing feature of interneurons is their expression of different types of calcium binding proteins (Figure 1.11). Three large subpopulations can be distinguished, which express: PV (20-25% of all GABAergic cells), calbindin (CB; 20-25%) or calretinin (CR; 45-50%) in a non-overlapping manner (Baimbridge et al., 1992; Druga, 2009; Hof et

al., 1999). In addition, the expression of several neuropeptides such as neuropeptide Y (NPY), somatostatin (SOM), cholecystokinin (CCK) and vasoactive intestinal peptide (VIP) serve as another distinctive marker (Markram et al., 2004). CB- and CR-positive interneurons mainly belong to the morphological classes of bipolar, bitufted and double-bouquet interneurons, while PV-positive interneurons are either basket cells or Chandelier cells (DeFelipe, 1997; Defelipe et al., 1999; Druga, 2009). Based on the presence of these calcium binding proteins, Gabbott and colleagues (1997) characterised the laminar distribution of different types of interneurons in ACC, PL and IL of the rat mPFC in an immunocytochemical study (Gabbott et al., 1997). While the distribution across mPFC areas was found to be consistent, they observed differences in the laminar density between the different subclasses of interneurons. Bipolar CR-positive cells were most frequently found in upper layer III, multipolar PV-positive cells were most dense in layers III and V, and multipolar CB-positive cells were mostly found in lower layer III, while some Martinotti and neurogliaform CB-positive cells also appeared in layer V/VI (Gabbott et al., 1997).

Inhibitory interneurons can be further distinguished based on their electrophysiological properties, such as firing rate, steady-state firing pattern and spike onset response types (Markram et al., 2004). Kawaguchi and colleagues (1993), for example, found two principal types of interneurons in layer V of the rat PFC. One was defined by its fast spiking pattern (FS cells), which showed no adaptation in spike frequency and possessed a more negative membrane potential, while the slower spiking cells possessed a low firing threshold (LTS) cells and exhibited spike-frequency adaptation and typically elicited burst-like discharges after a hyperpolarising pre-pulse (Kawaguchi, 1993). While FS cells were multipolar in shape and extended dendrites to layers II/III and V, LTS cells were mostly bitufted and their dendrites were restricted to layer V. More recently, electrophysiological distinctions have been made and have linked the three main subclasses of calcium-binding protein expressing interneurons to different firing categories. Thus, CR-positive interneurons usually show an irregular spike discharge pattern with an accommodating spike-frequency, CB-positive interneurons exhibit a burst-firing pattern, and PV-positive interneurons have the characteristics of FS cells (Markram et al., 2004).

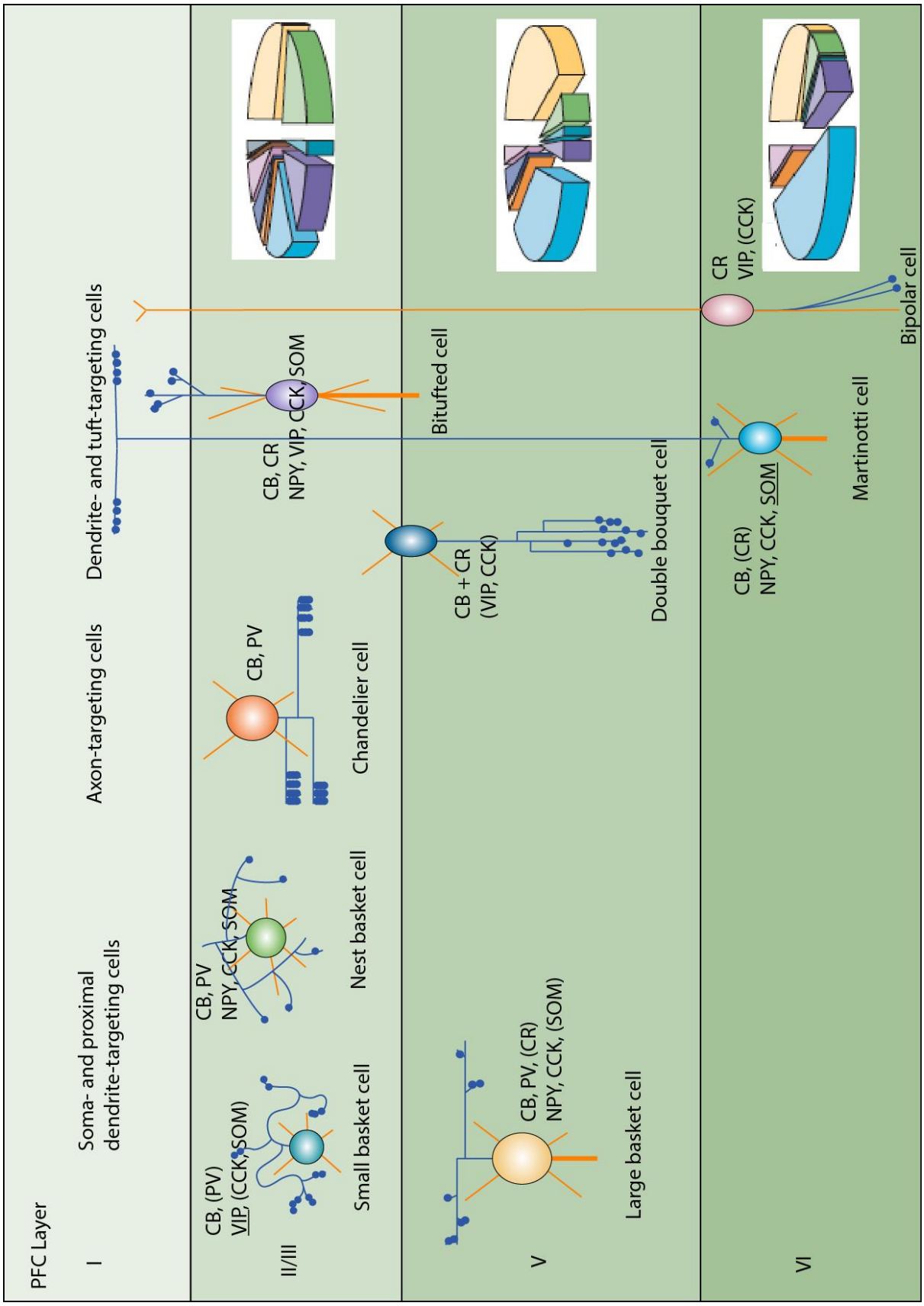
PFC Layer
I
II/III
V
VI
Soma- and proximal dendrite-targeting cells
Axon-targeting cells
Dendrite- and tuft-targeting cells
CB, (PV)
VIP, (CCK, SOM)
Small basket cell
CB, PV
NPY, CCK, SOM
Nest basket cell
CB, PV
Chandelier cell
CB, CR
NPY, VIP, CCK, SOM
Bitufted cell
CB + CR
(VIP, CCK)
Double bouquet cell
CB, PV, (CR)
NPY, CCK, (SOM)
Large basket cell
CB, (CR)
NPY, CCK, SOM
Martinotti cell
CR
VIP, (CCK)
Bipolar cell

Figure 1.11: Diversity of cortical interneurons
Schematic drawing of the morphology and laminar distribution of 8 different types of cortical interneurons (adapted from Markram et al., 2004). The original data stemmed from the somatosensory cortex (which, contrary to the PFC, has a granular layer IV) and has been adjusted to represent an agranular cortex here. Neurogliaform and Cajal-Retzius cells have been omitted for simplicity. The somata of each interneuron subtype are differentially coloured and placed in their preferred cortical layer location. Proportional laminar representation of each subtype is represented in the pie-charts on the right-hand side, with the colour of each slice corresponding to the soma of the respective interneuron. Axons are drawn in blue, axonal terminals are drawn as blue circles and dendrites are drawn in orange. Some interneurons possess an apical dendrite, which is shown as a thicker orange line. Calcium-binding proteins and neuropeptides typically expressed by each interneuron subtype are indicated. Those that are rarely expressed are shown in parentheses, while those that are frequently expressed are underlined.

Lastly, different interneuron subtypes preferentially target specific cellular compartments, which is of relevance for the type of modulatory influence they can exert over the postsynaptic cell (see Figure 1.2). For example, as mentioned in section 1.1.1, PV-positive cells are generally fast-spiking and inhibit the perisomatic region, thus controlling PC output, while somatostatin (SOM) interneurons, which target the dendritic arbour, modulate inputs onto PCs (Klausberger et al., 2002; Möhler, 2006b; Nyíri et al., 2001). Amongst PV-positive interneurons, basket cells form somatic or perisomatic connections onto mainly α1-$GABA_AR$ containing synapses, and Chandelier cells innervate the AIS (Somogyi, 1977), which is enriched with α2-$GABA_ARs$ (Nusser et al., 1996b), placing them in a crucial position to regulate sodium-generated APs (Cobb et al., 1995). Martinotti cells, on the other hand, which always express SOM and can additionally express CB, CR or CCK, are slow-spiking and innervate the apical dendrites, where they may inhibit Ca^{2+}-mediated dendritic spikes (Druga, 2009; Higley, 2014; Isaacson and Scanziani, 2011; Marlin and Carter, 2014).

In summary, this brief account of cortical connectivity and cortical cellular diversity demonstrates the challenges experimental studies on the PFC have to confront when trying to interpret results obtained from a non-uniform population of neurons.

1.5 Thesis objectives

The aim of this thesis is to study GABAergic inhibition in the PFC, with a particular focus on the mPFC, given that neurodevelopmental and psychiatric disorders (schizophrenia, depression, etc) are frequently linked to this part of the brain and dysfunctional GABA inhibition. Whilst there have been many studies addressing GABAergic inhibition in the hippocampus (Farrant and Nusser, 2005; Klausberger et al., 2003) and cerebellum (Marty and Llano, 1995), there is a significant gap in our understanding of such processes in the PFC. One of the principal goals, therefore, was to further elucidate the role of GABAergic inhibition and understand how key neuromodulators, such as dopamine and neurosteroids, in the mPFC, could regulate synaptic and extrasynaptic $GABA_A$Rs.

Dopamine modulation of inhibition, via the D4 receptor, has previously been shown to decrease $GABA_A$R surface expression and IPSCs in the PFC (Graziane et al., 2009; Wang et al., 2002). The dopaminergic system is strongly implicated in the pathophysiology of schizophrenia (Arnsten et al., 2015; Furth et al., 2013; Lewis and Gonzalez-Burgos, 2006; Masana et al., 2012). Alterations to the levels of inhibitory transmission at the Chandelier-AIS synapse (Lewis, 2011), including the concomitant increase in α2-$GABA_A$Rs in this region (Beneyto et al., 2011), have also been linked to schizophrenia. Since the α2-$GABA_A$R is a subtype of $GABA_A$R that is involved in anxiolysis (Dias et al., 2005; Löw et al., 2000; Vollenweider et al., 2011) and has been linked to some psychiatric diseases (Engin et al., 2012; Möhler, 2012), the possibility of a subunit-specific effect of D4 receptor activation, in particular on α2-$GABA_A$Rs, was one important focus of the study (see Chapter 3).

Neurosteroids are another endogenous family of neuromodulators implicated in psychiatric disease and they have been of interest in the development of novel psychopharmaca with less severe side-effects than the benzodiazepines. Their modulation of synaptic inhibition has been well studied and previous research using a knock-in mouse model expressing the neurosteroid-insensitive α2 subunit has shown electrophysiological effects of neurosteroid-modulation at α2-$GABA_A$Rs in the hippocampus and NAcc (Durkin, 2012). The same study has also shown a behavioural

effect of ablating endogenous neurosteroid-modulation via this receptor subtype. However, whether α2-$GABA_A$Rs contribute to neurosteroid-modulation in the mPFC has not been investigated and was therefore the key aim of this project (chapter 4). Furthermore, given their enrichment at the AIS, α2-$GABA_A$Rs were postulated to exert some control over pyramidal cell firing. Here, we made use of the neurosteroid knock-in mouse model to study the influence of α2-$GABA_A$Rs on neurosteroid-modulation of neuronal excitability and spike output in the mPFC (chapter 5).

In summary, the main objectives are:

- To assess the effect of D4 receptor activation on GABAergic inhibition in primary PFC cultures as well as to determine whether these effects are mediated via distinctive $GABA_A$R subtypes
- To elucidate the contribution of α2-$GABA_A$Rs and its modulation by neurosteroids to phasic and tonic prefrontal inhibition
- To investigate the role of neurosteroid-modulation of α2-$GABA_A$Rs in regulating pyramidal cell excitability

2 Materials & Methods

2.1 Materials

2.1.1 Reagents

For Western Blot (WB) analysis, the chemical reagents Bovine Serum Albumin (BSA) and sodium dodecyl sulphate (SDS) were obtained from First Link (UK) Ltd (Birmingham, UK) and National diagnostics (Atlanta, Georgia, USA), respectively. SDS-PAGE Molecular Weight Standards (Broad Range) and Tween20 were obtained from Bio-Rad Laboratories (Hemel Hempstead, UK) and NP-40 was obtained from Merck KGaA, (Darmstadt, Germany).

All cell culturing reagents were obtained from Invitrogen, except for papain, which was supplied by Worthington Biochemical Corporation (Lakewood, New Jersey, USA).
For electrophysiological experiments, the compounds (2R)-amino-5-phosphonovaleric acid (APV), 6-cyano-7-nitroquinoxaline-2,3-dione (CNQX), PD168077 maleate, tetrodotoxin (TTX) citrate, L-745870 and SB242084 were obtained from Abcam (Cambridge, UK) and MRK 016 was obtained from Tocris Bioscience (Bristol, UK). QX-314 bromide and leupeptin hemisulfate, which were supplements to the internal recording solution, were obtained from Insight Biotechnology (London, UK) and AppliChem GmbH (Darmstadt, Germany), respectively. All other chemicals were obtained from Sigma-Aldrich (Steinheim, Germany), VWR International (Leuven, Belgium) or ThermoFisher Scientific Inc. (Rockford, Illinois, USA) unless stated otherwise.

2.1.2 Antibodies

Antibody	Working concentration		Supplier
	WB	**ICC**	
Primary Antibodies			
Rabbit anti $GABA_A$ α1	-	1:20,000	Courtesy of Dr Jean-Marc Fritschy (University of Zurich)
Rabbit anti $GABA_A$ α1	1:250	-	Courtesy of Dr Jean-Marc Fritschy (University of Zurich) (2013)
Guinea-pig anti $GABA_A$ α2	1:200	1:200	Courtesy of Dr Jean-Marc Fritschy (University of Zurich)
Chick anti microtubule-associated protein 2 (MAP2)	-	1:5,000	Abcam
Mouse anti AnkyrinG	-	1:1,000	Neuromab
Mouse monoclonal anti-β-Tubulin	1:1,000	-	SigmaAldrich (clone TUB2.1)
Mouse anti dopamine receptor D4	1:200	1:10	Abcam
Secondary Antibodies			
Alexa Fluor® 488 conjugated to goat anti-guinea pig IgG (H+L)	-	1:500 or 1:1000	Thermo Fisher Scientific.

Antibody	Working concentration		Supplier
	WB	**ICC**	
Alexa Fluor® 488 conjugated to goat anti-rabbit IgG (H+L)	-	1:500 or 1:1000	Thermo Fisher Scientific
Alexa Fluor® 488 conjugated to goat anti-mouse IgG (H+L)	-	1:500 or 1:1000	Thermo Fisher Scientific
Alexa Fluor® 555 conjugated to goat anti-mouse IgG (H+L)	-	1:500 or 1:1000	Thermo Fisher Scientific
Alexa Fluor® 594 conjugated to goat anti-chick IgG (H+L)	-	1:500 or 1:1000	Thermo Fisher Scientific
Alexa Fluor® 647 conjugated to goat anti-chick IgG (H+L)	-	1:500 or 1:1000	Thermo Fisher Scientific
HRP-conjugated goat anti-rb IgG(H&L)	1:50,000	-	Rockland Immunochemicals for Research
HRP-conjugated donkey anti-guinea-pig IgG (H&L)	1:4,000	-	Jackson ImmunoResearch Laboratories
HRP-conjugated goat anti-mouse IgG (H&L)	1:10,000	-	Rockland Immunochemicals for Research

2.2 Animals

All procedures were performed according to the *Animals (Scientific Procedures) Act* (ASPA)*, 1986* and had obtained ethical approval. For obtaining tissue for electrophysiology or Western blotting, young adult male Sprague Dawley rats, α2 Q241M mutant mice (a knock-in mouse model generated in our lab expressing a neurosteroid-insensitive $GABA_AR$ α2 subunit, see Durkin, 2012) or C57Bl6/J mice (P28-

60 for both mouse strains) were decapitated subsequent to isoflurane anaesthesia (Abbott, Chicago, Illinois, USA). To avoid neurosteroid fluctuations known to occur throughout the oestrous cycle (Corpéchot et al., 1997), only male animals were used for the experiments.

Pregnant rats were culled by cervical dislocation and E18 embryonic rats, used for tissue culture, were extracted and decapitated under schedule 1 procedures of the Animals Act 1986.

2.2.1 Breeding and housing

For breeding purposes, heterozygous mice (PD > 42) of the N303 strain were kept in pairs to allow for comparison of homozygous and wild-type littermates. Breeding pairs were maintained for a maximum of 6 litters before being culled by exposure to carbon dioxide in a rising concentration in accordance with Schedule 1 of the ASPA. For experimental purposes, male animals were housed in cages of up to 5 littermates with *ad libitum* access to water and food. Cages were environmentally enriched and kept in a temperature-controlled room under a 12-hr light-dark cycle. Animals not suitable for experimental purposes (e.g. heterozygous and female animals) were culled in accordance with Schedule 1 of the ASPA.

2.2.2 Genotyping

The genotype of mice used for experimental purposes was determined using tissue obtained from ear clippings. The DNA was extracted by incubating tissue overnight in a lysis buffer (100 mM Tris-HCl pH 8.5, 5 mM EDTA, 0.2% w/v SDS, 200 mM NaCl and 0.1 µg/ml proteinase K (Roche Diagnostics, Mannheim, Germany)) at 37°C. This was followed by a centrifugation step (15 min, 13,000 rotations per minute (RPM)) at room temperature (RT) to remove debris. The DNA was precipitated in a second centrifugation step (10 min at RT and 13,000 RPM) using isopropanol and was washed using 70% ethanol in a final centrifugation step (5 min at RT and 13,000 RPM). Lastly, the DNA was resuspended in 0.05x TE (10 mM Tris, 1 mM EDTA, pH 8.0) and incubated at 42°C for 1 hr before storage at 4°C for further use.

To distinguish between genotypes, a polymerase chain reaction (PCR) was performed as outlined in Figure 2.1 and the product was separated on a 2% w/v agarose gel with added ethidium bromide (0.2 µg/ml, VWR international) using gel-electrophoresis. DNA bands were visualised under UV light. Mice homozygous for the $\alpha2^{Q241M}$ allele could be distinguished from wild-type animals by the presence of a loxP site (see Durkin, 2012). The DNA fragment obtained from the PCR described in Figure 2.1 was 100 base pairs larger for mice homozygous for the mutant allele compared to wild-type mice, while heterozygous animals expressed both fragments.

PCR protocol

Step	Temperature	Time [min]	
1 – Melt	98°C	30	
2 – Melt	98°C	10	
3 – Anneal	63°C	30	Repeat 35 x
4 – Extend	72°C	30	
5 - Extend	72°C	5	

PCR mix (50 µL reaction volume)

Reagent	[µL]
DNA	1
H_2O	37
GC buffer	10
dNTPs	1
Forward primer	0.25
Reverse primer	0.25
Polymerase	0.5

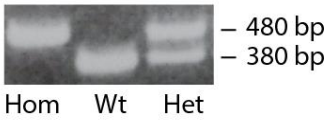

PCR Primers

Forward Primer

5’-GCATAGACTACACAAAGTCTCTAGAAC-3’

Reverse Primer

5’-GGAGGTGGTGGTGATATCAAGTATA-3’

Figure 2.1 PCR protocol used for genotyping Q241M knock-in mice
PCR protocol and primers from Eurofins MWG Operon (Ebersberg, Germany) used in a standard procedure for genotyping. The image in the middle depicts representative DNA fragments and their length obtained for the wild-type (Wt) and the neurosteroid-insensitive $\alpha2^{Q241M}$ allele (Hom). Animals heterozygous for the allele produced both DNA fragments (Het). The PCR was carried out using a G-Storm PCR cycler (G-Storm, Somerton, UK) and the Phusion Hot Start II polymerase kit (Thermo Fisher Scientific) using the primers shown in the bottom panel.

2.3 Tissue preparation

2.3.1 Neuronal cell culture

Primary neuronal cultures of the PFC were obtained from E18 rats. Cortices were removed and dissociated by incubating in papain (300 U in CO_2-independent medium) for 30 min followed by a series of gentle triturations using decreasing Pasteur pipette bore diameters. Cells were plated on Poly-D-Lysine (PDL, 100 µg/ml)-coated 22mm glass coverslips at a density of 1 - 2.6 x 10^5 cells/cm^2 in serum rich plating medium (DMEM, 10% heat-inactivated horse serum, 200 units/ml Penicillin and 200 µg/ml Streptomycin). Cells were allowed to attach to the surface for 3-4 hrs before exchanging the plating medium for a serum-free medium (DMEM with B27 supplement, 200 units/ml Penicillin and 200 µg/ml Streptomycin). By volume, 50% of this medium was replaced twice-weekly with fresh medium. Neurons were maintained in this manner for at least 10 days for the purpose of electrophysiological recordings. Some immunocytochemical and Western Blot experiments were carried out at earlier ages, as indicated in the Results section.

2.3.2 Brain slices

Coronal slices (300 µm thick) of the PFC were obtained from P22 male rats or male mice (P28 – 60). For slices obtained from rats, sections were cut in ice-cold bicarbonate-buffered solution (85 mM NaCl, 2.5 mM KCl. 1.25 mM $NaH_2PO_4 \cdot H_2O$, 26 mM $NaHCO_3$, 75 mM Sucrose, 1 mM $CaCl_2$, 4 mM $MgCl_2$, 25 mM Glucose, 2 mM kynurenic acid (KA)) using a vibrating blade microtome (VT 1200 S, Leica Microsystems GmBH, Wetzlar, Germany) whilst under constant perfusion with 95% O_2 / 5% CO_2. For slices obtained from mice, a HEPES-buffered potassium gluconate solution was used (130 mM K-Gluconate, 15 mM KCl. 0.05 mM EGTA, 20 mM HEPES, 4 mM Na-pyruvate, 25 mM Glucose, 2 mM KA, pH adjusted to 7.4 using 1 M NaOH). Slices were transferred into a holding chamber pre-warmed to 37˚C and maintained at this temperature for 1 hr during which time the solution was slowly exchanged for sucrose-free artificial cerebrospinal fluid (aCSF) containing 125 mM NaCl, 2.5 mM KCl, 1.25 mM $NaH_2PO_4 \cdot H_2O$, 26 mM $NaHCO_3$, 2 mM $CaCl_2$, 1mM $MgCl_2$ and 25 mM glucose. For voltage-clamp experiments, 2 mM KA was added to block ionotropic glutamatergic transmission. Slices

were subsequently maintained in this solution at room temperature (RT). All solutions were continuously perfused with 95% O_2 / 5% CO_2 (BOC Healthcare, Manchester, UK).

2.4 Electrophysiology

2.4.1 Primary culture electrophysiology

Electrophysiological recordings from pyramidal neurons grown in culture for at least 10 days were obtained using standard whole-cell patch clamp techniques. Electrodes were pulled using thin-walled filamented borosilicate capillaries (10 cm long, 1.5 mm outer diameter; World Precision Instruments, Sarasota, Florida, USA) to a resistance of 3-5 MΩ when filled with a recording solution containing 140 mM CsCl, 2 mM NaCl, 10 mM 4-(2-hydroxyethyl)-1-piperazineethanesulfonic acid (HEPES), 5 mM ethylene glycol tetraacetic acid (EGTA), 2 mM $MgCl_2$, 0.5 mM $CaCl_2$, 2 mM Na_2-ATP, 0.5 mM Na-GTP and 2 mM QX-314. For recordings examining the activation of G-protein-coupled inwardly-rectifying potassium channels (GIRKs, see Chapter 3), a high K^+, low Cl^- recording solution was used instead, consisting of: 130 mM K-Gluconate, 10 mM KCl, 10 mM HEPES, 5 mM EGTA, 2 mM $MgCl_2$, 0.5 mM $CaCl_2$, 2 mM Na_2-ATP and 0.5 mM Na-GTP. The osmolarities of the recording solutions ranged between 280-290 mOsm/l and were adjusted to 300-310 mOsm/l by supplementing with 10-20 mM sucrose. The osmolarity was measured using a vapour pressure osmometer (Wescor Inc, Utah, USA). All recording solutions were adjusted to pH 7.3.

For recordings from cultured neurons an external solution (Krebs) containing 140 mM NaCl, 4.7 mM KCl, 1.2 mM $MgCl_2$, 2.5 mM $CaCl_2$, 11 mM Glucose and 5 mM HEPES was used and supplemented with 10 µM CNQX plus 20 µM APV to block ionotropic non-NMDA and NMDA glutamatergic transmission, respectively. Neurons were visualised using an inverted microscope (Nikon Eclipse TE300, Nikon Instruments Europe B.V., Surrey, UK) and recordings were carried out at RT using an Axopatch 200B amplifier (Molecular Devices, Sunnyvale, California, USA). Membrane currents were digitized using a Digidata 1440A (Molecular Devices) and recorded using Clampex software (version 8.2, Molecular Devices). Membrane voltage was clamped at -70 mV. Drugs

were kept as concentrated stock solutions in either H_2O (GABA, TTX, CNQX, APV, pentobarbitone, L-745870, THIP) or dimethyl sulfoxide (DMSO) (PD168077, bicuculline, SB242084, Diazepam, RO-60-0175, THDOC, MRK-016) and diluted to working concentrations in recording solution prior to use. Applications were carried out using a custom-built U-tube controlled by rapid solenoid switching (Thomas and Smart, 2005) for 1-2 s with 30 s - 2 min washout periods between applications. For the generation of concentration response curves, a series of GABA concentrations (0.1 µM, 0.3 µM, 1 µM, 3 µM, 10 µM, 30 µM, 100 µM, 300 µM, 1 mM) were randomly applied. Peak GABA-activated currents were measured and normalised to the maximal response evoked by 1 mM GABA. Concentration response relationships were fitted with OriginPro (version 9.1, OriginLab Corporation, Northampton, MA, USA) and half-maximal effective concentrations (EC_{50}) as well as the Hill coefficient were determined using a non-linear least squares fitting routine based on the Hill equation:

$$\frac{I}{I_{max}} = \frac{1}{1 + \frac{EC_{50}}{[A]^n}}$$

Where EC_{50} is the GABA concentration that elicits a half-maximal response, n is the Hill coefficient, I is the current measured at concentration of GABA, A, and I_{max} is the maximal GABA current response measured. Mean EC_{50} values and standard errors of the mean (SEM) were determined from the EC_{50} values obtained from individually fitted concentration-response curves.

2.4.2 Brain slice recordings

Pyramidal neurons in layers II-VI of PFC slices were located using infra-red optics (Nikon Eclipse E600FN, Nikon Instruments Europe B.V. Surrey, UK) fitted with a Basler SLA750-60fm Camera (Basler Vision Technologies, Ahrensburg, Germany). Whole-cell patch clamp recordings in voltage-clamp were carried out using the same internal solution and recording electrodes as described for cultured neurons, except for supplementation of the recording solution with 2 mM Lucifer Yellow CH dipotassium salt in initial experiments, to allow *post-hoc* confocal imaging and identification of the morphology for the recorded neurons in fixed (4% PFA) slices. Membrane currents were filtered at 4

kHz (Bessel filter), digitised at 50 kHz (Digidata 1322A, Molecular Devices) and membrane voltage was clamped at -60mV using a MultiClamp 700A amplifier (Molecular Devices). For current clamp recordings a potassium-gluconate based internal solution was used consisting of: 130 mM K-Gluconate, 10 mM KCl, 10 mM HEPES, 10 mM Na_2-phosphocreatine, 0.2 mM EGTA, 4 mM Mg-ATP and 0.3 mM Na-GTP. All recordings were carried out at RT.

Slices were continuously perfused with aCSF (supplemented with 2 mM KA in voltage-clamp experiments, and without KA supplementation in the current-clamp experiments) and bubbled with 95% O_2 / 5% CO_2. Drugs were applied to cells via the bath perfusion subsequent to a stable period of recording in control solution. An equilibration period (1 min for bicuculline, 5 min for RO-60-0175 and 3 min for all other drugs) was allowed before acquiring any data. The access resistance, R_A, was monitored at regular intervals (i.e. every 3 min) and recordings were discarded if it changed by more than 25%. At the end of each set of recordings, 20 µM bicuculline was added to the cells to confirm that currents recorded were GABAergic and to reveal the extent of GABA-mediated tonic currents. For an initial selection of recordings, the electrode was carefully removed after the experiment to reduce damage to the cell and surrounding tissue and slices were fixed for the purpose of assessing cell morphology and localisation.

2.4.3 Data analysis

Voltage clamp

Synaptic events were analysed using WinWCP v4.7.6 and WinEDR v3.5.6 software (John Dempster, University of Strathclyde, UK). A spontaneous event was detected when the membrane current exceeded a threshold of 4-7 pA for 0.6 ms (compared to a baseline current averaged over 2 ms prior to the event). Exact parameters were individually adjusted for each recording and all detected events were subsequently manually screened and validated. For the purpose of kinetic analysis of spontaneous synaptic events, only clean, unfiltered events were chosen, i.e. events that had a fast rise-time (< 1.5 ms), a sharp peak and a steady decay without contamination from secondary events.

For each individual event, 10-90 % rise times were determined using WinWCP and decay times were calculated as event area divided by peak amplitude.

Tonic currents were measured as the average deflection of baseline (or drug-induced) holding current in the presence of 20 µM bicuculline using Clampfit version 10 (Molecular Devices). Holding currents were measured over 20-30 s of current traces, including synaptic events.

Changes in root mean square (RMS) current noise in the presence of bicuculline were used as another measure for tonic current. To this end, the RMS current noise was obtained using WinEDR v3.5.6 software (John Dempster) and averaged over 100 ms long epochs uncontaminated by synaptic events. Contaminated epochs were filtered and excluded using an automated process in Microsoft Excel by comparing the RMS noise to a user-defined threshold. Epochs exceeding the threshold value were excluded. The threshold was defined as a proportion of the median RMS noise over a 5 s epoch and adjusted for each cell.

Access resistance (R_A), membrane capacitance (C_m) and input resistance (R_{in}) were calculated from the average capacity transients evoked in response to a set of 20 x -10 mV voltage command steps (100 ms each, Figure 2.2) from holding (-60 mV). R_A was calculated as the command voltage (-10 mV) divided by the peak current deflection (I_{peak}). R_{in} was calculated as

$$R_{in} = \frac{-10\ mV}{I_{ss}} - R_A$$

where I_{ss} is the steady-state current deflection due to the voltage step. C_m was calculated as

$$C_m = \frac{\tau_{dec} * (R_{in} + R_A)}{R_{in} * R_A}$$

where τ_{dec} is the decay time of the capacitance transient (area/I_{peak}).

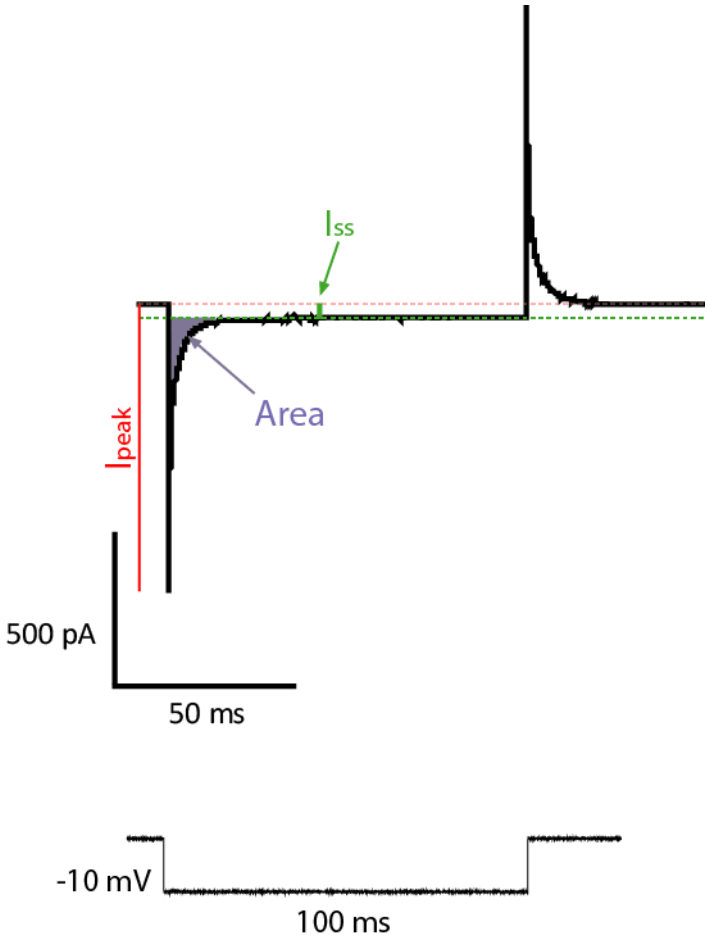

Figure 2.2: Capacity transients in response to a -10 mV voltage command step
Top, current trace showing representative average capacity transients in response to a negative voltage command of -10 mV (100 ms), bottom. I_{peak} is the peak amplitude of the current deflection. I_{ss} is the steady-state current deflection which is maintained for the duration of the voltage command. "Area" demarcates the area defined by the peak deflection of the current trace and I_{ss}.

Current clamp

Principal neurons recorded under current-clamp were characterised electrophysiologically using a set of constant current injection steps (-200 to +200 pA in 20 pA increments, with a duration of 200 ms, Figure 2.3). From this, the rheobase was defined as the minimal current injection necessary to elicit an AP and R_{in} was calculated as the change in membrane potential in response to a subthreshold current injection divided by the magnitude of that current (ie., $\Delta V/\Delta I$). Since this current step protocol did not lead to saturation of the AP firing rate, truncated forms of input-output curves (change in the number of spikes fired / change in the injected current) were generated from the data using OriginPro (version 9.1, OriginLab). Individual input-output curves

were then fitted using linear regression to compare values for the offset (x-axis intercept) and slope in the presence of different drugs. Only recordings from neurons with a stable membrane potential lower than -60 mV were accepted for analysis.

Neuronal excitability was assessed by depolarising neurons from their resting potential with a 1 s current-injection step above threshold (usually 200 pA, though the magnitude was adjusted based on the threshold for the first spike during the initial current step protocol, Figure 2.3). After this, a 30 s recovery period was allowed between consecutive current-injection steps. AP frequency was measured as the average inter-event-interval (IEI) between spikes elicited by a current injection step, and this value was averaged over at least 5 consecutive repeat recordings (i.e. a period of 2.5 min).

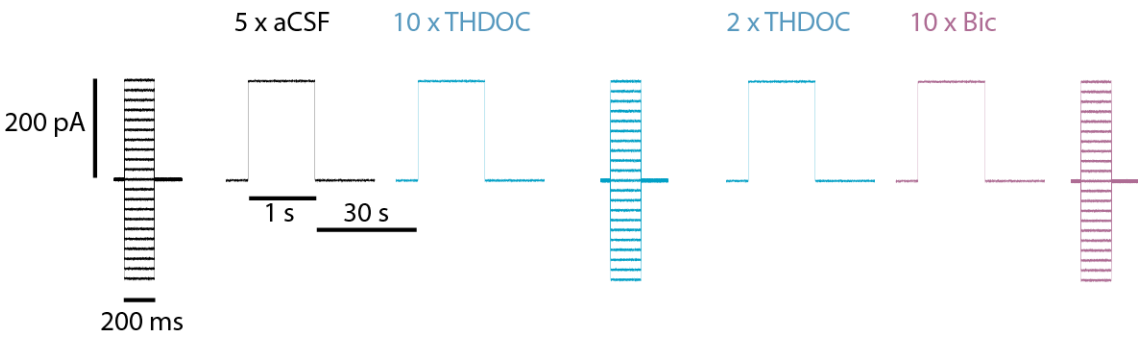

Figure 2.3: Current-step protocol used to assess cellular excitability
Spike threshold was assessed before each recording and after equilibration in each drug by applying brief consecutive current injections of 200 ms with increasing amplitude (-200 pA to + 200 pA). The excitability of cells following each drug exposure was subsequently measured by stimulating neurons with a current-injection step above threshold for 1 s (usually 200pA, but the magnitude was adjusted based on the first spike threshold during the initial current step protocol). The first 5 current injections were measured in aCSF, before applying the drug (in this example, THDOC). After 10 current injections in the presence of drug, the spike threshold was re-assessed using the same initial incremental current step protocol. Following this, a further two current injections were applied before changing to another drug. IEIs in the presence of drugs were measured over 5 current injections after an equilibration period appropriate for the drug. Each experiment ended with a total of 10 current injections in the presence of bicuculline (20 µM).

2.5 Immunocytochemistry and imaging

Neurons grown in culture were washed in warm (37°C) phosphate-buffered saline (PBS) supplemented with 1% bovine serum albumin (BSA) prior to fixation with pre-warmed (37°C) paraformaldehyde (PFA; 4% w/v in PBS) for 2 min at 37°C followed by 10 mins at RT. The fixative was removed through a series of three washing steps using PBS supplemented with 1% BSA. For staining of cell surface receptors, fixed cells were incubated for at least 30 min in a blocking solution consisting of 10% v/v normal goat serum (NGS) prior to incubating in primary antibody diluted to a working concentration (see table section 2.1.2) in 1% BSA in PBS for at least 1 hr. Coverslips were washed thoroughly with PBS, followed by an optional permeabilisation step in 0.1% Triton-X in PBS supplemented with 1% BSA for 10 min, in order to allow labelling of intracellular protein. If cells were permeabilised in this manner, two further washing steps followed in PBS before undergoing a second period of 30 min in blocking solution prior to incubating in the second primary antibody for at least 1 hr. Following another set of three washes in PBS, neurons were incubated in the appropriate combination of secondary antibodies diluted to working concentrations in PBS supplemented with 1% BSA, for 45 min. After a final set of washes in PBS, coverslips were mounted onto microscope slides using glycerol gelatine (Sigma) following another series of washing steps in PBS.

Brain slices previously used in electrophysiological recordings were fixed in 4% PFA in PBS overnight at 4˚C. Slices were subjected to two 15 min washes with gentle agitation in PBS prior to mounting onto microscope slides using Vectashield mounting medium (Vector Laboratories, Burlingame, California, USA).

All cells were imaged using a Zeiss Axioskop LSM 510 confocal microscope with either a Plan Neofluor 10x (Numerical aperture (NA) 0.3) differential interference contrast (DIC) or a 40× (NA 1.3) or 63x (NA 1.4) oil immersion DIC objective. The mid-optical confocal slice in the sample was chosen and imaged as a mean of four scans in 8-bit (i.e. 256 grayscales). For analysing $GABA_A$ receptor distribution within the cell, a set of slices was acquired as z-stacks spanning the cell body using a pinhole diameter of 1 airy unit (AU),

which optimises the signal-to-noise ratio, and optimal section thickness as determined by the operating software. Neurons filled with Lucifer yellow were imaged as z-stacks of 20-60 slices while opening the pinhole to 2-4 AU, to enable the detection of the weaker signal of this dye within the tissue of the brain slice. A 543-nm helium-neon laser (560 – 615 nm band pass filter), a 488-nm argon laser (505 – 530-nm band pass filter) and a 633-nm argon laser (638-798 nm band pass filter) were used for imaging AlexaFluor(AF)555/AF594 (excitation/emission peaks of 555/565 nm and 590/617 nm, respectively), AF488 (excitation/emission peaks of 496/516 nm) or neurons filled with Lucifer yellow (Sigma, excitation/emission peaks of 428/536 nm) and AF647 (excitation/emission peaks of 650/665 nm), respectively.

2.5.1 Image analysis

Images were analysed using Image J (version 1.49; Schneider et al., 2012). In detail, image files were imported into Image J and z-stacks were compiled using a maximum intensity projection. Green (488 nm, $GABA_AR$ α2 subunits), blue (633 nm, MAP2) and red (543 nm, AnkyrinG) channels were separated. Individual thresholds were set manually in the blue (MAP2) and red channels (AnkyrinG) in areas that matched the regions of interest (ROIs) for dendrites and soma, and the AIS, respectively (see Figure 2.4). Both area and mean signal intensity levels in the green channel were recorded for these ROIs. In addition, for each image an ROI was manually drawn in a cell-free area of the green channel to set the background intensity.

To select and analyse α2 subunit puncta, the green channel was processed to reduce background noise using a rolling ball background subtraction with a radius of 20 pixels. This method calculates the average background for a spherical region of the chosen radius around every pixel and subtracts that value from the original image (Sternberg, 1983). The image was subsequently converted into a binary image using Image J's "Auto Local Threshold" plugin with a Bernsen filter and 20 pixel diameter. The Bernsen filter calculates the threshold for each pixel using the local contrast in a circular area of the chosen diameter around the pixel. It compares the pixel's grey value to the midrange grey value of the surrounding area (for a review, see Sezgin, 2004). Punctate α2 subunit

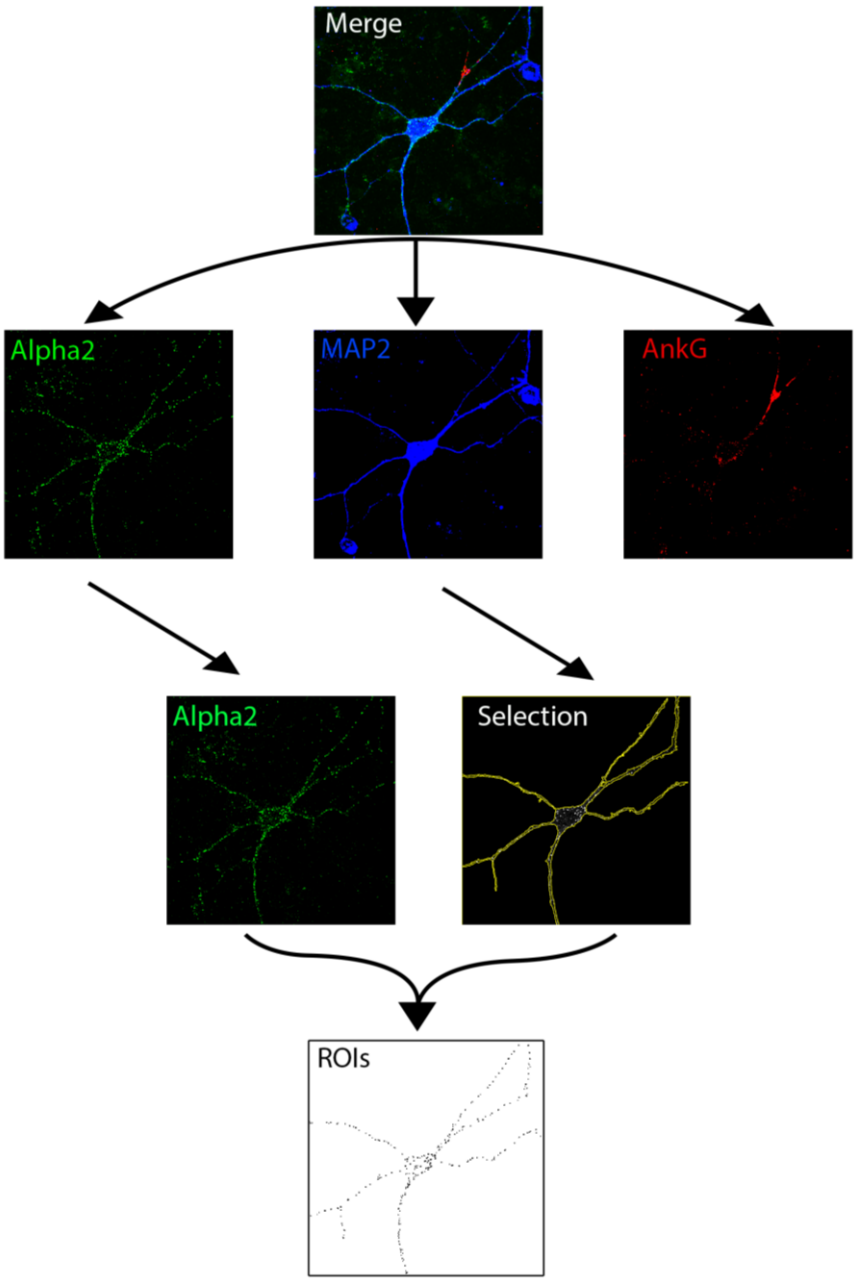

Figure 2.4: Procedure for image analysis of antibody labelled cultures
To assess the effects of D4 receptor activation on $GABA_A$ subunit localisation, cultured neurons were treated and imaged as described in the text and files were imported into Image J for further processing. Z-stacks were compiled using a maximum intensity projection. Green (α2 subunits), blue (MAP2) and red (AnkyrinG) channels were separated. MAP2 labelling was used to select dendrites and soma, and AnkyinG was used to select the AIS. The green channel was processed to reduce background noise and punctate α2 structures within each of the ROIs were detected and analysed using Image J's "Particle Analysis" plugin. This data was imported into Excel for further analysis and presentation.

structures within each ROI (dendrites, soma and AIS) were detected and analysed using Image J's "Particle Analysis" plugin. Particles smaller than 0.01 pixels in diameter were regarded to represent 'salt and pepper' noise and excluded from the analysis. This cut-off diameter was chosen arbitrarily. Information obtained in this manner contained the number of particles and their mean intensity. Data thus obtained was imported into Excel for further analysis and presentation. The α2 subunit particle density was obtained by dividing the number of particles by the area of the ROI and the background noise was subtracted from their intensity level.

2.6 Western Blots

Cultured neurons that were used for cell lysates were grown on PDL-coated 6 cm dishes at a density of 3 – 5 x 10^6 cells per dish. Samples were then placed on ice and washed once with cold PBS, before being dissociated from the surface using 300 µl radio-immunoprecipitation assay (RIPA) lysis buffer (150 mM NaCl, 50 mM Tris pH 8.09, 5 mM EDTA, 1% NP40 (v/v), 0.5% DOC (w/v), 0.1% SDS (w/v), 1mM phenylmethylsulfonyl fluoride (PMSF), 1x protease inhibitor cocktail) and collected in a clean Eppendorf tube. Cells were then incubated at 4^{o}C for 1 hr with mild agitation and subsequently spun down at 13,000 RPM at 4 ^{o}C for 15 min. The supernatant was transferred into a fresh tube and protein concentration was determined spectrophotometrically (Bio-Rad SmartSpec Plus, Bio-Rad Laboratories) using a bicinchoninic acid (BCA) assay (Thermo Fisher Scientific).

For tissue lysates, the brain structure of interest was dissected and homogenised in RIPA buffer using a glass pipette homogeniser. Tissue homogenates were then collected on dry ice until frozen, thawed on ice and subsequently spun down at 13,000 RPM at 4 ^{o}C for 15 min. The supernatant was removed to a clean tube and the freeze-thaw cycle was repeated once more before determining protein concentration of the final supernatant using a BCA assay.

An appropriate amount of 3x sample buffer (150 mM Tris-Cl pH 6.8, 6% SDS (w/v), 0.3% bromophenol blue (w/v), 30% glycerol (w/v), 15% β-mercaptoethanol (v/v)) was added to the protein extract and heated to 95 °C for 5 min, prior to loading 50 µg onto a 10% SDS (w/v) gel and subsequent separation using gel electrophoresis (Mini-Protean Tetra Cell, Bio-Rad). The sample was then transferred onto a nitrocellulose membrane (Hybond C Extra, Amersham Biosciences, Buckinghamshire, UK) using an XCell SureLock electrophoresis cell (Thermo Fisher Scientific) and the presence of protein was confirmed using Ponceau staining.

Membranes were blocked using 4% dry milk (w/v) or 6% bovine serum albumin (w/v) in PBS with 1% Tween-20 (PBST) for 30 min – 1 hr. Primary antibodies were diluted to their working concentrations (see table in section 2.1.2) in the respective blocking buffer and membranes were incubated at 4°C with mild agitation overnight. This was followed by three 20 min washing steps in blocking buffer and a 2 hr long incubation in secondary antibody coupled to horseradish peroxidase (HRP) in blocking buffer. The membranes were finally washed 3x for 20 min in PBST. Signals were detected using SuperSignal West Pico or West Femto Chemiluminescent Substrate (Thermo Scientific) and developed using the ImageQuant LAS 4000 Mini digital imaging system (GE Healthcare Biosciences AB, Uppsala, Sweden).

2.7 Statistics

Statistical analysis was carried out using GraphPad InStat software (Version 3.06, GraphPad Software Inc., La Jolla, CA, USA) and SPSS Statistics 22 (IBM, Armonk, New York, USA). Data were checked for a normalised distribution using a Kolmogorov-Smirnov test. If data were not normally distributed, a transformation (i.e. comparing the log or reciprocal of the values) was first attempted. Only if transformation was not successful in normalising the distribution of data were non-parametric tests used. For pairwise comparisons of normally distributed data, two-tailed Student's t-test was applied. Only where a presumption about the direction of the difference between the means could rightfully be made and confirmed, were one-tailed t-tests used. In the case

of normally distributed data whose standard deviations vary significantly from one another (assessed using an F test), the t-test is prone to type I errors, i.e. detecting false positives. The reason for this is that it pools the standard deviations of both samples. A Welch-corrected t-test avoids this issue by making no assumption about the equality of variance of the datasets (Ruxton, 2006), and hence this test was used in those cases. For pairwise comparisons of non-normal data, the Mann-Whitney test was used, which, rather than comparing means of populations, ranks values in both datasets according to their size and compares the means of those ranks (Sheskin, 2007).
When comparing dependent, i.e. paired variables, a paired t-test was used for normally distributed data and the Wilcoxon matched pairs test was used for non-normal data. This method computes the difference between each paired set, ranks them and then compares the sum of ranks (Sheskin, 2007).

When comparing more than two unpaired datasets, a one-way analysis of variance (ANOVA) or Kruskal-Wallis test was used for normally distributed or non-normal data, respectively. These test whether the difference between the means (or the sum of ranks for the Kruskal-Wallis test) of the datasets can be explained by random sampling. In case of a rejection of the null-hypothesis, i.e. a significant difference between the means (or sum of ranks) at the 5% margin, *post-hoc* pairwise comparisons were carried out. To correct for type I errors, which are more likely to occur in multiple comparisons, the Bonferroni correction was used for pairwise comparisons of more than three datasets. The Bonferroni correction uses a family-wise error, i.e. it multiplies the threshold of significance by the number of comparisons made, thus reducing the risk of type I errors (Sheskin, 2007). However, it should be noted that if the comparisons are not independent from one another (e.g. when comparing A to B and A to C), the Bonferroni correction is more prone towards type II errors, i.e. false negatives.

3 Dopaminergic modulation of GABAergic inhibition in PFC

3.1 Introduction

Dopamine (DA) is a powerful modulator of CNS networks and it plays an essential role in reward circuits and as such is important in learning (Schultz, 1997) and is involved in the addictive properties of drugs of abuse (Di Chiara and Imperato, 1988). In the PFC, dopaminergic signalling is a key component of normal cortical function such as working memory (Seamans and Yang, 2004; Yang et al., 1999). The modulatory function of dopaminergic signalling comprises long-term changes in plasticity by altering gene expression, as well as more immediate effects on neuronal communication by changing cellular transmission, excitability and sensitivity to neurotransmitter receptors (reviewed in Tritsch and Sabatini, 2012). Dopaminergic input into the cortex mainly stems from mesocortical dopaminergic neurons based in the VTA. In the rodent brain, these mainly project to the cingulate, entorhinal and medial prefrontal cortices (see Seamans and Yang, 2004 for a review). The deep layers V-VI receive the most dense mesocortical inputs, which have been shown to form symmetric synapses onto somata, dendritic shafts and spines of pyramidal neurons (Goldman-Rakic et al., 1989). The resulting dopaminergic control over a wide range of synaptic inputs onto prefrontal PCs potentially places DA as a powerful regulator of cognitive function. Consequently, dysfunction of prefrontal DA signalling has been linked to a plethora of psychological conditions, such as schizophrenia, addiction and attention-deficit hyperactivity disorder (reviewed in Arnsten et al., 2015).

3.1.1 Dopamine receptor signalling and distribution

DA receptors are GPCRs. The five currently identified subtypes are classified into two families, the D1-like (includes D1 and D5, D1 being the most prominent) and D2-like (D2, D3 and D4, D2 being the most prominent; Alexander et al., 2011). D1-like receptors are coupled to G_S, which activates the cyclic adenosine monophosphate (cAMP)-dependent signalling pathway and are generally thought to mediate excitatory transmission. D2-like receptors, on the other hand, are coupled to G_i, which inhibits the cAMP pathway,

and mediate inhibitory neurotransmission (see reviews Girault and Greengard, 2004; Tarazi et al., 2004). In addition, D2-like (and to some extent D1-like) receptors can modulate intracellular calcium levels, protein trafficking or ion channel gating either directly through the $G_{\beta\gamma}$-subunit or through activation of phospholipase C (PLC) (reviewed in Tritsch and Sabatini, 2012). An example is the coupling of D2-like receptors to GIRKs, which has been explored in *Xenopus* oocyte expression systems (Pillai et al., 1998) and was also found in dopaminergic midbrain neurons, where it elicits an inhibitory postsynaptic current (Beckstead et al., 2004).

D1-like receptors are expressed in structures such as the caudate-putamen, NAcc and SN (Wamsley et al., 1992). In the PFC, DA receptors are expressed throughout layers II-VI, most prominently in the deeper layers, coinciding with the main dopaminergic inputs onto the PFC. D1-like receptors are more abundant than D2-like receptors and they are expressed on both PCs and GABAergic interneurons. D1 receptors show a proportionately stronger expression in interneurons compared to PCs (Santana et al., 2008), most of which are PV-expressing interneurons (Le Moine and Gaspar, 1998).

D2-like receptors are found throughout the cortex, with the highest concentrations detected in the PFC (Lidow et al., 1989). In the mPFC, D2 receptors are most strongly expressed on layer V PCs and, to a lesser extent, on layer V GABAergic interneurons as well as layer VI PCs and interneurons (Santana et al., 2008). While both, D1 and D2 receptors, are evenly expressed in the deep layer V, D1 receptors are much more prominent in layers II/III and in layer VI compared to D2 receptors (Santana et al., 2008). This heterogeneous expression pattern of DA receptor subtypes underlies difficulties in delineating specific functions of different dopaminergic inputs and is reflected in the multitude of effects DA exerts on PFC function, as described below.

3.1.2 Functional effects of dopamine in the PFC

On a behavioural level, DA signalling is believed to play a vital role in modulating PFC functions. Pioneering work by Goldman-Rakic showed that the impact of dorsolateral PFC (dlPFC) depletion of dopamine is almost as severe on delayed-response tasks (a

behavioural test where a delay is interposed between cue presentation and response, to test working memory processes) as removing the PFC altogether (Brozoski et al., 1979). Other research has continued to show elevated DA levels during memory acquisition and retrieval tasks, and found that disruptions of DA signalling, in particular D1-like receptors, decreases working memory task performance (Seamans and Yang, 2004).

The exact underlying cellular mechanisms behind these observations, however, are difficult to define, due to the differential effects on cortical cell excitability mediated by DA (Yang et al., 1999). There are a number of key factors determining the net direction of DA effects on PCs (reviewed in Seamans and Yang, 2004). Amongst these are biphasic effects of DA (producing an initial reduction in IPSC amplitude, followed by a delayed increase; Seamans et al., 2001) as well as the involvement of different signalling pathways, which are activated either by different DA receptor subtypes or by the same receptor but the signalling effect varying with intracellular Ca^{2+}-states (Seamans and Yang, 2004; Tarazi et al., 2004).

The PFC encompasses a range of different types of PCs (Wang et al., 2006), which receive different inputs and express different DA receptor subtypes, adding complexity to DA's action. DA can also act in a target specific manner at different synapses from the same cell. In layer V of the ferret PFC, for example, DA depresses excitatory transmission between PCs (Gao et al., 2001) while enhancing excitation at PC synapses onto fast-spiking (FS) interneurons (Gao and Goldman-Rakic, 2003). To add to the complexity, DA can modulate PC excitability both directly and indirectly through GABAergic interneurons (Gorelova et al., 2002; Tseng et al., 2007; Zhou and Hablitz, 1999a). In the PFC, D1 and D2 receptors have been shown to decrease GABA release onto FS interneurons and PCs (reviewed in Tritsch and Sabatini, 2012). In addition to GABA, DA can also modulate the release of other neurotransmitters such as glutamate and acetylcholine (Tritsch and Sabatini, 2012). The net effect of DA can furthermore vary with development, membrane potential, network activity and the concentration of DA (see Seamans and Yang, 2004 for a review).

While the evidence presented here is not an exhaustive account of the scope of prefrontal dopaminergic function, it gives an impression of its vital role in modulating and tuning circuit function and touches upon some of the difficulties ongoing research encounters.

3.1.3 Dopaminergic modulation of GABA transmission

While DA receptors can directly affect pyramidal neuron activity, many of their functions are relayed indirectly via GABAergic interneurons. For example, dopaminergic excitation of VTA DA neurons is mediated via an inhibition of GABAergic interneurons, called the "inhibition gate" (Michaeli and Yaka, 2010). In the PFC, GABAergic inhibition can shape the modulatory action of DA, which has been shown by a reversal in DA effect from inhibitory to excitatory upon $GABA_AR$ blockage (Zhou and Hablitz, 1999a). More research elucidating the interplay of DA and GABAergic inhibition in the PFC has been conducted over the last decade and continues to be a topic of interest (Gao et al., 2003; Gorelova et al., 2002; Graziane et al., 2009; Wang et al., 2002; Zhong and Yan, 2014). For example, similar to the reported bidirectional effects on PC excitability, DA has been found to both increase and decrease GABAergic inhibition in the PFC, depending on DA receptor subtype and the cortical layer (Seamans and Yang, 2004). In addition, dopaminergic modulation of inhibition in the PFC has been shown to be dependent on the developmental stage of the animal (Gorelova et al., 2002; Paul et al., 2013; Tseng and O'Donnell, 2007) and can vary with the stimulating input (Paul et al., 2013) or postsynaptic target (Gao et al., 2003). Furthermore, the effects of DA on GABAergic inhibition can be presynaptic (i.e. an increase or decrease in GABA release via a change in interneuron excitability, see (Tritsch and Sabatini, 2012; Tseng and O'Donnell, 2007) or postsynaptic (via a direct modulation of postsynaptic $GABA_ARs$ see Graziane et al., 2009; Li et al., 2012; Wang et al., 2002). Interestingly, DA receptors are mainly depolarising on FS interneurons, which innervate the perisomatic region and AIS, while having little effect on other interneuron subtypes in rat PFC (Gorelova et al., 2002). This may have implications for a network-modulating effect of DA, given the role of FS interneurons in synchronising and modulating firing patterns (Cobb et al., 1995; Whittington and Traub, 2003).

3.1.4 D4 receptors are linked to psychiatric conditions and modulate $GABA_AR$ expression

D4 is a member of the D2-type receptor family and is highly expressed in PFC interneurons and PCs (Mrzljak et al., 1996) and is enriched in rodent cortical layers III-VI (Ariano et al., 1997). It is widely suggested that D4 plays a role in cognitive function and it has been implicated in the pathologies underlying neuropsychiatric disease (Furth et al., 2013; Oak et al., 2000; Sanyal and Van Tol, 1997; Tarazi et al., 2004). For example, it is targeted in certain treatments for schizophrenia due to its higher sensitivity to the antipsychotic drug clozapine (Van Tol et al., 1991), and due to the increased expression of D4 found in schizophrenic patients (Seeman et al., 1993 - other studies, however, have not confirmed this, see Tarazi et al, 2004). In addition, D4 receptor expression has been shown to be upregulated in response to treatment with various antipsychotic drugs (Tarazi et al., 2004). Besides schizophrenia, D4 variants have also been linked to attention deficit hyperactivity disorder (Li et al., 2006) and D4 receptors have been suggested to play an important role in working memory due to impairments observed in performance in memory tasks after treatment with the D4 antagonist L-745,870 (Zhang et al., 2004). More recent research is investigating a possible involvement of D4 receptors in the regulation of sleep-wake states (Nakazawa et al., 2015) and in treatments for the management of cocaine addiction (Bergman and Rheingold, 2015).

Since GABAergic inhibition is one of the main recipients of dopaminergic modulation in the PFC, and since there is evidence for its involvement in many of the same pathological conditions, studying D4-mediated modulation on GABAergic inhibition is of particular interest. It has previously been shown that activation of the D4 receptor reduces GABAergic transmission in cortical slice preparations (Graziane et al., 2009; Wang et al., 2002) and cortical cultures (Graziane et al., 2009; Li et al., 2012) via a postsynaptic mechanism down-regulating $GABA_AR$ surface expression (see Figure 3.1 for a schematic model). The $GABA_AR$ down-regulation induced by D4 receptor activation has been linked to activation of the PKA/PPI pathway (Wang et al., 2002) and is mediated via a cofilin/actin-dependent mechanism (Graziane et al., 2009). However, it has not been elucidated whether D4 preferentially affects specific isoforms of $GABA_ARs$.

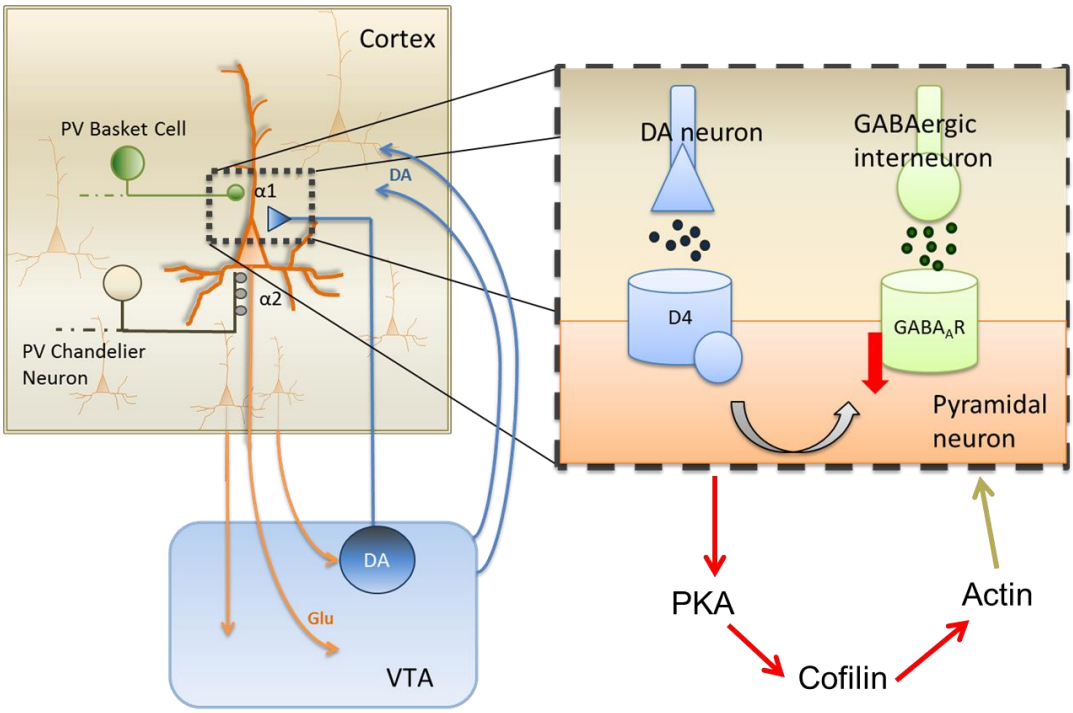

Figure 3.1: Dopaminergic modulation of principal cell output in the PFC
Model depicting cortical PC innervation by different inputs and indicating differential distribution of GABA$_A$Rs containing the α1 and α2 subunits on the cell's surface (Fritschy and Möhler, 1995; Nusser et al., 1996b). The box on the right highlights a postsynaptic mechanism for downregulation of GABA$_A$Rs via D4 receptors as previous research has shown (Graziane et al., 2009; Li et al., 2012; Wang et al., 2002). PCs in the cortex receive inputs regulating their excitation, amongst them dopaminergic signals from the VTA. In turn, they send glutamatergic projections to the VTA, affecting dopamine release (Carr and Sesack, 2000). GABAergic interneurons play a crucial role in balancing this interaction and their impairment has been implicated in psychiatric disease (Lewis, 2011). Two types of fast-spiking, PV-positive interneurons are displayed here: Basket cells, which mainly synapse onto the PC soma and proximal dendrites (Armstrong and Soltesz, 2011), and Chandelier cells, which are known to innervate the AIS (Somogyi, 1977).

3.1.5 Objectives

The objective in this chapter was to explore how dopaminergic pathway signalling affects surface GABA$_A$R expression in the PFC by studying the underlying mechanisms and exploring GABA$_A$R isoform target specificity. In particular, α2-GABA$_A$Rs have been linked to CNS disorders (Engin et al., 2012) and recent research in mouse models has shown that disruption of α2 subunit clustering impacts γ-oscillations and induces cognitive deficits similar to those seen in schizophrenia (Hines et al., 2013). Due to these

findings, as well as their relative enrichment at the AIS, α2 containing $GABA_A$Rs were the main focus of this project. To this end, we focused on pyramidal neurons in PFC cultures as well as in layer II/III of acute PFC slices to elucidate the effects of DA on inhibitory transmission using a combination of electrophysiological, imaging and biochemical techniques.

Primary cortical cultures were established and characterised in terms of expression of different $GABA_A$R subtypes as well as their response to neuromodulators, and the properties of GABA-mediated inhibition in those cultures were investigated. Furthermore, effects of D4 receptor activation on $GABA_A$R subunit surface expression in different subcellular compartments have been probed in cell cultures. Simultaneously, acute PFC slice preparations have been used to investigate the previously described electrophysiological effects of D4 receptor activation on GABAergic transmission (Graziane et al., 2009; Li et al., 2012).

3.2 Results

3.2.1 Establishment and characterisation of primary cortical cultures

Initially, a primary culture of PFC neurons was established from E18 rat embryos as the basis for all experimental procedures. PFC neurons were successfully cultured using an established lab protocol for hippocampal primary cultures (Hannan et al, 2011).

Presence of tonic and phasic GABAergic transmission.

To assess whether cultures had indeed formed active networks and to determine the properties of their GABAergic transmission, currents were recorded from pyramidal-shaped neurons of cultures at DIV 10-21 using whole-cell voltage clamp (see Materials & Methods). The presence of tonic currents, which are mainly attributable to extrasynaptic $GABA_A$Rs containing αβδ or α5βγ subunits (reviewed in Mody and Pearce, 2004), was assessed by applying 20 µM bicuculline, which is sufficient to block the activity of all cell surface $GABA_A$Rs. The revealed shift in holding current (29.5 ± 5.5 pA, Figure 3.2 A1 & A2) confirmed the presence of a tonic current mediated by extrasynaptic $GABA_A$Rs.

To explore the properties of native $GABA_A$Rs, a series of GABA concentrations were applied (see Materials & Methods) and a half-maximally effective concentration (EC_{50}) of 8.9 ± 1.9 µM (n = 3) was determined from the concentration-response curves (Figure 3.2 C). Next, intrinsic GABAergic synaptic activity was assessed by recording synaptic responses to spontaneous GABA release in the presence of 2 mM KA, which non-specifically blocks ionotropic glutamate receptors (Elmslie and Yoshikami, 1985). Neurons received spontaneous inhibitory synaptic inputs (sIPSCs) with a relatively low mean frequency of 1.7 ± 0.3 Hz (Figure 3.2 B). In the same population of synaptic events, average peak amplitudes measured -96.2 ± 9.7 pA (calculated from >1000 detected events in 7 cells), with a mean decay time of 25.4 ± 0.5 ms and mean rise time of 2.4 ± 0.1 ms (see Figure 3.2 B; both calculated from 264 selected 'clean' events from 7 cells). In summary, these results show that cortical neurons form active networks and show intrinsic GABAergic transmission after 10 days in culture.

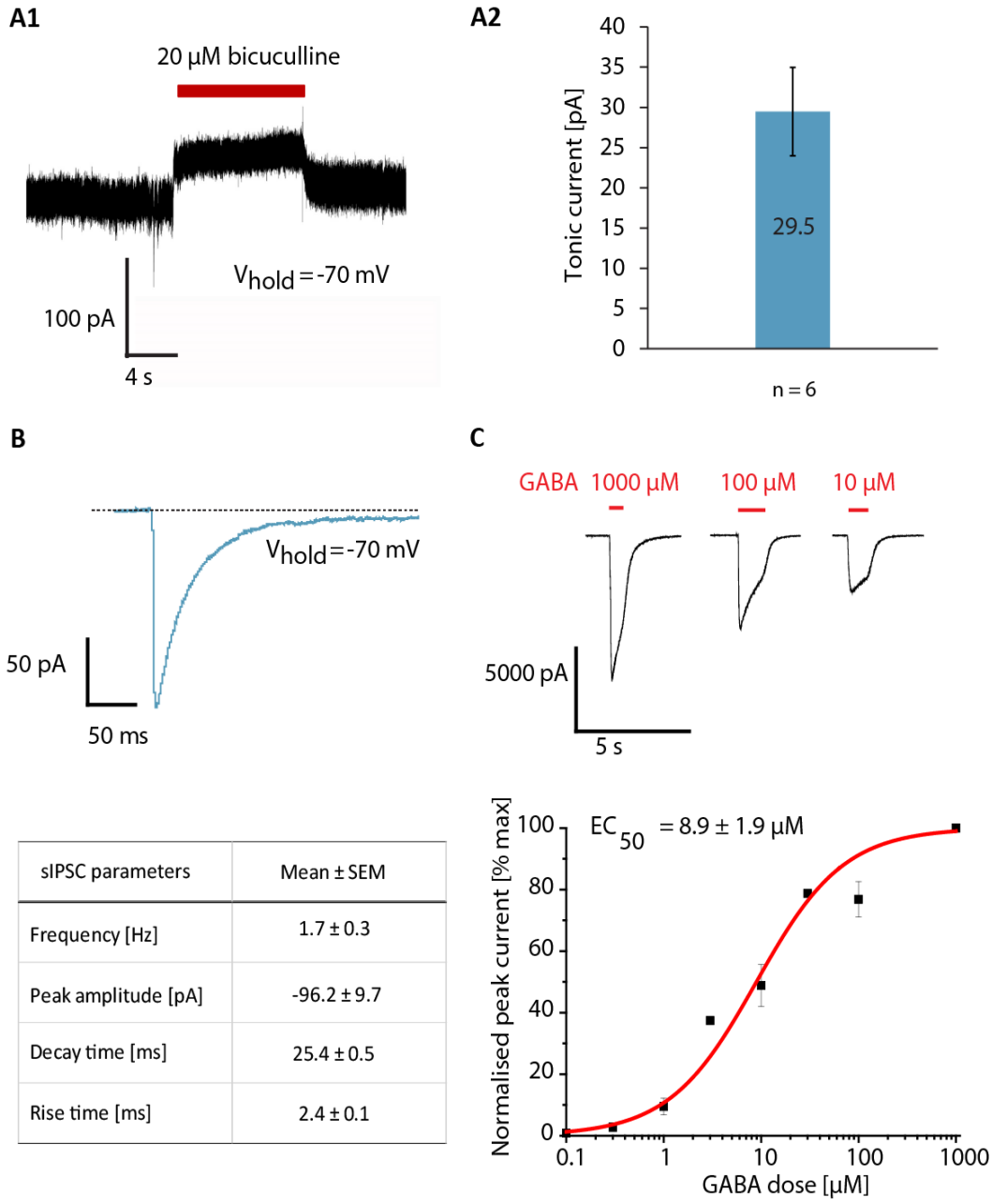

sIPSC parameters	Mean ± SEM
Frequency [Hz]	1.7 ± 0.3
Peak amplitude [pA]	-96.2 ± 9.7
Decay time [ms]	25.4 ± 0.5
Rise time [ms]	2.4 ± 0.1

Figure 3.2 Inhibitory properties of cultured PFC neurons

A1. Example of a tonic current revealed by 20 µM bicuculline, applied through a "U-Tube" (see Materials & Methods). **A2**. Average size of tonic currents; n = 6. Error bars represent standard error of the mean (SEM). **B**. representative averaged spontaneous GABAergic event recorded in the presence of 2 mM KA, generated from 264 selected 'clean' events from one neuron. Table presents frequency and amplitude (calculated from all events) and decay and rise times (calculated from a subset of events, see Materials & Methods; n = 7 neurons, DIV 11-21). **C**. Top: Representative GABA currents in response to U-tube applications of GABA at varying concentrations. Bottom: GABA concentration response curve, n = 3. All recordings carried out in cultured primary PFC neurons at DIV 10 – 20 in the presence of 2 mM KA.

Developmental change in α1- and α2- $GABA_A$Rs in PFC cultures and presence at the AIS

$GABA_A$R subunit expression is known to vary with subcellular localisation (Klausberger et al., 2002; Nusser et al., 1996b) and can also change during development (Dunning et al., 1999; Möhler et al., 2004; Tarazi and Baldessarini, 2000). Together with evidence showing that synapses in cultured neurons only reach maturity after at least two weeks in *vitro* (Kraszewski and Grantyn, 1992), this prompted us to assess the change in expression of α1 and α2 subunits over time in culture. In addition to this, we also wished to establish whether enrichment of α2 subunits at the AIS (Nusser et al., 1996b) was occurring in the primary culture used here.

To verify the presence of the receptor subunits in question and to determine if any developmental changes in expression occurred, protein expression was determined using Western Blots (WBs). To this end, neurons were cultured for different durations (4, 10, 17, 25 DIV) before harvesting. Total protein content was probed for $GABA_A$R α1 and α2 subunits using standard WB techniques (see Materials & Methods). The WBs revealed that $GABA_A$R α1 increased between DIV 4-10 and DIV 17 - 25 ($P = 0.05$, one-tailed Welch-corrected t-test), whereas α2 subunits were more or less stably expressed over this period (Figure 3.3 A1 & A2). To complement the WB results, neurons were grown in culture for 2-4 weeks before fixation and permeabilisation in methanol or acetone and subsequent labelling of target proteins using immunocytochemistry (ICC) as described in the Materials & Methods section. Both $GABA_A$R α1 and α2 subunits were expressed in punctate structures along the soma and dendritic tree (Figure 3.3 B1) and total somatic surface labelling appeared to increase between weeks two and four (Figure 3.3 B2, $P = 0.04$, $P=0.02$, respectively, Mann-Whitney test). This difference in ability to detect changes in α2 or α1 subunit expression in WBs or ICC, respectively, may stem from a variation in groups of neurons targeted by either technique: while WBs probe the entire cellular population of the extracted PFC (including interneurons, PCs and astrocytes), ICC allowed more specific targeting of pyramidal shaped neurons.

Co-labelling of cultured neurons for α1 or α2 subunits and ankyrin G (AnkG), a scaffold protein that is expressed at the AIS (Kordeli et al., 1995), was used to assess the relative

expression of α1 and α2 subunits in this membrane domain (Figure 3.3 C). To compare the relative subunit enrichment at the AIS, signal intensities measured in this area were normalised to somatic signal strength to account for variations in antibody efficiency and total neuronal expression. As previous research suggested (Nusser et al., 1996b), normalised α2 subunit labelling was stronger at the AIS compared to α1 labelling (P = 0.0002, unpaired t-test; Figure 3.3 C).

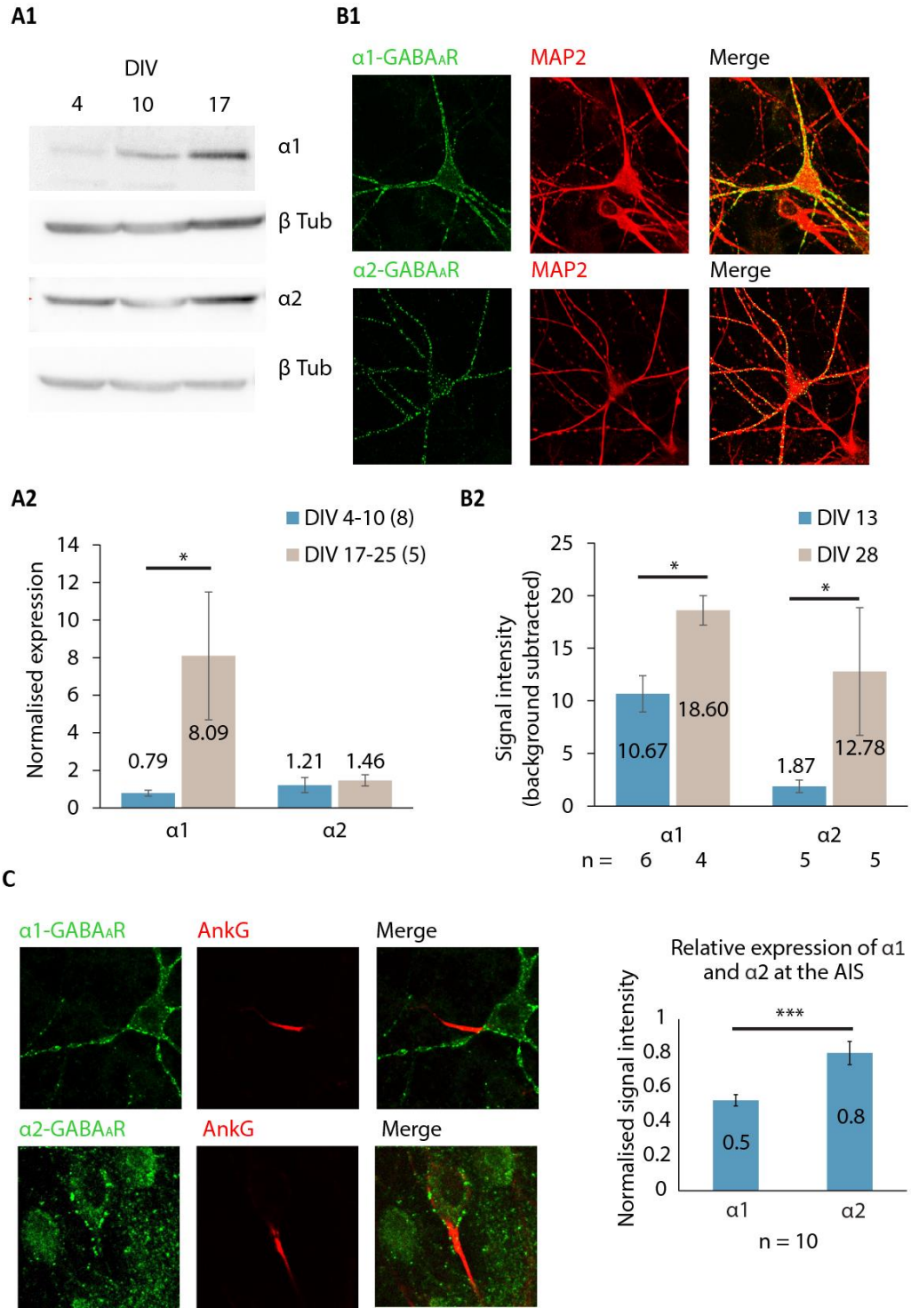

Figure 3.3 Varying expression levels of α1- and α2-$GABA_A$Rs in cultured PFC neurons of different ages
A1. Sample WBs showing α1 (row 1) and α2 (row 3) protein expression in whole cell lysates of primary PFC neurons after different durations in culture. Row 2 and 4 show respective loading controls using β-tubulin (β-Tub). **A2**. Expression of α1 and α2 subunits obtained from 5 (DIV 17-25) or 8 (DIV 4-10) WBs, normalised to β-tubulin control. Data for weeks one and two as well as weeks three and four were pooled into two groups. * - $P < 0.05$, one-tailed Welch-corrected t-test. **B1**. Representative images showing whole-cell expression of $GABA_A$R α1 and $GABA_A$R α2 relative to the somato-dendritic marker MAP2 in primary PFC neurons at DIV 28. PFC neurons were fixed and permeabilised using methanol and immunolabelled using primary antibodies directed against MAP2 and either α1 or α2 subunits. Secondary antibodies used were coupled to AlexaFluor594 (red) or AlexaFluor488 (green). **B2**. Quantified background-subtracted immunolabelling of somatic α1 and α2 in cultured PFC neurons fixed at different ages. * - $P < 0.05$, one-tailed t-test. **C.** Left: Representative images showing $GABA_A$R α1 and $GABA_A$R α2 expression relative to the AIS (AnkG) in a primary PFC neuron at DIV 28. Right: Quantified immunofluorescent signal strengths at the AIS normalized to somatic signal intensity. *** - $P < 0.001$ unpaired t-test. Error bars represent SEM.

Since the PFC cultures prepared in this study were grown in the absence of subcortical dopaminergic input, D4 receptor surface expression may have been affected. To ascertain if D4 receptors were present in our cell culture, neurons were fixed and immunolabelled as described above. Staining of permeabilised cells for D4 receptor revealed a punctate distribution throughout the soma and dendrites (Figure 3.4 A). Furthermore, WBs of whole cell lysates of rat PFC were positive for D4 receptor and showed an increased expression over the first three weeks in culture (Figure 3.4 B). Since both these methods did not allow assessment of the surface expression of functional D4 receptor, whole-cell patch clamp recordings using a high K^+ internal solution (140 mM) were carried out to detect the activation of GIRKs by D4 receptors (Pillai et al., 1998). Under physiological conditions, the resting membrane potential is more positive with respect to the equilibrium potential for K^+. Activation of D4 receptor should therefore lead to the opening of GIRKs, resulting in an efflux of K^+ out of the cell, consistent with a hyperpolarising effect. Consistent with this, recording from cultured PFC neurons using a high K^+ internal solution, the application of 30 µM PD168077, a D4 agonist with 400-fold selectivity over D2 and 300-fold selectivity over D3 receptors (Glase et al., 1997), evoked an outward current (Figure 3.4 C), while simple application of external recording

solution without PD168077 did not elicit this response [data not shown]. This indicates the presence of functional D4 receptors on the cell surface that couple to GIRKs.

In summary, these results indicate that $GABA_A$ receptor α1 and α2 subunits, and D4 receptors, are expressed in cultured cortical neurons and that they are functional. Furthermore, their expression levels increase significantly for at least the first three weeks in culture.

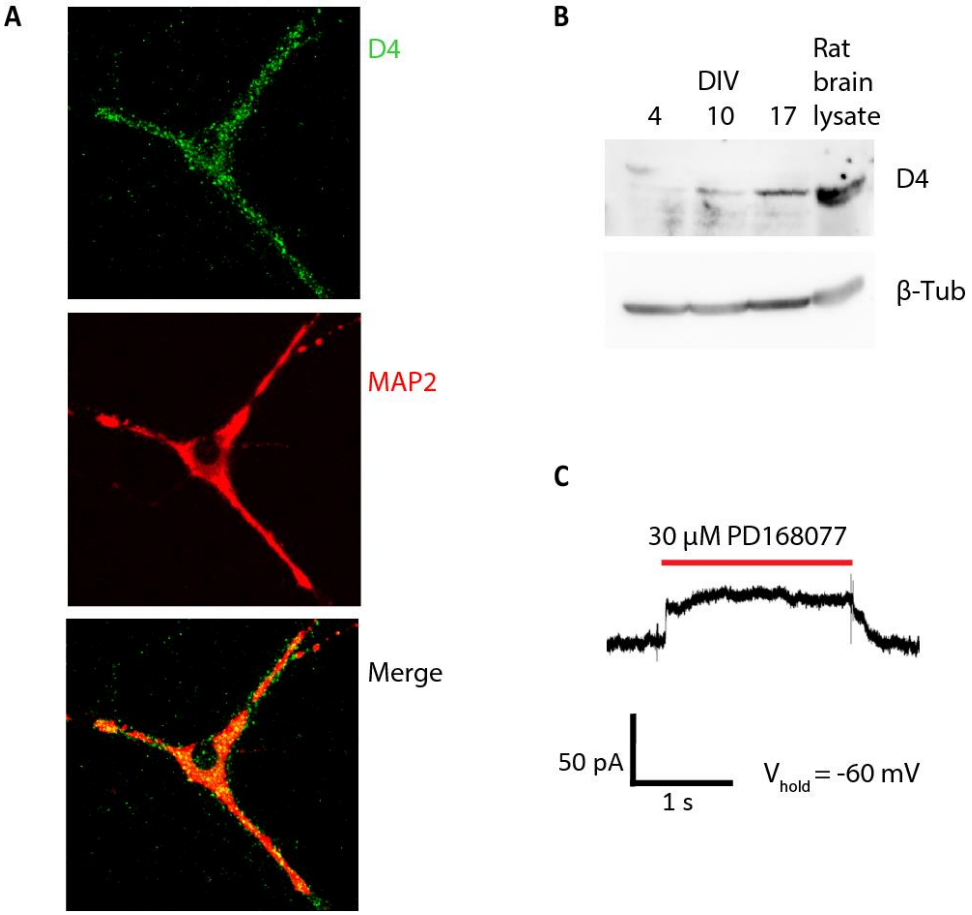

Figure 3.4: Primary cortical cultures expression of D4 receptors
A. Representative labelling of a primary cultured cortical neuron at DIV 19 for the expression of D4 receptors. **B.** Representative WB showing D4 receptor expression in cortical culture lysate from DIV 10 onwards. Last lane shows protein expression in rat whole brain lysate as a positive control. Bottom row: β-tubulin loading control. **C.** Outward current evoked in a DIV 11 neuron by the application of the selective D4 receptor agonist, PD168077 (30 µM).

3.2.2 Activation of D4 receptors has no effect on postsynaptic GABAergic inhibition

Next, we sought to expand on previous observations showing a decrease in GABAergic inhibition in mPFC PCs in the presence of the D4 receptor agonist, PD168077 (Graziane et al., 2009; Wang et al., 2002). While these studies had shown a reduction in mIPSC amplitude as well as reduced surface expression of $GABA_A$Rs, we wanted to assess whether the effect was mediated via specific $GABA_A$R subtypes, with a particular focus on α2-containing $GABA_A$Rs. Initially, we endeavoured to confirm their previous results.

In order to evaluate the effect of D4 receptor activation on GABAergic inhibition, 30 µM PD168077 was applied to cultured PFC neurons (DIV 14) in the presence of 2 mM KA (Figure 3.5 A & B) to block ionotropic glutamatergic receptors. sIPSC frequency and amplitude in PD168077 were measured and compared to a control recording period in Krebs. There was no significant effect of PD168077 on either sIPSC frequency or amplitude (Figure 3.5 A & B). However, the frequency in those recordings was noticeably low. To improve the resolution of the recordings, since there is evidence for an increase in GABAergic transmission in CNQX, another blocker of AMPA receptors (Brickley et al., 2001), the effect of PD168077 was assessed after replacing KA with a combination of CNQX and APV (to block NMDARs).

When 30 µM PD168077 was applied to cultured PFC neurons (DIV 12-20) in the presence of 10 µM CNQX and 20 µM APV (Figure 3.5 C & D), neurons did indeed show much larger sIPSC frequencies. However, as before, the results showed no significant effect of D4 receptor activation on frequency or peak amplitude of sIPSCs.

Since previous work had examined mIPSCs (Graziane et al., 2009; Wang et al., 2002), we reasoned that variability in action potential-driven GABA-release might mask a D4 receptor effect on sIPSCs. Therefore, action-potential generation was blocked by supplementing the bath with 0.5 µM TTX and the effects of D4 receptor activation on mIPSCs were reassessed.

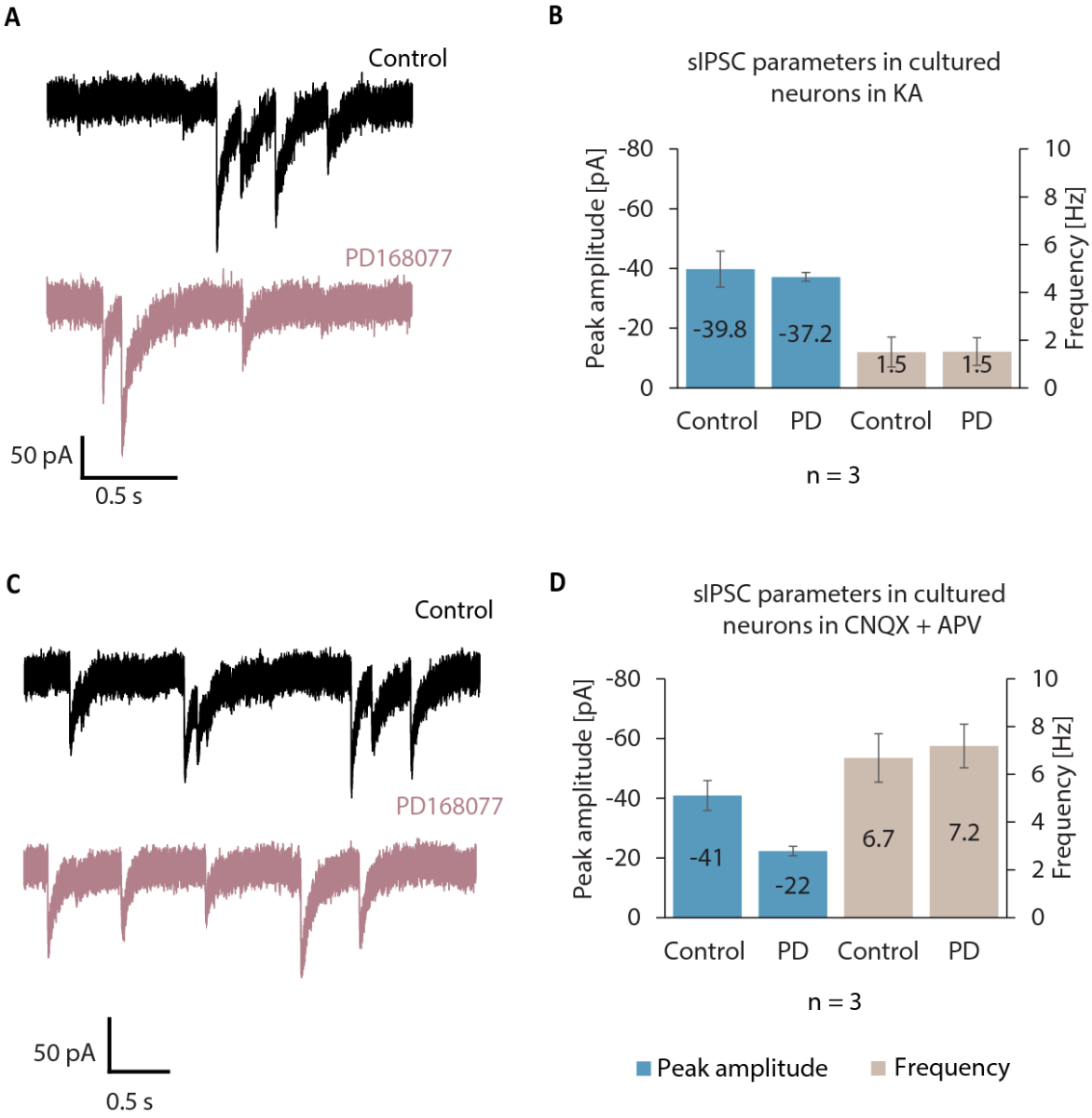

Figure 3.5: D4 receptor modulation of GABAergic inhibition in cultured neurons
A. & B. sIPSCs recorded from cultured pyramidal-shaped neurons using 2 mM KA. A standard CsCl internal pipette solution was used. **A.** Representative current traces showing sIPSCs before and after exposure to PD168077 (30 µM). **B.** sIPSC amplitude and frequency recorded from cultured neurons (DIV 14). **C. & D.** sIPSCs recorded from cultured pyramidal-shaped neurons using 10 µM CNQX plus 20 µM APV. A standard CsCl internal solution was used. **C.** Representative current traces showing sIPSCs before and after exposure to PD168077 (30 µM). **D.** sIPSC amplitude and frequency recorded from cultured neurons (DIV 12-20). All pairwise comparisons were carried out using the Wilcoxon matched-pairs signed ranks test.

Furthermore, leupeptin and phosphocreatine were added to the internal solution to prevent protein degradation and dilution of phosphates, respectively, through the intracellular recording solution. This could potentially negatively affect protein kinase

function, which is thought to be involved in the D4 receptor modulation of $GABA_A$Rs (Wang et al., 2002). However, while responses of individual cells were more consistent under these conditions, recordings did not reveal any significant effects of PD168077 on mIPSC frequency or amplitude (Figure 3.6 A & B).

At this point, having been unable to observe an effect of D4 receptor activation on $GABA_A$R mediated currents in cultured PFC neurons, it was considered whether the lack of dopaminergic inputs during neuronal maturation in culture might have led to an alteration in dopaminergic function. Furthermore, the previous studies on which our work was based (Graziane et al., 2009; Wang et al., 2002) had used both acutely dissociated neurons and acute slices for their experiments, both of which may have approximated physiological conditions more closely than primary cultures. Hence, we emulated those conditions by recording both sIPSCs and mIPSCs from acute PFC slices of 3-week old rats (Figure 3.6 C & D). While previous studies had recorded from neurons located in the intermediate to deep layers (III-VI), in the present study, the intermediate layer (III) was chosen in order to target an area with higher α2-$GABA_A$R expression, which were the intended receptor target for subsequent experiments.

Similar to the results obtained from cultured neurons, in pyramidal neurons from acute mPFC slices neither sIPSC nor mIPSC peak amplitudes were affected by PD168077 and there was no change in mIPSC frequency. However, there was a significant decrease in sIPSC frequency in the presence of PD168077 ($P = 0.01$, paired t-test), indicative of a reduction in action potential-dependent GABA release. This is most likely caused by D4 receptor activity on presynaptic interneurons leading to a reduction in interneuron excitability.

In summary, the potential effects of D4 receptor activation were assessed in both primary cultures and acute PFC slices. Overall, while there was a decrease in sIPSC frequency in slices, no changes in sIPSC or mIPSC amplitude consistent with a postsynaptic effect on $GABA_A$R surface expression were observed.

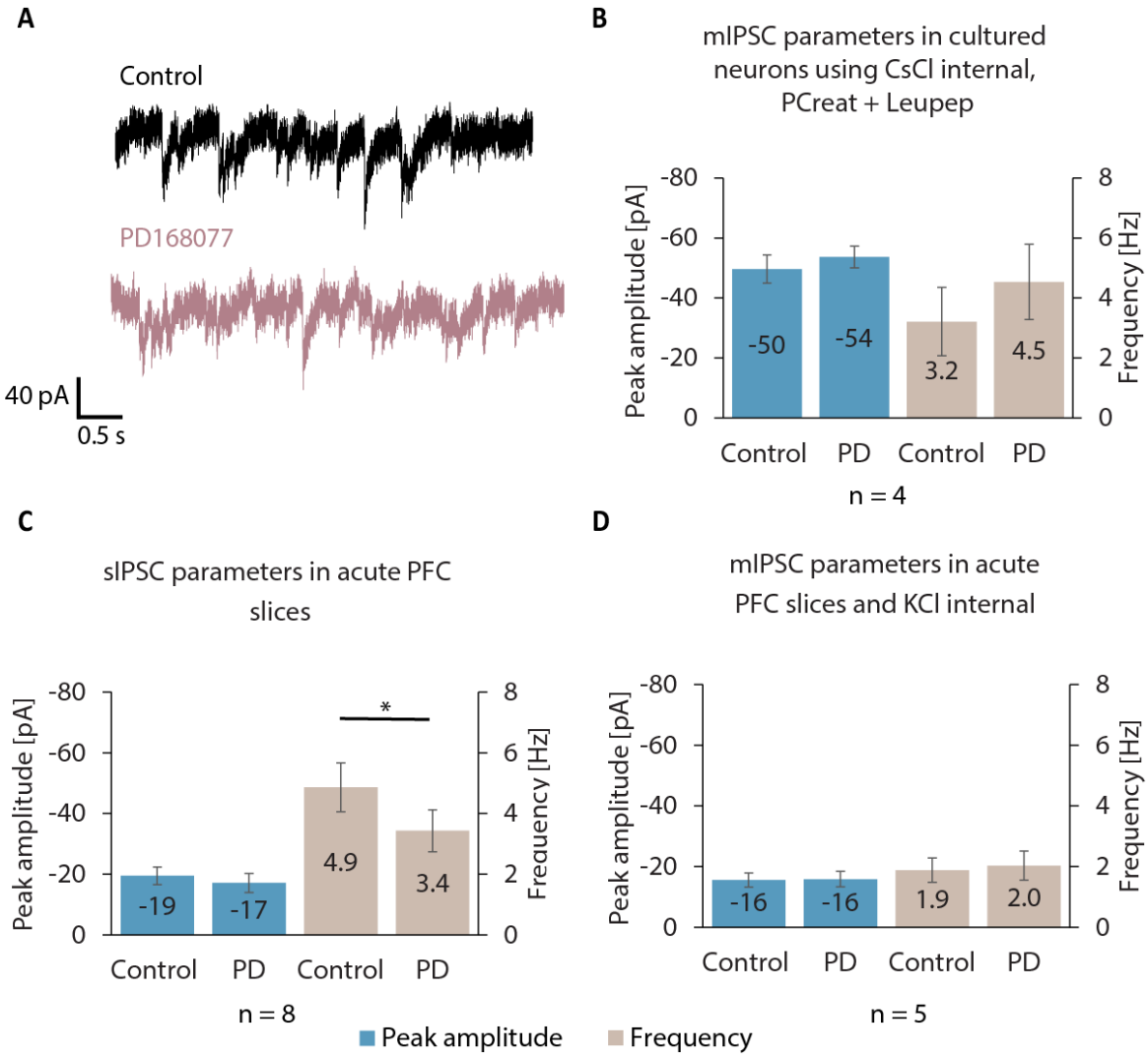

Figure 3.6: D4 receptor modulation of sIPSCs and mIPSCs in cultured neurons and acute PFC slices under varying experimental conditions

A. Representative current traces showing mIPSCs recorded from cultured pyramidal-shaped neurons using 10 µM CNQX and 20 µM APV before and after exposure to PD168077 (30 µM). **B-D.** Mean peak amplitude and frequency of IPSCs recorded under different conditions. **B.** mIPSCs recorded from cultured neurons (DIV 19-21) in Krebs (+ 10 µM CNQX, 20 µM APV and 0.5 µM TTX) using a CsCl internal supplemented with 12 mM phosphocreatine (PCreat) and 0.1 mM leupeptin (Leupep). **C.** sIPSCs recorded from PCs in acute PFC slices (P21-22) in aCSF supplemented with 2 mM KA using a CsCl internal. **D.** mIPSCs recorded from pyramidal neurons in aCSF + TTX using a KCl internal to replicate experimental methods used by Graziane et al (2009). All pairwise comparisons were carried out using the Wilcoxon matched-pairs signed ranks test (B) or paired t-tests (C & D).

3.2.3 The D4 receptor agonist PD168077 may affect α2 subunit surface expression but does not alter subcellular localisation

While we could not corroborate previous findings for a reduction in $GABA_AR$-mediated IPSC amplitude in response to D4 receptor activation, the inevitable variability in experimental conditions also did not allow the dismissal of a potential effect. However, in addition to a D4 receptor mediated decrease in synaptic GABA current amplitudes, Graziane et al. (2009) also showed a reduction in $GABA_AR$ surface expression using ICC. To assess whether this could be replicated in our cultures and to further investigate differential effects on subcellular location, we used ICC to visualise and quantify changes in receptor surface expression in response to PD168077, focusing on α2-$GABA_AR$ at the soma, dendrites and AIS.

Since our previous characterisation of the cortical cell culture used here had shown that expression of α1 and α2 subunit containing $GABA_ARs$ and D4 receptors increased until at least three weeks in culture and because it had previously been shown that $GABA_AR$ mediated IPSC kinetics change during that same period in culture (Hutcheon et al., 2000), neurons were maintained for a longer period in culture (at least 19 days) before being used for the following experiments. To this end, the cell culture protocol was modified to maintain healthy neurons for a longer period of time. After testing a range of different protocols, satisfactory results were eventually achieved with the method described in the Materials & Methods section. This method was used henceforth. Furthermore, the ICC protocol was modified and a non-permeabilising fixative (PFA) was used to allow labelling of surface membrane receptors only.

We initially focused on α2 subunit expression, due to its concentration around the AIS (Nusser et al., 1996b), a neuronal compartment that is strongly innervated by a subclass of FS interneurons, the Chandelier cells (Somogyi, 1977). Neurons were cultured for 19 days and were subjected to one of two different treatment protocols (10 min in 30 µM of the D4 receptor agonist PD168077 (PD) or 20 min in 30 µM of the D4 receptor antagonist L745870 plus a further 10 min in both PD168077 and L745870 (L74)) or a

control condition (10 min in fresh maintenance medium). Subsequently, neurons were fixed and immunolabelled as described in Materials & Methods.

Images of individual neurons were acquired and analysed as described in Materials & Methods – in brief, α2 cluster sizes were measured and their density was calculated by counting clusters at the AIS, the soma and dendrites, and dividing them by the size of their respective subcellular compartment.

The results revealed an increase in α2 cluster size after exposure to PD (Figure 3.7 A & B, $P = 0.005$, Kruskal-Wallis test; $P = 0.03$ PD vs control, Mann-Whitney test), which was inhibited by the antagonist L74, though there was no effect of PD on cluster density compared to control. However, none of the pairwise comparisons between cluster size in different subcellular compartments of control and PD-treated cells were significantly different, suggesting that the individual effects were relatively small. This suggests a weak, general, rather than a membrane compartment-specific effect of D4 receptor activation on $GABA_AR$ surface expression. Interestingly, co-treatment with the antagonist L74 reduced α2 cluster density in all three subcompartments compared to control (Figure 3.7 B, $P < 0.0001$, Kruskal-Wallis test; $P < 0.0001$, Mann Whitney test, $P < 0.0007$ and $P < 0.008$ Welch-corrected t-test for soma, dendrites and AIS, respectively), possibly indicating constitutive activity of D4 receptors (see Discussion).

In conclusion, we were unable to demonstrate an effect of D4 receptor activation on GABAergic transmission in either cultured neurons or in recordings from acute PFC slices. However, while the assessment of subunit-specific surface expression suggested there was no evidence for a region-specific effect of D4 receptor activation on $GABA_AR$ α2 subunit expression, the results did suggest an overall increase compared to control, whereas a global decrease was seen when D4 receptors where inhibited, possibly indicating constitutive activity of D4 receptors. Nevertheless, such a change in surface $GABA_A$ receptors did not appear to have a functional impact on inhibition in cortical neurons.

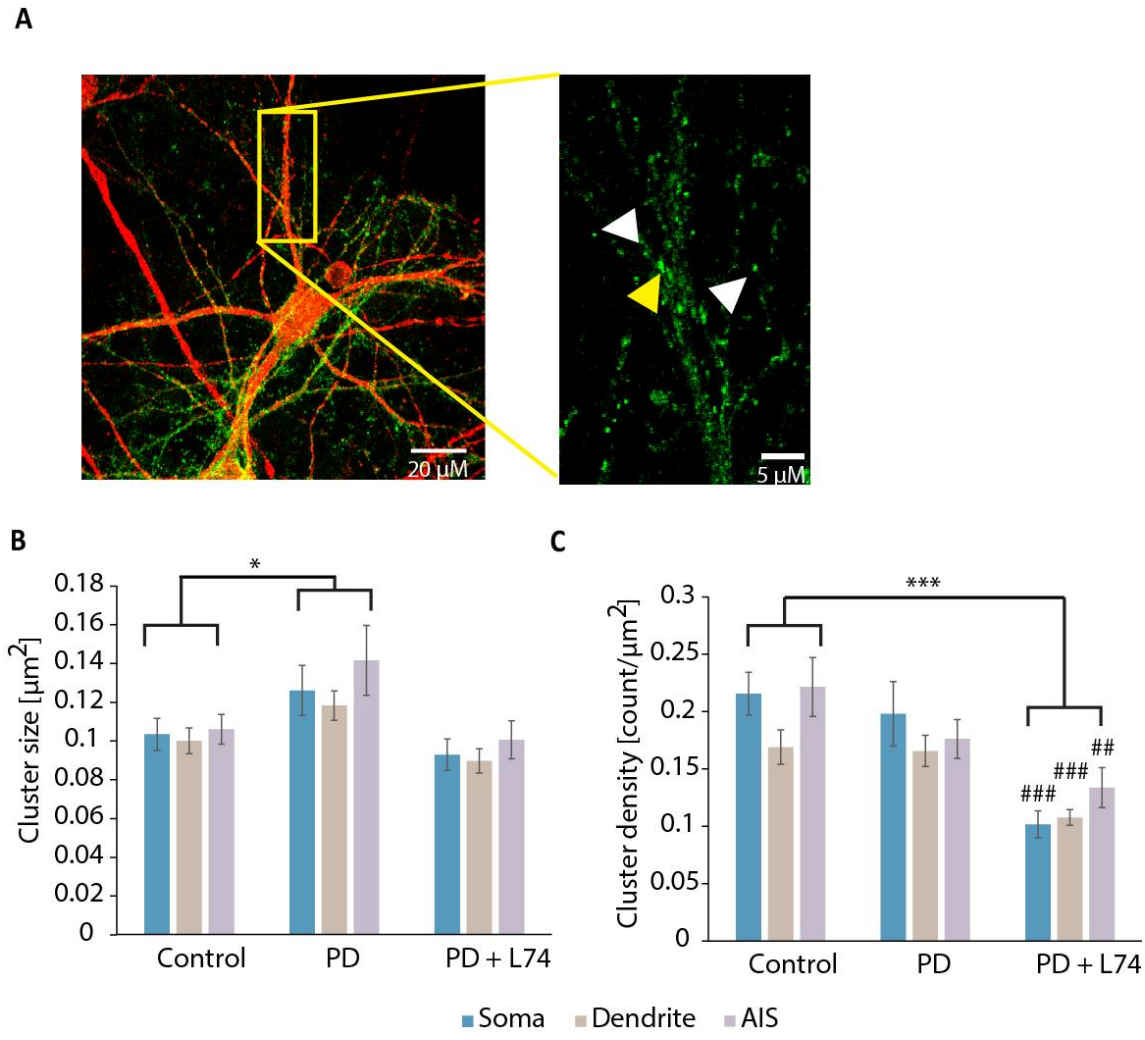

Figure 3.7: Effect of D4 receptor activation on α2 subunit surface expression and subcellular localisation

A. Representative image of a cultured neuron (DIV 19) which was used for the analysis of PD168077 effects on α2-$GABA_A$R surface expression and subcellular localisation. Surface α2 subunit labelling is shown in green, while the somatodendritic marker, MAP2, is shown in red. The right-hand image shows a dendrite at higher resolution (yellow box from A). White arrowheads mark representative α2 clusters, while the yellow arrowhead marks a fused α2 cluster. **B & C.** Bar graphs showing different measurements of α2 surface subunits acquired from fixed and immunolabelled cultured PFC neurons, including: comparison of surface expression in control medium; + PD168077 (PD; 30µM for 10 min); and PD168077 + L745870 (L74; 10 min in 30 µM L74 before addition of PD for a further 10 min) for three subcellular compartments (soma, dendrites, AIS). For both control and PD treatment, 32 cells were analysed, while 23 cells were analysed for L74. **B.** Comparison of α2 cluster sizes between subcellular compartments of control and PD-treated cells. **C.** Density of α2 clusters (cluster signal intensity divided by the area of their origin, i.e. dendrites, soma, or AIS). Error bars represent SEM. *** - P<0.001, * - P<0.05 treatment vs control, Kruskal-Wallis test between treatment groups; ### - P<0.001, ## - P<0.01 treatment vs control, Mann-Whitney (soma) or Welch-corrected unpaired t-tests (dendrites and AIS) between treatment and control conditions of respective cellular subcompartments .

3.3 Discussion

The objective of this chapter was to investigate the basis for neurotransmitter modulation of GABAergic inhibition in the PFC. Here, the main focus was placed on the D2-like dopamine receptor, D4, and an in-depth investigation of its potential for modulation/down-regulation of $GABA_A$Rs, specifically at the AIS.

3.3.1 Cortical cultures express functional $GABA_A$ and dopamine D4 receptors after two weeks in culture

Cultured neurons grow in an artificial environment and lack most of the synaptic inputs they would normally receive from other brain areas (e.g. dopaminergic projections from the VTA). Since this can, in turn, influence synapse formation and expression of neurotransmitter receptors, it was important to assess whether the receptors of interest were indeed present and functional. While this was confirmed for $GABA_A$Rs, both electrophysiologically as well as biochemically, it was also shown that expression levels are low in the first two weeks and only stabilise after at least 17 days in culture. Furthermore, we showed an increase in the expression of α1 and α2 subunits during the first three weeks in culture. In comparison, previous studies report a developmental shift in receptor expression in slices and cultured neurons, where embryonic rodent cortical $GABA_A$Rs are mainly composed of α2 and α5 subunits, and α1 subunit expression increases shortly before birth and during the first few weeks of postnatal development (Dunning et al., 1999; Möhler et al., 1995; Nusser et al., 1996b; Paysan and Fritschy, 1998). Since only whole-cell receptor expression was assessed here, this may not reflect the relative contribution of α1- vs α2-$GABA_A$Rs on the cell surface.

A developmental shift in α subunit expression is relevant for the biophysical properties of sIPSCs recorded in two week-old cultured neurons, since the α subunits in particular bestow different kinetic properties onto $GABA_A$Rs (see Mody and Pearce, 2004 for review). This may explain the slow decay time (35 ms compared to ~ 10 ms obtained later in acute PFC slices, see chapters 4 & 5) observed in our characterisation of inhibition in cultured PFC neurons. Further support for this assumption stems from

previous research observing a significant decrease in decay times by comparing neurons grown for 2 weeks to those grown for 4 weeks in culture (Dunning et al., 1999).

Similar changes in developmental expression have also been reported in the dopaminergic system. For example, cortical pyramidal cell output has been found to be differentially modulated by the release of dopamine in an age-dependent manner (Paul et al., 2013). Here, the presence of D4 receptors in cortical lysates was shown, and an increase in D4 receptor levels was observed over the first three weeks in culture. Furthermore, evidence for a functional expression of D4 receptors coupled to GIRKs at the cell surface was found in the form of an outward current in response to PD168077 using a high K^+-internal solution.

Hence, this primary cortical culture was considered an appropriate model system to elucidate D4 receptor mediated effects on GABAergic inhibition. Due to observed changes in receptor expression in cultured neurons, as well as evidence from other groups showing that synapses in cultured neurons continue to mature until at least 3 weeks in culture (see, for example, Kraszewski and Grantyn, 1992), the use of more mature neurons (3 - 4 weeks in culture) for the planned experiments was intended. However, the increase in experimental suitability with culture age was paralleled by a decrease in cell health and viability, despite rigorous attempts to improve dissection and maintenance protocols. As a compromise, neurons between DIV 10 – 20 were used for most experiments.

3.3.2 Activation of dopamine receptor D4 does not affect GABAergic transmission in primary cultures or PFC slices

Dopaminergic modulation of cortical GABAergic transmission has been shown previously in *vitro* and in *vivo* (Graziane et al., 2009; O'Donnell, 2010; Paul et al., 2013; Tritsch and Sabatini, 2012; Tseng and O'Donnell, 2007; Tseng et al., 2007; Wang et al., 2002; Yagüe et al., 2013). Here, the effects of D4 receptor activation on GABAergic inhibition were to be confirmed using the selective agonist PD168077. Both mIPSCs and sIPSCs were assessed, the latter to account for indirect, action-potential driven effects

of D4 mediated via GABAergic interneurons. However, a reduction in IPSC amplitude as a result of D4 receptor activation, seen previously (Graziane et al., 2009), could not be corroborated in cultured PFC neurons. This may, in part, be due to the lack of physiological dopaminergic input and hence an alteration in the dopaminergic signalling system. Cultures comprise an array of neurons from different subregions and layers of the original cortical tissue and may vary morphologically and physiologically from their in *vivo* counterparts. This makes identification of particular neuronal subtypes difficult and even though pyramidal-shaped neurons were chosen for study, it cannot be ascertained whether these were a physiological equivalent of PCs in the PFC. This is especially important since it has been shown that principal cells of different cortical layers possess different inhibitory properties (van Aerde and Feldmeyer, 2015; Nicoll et al., 1996) and show lamina-specific alterations in psychiatric diseases such as schizophrenia (Beneyto et al., 2011). Furthermore, studies of dopaminergic activity in the PFC have shown variability due to different cell types, laminar differences, network activity states, to name just a few variables (Seamans and Yang, 2004). In the case of D4 receptors in particular, cortical PCs have been found to respond differently to D4 activation compared to interneurons (Zhong and Yan, 2014). Consequently, the failure to reproduce previous data in the cell culture system described here may in part stem from a lack of distinction between different cell types. Therefore, the cellular system was changed to acute slices.

While PFC slices are more limited in terms of conducting ICC or other imaging-based experiments, they are a valuable tool for electrophysiological recordings. Some of their most prominent advantages are that neurons have matured in a physiological environment, they can be more easily distinguished morphologically and, as opposed to cell cultures which contain a mix of all cortical layers, can be targeted in a layer-specific manner. However, even in slice preparations and when trying to closely emulate the experimental conditions of a previous study (Graziane et al., 2009), no effect was found on either mIPSC amplitude or frequency in the presence of D4 receptor activation with PD168077. We did, however, observe a significant decrease in sIPSC, but not mIPSC, frequency. Since sIPSCs are action potential-driven, a decrease in sIPSC frequency may

result from decreased activity of presynaptic GABAergic interneurons. This is consistent with an inhibitory action of D4 receptor activation at PFC GABAergic interneurons (Acosta-García et al., 2009; Azdad et al., 2003; Gasca-Martinez et al., 2010; Govindaiah et al., 2010). It is noteworthy, however, that there is also evidence to the contrary, i.e an increase in PFC GABAergic transmission in response to DA (Gorelova et al., 2002; Tseng et al., 2007).

Despite a lack of D4-mediated effect on sIPSC amplitudes in the slice preparation, there could still be other effects that have not been investigated here, such as changes to oscillation states mediated by effects on frequency. For example, Andersson and colleagues show that D4 activation increases γ-oscillations, which are linked to working memory (Pesaran et al., 2002) and learning (Bauer et al., 2007) in hippocampal PCs, but, similar to the present study, did not detect any effects on IPSCs (Andersson et al., 2012). In addition, Zhong and colleagues (2014) discovered a significant D4-mediated increase of PC excitability in PFC, while they only observed a non-significant trend towards a reduction in sIPSC amplitude (Zhong and Yan, 2014). However, they did find the reduction in mean amplitude to be mainly caused by a loss of large events. Contrary to our findings though, this study continues to show a significant reduction in mIPSC amplitude, but not frequency, in PFC pyramidal neurons.

Therefore, the effect of PD168077 appears to be inconsistent between studies and may reflect different experimental conditions, though by studying dissociated cultures and acute slices, and both mIPSC and sIPSCs, a robust effect of D4 receptor activation should have been apparent.

3.3.3 Activation of dopamine receptor D4 increases cell-surface expression of α2-$GABA_A$Rs

The second approach implemented to elucidate D4 effects on $GABA_A$Rs was to investigate possible changes in the expression of specific $GABA_A$R subunits in response to PD168077 treatment. We initially focused on α2 subunit surface expression in different subcellular compartments. To this end, we analysed ICC labelling of α2-

$GABA_AR$s, which presented itself as punctate structures, henceforth referred to as "clusters". An increase in cluster size can be explained by an increase of α2-$GABA_AR$s incorporated into postsynaptic sites with a concomitant expansion of the postsynaptic area. Another explanation for this acknowledges the limitations of the resolution which can be achieved using confocal imaging and the image analysis paradigm described here (see Materials & Methods). In that case, an increase in the number of $GABA_AR$s present at the cell surface can lead to "fusion" of distinct clusters. Thus, an increase in cluster area may in fact stem from an increase in cluster number. In this case, using cluster density alongside cluster size provides a more accurate representation of receptor surface expression. Therefore, both cluster size and density were used as measures for receptor surface expression here.

Interestingly, contrary to previous work by Graziane et al showing a down-regulation of $GABA_AR$s (Graziane et al., 2009), the present study showed an *increase* in α2 cluster size in the presence of D4 agonist and a decrease in cluster density in the presence of the D4 antagonist. The lack of an effect on cluster density in the presence of the agonist, concomitant with a reduction in the antagonist, points to an increase in density in response to PD168077 that was probably masked by the fusion of distinct α2 clusters. This is reflected by the observed increase in cluster size. The absence of a reduction in cluster size in the antagonist L74 could indicate that, while receptor expression was reduced, the number of previously fused clusters probably remained unaltered, therefore cluster size remained unaffected. Together, this is indicative of an insertion or removal of distinct α2-$GABA_AR$ populations from the membrane, rather than a lateral movement of "free" receptors into more confined clusters. However, and most important, concomitant with an increase in α2-$GABA_AR$ surface expression, an increase in sIPSC amplitude would be expected, which was not observed in this study. It is conceivable that an increase in α2-containing $GABA_AR$s might be counterbalanced by a decrease in other $GABA_AR$s, for example containing the α1 subunit, and therefore no net change in sIPSC amplitude would be observed.

This is particularly interesting in light of the observed increase in α2- and decrease in α1-levels in the cortices of schizophrenic patients (Beneyto et al., 2011). Together with the fact that the antipsychotic drug clozapine is a more efficient antagonist at D4 receptors (Van Tol et al., 1991) it may be possible that a clinical improvement seen by D4 targeted treatments could in part be mediated by a change in expression of α2-$GABA_A$Rs. Nevertheless, there is no functional correlate of the apparent changes in α2 subunit expression by D4 receptor activation.

Another interesting observation is the reduction in α2 subunit surface expression observed in L74 compared to control. Since this compound is highly potent and selective for D4 receptors (Kulagowski et al., 1996), this reduction points to intrinsic (constitutive) activity of D4 receptors in our primary cortical culture. This could either be due to the presence of basally active dopaminergic terminals in the culture, which seems unlikely, considering that these processes will have been severed from their somatic origin in the midbrain during the culturing process. A second explanation involves constitutive activity of D4 receptors in the absence of agonist, which has been evidenced previously for D2 and D3 receptors (Malmberg et al., 1998; reviewed in Strange, 1999). Potential constitutive activity of GPCRs has been suggested by the "allosteric ternary complex model", wherein the receptor (R) can spontaneously activate (R*G) and form an active complex with the G-protein (RG) (Lefkowitz et al., 1993). The presence of constitutively active D4 receptors in cultured prefrontal neurons requires further corroboration, possibly using a combination of inverse agonists and antagonists.

In conclusion, while the experiments conducted have been unable to corroborate previous studies reporting a reduction in IPSC amplitude in response to D4 receptor activation, they did show an increase in α2 subunit expression which is congruent with upregulation of $GABA_A$R α2 subunits seen in schizophrenic patients (Beneyto et al., 2011). Nevertheless, since we failed to see an effect of D4 activation on postsynaptic inhibition in both cultured neurons and acute slices, this change in $GABA_A$R numbers may be below threshold for a functional effect. We therefore investigated other potential modulators that may affect $GABA_A$R receptor function in the mPFC.

3.4 Conclusions

1. A primary cortical culture was developed that possessed both tonic and phasic $GABA_AR$ conductances and expressed $GABA_ARs$ as well as D4 receptors that varied over the first three weeks in *vitro*.

2. In primary cultures, whole-cell expression of $GABA_AR$ α1 and α2 subunits increased over the course of the first three weeks in *vitro* as revealed by both WB and ICC.

3. The α2 subunit is relatively enriched at the AIS of cultured pyramidal-shaped neurons compared to α1 subunits.

4. Contrary to previous reports, activation of D4 receptors had no effect on the amplitudes of either action potential-dependent or –independent IPSCs in either primary cultures or acute mPFC slices.

5. D4 receptor activation does appear to decrease action potential-driven release of GABA from interneurons, leading to a decrease of sIPSC frequency at postsynaptic pyramidal neurons in acute mPFC slices.

6. D4 receptor activation universally increased cell surface expression of α2 subunits, but does not appear to have subcompartment-specific effects.

7. The concomitant down-regulation of α2 subunit surface expression observed when blocking D4 receptors is probably indicative of constitutive activity of D4 receptors in PFC cultures.

4 Neurosteroid modulation of GABAergic inhibition in the mPFC

4.1 Introduction

Neurosteroid modulation of GABAergic inhibition plays a critical role in shaping both synaptic and tonic inhibition in the CNS. While neurosteroids are seemingly synthesised and released ubiquitously throughout the brain, their effect on inhibition can be very specific and vary between brain regions and even different cell types within a certain brain area (for reviews, see Belelli and Lambert, 2005; Lambert et al., 2003). This has been largely attributed to fluctuations in local neurosteroid concentrations as well as to the expression of $GABA_AR$ subtypes with varying neurosteroid sensitivities. In addition, post-translational modification, such as phosphorylation of $GABA_ARs$, can alter their neurosteroid sensitivity (Abramian et al., 2014; Adams et al., 2015; Fáncsik et al., 2000; Tasker, 2000). The enzymatic pathways for neurosteroid metabolism are differentially expressed throughout the brain (Gunn et al., 2015) and steroid levels can change with development, oestrous cycle, pregnancy, or in response to external stressors (Gunn et al., 2015; Mody and Maguire, 2011; Purdy et al., 1991). Hippocampal DGGCs, for instance, show a much larger effect on tonic currents in response to THDOC with only minimal effects on phasic inhibition (Farrant and Nusser, 2005; Stell et al., 2003), while in CA1 PCs, neurosteroid exposure results in an increase in phasic decay (Harney et al., 2003) without affecting tonic inhibition (Stell et al., 2003). The particular subunit-composition of the $GABA_AR$ also appears to determine the affinity for neurosteroids and their relative efficacy, as well as the type of modulation they exert. For example, the affinity of αβγ-containing $GABA_ARs$ for neurosteroids is in the low nM range and varies with the specific α subunit incorporated (Belelli et al., 2002). By contrast, αβδ-containing $GABA_ARs$, possess a similar affinity for neurosteroids, but show a much higher efficacy in neurosteroid modulation (Belelli et al., 2002; Hosie et al., 2009; Lambert et al., 2003). In addition, αβγ-$GABA_ARs$ are mostly located at synaptic sites and neurosteroid potentiation leads to an increase in IPSC decay times and prolongation of IPSC durations (Belelli and Herd, 2003; Belelli and Lambert, 2005; Harney et al., 2003),

while αβδ-$GABA_A$Rs are mainly found at extrasynaptic sites where neurosteroids enhance the level of tonic inhibition (Stell et al., 2003).

Many studies have shown a link between neuroactive steroid levels and psychiatric disease, such as anxiety disorders (Eser et al., 2008; Rupprecht et al., 2001; Schüle et al., 2014; Strous et al., 2006). However, little is known about how neurosteroids modulate inhibition in the PFC, an area which is strongly interconnected with subcortical regions such as the amygdala and striatum (Berkowitz et al., 2007; Carr and Sesack, 2000). The mPFC in particular is thought to exert executive control over fear and reward pathways (Riga et al., 2014), and both hypo- and hyperactivity of this region have been implicated in different types of anxiety disorders (Arnsten, 2007; Gamo and Arnsten, 2011). Furthermore, recent research has demonstrated that enhancing neurosteroid synthesis in mouse mPFC increases GABAergic IPSC duration and amplitude and has anxiolytic effects in rodent behavioural tests (Rupprecht et al., 2009). There is evidence for neurosteroid synthetic pathways in the PFC (Castelli et al., 2013; Gunn et al., 2015) that may influence neurodevelopment (Grobin et al., 2006) and could also be crucial for providing neuroprotection in Alzheimer's disease (Luchetti et al., 2011; Marx et al., 2006). Hence, elucidating how neurosteroids modulate PFC activity could help to understand the underlying mechanisms associated with neurological and psychiatric disease.

In this chapter, we focus on effects mediated via the α2 subunit-containing $GABA_A$Rs, given their high expression in brain areas linked to mental illness, such as the amygdala and NAcc (Fritschy and Möhler, 1995; Möhler, 2002; Pirker et al., 2000) and the strong links which have been identified between alterations in α2 subunit function and CNS disorders (Engin et al., 2012). One interesting feature of α2-$GABA_A$R is their preferred localisation at the AIS in hippocampal PCs (Nusser et al., 1996b), a neuronal region crucially involved in action potential generation. Since the synchronised, regular activity of PCs generates neuronal network oscillations, which are an important functional characteristic of many brain regions (Fries, 2009), an involvement of α2-$GABA_A$Rs in regulating PC output may therefore have profound effects on network activity. Evidence

for this has been shown in the hippocampus, where cholinergic oscillations are controlled by α2 subunit $GABA_A$Rs in the CA3 region (Heistek et al., 2013). It is therefore conceivable that $GABA_A$Rs containing this subunit may play a similar role in modulating the concerted activity of neuronal networks in the PFC.

4.1.1 Probing α2-mediated neurosteroid effects in the mPFC using an $\alpha2^{Q241M}$ knock-in mouse

There are two distinct neurosteroid binding sites on $GABA_A$Rs: One is formed entirely by the α subunit transmembrane domain and mediates allosteric potentiation by neurosteroids, whilst the other is thought to lie at the β-α interface and mediates direct receptor activation by neurosteroids (Hosie et al., 2006). Previously, an α2 knock-in mouse (henceforth referred to as "hom" or $\alpha2^{M/M}$ to distinguish from wild-type mice, $\alpha2^{WT}$) has been created by exchanging glutamine at position 241 for methionine in the allosteric binding site (Durkin, 2012). This mutation of a conserved glutamine residue in the first transmembrane domain, has been introduced into different α subunits and shown to remove neurosteroid sensitivity without affecting other allosteric sites, such as benzodiazepine binding, in heterologous expression models (Hosie et al., 2009). Since binding at the potentiating site is also required to facilitate direct receptor activation by neurosteroids, this mutation (Q241M) renders the subunit insensitive to both the allosteric and direct effects of neurosteroids.

Previous work from our laboratory has used the $\alpha2^{M/M}$ mouse to explore GABA receptor subunit-specific effects of neurosteroid modulation. It has been assessed for compensatory changes in the expression of other $GABA_A$R α subunits, which were unchanged (Durkin, 2012). This study also confirmed the reduced neurosteroid sensitivity of $GABA_A$R-mediated inhibition in the NAcc and hippocampus of $\alpha2^{M/M}$ mice compared to $\alpha2^{WT}$ littermates. Interestingly, a novel potential involvement of α2 subunits in mediating tonic inhibition was discovered in addition to a significant contribution towards synaptic inhibition. Furthermore, behavioural experiments showed a role for α2 subunits in mediating anxiolytic effects of endogenous as well as exogenously-administered neurosteroids (Durkin, 2012).

4.1.2 Objectives

The aim of this project was to elucidate and characterise the properties and laminar differences of mPFC GABAergic inhibition, and how this is affected by neurosteroids. A particular focus was placed on the significance of signalling via α2-$GABA_A$Rs. To this end, acute coronal brain slices from $\alpha2^{WT}$ mice as well as from $\alpha2^{M/M}$ littermates were initially probed for functional differences in cortical GABAergic inhibition between the two genotypes. Furthermore, since $GABA_A$R receptor expression varies with the cortical layer (Pirker et al., 2000; Wisden et al., 1992), differences between superficial (II/III) and deeper layers (V/VI) were investigated (note there is no discernible layer IV in the mPFC). Using whole-cell patch-clamp recording, sIPSCs were recorded and their properties compared. Subsequent to assessing potential differences in baseline inhibitory properties between layers or genotypes, the neurosteroid THDOC was used to explore the effects of neurosteroids in different layers of the mPFC as well as, more specifically, the contribution of α2 subunit-containing $GABA_A$Rs to prefrontal cortical inhibition.

4.2 Results

In order to investigate neurosteroid modulation of GABAergic inhibition in the mPFC, acute coronal slices of murine mPFC were prepared as described in Materials & Methods. Only male mice between the ages P28 - P60 were used to avoid oestral cycle (Finn and Gee, 1993) and developmental fluctuations known to occur in endogenous neurosteroid levels (Grobin and Morrow, 2001). The age range was set to avoid inconsistent results due to changes in $GABA_AR$ subunit expression levels and, consequently, IPSC decay times that occur in early postnatal development (Dunning et al., 1999; Kobayashi et al., 2008). All recordings were carried out at room temperature in aCSF supplemented with 2 mM KA to block excitatory synaptic activity via glutamate receptors.

Typically, the first 4-6 slices (300 µm thick) below the olfactory bulb and anterior to the corpus callosum, were collected (approximately matching Bregma + 4.5 to + 2, see Figure 4.1). Cells were chosen from layer II/III or layer V/VI in the anterior cingulate cortex (ACC) or prelimbic cortex (PL) of the mPFC (Figure 4.2 A). The border between layer I and layer II/III was identified visually as a dark band approximately 100 µm from the midline (Figure 4.2 A), which had a characteristically dense distribution of somata. Any cells within approximately 200 µm from the pial surface were classified as layer II/III, while neurons located further from the pial surface were classified as layer V/VI.

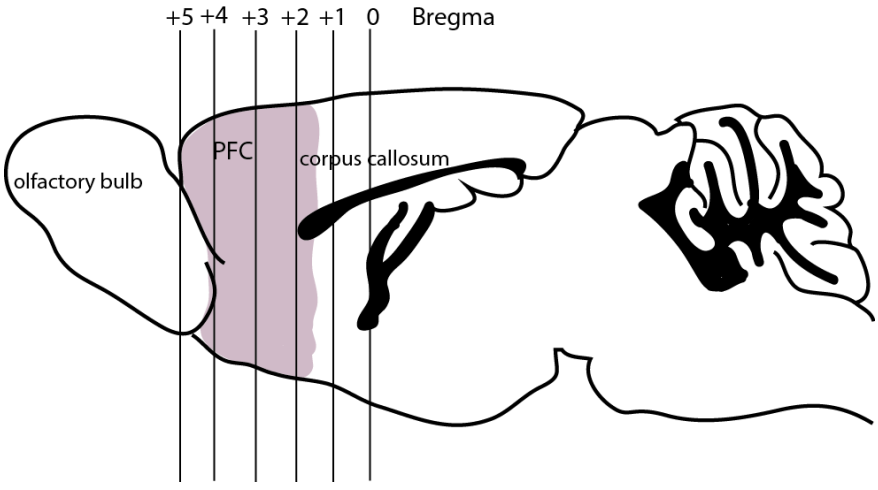

Figure 4.1: Schematic model of a mouse brain
Schematic parasagittal view of a mouse brain that includes the segmentation guidelines denoted by Bregma. The PFC, from which acute slices were collected for the purpose of the experiments carried out here, is colour highlighted. The brain model was based on Barral et al., 2014, Fig. 6 and Gabbott et al., 2005.

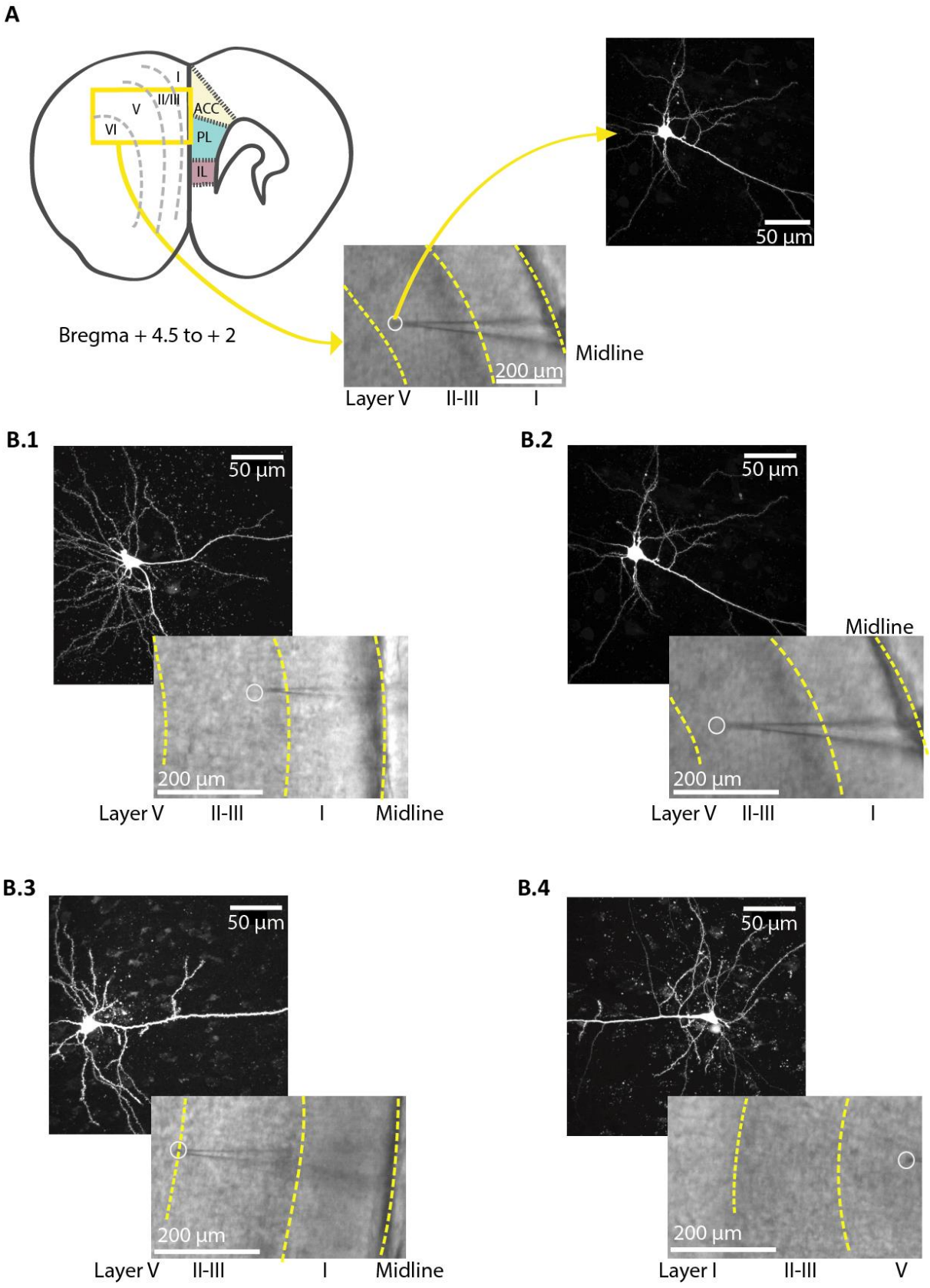
A
I
II/III
V
VI
ACC
PL
IL
Bregma + 4.5 to + 2
50 µm
200 µm
Midline
Layer V
II-III
I
B.1
50 µm
200 µm
Layer V
II-III
I
Midline
B.2
50 µm
Midline
200 µm
Layer V
II-III
I
B.3
50 µm
200 µm
Layer V
II-III
I
Midline
B.4
50 µm
200 µm
Layer I
II-III
V

Figure 4.2: Localisation and morphologies of neurons typically chosen for electrophysiological recordings in acute mPFC brain slices.
A. Schematic drawing depicting the mPFC with identified subregions (ACC – anterior cingulate cortex; PL – prelimbic cortex; IL – infralimbic cortex), and main laminar subdivisions (left). On the right of each panel are representative images of patch electrode placement within the slice (centre) and morphology of dye-filled neurons that were imaged *post hoc* (right). **B.** Selection of images showing morphology of neurons used for electrophysiological recordings from the different layers of the mPFC.

Pyramidal neurons were identified morphologically by their characteristic large, triangular somata and apical dendrite extending towards the midline. This identification was verified electrophysiologically by whole-cell capacitance: Due to their size, they possess larger membrane capacitances (in layer V/VI, on average 180 ± 7 pF, n = 13) than interneurons (here usually < 100 pF). Initial *post hoc* imaging of neurons, filled with Lucifer yellow from the patch pipette (Figure 4.2 B) confirmed that the majority of neurons recorded from in the identified cell layers of the mPFC were PCs (pyramidal neurons were easily identifiable not just by their typical gross morphology, but also by the presence of spines). Hence, *post hoc* confirmation of cell-type was discontinued in later experiments.

For analysing the kinetics of spontaneous IPSCs and for RMS noise analysis, recordings were only considered if the R_A remained stable (i.e. less than a 25% change) throughout the duration of the recording. IPSC decay times were determined as charge transfer (IPSC area) divided by the peak IPSC amplitude (Ye et al., 2013). IPSC frequencies were calculated as the reciprocal of the average inter-event intervals. Tonic currents were measured as absolute shifts in the holding current after bath-application of 20 µM bicuculline. For the measurement of tonic currents, recordings were discarded if baseline holding currents were unstable (i.e. fluctuating or gradually drifting).

4.2.1 THDOC enhances sIPSC decay times and tonic currents in mPFC of C57Bl6/J mice

The first step was to verify an effect of a physiological concentration of the neurosteroid THDOC (100 nM; Paul and Purdy, 1992) on pyramidal neuron sIPSC decay times in

superficial layers (i.e. layers II/III) of mPFC in C57Bl6/J mice. This is the animal strain that supplied the genetic background for the neurosteroid binding site mutant mouse model. THDOC was diluted to a working concentration in aCSF and applied to the slices via the bath circulation system. Neuronal currents were measured after an equilibration period of 3 min.

Similar to previous findings in other brain regions such as the hippocampus (Belelli and Herd, 2003; Cooper et al., 1999), 100 nM THDOC was found to significantly prolong sIPSC decay times by about 16% compared to a preceding control period in aCSF (7.6 ± 0.2 ms in aCSF vs 8.9 ± 0.4 ms in THDOC, $P < 0.001$, paired t-test, see Table 4.1). This prolongation in sIPSCs was also significantly larger ($P < 0.0001$, unpaired t-test, Figure 4.3 A & B) than the change observed in a "mock" application of aCSF (9 ± 0.3 ms in aCSF vs 8.9 ± 0.3 ms in "mock", see Table 4.1). Furthermore, THDOC appeared to enhance the tonic current by more than four-fold as revealed by the subsequent application of 20 µM bicuculline (5.3 ± 1.4 pA in "mock" vs 24 ± 2.7 pA in THDOC, $P < 0.0001$ unpaired t-test, Figure 4.3 C). This is also in agreement with the previously shown effect of neurosteroids on GABA-mediated tonic inhibition in the hippocampus (Mody, 2005; Stell et al., 2003).

THDOC did not have a significant influence on the sIPSC frequency or rise times (Table 4.1) when comparing absolute values to those measured in aCSF ($P = 0.4$, $P = 0.3$, respectively, paired t-tests). Furthermore, neither sIPSC frequency ($P = 0.1$, unpaired t-test) nor rise times ($P = 0.3$, unpaired t-test), if normalised to measurements taken during a control period in aCSF prior to THDOC application, were significantly different from a "mock" control recording (see Table 4.1 for absolute values). A small tendency for an increase in the peak amplitude was observed in the presence of THDOC ($P = 0.04$, paired t-test; Table 4.1); however, normalised peak amplitudes in THDOC (5.5 ± 2.2 % change) were not significantly different from a "mock" control (1.4 ± 4.3 % change, $P = 0.4$, unpaired t-test).

sIPSC parameters & GABA tonic currents	aCSF	THDOC	n
Frequency [Hz]	10.09 ± 0.86	10.43 ± 0.82	(12)
Peak amplitude [pA]	-29.26 ± 1.38	-30.83 ± 1.55*	(12)
Decay time [ms]	7.59 ± 0.22	8.85 ± 0.37***	(12)
Rise time [ms]	0.47 ± 0.02	0.48 ± 0.02	(12)
Tonic current [pA]	-	23.97 ± 2.65###	(25)

sIPSC parameters & GABA tonic currents	aCSF	"Mock" Control	n
Frequency [Hz]	7.26 ± 1.12	6.88 ± 1.08	(9)
Peak amplitude [pA]	-30.81 ± 1.53	-31.56 ± 1.70	(9)
Decay time [ms]	9.02 ± 0.25	8.89 ± 0.33	(9)
Rise time [ms]	0.5 ± 0.04	0.47 ± 0.02	(9)
Tonic current [pA]	-	5.3 ± 1.39	(11)

Table 4.1: THDOC effects on sIPSC parameters and tonic current in mPFC pyramidal neurons

Comparison of sIPSC kinetics and tonic currents before (aCSF) and after application of 100 nM THDOC or in a "mock" control (application of aCSF) in C57Bl6/J slices. Recordings were obtained from layer II/III pyramidal neurons of mPFC. Cell numbers (n) are shown in parentheses. All values are given as mean ± SEM. * - $P < 0.05$, *** - $P < 0.001$, aCSF vs THDOC/"mock", paired t-test. ### - $P < 0.001$, tonic currents in THDOC vs "mock" control, unpaired t-test.

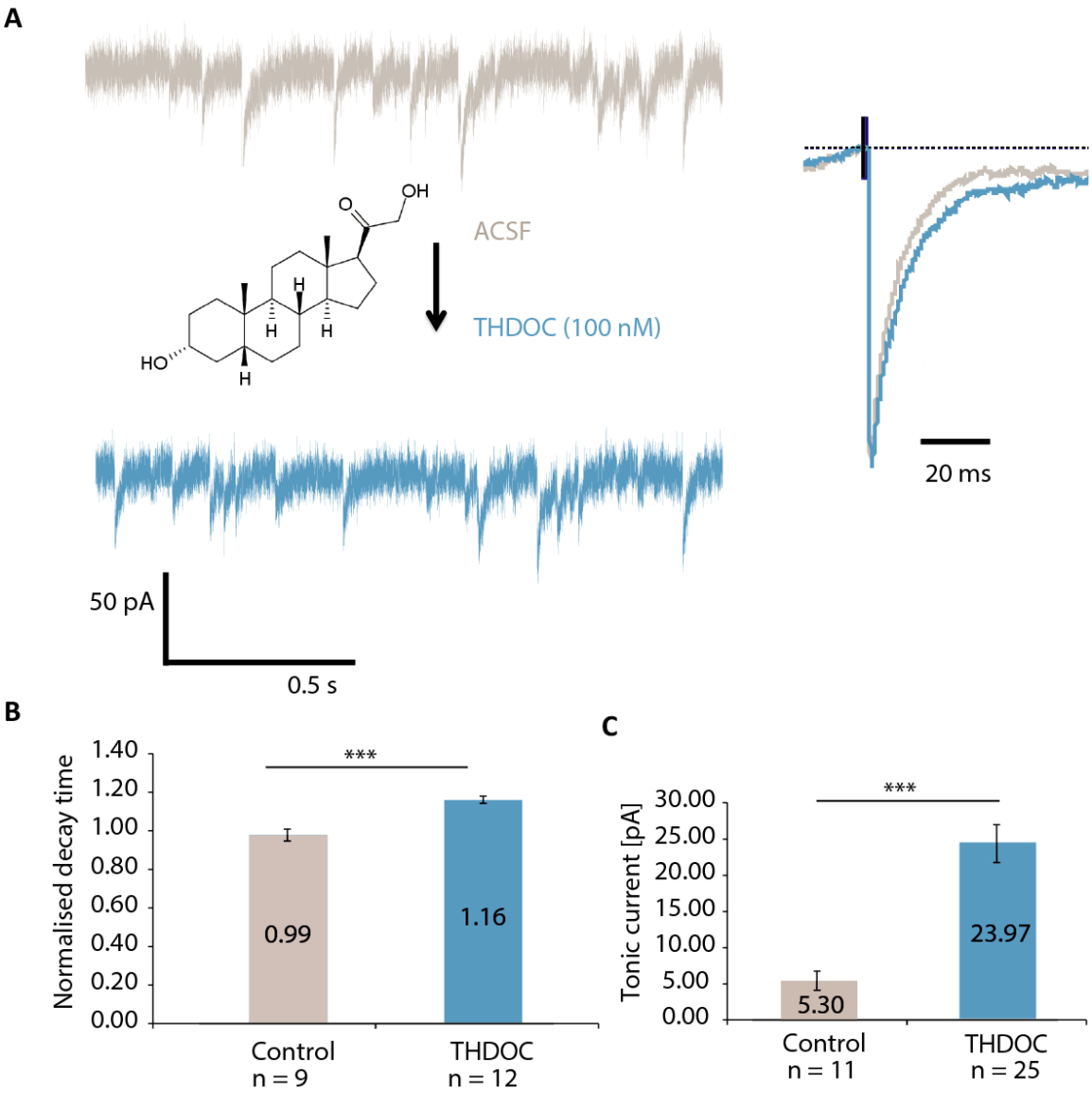

Figure 4.3: THDOC prolongs sIPSC decay times and enhances tonic currents

A. Representative sIPSCs recorded from a layer II/III pyramidal neuron of C57Bl6/J mPFC in aCSF and THDOC. Shown in the centre is the chemical structure of THDOC. Currents shown on the right-hand side represent peak-scaled average sIPSCs observed in either aCSF or THDOC and which were obtained from averaging at least 100 events for each condition. **B & C.** Bar graphs of the effects of 100 nM THDOC on decay times and tonic currents, compared between drug application and a "mock" control (aCSF). Decay time was normalised to those measured in aCSF alone. Error bars represent mean ± SEM. *** - $P < 0.001$, unpaired t-test.

4.2.2 Baseline sIPSC kinetics do not vary between mPFC layers of $\alpha2^{WT}$ mice

Having established the effects of THDOC on sIPSC decays in C57Bl6/J mouse mPFC pyramidal neurons, the mouse model expressing neurosteroid insensitive α2 subunits was used henceforth. Initially, baseline cellular parameters and sIPSC kinetics of pyramidal neurons from different layers of wild-type ($\alpha2^{WT}$) mPFC neurons were compared in slices taken from wt littermates. With the exception of membrane capacitance, most parameters were similar between layers II/III and V/VI (Table 4.2). Membrane capacitance, however, was found to be larger for cells located in the deeper layers ($P < 0.0001$, unpaired t-test), which is likely to reflect the typically larger somata found in this layer (van Aerde and Feldmeyer, 2015).

Pyramidal neuron parameters	Layer II/III	Layer V/VI
R_{in} [MΩ]	186.65 ± 14.26 (13)	212.15 ± 17.06 (13)
C_m [pF]	124.3 3± 8.11 (13)	179.75 ± 7.40 (13)***
Baseline sIPSC parameters & tonic current	**Layer II/III**	**Layer V/VI**
Frequency [Hz]	10.67 ± 1.59 (12)	10.38 ± 0.94 (13)
Peak amplitude [pA]	-28.03 ± 1.95 (12)	-25.78 ± 1.02 (13)
Decay time [ms]	8.55 ± 0.51 (12)	8.49 ± 0.35 (13)
Rise time [ms]	0.57 ± 0.07 (12)	0.64 ± 0.02 (13)
Tonic current [pA]	10.28 ± 2.71 (7)	13.97 ± 1.98 (10)

Table 4.2: Membrane capacitance varies between different layers of $\alpha2^{WT}$ mPFC

Table comparing electrophysiological parameters of pyramidal neurons in different layers of $\alpha2^{WT}$ mouse mPFC. Values for the input resistance (R_{in}) and membrane capacitance (C_m) were calculated from the average hyperpolarising capacity transients recorded by applying 20 x 10 mV steps (see Materials & Methods section). sIPSC frequency, rise-time, amplitude and decay time were obtained by averaging measurements from sIPSCs over a period of at least 2 min (>100 events). Cell numbers are shown in parentheses. All values are given as means ± SEM. *** - $P < 0.001$, unpaired t-test.

4.2.3 THDOC prolongation of decay times is greater in layers V/VI compared to II/III

We then compared the effects of THDOC on pyramidal cell GABA-mediated inhibition between the superficial mPFC layers (II/III) and deeper layers (V/VI) in $\alpha2^{WT}$. While initial comparisons of baseline parameters and sIPSC kinetics between those regions revealed a difference only in cell capacitance (Table 4.2), the differential distribution of $GABA_AR$ subtypes that is known to occur across different cortical layers (Pirker et al., 2000; Sieghart and Sperk, 2002) could nevertheless lead to changes in the response to neurosteroids. Indeed, comparing the effect of THDOC (100 nM) on decay times, a greater prolongation of sIPSCs was detected in layers V/VI compared to II/III: while decay times in the outer layers were prolonged by ~16 %, inner layer sIPSC decay times were prolonged in THDOC by 27 % ($P = 0.012$, unpaired t-test, Table 4.3), equating to an approximate 69% larger effect by THDOC. This could be indicative of a larger population of neurosteroid-sensitive $GABA_ARs$ in the deeper layers (see Discussion). None of the other parameters examined exhibited a significant laminar difference, which indicates that GABA release is likely to be similar across the different layers and also points to an overall similar density of synaptic and extrasynaptic $GABA_ARs$. Interestingly, sIPSC frequency was increased in THDOC in PCs of $\alpha2^{WT}$, an effect we did not observe before in C57Bl6/J (Table 4.1, Table 4.3). While a change in sIPSC frequency was not expected after THDOC treatment, there is no consensus on neurosteroid effects on sIPSC frequency in the literature (Reith and Sillar, 1997; Stell et al., 2003). Such changes may conceivably involve neurosteroid action at presynaptic Ca^{2+} channels and/or presynaptic $GABA_ARs$ (Haage et al., 2002; Poisbeau et al., 1997). Another difference to the results obtained in C57Bl6/J mice is the lack of an effect of THDOC on tonic currents (Table 4.4).

In summary, using electrophysiology, the cellular properties of pyramidal neurons and underlying parameters of GABA inhibition in the mPFC were characterised. Most of these parameters were found to be largely independent of the cortical layer, with the exception of a larger membrane capacitance observed in layers V/VI. Furthermore, THDOC significantly prolonged sIPSC decay times in layers II/III and V/VI of $\alpha2^{WT}$ mice, and this increased duration of synaptic inhibition was significantly more pronounced in

the deeper cortical layers. Finally, there appeared to be an equal increase in sIPSC frequency in response to THDOC in both layers of $\alpha2^{WT}$ slices.

Normalised sIPSC parameters after THDOC	Layer II/III (12)	Layer V/VI (8)
Frequency	1.14 ± 0.06$^{\#}$	1.13 ± 0.05$^{\#}$
Peak amplitude	1.05 ± 0.03	1.06 ± 0.06
Decay time	1.16 ± 0.02	1.27 ± 0.03*
Rise time	1.16 ± 0.08	1.09 ± 0.06

Table 4.3: Effect of THDOC on sIPSC parameters in layers II/III and V/VI of the mPFC

Comparison of sIPSC frequency and kinetics after application of 100 nM THDOC normalised to a control period (= 1) in aCSF in different layers of the mPFC. Recordings were obtained from pyramidal neurons of $\alpha2^{WT}$ mouse mPFC. The numbers of cells are shown in parentheses. All values are means ± SEM. * - P < 0.05 layer V/VI vs layer II/III, unpaired t-test. # - P < 0.05, aCSF vs THDOC, paired t-test.

Tonic currents [pA]	Layer II/III (12)	Layer V/VI (8)
aCSF	10.28 ± 2.71 (7)	13.96 ± 1.98 (7)
THDOC	12.98 ± 1.44 (13)	8.81 ± 1.91 (8)

Table 4.4 Effect of THDOC on tonic currents in layers II/III and V/VI of the mPFC

Absolute tonic currents in the presence and absence of THDOC. Recordings were obtained from pyramidal neurons of $\alpha2^{WT}$ mouse mPFC. The numbers of cells are shown in parentheses. All values are means ± SEM. Statistical tests compared tonic currents between layers (unpaired t-test) and between THDOC and aCSF treatment (paired t-test); both were found to be insignificant (P<0.05).

4.2.4 Ablating neurosteroid sensitivity of $GABA_AR$ α2 subunits in layer II/III PCs

In order to study the specific effects of neurosteroid modulation of GABAergic inhibition via α2-containing $GABA_ARs$, a mutant knock-in mouse line has been generated by introducing a point mutation in the neurosteroid binding site of the α2 subunit (Durkin, 2012). Previous work has provided evidence that this residue renders $GABA_ARs$ containing α2 subunits insensitive to allopregnanolone and THDOC, without affecting GABA or benzodiazepine binding, or the function of the $GABA_AR$ (Hosie et al., 2006, 2009). Work from our lab has previously characterised this knock-in mouse-model in the hippocampus and NAcc with regards to its effect on neurosteroid responses, as well as potential compensation resulting from the knock-in. However, the effects of neurosteroid modulation and the role of the α2 subunit in the mPFC of the knock-in line have not been characterised.

Initially, baseline cellular parameters (Table 4.5) and GABA inhibitory neurotransmission (Table 4.6) in layers II/III and V/VI were compared between $\alpha2^{WT}$ animals and $\alpha2^{M/M}$ littermates. These data also allowed us to assess the potential presence of any endogenous neurosteroid tone on α2-$GABA_ARs$.

By comparing sIPSC decay times between neurons from $\alpha2^{WT}$ and $\alpha2^{M/M}$ slices (Table 4.6), a difference in baseline decay was noted only in layer II/III ($P = 0.04$, one-tailed unpaired t-test). Such a result could be indicative of an endogenous neurosteroid tone that is removed by the Q241M mutation in the α2 subunit of slices from homozygote mice (see Discussion). There were no differences in other sIPSC parameters or tonic inhibition between the genotypes or between the different cell layers (Table 4.6). Similar to the results with $\alpha2^{WT}$, layer V/VI neurons had a larger membrane capacitance than their layer II/III counterparts in $\alpha2^{M/M}$ animals ($P < 0.001$, unpaired t-test; Table 4.5). There was no difference in the membrane capacitance between genotypes.

Pyramidal neuron baseline parameters		$\alpha2^{WT}$(13)	$\alpha2^{M/M}$ (12)
R_{in} [MΩ]	Layer II/III	189 ± 14 (13)	197 ± 29
	Layer V/VI	212 ± 17	267 ± 25
C_m [pF]	Layer II/III	124 ± 8	139 ± 10
	Layer V/VI	180 ± 7***	191 ± 9***

Table 4.5: Comparison of baseline cellular parameters between $\alpha2^{WT}$ and $\alpha2^{M/M}$ mice
Comparison of R_{in} and C_m measured in aCSF at the beginning of an experiment between slices from $\alpha2^{WT}$ mice and $\alpha2^{M/M}$ littermates, in layers II/III and V/VI of the mPFC. *** - $P < 0.001$ layer II/III vs layer V/VI, unpaired t-test.

Baseline sIPSC parameters and GABA tonic current		$\alpha2^{WT}$	$\alpha2^{M/M}$
Frequency [Hz]	Layer II/III	10.67 ± 1.59 (12)	13.70 ± 1.73 (12)
	Layer V/VI	10.38 ± 0.94 (13)	9.24 ± 1.3 (9)
Peak amplitude [pA]	Layer II/III	-28.03 ± 1.95 (12)	-25.99 ± 1.16 (12)
	Layer V/VI	-25.78 ± 1.02 (13)	-27.55 ± 0.73 (9)
Decay time [ms]	Layer II/III	8.55 ± 0.51 (12)	7.37 ± 0.31 (12)*
	Layer V/VI	8.49 ± 0.35 (13)	9.19 ± 0.38 (9)##
Rise time [ms]	Layer II/III	0.57 ± 0.07 (12)	0.60 ± 0.05 (12)
	Layer V/VI	0.64 ± 0.02 (13)	0.59 ± 0.02 (9)
Tonic current [pA]	Layer II/III	10.28 ± 2.71 (7)	10.79 ± 3.18 (8)
	Layer V/VI	13.97 ± 1.98 (10)	9.74 ± 1.59 (6)

Table 4.6: Comparison of sIPSC parameters and tonic current properties between neurons of $\alpha2^{WT}$ and $\alpha2^{M/M}$ mice

Comparison of absolute baseline values for sIPSC kinetics and tonic currents between neurons from $\alpha2^{WT}$ mice and $\alpha2^{M/M}$ littermates, as well as between different layers of the mPFC. Cell numbers are shown in parentheses. All values are given as means ± SEM. ## - $P < 0.01$ layer II/III vs layer V/VI unpaired t-test, * - $P < 0.05$ $\alpha2^{WT}$ vs $\alpha2^{M/M}$ unpaired t-test.

While changes in GABA tonic currents overall did not vary significantly between either genotype or cell layers (Figure 4.4 A & B, Table 4.6), there was a tendency towards a reduced current in layer V/VI neurons of $\alpha^{M/M}$ mutant mice. Furthermore, since a novel involvement of $GABA_AR$ α2 subunits in tonic inhibition had previously been suggested for DGGCs (Durkin, 2012), and differences in tonic currents have been reported for wt cells from different cortical layers of visual and somatosensory cortex (Jang et al., 2013; Yamada et al., 2007), the possibility for changes in tonic current were further explored. In addition to measuring absolute shifts in the holding current, the tonic current density (holding current change normalised to cell capacitance) was determined, to account for any effects that different cell sizes might have on the measured GABA currents (Figure 4.4 C). However, these normalised tonic currents did not vary significantly between genotypes or the different cortical layers. As a third check, changes in RMS current noise were also analysed (Figure 4.4 D), but, as before, they did not reveal any significant differences in the tonic currents.

4.2.5 $GABA_ARs$ containing δ or α5 subunits contribute to tonic currents in layer V/VI pyramidal neurons

While overall tonic currents appeared unaltered for $\alpha2^{M/M}$, there may still have been alterations in the relative contribution of different populations of $GABA_AR$ subtypes to tonic inhibition in the mPFC. The two subtypes most commonly implicated in tonic inhibition are α5 and δ subunit-containing $GABA_ARs$ (Brickley and Mody, 2012; Caraiscos et al., 2004; Glykys et al., 2008; Lee and Maguire, 2014; Marowsky and Vogt, 2014). Overall, δ-$GABA_ARs$ tend to be more highly expressed in superficial layers of the PFC, while α5-$GABA_ARs$ are found more concentrated in the deeper layers (Pirker et al., 2000). Since the initial investigation of changes in tonic currents between $\alpha2^{WT}$ and $\alpha2^{M/M}$ showed a slight tendency towards a reduction in tonic currents in $\alpha2^{M/M}$ layer V/VI PCs (Figure 4.4 B), the presence of functional δ- and α5-$GABA_ARs$ was elucidated further in this area and compared between genotypes.

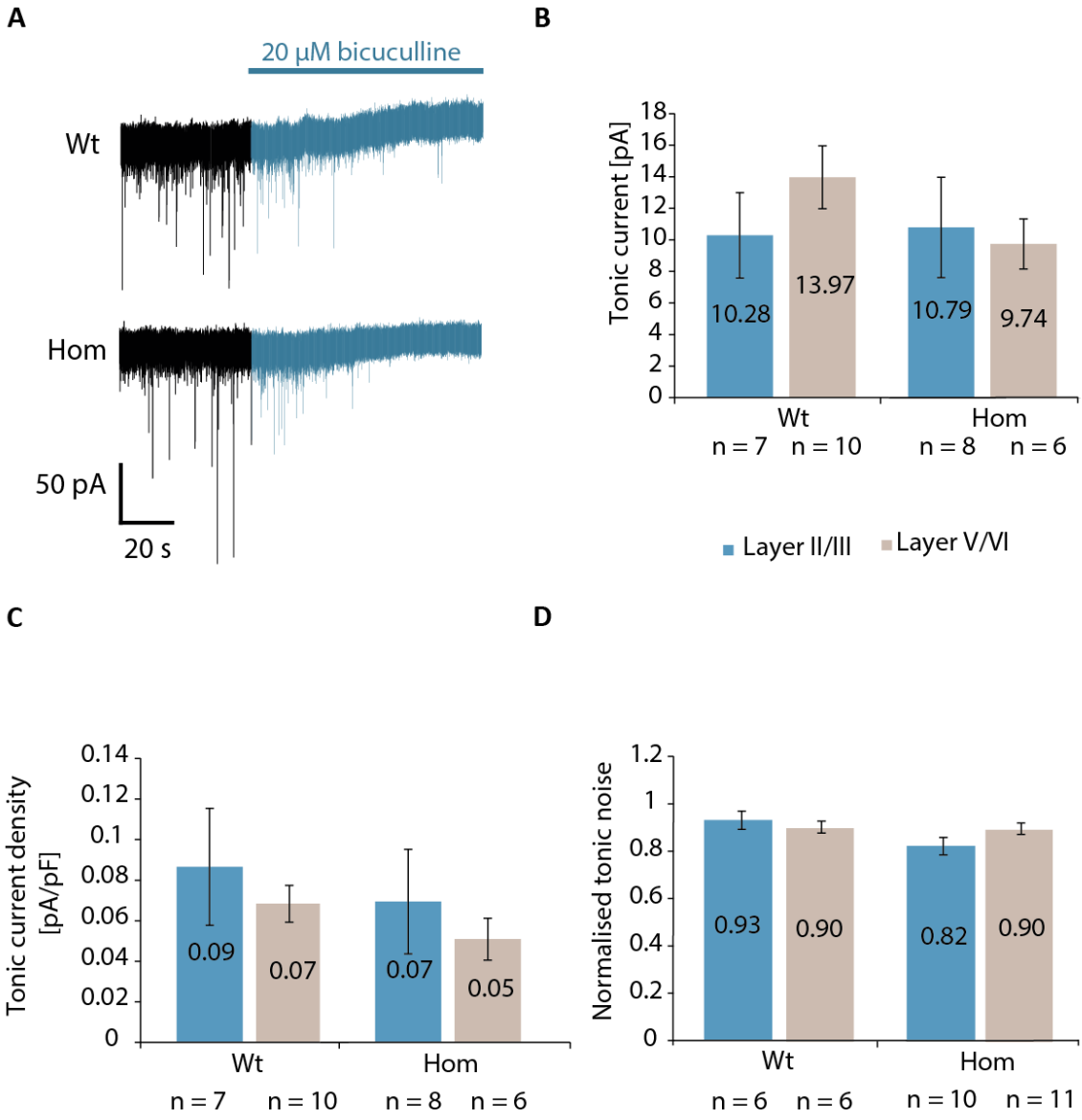

Figure 4.4: GABA tonic currents recorded from mPFC cell layers and different genotypes

A. Representative tonic currents for layer V/VI PCs of $\alpha2^{WT}$ and $\alpha2^{M/M}$ mice recorded under whole-cell voltage clamp. Traces show the current shift in response to bath application of 20 µM bicuculline. Cells were held at -60 mV and currents were allowed to equilibrate for at least 1 min after drug application before any measurements were taken. **B.** Comparison of GABA-mediated tonic currents between different genotypes and cell layers. **C.** Tonic current densities calculated using the same currents as measured in B, but normalised to cell capacitance. **D.** Tonic noise measured by calculating the RMS noise of current traces in bicuculline (see Material & Methods), normalised to a preceding control period in aCSF. Only current traces uncontaminated by synaptic events were chosen and averaged over at least 30 s. All datasets were tested using pairwise comparisons. Bars represent mean ± SEM.

First, the presence of δ subunit-containing $GABA_A$Rs was explored using THIP, an agonist selective for this receptor subtype when used at appropriate concentrations (Krogsgaard-Larsen et al., 2004; Mortensen et al., 2010). After establishing a stable baseline recording from layers V/VI in aCSF (usually after 3-4 min), 1 µM THIP (a δ-subunit selective agonist) was applied through the bath perfusion system. As expected for THIP, which is a more potent agonist at αβδ receptors compared to the natural transmitter (Brown et al., 2002; Krogsgaard-Larsen et al., 2002; Mortensen et al., 2010), tonic currents approximately doubled in amplitude (Figure 4.5) in both $\alpha2^{WT}$ and $\alpha2^{M/M}$ cells when compared to tonic currents in aCSF (P = 0.002 both, unpaired t-test). However, there was no effect of genotype on the THIP-induced tonic currents, suggesting that both $\alpha2^{WT}$ and $\alpha2^{M/M}$ neurons are expressing near-equal numbers of δ subunit-containing $GABA_A$Rs in layer V/VI pyramidal neurons.

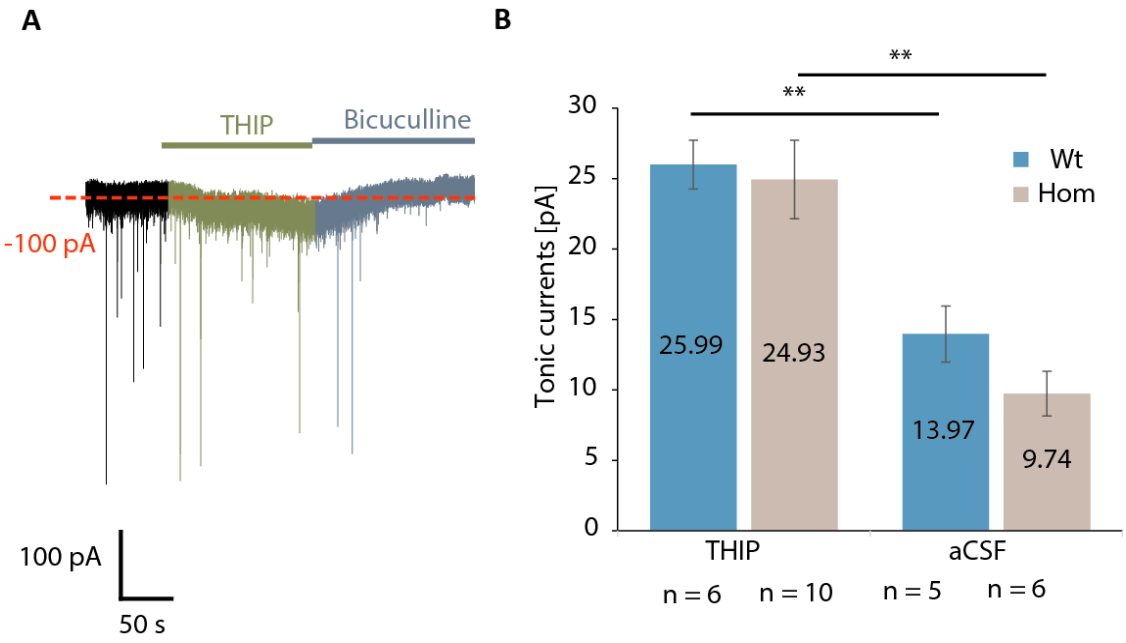

Figure 4.5: $GABA_A$Rs containing δ subunits are present in layer V/VI pyramidal neurons but do not vary between genotypes

A. Representative membrane current trace showing an increase in holding current after bath application of 1 µM THIP and a decrease in 20 µM bicuculline. **B.** Tonic GABA currents in THIP and aCSF compared between $\alpha2^{WT}$ and $\alpha2^{M/M}$ neurons. Bars represent mean ± SEM. **-P < 0.01, THIP vs aCSF, unpaired t-test.

The presence of α5 subunit-containing $GABA_AR$s was also probed in layers V/VI using a selective inverse agonist, (MRK-016). This compound has previously been shown to selectively inhibit α5-containing $GABA_AR$s with 50% relative inhibitory efficacy and a high potency indicated by the low IC_{50} of 3 nM (Atack et al., 2009; Chambers et al., 2004). A comparison of tonic GABA currents recorded from neurons from the two genotypes, exposed to either MRK-016 (100 nM) or just aCSF, showed a significant difference in $\alpha2^{M/M}$ only (P = 0.03, one-tailed unpaired t-test; Figure 4.6 A), while $\alpha2^{WT}$ just failed significance at the 5% margin (P = 0.06, one-tailed unpaired t-test). However, MRK-016 induced significant changes to the holding current compared to a null-effect for both $\alpha2^{WT}$ (P = 0.006, one-sample t-test, Figure 4.6 C) and $\alpha2^{M/M}$ (P = 0.009; Figure 4.6 C). There is no significant difference in holding current shifts by MRK-016 between the genotypes (P = 0.06, unpaired t-test). Furthermore, the contribution of MRK-016-mediated inhibition of α5-$GABA_AR$ to tonic currents in layer V/VI PCs, measured as current shift relative to total tonic current after bicuculline, is not significantly different between genotypes (P = 0.6, unpaired t-test; Figure 4.6 D).

Together, these data suggest that α5-$GABA_AR$s do contribute significantly to tonic inhibition in layer V/VI PCs in both genotypes. While there may be differences in the absolute values for current shifts observed in MRK-016 between $\alpha2^{M/M}$ and $\alpha2^{WT}$ mice, their relative contribution towards tonic currents are broadly similar. Therefore, the most likely conclusion is that the α5-$GABA_AR$ contribution to GABA tonic current is unaffected in $\alpha2^{M/M}$ animals.

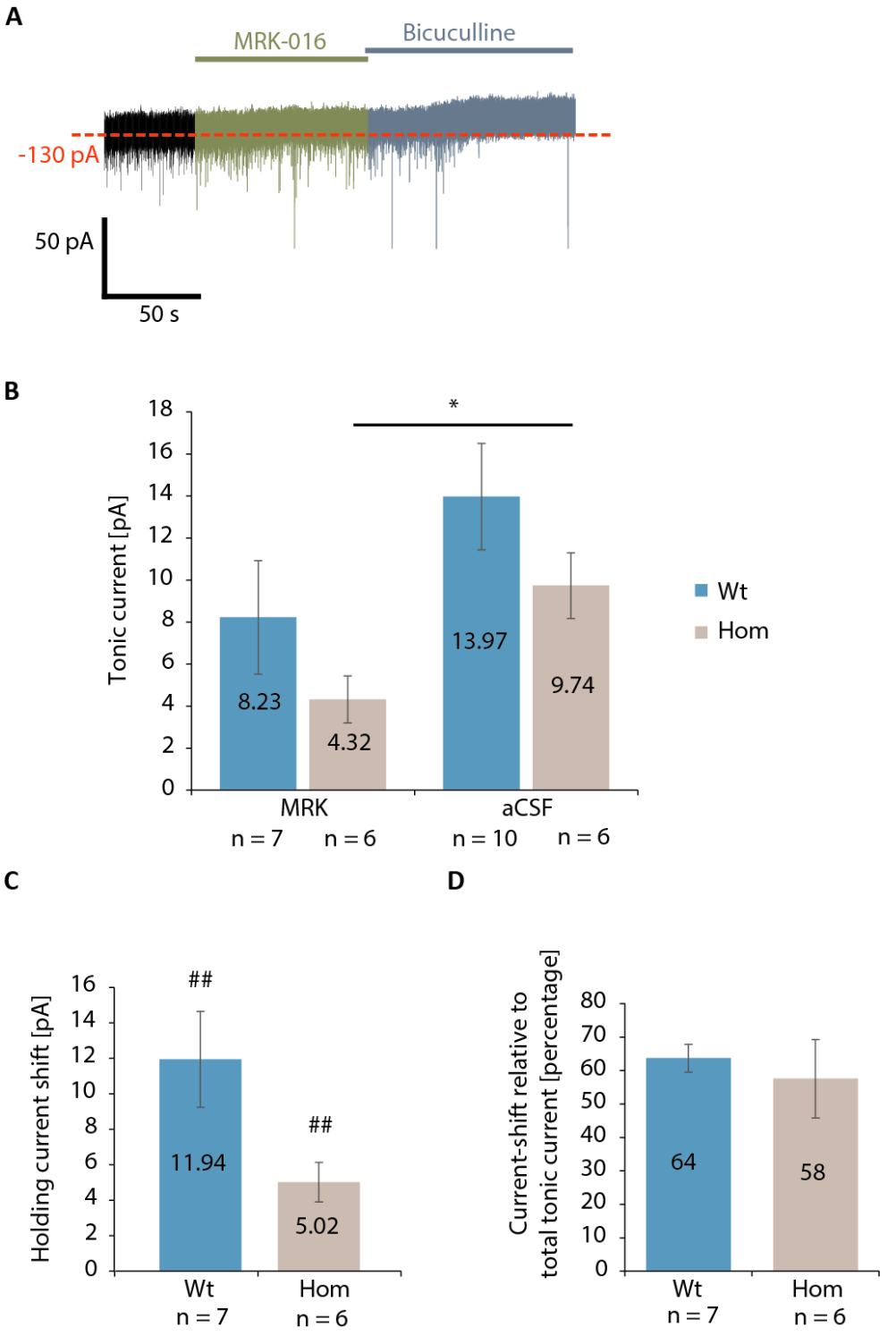

Figure 4.6: α5-GABA$_A$Rs contribute to tonic current in layer V/VI pyramidal neurons
A. Representative current trace of a layer V/VI PC showing reductions in the holding current after application of 100 nM MRK-016 and 20 µM bicuculline. **B.** Comparison of tonic currents in MRK-016 or aCSF between $\alpha2^{WT}$ and $\alpha2^{M/M}$ neurons. *-P < 0.05, MRK vs aCSF, one-tailed unpaired t-test. **C.** Shifts in holding current upon exposure to MRK-016. ##-P < 0.01, one-sample t-test vs null-effect. **D.** Relative contribution of MRK-016-mediated current shift towards tonic currents. Unpaired t-test revealed no difference between genotypes. Bars represent mean ± SEM.

4.2.6 $GABA_ARs$ containing the α2 subunit contribute to neurosteroid-mediated modulation of prefrontal cortical inhibition

The aim of using the $\alpha2^{Q241M}$ mutant knock-in was to assess the contribution of $GABA_ARs$ containing the α2 subunit towards synaptic inhibition in pyramidal neurons from different layers in the mPFC. To this end, THDOC-induced changes in sIPSC kinetic parameters and tonic GABA currents were compared between $\alpha2^{M/M}$ mice and $\alpha2^{WT}$ mutant littermates. Furthermore, we also assessed whether the contribution of α2 subunits towards GABA inhibition differed between cortical layers II/III and V/VI.

For the sIPSC decay times, prolongation was found to be more pronounced in $\alpha2^{WT}$ neurons compared to $\alpha2^{M/M}$ counterparts (by approximately 12% in both layers, Figure 4.7). However, in layer II/III, comparing $\alpha2^{WT}$ with $\alpha2^{M/M}$ neurons, the incremental effect of THDOC on sIPSC decay times was 75% smaller (only a 4% increase in decay time in $\alpha2^{M/M}$ compared to a 16% increase for $\alpha2^{WT}$). By comparison, THDOC was more effective (only 48% smaller effect) in layer V/VI (14% increase in decay time for $\alpha2^{M/M}$ compared to a 27% increase for $\alpha2^{WT}$). This suggests that α2 subunits do indeed make up a significant proportion of $GABA_AR$ subunits involved in synaptic inhibition in the mPFC, and that their relative contribution is greater in the more superficial cortical layers. This would be consistent with a higher expression of α2-$GABA_ARs$ in those layers compared to deep layers V/VI (Pirker et al., 2000).

Furthermore, $GABA_AR$-mediated synaptic currents display a higher sensitivity to THDOC in layers V/VI compared to layers II/III, with a relative increase in sensitivity of about 68% in $\alpha2^{WT}$ (27% prolongation of decay times in layer V/VI against a 16% prolongation in layer II/III; Figure 4.7 A). This suggests there is an increased responsiveness of $GABA_ARs$ to THDOC in layers V/VI compared to layers II/III (see Discussion).

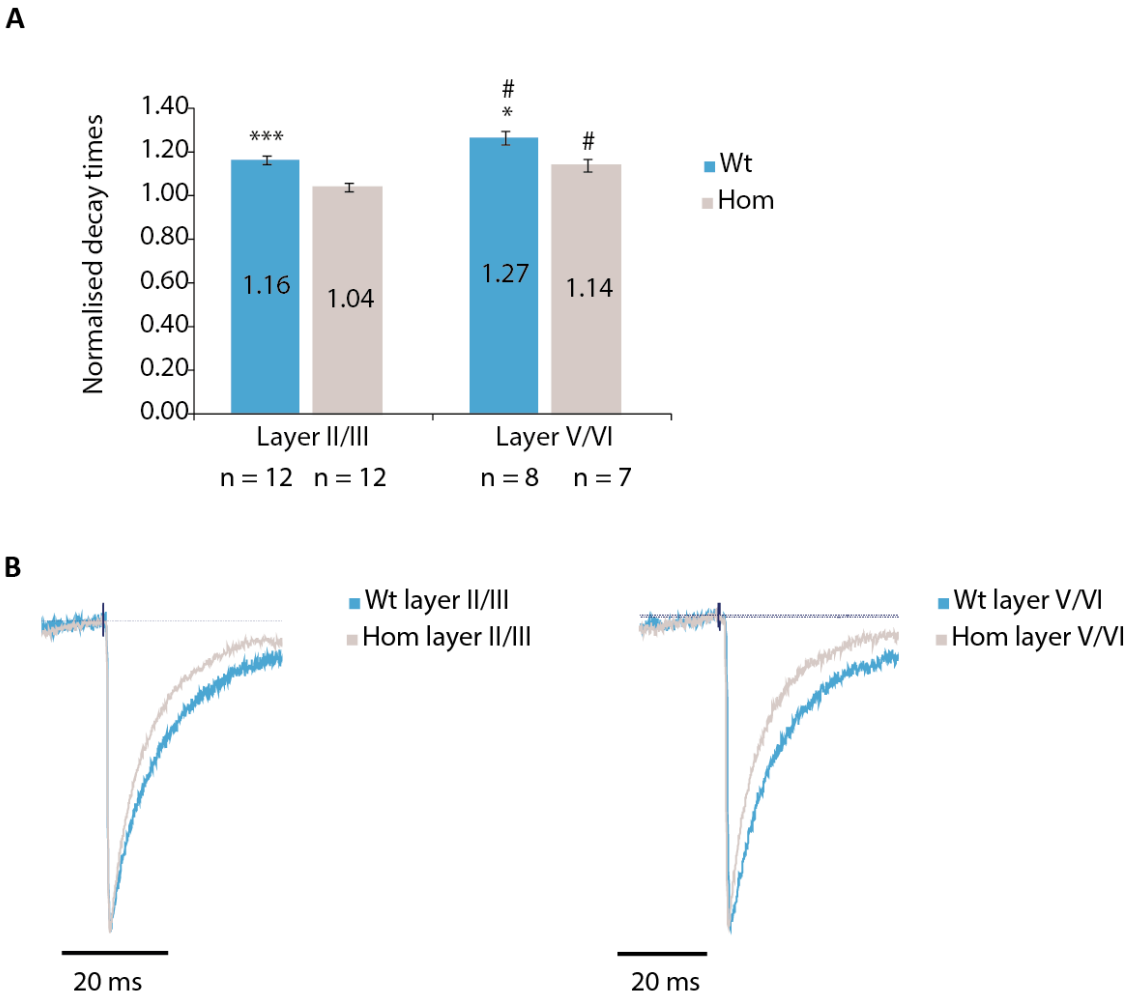

Figure 4.7: Prolongation of sIPSCs in response to THDOC depends upon cortical cell layer and genotype

A. Bar plot showing changes in sIPSC decay times normalised to aCSF for $\alpha2^{WT}$ and $\alpha2^{M/M}$ littermates in different layers of the mPFC following the application of 100 nM THDOC. # - P <0.05 layer V/VI vs layer II/III, unpaired t-test, * - P < 0.05, ***-P < 0.01 $\alpha2^{M/M}$ vs $\alpha2^{WT}$ unpaired t-test. **B**. Representative peak-scaled averaged sIPSCs (from > 100 sIPSCs). Note prolonged decay times for $\alpha2^{WT}$ compared to $\alpha2^{M/M}$ sIPSCs in layer II/III and layer V/VI. Bars represent mean ± SEM.

The sIPSC frequency, while increased in $\alpha2^{WT}$ in the presence of THDOC (Table 4.7), did not appear significantly elevated in $\alpha2^{M/M}$ (Table 4.8) and, overall, changes in frequency did not differ between genotypes (Table 4.9). This could potentially be due to subtle changes in activity of GABAergic interneurons in $\alpha2^{M/M}$ mice. A loss (disinhibition) of endogenous neurosteroid-mediated inhibition of interneurons at α2-$GABA_A$Rs could explain an increased release of GABA onto PCs in this case.

sIPSC parameters in $\alpha2^{WT}$		aCSF	THDOC
Frequency [Hz]	**Layer II/III**	10.67 ± 1.59 (n=12)	11.63 ± 1.42 (n=12)*
	Layer V/VI	10.77 ± 1.27 (n=8)	12.05 ± 1.37 (n=8)*
Peak amplitude [pA]	**Layer II/III**	-28.03 ± 1.95 (n=12)	-28.97 ± 1.73 (n=12)
	Layer V/VI	-25.32 ± 0.99 (n=8)	-26.93 ± 1.74 (n=8)
Decay time [ms]	**Layer II/III**	8.55 ± 0.51 (n=12)	9.86 ± 0.48 (n=12)***
	Layer V/VI	8.11 ± 0.35 (n=8)	10.23 ± 0.40 (n=8)***
Rise time [ms]	**Layer II/III**	0.57 ± 0.07 (n=12)	0.67 ± 0.10 (n=12)
	Layer V/VI	0.62 ± 0.03 (n=8)	0.67 ± 0.03 (n=8)

Table 4.7: Comparison of sIPSC parameters before and after THDOC in $\alpha2^{WT}$ pyramidal neurons
Comparison of 100 nM THDOC-mediated changes on sIPSC parameters in $\alpha2^{WT}$ PCs across different layers of the mPFC. Cell numbers are shown in parentheses. * - $P < 0.05$; *** - $P < 0.001$ THDOC vs aCSF, paired t-test (decay time) or Wilcoxon matched pairs test (frequency).

sIPSC parameters in $\alpha2^{M/M}$		aCSF	THDOC
Frequency [Hz]	**Layer II/III**	13.7 ± 1.7 (12)	14.8 ± 2.2 (12)
	Layer V/VI	10.2 ± 1.5 (7)	10.4 ± 1.2 (7)
Peak amplitude [pA]	**Layer II/III**	-26.0 ± 1.2 (12)	-27.0 ± 1.1 (12)
	Layer V/VI	-27.8 ± 0.7 (7)	-28.2 ± 0.8 (7)
Decay time [ms]	**Layer II/III**	7.4 ± 0.3 (12)	7.6 ± 0.3 (12)
	Layer V/VI	9.7 ± 0.3 (7)	11.0 ± 0.4 (7)**
Rise time [ms]	**Layer II/III**	0.6 ± 0.05 (12)	0.61 ± 0.04 (12)
	Layer V/VI	0.6 ± 0.02 (7)	0.65 ± 0.02 (7)

Table 4.8: Comparison of sIPSC parameters before and after THDOC in $\alpha2^{M/M}$ pyramidal neurons
Comparison of 100 nM THDOC-mediated changes on sIPSC parameters in $\alpha2^{M/M}$ PCs across different layers of the mPFC. Cell numbers are shown in parentheses. ** - $P < 0.01$ THDOC vs aCSF, paired t-test.

Normalised sIPSC and tonic parameters after THDOC		$\alpha2^{WT}$	$\alpha2^{M/M}$
Frequency	**Layer II/III**	1.14 ± 0.06 (12)	1.07 ± 0.04 (12)
	Layer V/VI	1.13 ± 0.05 (8)	1.06 ± 0.06 (7)
Peak amplitude	**Layer II/III**	1.05 ± 0.03 (12)	1.05 ± 0.05 (12)
	Layer V/VI	1.06 ± 0.06 (8)	1.02 ± 0.02 (7)
Decay time	**Layer II/III**	1.16 ± 0.02 (12)	1.04 ± 0.02 (12)**
	Layer V/VI	1.27 ± 0.03 (8)$^{\#}$	1.14 ± 0.03 (7)*$^{\#}$
Rise time	**Layer II/III**	1.16 ± 0.08 (12)	1.04 ± 0.03 (12)
	Layer V/VI	1.09 ± 0.06 (8)	1.09 ± 0.06 (7)

Table 4.9: Effect of THDOC on sIPSC parameters for $\alpha2^{WT}$ and $\alpha2^{M/M}$ mPFC neurons

Comparison of 100 nM THDOC-mediated changes in sIPSC kinetics (normalised to values in aCSF) between $\alpha2^{WT}$ and $\alpha2^{M/M}$ littermates across different layers of the mPFC. Cell numbers are shown in parentheses. # - $P < 0.05$ layer V/VI vs layer II/III, unpaired t-test. * - $P < 0.05$, **- $P < 0.01$, $\alpha2^{WT}$ vs $\alpha2^{M/M}$, unpaired t-test.

4.3 Discussion

4.3.1 Pyramidal cell parameters and GABA inhibition varies across mPFC layers

The rodent mPFC correlates functionally with dorso-lateral regions of the human PFC and has a similar responsibility for executive function, i.e. the selection of context-specific behavioural responses (Uylings et al., 2003).

It is a highly compartmentalised yet interconnected structure. While the superficial layers (I-III) are mainly thought to receive and process inputs, layers V-VI of the rodent mPFC are thought to provide the main outputs, sending efferents to subcortical brain structures such as the striatum, amygdala and thalamus (Riga et al., 2014). It is not surprising then, given the distinct functional roles and different structural connectivity pertaining to specific cortical layers, that these should vary in their cytoarchitecture all the way down to their molecular composition of receptors (Dégenètais et al., 2002; Dembrow and Johnston, 2014; Riga et al., 2014).

Previous studies have shown that $GABA_AR$ subtype expression profiles vary in different cortical layers. For example, α2-$GABA_ARs$ and αβδ-$GABA_ARs$ are more strongly expressed in superficial layers, while α5-$GABA_ARs$ are mostly found in the deeper layers (Pirker et al., 2000; Sieghart and Sperk, 2002). Morphologically, PCs in superficial layers vary from those in deeper layers in that they tend to have smaller somata and shorter principal dendrites (van Aerde and Feldmeyer, 2015; Amatrudo et al., 2012; Kawaguchi, 1993).

In the present study, Lucifer yellow-filled PCs in different layers did not show obvious differences in morphology, at a qualitative level; though while most cellular parameters (e.g., input resistance) did not vary significantly between the layers, we did resolve a larger membrane capacitance in layer V/VI. This would be in accord with the typically larger cell soma sizes found in the inner PFC layers (van Aerde and Feldmeyer, 2015).

4.3.2 There are no laminar differences in GABAergic tonic inhibition

Interestingly, previous studies could not detect the presence of a GABA-mediated tonic current in either layer II/III (Hoestgaard-Jensen et al., 2010; Salling and Harrison, 2014) or layer V/VI (Drasbek and Jensen, 2006; Weitlauf and Woodward, 2008) by using a selection of GABA blockers such as gabazine, picrotoxin and bicuculline. In murine mPFC slices in the present study, however, tonic GABA currents of approximately equal amplitude across the cortical layers were found. The difference in detection may be due to different species (rat vs mouse) and the cortical regions examined - not all of the published studies specified which area of the cortex was chosen for recording. This is important as electrophysiological properties can vary greatly between cortical regions (van Aerde and Feldmeyer, 2015; Kawaguchi, 1993).

Furthermore, tonic currents are by their nature quite small and can vary greatly with slightly different experimental recording methodologies (Bright and Smart, 2013). For example, different $GABA_AR$ blockers, typically used to reveal tonic currents, vary in their pharmacological properties (Bright and Smart, 2013; Ueno et al., 1997). Notably, whereas bicuculline was used here, some of the aforementioned studies used gabazine or picrotoxin. While both bicuculline and gabazine are competitive agonists, they can also act as negative allosteric inhibitors but to different extents, with bicuculline being considerably more effective in this role and more efficient at blocking tonic $GABA_AR$-mediated currents (Yeung, 2003) especially if there is a spontaneous component to the tonic current. Picrotoxin, on the other hand, has conventionally been described as a non-competitive blocker, inhibiting ion-flow by binding inside the channel pore (Inoue and Akaike, 1988; Sedelnikova et al., 2006). There is, however, contrasting evidence suggesting picrotoxin is a mixed / non-competitive inhibitor acting allosterically by stabilising a closed or desensitised channel state (Newland and Cull-Candy, 1992; Smart and Constanti, 1986).

Laminar differences in tonic GABA currents have been reported for cortical PCs in visual and somatosensory cortex (Jang et al., 2013; Yamada et al., 2007). However, no such difference was observed here in the mPFC (Table 4.6, Figure **4.4**). Despite the differential

laminar distribution of α5-$GABA_A$Rs and αβδ-$GABA_A$Rs (Pirker et al., 2000; Sieghart and Sperk, 2002), the main contributors to tonic GABAergic inhibition (Brickley and Mody, 2012; Caraiscos et al., 2004; Glykys et al., 2008; Lee and Maguire, 2014; Marowsky and Vogt, 2014), results shown here suggest both of them play a role in tonic inhibition in layer V/VI of the mPFC. However, the relative contribution of either receptor subtype cannot easily be measured. While the superagonist, THIP, was used to probe the presence of αβδ-$GABA_A$Rs, a partially selective inverse agonist (MRK-016) was used to detect the presence of α5-$GABA_A$Rs. The use of an agonist, while detecting the presence of the targeted $GABA_A$Rs, does not necessarily allow conclusions about whether these same receptors contribute to postsynaptic currents under physiological conditions. Factors such as the level of released GABA will be important determinants as to which extrasynaptic $GABA_A$RS are activated, particularly as different $GABA_A$Rs can exhibit different affinities for GABA (Bright and Smart, 2013; Scimemi et al., 2005).

In addition, there is evidence for a considerable fraction of extrasynaptic δ-$GABA_A$Rs existing in a desensitised state (Bright et al., 2011; Mortensen et al., 2010), which would tend to decrease their responsiveness to THIP. Furthermore, THIP could be displaced by GABA due to the high affinity for GABA of δ-$GABA_A$Rs (Brown et al., 2002; Houston et al., 2012; Mortensen et al., 2011) and it may therefore show reduced efficacy at receptors in a physiological context, but this would need quite high levels of GABA. A similar caveat presents itself for using MRK-016. The present study suggests a significant contribution for α5-$GABA_A$Rs to tonic inhibition by revealing MRK-016-mediated current shifts can account for 50 – 60% of the current shift observed from applying bicuculline. However, the inverse agonist only shows an efficacy of ~50% at $GABA_A$Rs (Chambers et al., 2004), suggesting α5-$GABA_A$Rs to be almost exclusively responsible for tonic inhibition in layer V/VI pyramidal neurons. This, despite the larger expression of α5 in the inner layers, seems unlikely and may in part stem from non-selective inhibition of other $GABA_A$Rs by MRK-016 at the concentration used (100 nM). Therefore, with the current set of pharmacological tools, it is difficult to precisely quantify the contributions of different $GABA_A$Rs to tonic inhibition in mPFC PCs. Nevertheless, it is clear from using

THIP and MRK-016 that both α5 and δ subunit-containing $GABA_A$Rs are contributing to tonic inhibition in layer V/VI.

For layer II/III PCs, we might expect extrasynaptic $GABA_A$Rs composed of αβδ subunits to show clear responses to THIP, and these would be expected to be greater in layer II/III compared to layer V/VI (as observed by Salling and Harrison, 2014) and the reverse should be the case for α5-$GABA_A$Rs, given their reported laminar distribution (Pirker et al., 2000).

4.3.3 $\alpha2^{Q241M}$ mutation reveals laminar differences in neurosteroid modulation of GABAergic inhibition

Of the $GABA_A$ α subunit family (α1-α6), the homologous mutation, $\alpha1^{Q241M}$, has been introduced and demonstrated to ablate the potentiation by neurosteroids for all αβγ and αβδ $GABA_A$RS so far investigated, without affecting the fundamental properties of the receptors and their responsivity to GABA, and for α1,2,3 and α5βγ receptors, to benzodiazepines (Hosie et al., 2006, 2009). The $\alpha2^{Q241M}$ mutation has been introduced into a knock-in mouse model and explored with regards to compensatory changes in $GABA_A$R α subunit expression as well as the electrophysiological properties of GABA inhibition in the hippocampus and NAcc (Durkin, 2012).

Here, we studied laminar differences in sIPSC kinetics and tonic inhibition of mPFC PC between $\alpha2^{WT}$ and $\alpha2^{M/M}$ littermates under baseline conditions and in the presence of the neurosteroid THDOC. No differences between $\alpha2^{WT}$ and $\alpha2^{M/M}$ mice were detected with regards to the basal level of tonic inhibition, or baseline sIPSC frequency, amplitude and rise time. Furthermore, no differences in the expression of δ or α5 subunit containing $GABA_A$Rs were detected by changes in holding current or RMS noise after applying the relatively selective ligands, THIP or MRK-016.

With regard to synaptic GABA inhibition, interestingly, there was a difference in basal sIPSC decay time in layer II/III between $\alpha2^{WT}$ and $\alpha2^{M/M}$ PC, with faster decay noted for sIPSCs recorded from $\alpha2^{M/M}$ neurons. Given that there is no evidence for a difference in

subunit expression between $\alpha2^{M/M}$ and $\alpha2^{WT}$ in the cortex, cerebellum, hippocampus and NAcc (Durkin, 2012), the difference in decay time observed here is most likely not due to varying $GABA_AR$ subunit composition. Instead, it is more likely indicative of an endogenous neurosteroid tone. Since endogenous neurosteroids prolong the decay time for αβγ-$GABA_ARs$ (Belelli and Herd, 2003), and this effect has been abolished for a subset of $GABA_ARs$ (i.e. those that contain α2 subunits) in $\alpha2^{M/M}$, the faster decay time in $\alpha2^{M/M}$ PCs might reflect the absence of a physiological sIPSC prolongation via neurosteroids, under basal conditions (i.e., no exogenous neurosteroids applied). The interesting absence of a significant difference basal decay time for sIPSCs in layer V/VI may either imply a lack of, or lower levels of, endogenous neurosteroids, or might be a reflection of a much lower expression level of α2 subunits in this layer (Pirker et al., 2000; Sieghart and Sperk, 2002). Furthermore, while expression patterns of $GABA_AR$ subunits are overall unaltered in $\alpha2^{M/M}$ cortex (Durkin, 2012), the possibility of changes pertaining to individual cortical layers cannot be excluded, which will have to be ascertained by using immunohistochemical methods.

Another discovery from the present study was a laminar difference in both $\alpha2^{M/M}$ and $\alpha2^{WT}$ neurons in their response to THDOC. sIPSCs recorded from deep, inner layers showed a significantly larger increase in decay times after applying THDOC than sIPSCs recorded from outer, superficial layers. A similar observation was made in human cortex, showing an enhanced effect on GABAergic inhibition in response to high doses of THDOC in deeper compared to more superficial layers (Nguyen et al., 1995) and is in line with known regional differences in the expression of $GABA_AR$ subtypes with varying pharmacological properties. These results might also suggest that the reason for not observing an effect on the sIPSC decay in layer V/VI PCs of $\alpha2^{M/M}$ slices is that steroid production is possibly lower in this region.

Independent of the genotype, the laminar difference in sensitivity to THDOC may be a result of altered neurosteroid-sensitivity of synaptic $GABA_ARs$, either caused by post-translational modifications or changes in $GABA_AR$ expression across those layers. For example, phosphorylation has been shown to alter neurosteroid sensitivity of synaptic

α1- and extrasynaptic α4-containing $GABA_AR$s (Adams et al., 2015). In addition, the neurosteroid sensitivity of $GABA_AR$s is influenced mainly by the identity of the α subunit and whether a γ or δ subunit has been incorporated. Notably, $GABA_AR$s containing α2, α4 or α5 subunits are less sensitive to THDOC compared to those with α1, α3 and α6 subunits, while receptors incorporating γ2 subunits show higher sensitivity to neurosteroids compared to γ1 subunit counterparts. It is also important to note that δ subunit-containing $GABA_AR$s show the highest neurosteroid-mediated augmentation of GABA currents, as assessed in *Xenopus* oocyte expression systems (Belelli et al., 2002). Presumably this reflects the increased efficacy of neurosteroids at αβδ receptors.

By examining $GABA_AR$ subunit expression profiles in rat brain, only α3, α5 and γ2 subunits are more highly expressed in the inner cortical layers compared to the superficial layers (Pirker et al., 2000; Wisden et al., 1992). On this basis, α3βγ2 receptors may be the most likely candidates underlying the increased THDOC sensitivity in deeper layers. This is supported by our findings showing only 25% of THDOC effect on decay time prolongation remains in layer II/III of $\alpha2^{M/M}$ mPFC, while 52% remains in Layer V/VI, suggesting the presence of other $GABA_AR$s contributing towards THDOC mediated prolongation of sIPSCs in that area. Further studies involving $GABA_AR$ selective compounds and kinase inhibitors, in conjunction with THDOC, would be necessary to explore the implications of these results.

4.3.4 The physiological role of α2-$GABA_AR$ in mPFC inhibition

Generally, from an *in vivo* viewpoint, $GABA_AR$s containing the α2 subunit are of importance to an array of processes in the brain. They are thought to mediate the anxiolytic effect of the benzodiazepines (Dixon et al., 2008; Löw et al., 2000); they have been linked to addiction by being involved in behavioural sensitisation to substances such as cocaine (Dixon et al., 2010; Jin et al., 2014; Morris et al., 2008); they are involved in neural circuits underpinning fear and are therefore likely to play roles in neuropsychiatric disorders such as schizophrenia, anxiety and depression (Engin et al., 2012; Rudolph and Möhler, 2014; Vollenweider et al., 2011). Overall, α2 subunits are the second-most expressed α subunit after α1, being incorporated in about 15-20% of

all $GABA_ARs$ (Möhler, 2002). While α1 is ubiquitously expressed throughout the brain, α2 subunits are mostly found in the forebrain, particularly in regions that are generally linked to anxiety disorders such as the amygdala and NAcc (Möhler, 2012; Sieghart and Sperk, 2002). In the rat mPFC, layers II/III show the highest levels of α2 subunit expression (Pirker et al., 2000). The decay kinetics of IPSCs show a slightly slower profile when compared to the decays of currents mediated by α1-$GABA_ARs$ (Lavoie et al., 1997) and they are enriched at the AIS of PCs (Nusser et al., 1996b), suggesting a possible role in controlling neuronal output activity. An observation supporting this notion of controlling neural activity has been made in the hippocampus, where cholinergic network oscillations were found to be regulated by α2-$GABA_ARs$ located in the CA3 region (Heistek et al., 2013).

Using an $\alpha2^{Q241M}$ mouse model, the electrophysiological consequences of neurosteroid insensitivity of this subunit were explored in the hippocampus (DG, CA1) and NAcc (Durkin, 2012), brain areas showing a high expression of α2 (Fritschy and Möhler, 1995; Pirker et al., 2000; Sieghart and Sperk, 2002). There, introduction of the mutation significantly decreased THDOC-mediated potentiation of IPSC decay times in all areas, revealing an important contribution of α2 to synaptic GABAergic inhibition. Interestingly, inhibiting neurosteroid modulation at the α2 subunit also reduced a tonic current in DGGCs, suggesting a novel role for α2 in mediating tonic inhibition. On a behavioural level, this study also showed an increased anxiogenic phenotype of $\alpha2^{M/M}$ mice compared to $\alpha2^{WT}$ littermates and a lack of response to neurosteroid treatment.

In the present study, a significant contribution of α2 subunits towards synaptic inhibition has now been identified across the mPFC cell layers, II/III and V/VI. Neurons expressing $\alpha2^{M/M}$ $GABA_ARs$ showed a reduced prolongation of decay times compared to $\alpha2^{WT}$ (25% effect remaining in layer II/III, 52% in layer V/VI), which, in the absence of any evidence for compensatory changes, can be attributed to a lack of neurosteroid modulation at α2 subunit-containing receptors. Interestingly, the difference in sIPSC prolongation across mPFC layers between $\alpha2^{M/M}$ and $\alpha2^{WT}$ neurons suggests that the contribution of α2-$GABA_ARs$ towards synaptic inhibition also varies and is smaller in the deep, inner layers

compared with the superficial, outer layers of the mPFC. This is in accord with their higher expression levels noted in layer II/III from ICC studies (Pirker et al., 2000).

In regard to physiological roles, the outer layers of the mPFC are thought to be mostly responsible for processing inputs from sensory-motor areas and thalamus (targeting the dorsal mPFC and ACC) and inputs from the hippocampus and amygdala (to the ventral mPFC) and forwarding them to the deep, inner layers, which are the main efferent outputs to subcortical regions such as the thalamus and NAcc (Gabbott et al., 2005; Heidbreder and Groenewegen, 2003; Kesner and Churchwell, 2011; Riga et al., 2014; Shepherd, 2009). Given this distribution of different functions across cortical layers, this suggests α2-$GABA_A$Rs are most likely to be broadly involved across the spectrum of mPFC functions. For example, the previously observed anxiogenic phenotype of $\alpha2^{Q241M}$ mutant mice (Durkin, 2012) might, in part, be due to the reduced basal potentiation of mPFC GABA-mediated inhibition described in the present study. The results of other studies tend to support this notion, having shown links between changes in PFC α2 subunit expression and psychological conditions. For example, stress exposure of adult mice can induce anxiety-like behaviours and increases PFC α2 subunit expression (Jacobson-Pick et al., 2012), while an upregulation of α2 subunits has been found in layer II dlPFC neurons in schizophrenic patients (Beneyto et al., 2011). Furthermore, certain genetic $GABA_A$R α2 subunit polymorphisms have been associated with greater sensitivity to alcohol (Haughey et al., 2008) and alcohol dependence (Edenberg et al., 2004), and fMRI studies have shown that human subjects carrying such polymorphisms had a greater mPFC response to odour cues from their preferred alcoholic drinks (Kareken et al., 2010).

The $\alpha2^{Q241M}$ mutation had no effect on tonic inhibition in layers II/III or V/VI, which indicates that α2-$GABA_A$Rs are involved exclusively at inhibitory synaptic sites in the mPFC. This could have implications for their functional role in cortical networks given the distinct physiological effects of tonic and phasic inhibition (Farrant and Nusser, 2005; Mody and Pearce, 2004; Semyanov et al., 2004). Consequently, α2-$GABA_A$Rs are well placed to be involved in the dendritic integration and regulation of PC spike patterns as

well as generating network oscillations, rather than modulating thresholds for cellular and network excitability and adjusting cellular “gain” through an increase in membrane conductance. The potential for neurosteroid-mediated influences on PC excitability via α2-containing receptors, as well as the effect of tonic and phasic inhibition on mPFC PC excitability, is explored in the next chapter.

4.4 Conclusions

1. The cellular properties of pyramidal neurons are mostly uniform across layers II/III and V/VI, apart from a larger cell membrane capacitance in deep, inner layers, reflecting the larger average cell size of PC somata in layers V/VI.

2. By measuring the basal properties of GABA-mediated synaptic and tonic inhibition, there was no evidence for compensatory changes in the $\alpha2^{M/M}$ neurons in the mPFC.

3. In layer II/III, measuring GABA-mediated sIPSC kinetics in $\alpha2^{WT}$ and $\alpha2^{M/M}$ neurons revealed that basal sIPSC decay times are shorter for $\alpha2^{M/M}$, which is indicative of an endogenous neurosteroid tone in these neurons.

4. Neurons in the deep, inner layers of the mPFC exhibited a greater prolongation of their sIPSC decays in response to applied THDOC, which most likely reflects variations in the laminar expression of synaptic $GABA_A$Rs subtypes, or changes in their post-translational modification.

5. Examining GABA-mediated tonic inhibition using pharmacological probes indicated the presence of both α5 subunit and δ subunit-containing extrasynaptic $GABA_A$Rs in layer V/VI PCs of the mPFC.

6. No difference was noted for $\alpha2^{WT}$ and $\alpha2^{M/M}$ neurons in the level of tonic inhibition suggesting α2 subunits play little or no role in extrasynaptic $GABA_A$Rs in the mPFC.

7. $GABA_A$Rs containing α2 subunits contribute significantly to the level of synaptic inhibition of mPFC pyramidal cells, and their modulation by neurosteroids. Their contribution varies with the cortical layer, amounting to ~75% in layer II/III and ~48% in layer V/VI neurons.

5 The influence of GABAergic inhibition on PC excitability

5.1 Introduction

The main function of neurons is to communicate information from the external or internal environment and to produce an adequate physiological response. The brain serves as the central processing and relay station, selecting and integrating relevant information. At a cellular level, this information is coded by the frequency of action potentials (APs) travelling along the axon. On a network scale, the interchanging phases of excitation and inhibition of many neurons firing together create oscillations in electrical activity, a prominent characteristic of cortical networks. These are thought to play a role in transmitting information within the cortex by connecting neuronal populations that are oscillating in phase (Isaacson and Scanziani, 2011).

5.1.1 What are the factors that govern neuronal excitability?

Whether a neuron is stimulated to fire an AP depends on the temporal and spatial integration of the multitude of inputs it receives along its dendritic tree, somatic and perisomatic regions. The impact any given input has on the cell it targets, therefore, not only depends on the strength of a single PSP, but also on its location and temporal origin relative to other inputs. According to the traditional, linear view of dendritic integration, PSPs will travel passively along the dendrite and gradually decay in amplitude (according to the cell's space constant; Rall, 1967, 2006; Rall and Rinzel, 1973) unless they are reinforced (or diminished) by further coincident inputs. The sum of inhibitory and excitatory inputs onto a single neuron will trigger an AP, only if a threshold depolarisation is attained at the AIS. The magnitude and time-course of depolarisation is reflected by the varying frequencies of AP trains. In addition to this traditional view of AP generation at the AIS, which is dependent on voltage-gated sodium-channels, more recent evidence highlights the significance of non-linear dendritic properties wherein the dendritic tree possesses the ability to actively process and integrate incoming signals (see Branco and Häusser, 2011; Major et al., 2013; Palmer, 2014 for recent reviews). Amongst these properties are AP back-propagation (antidromic) into the dendritic tree

and dendritic spikes driven by local activation of voltage-gated Ca^{2+}-channels and NMDARs, which contribute to modulating synaptic integration and thus cellular signalling.

A number of factors can impact on the linear and non-linear integration of inhibitory and excitatory inputs a neuron receives and hence how likely it is to generate an AP. For example, the ion channel composition of the cell membrane influences its input resistance and conductance and thus affects the amplitude of PSPs as well as their temporal decay while travelling along the dendritic tree before reaching the AIS or being integrated with another input (Rall, 1967, 2006; Rall and Rinzel, 1973). Furthermore, the diameter and length of the dendrite a particular PSP has to travel also determine the time-course of decay. In addition to the number and type of ion channels present, the electrochemical gradient of ions across the membrane determines the driving force and direction of current flow, ultimately defining the size and shape of the PSP. As described in the introduction, the distribution of ions across the membrane is regulated by a number of different ion transporters and hence the type of transporter can significantly shape the postsynaptic response to a neurotransmitter. An example is the developmental shift from a depolarising to a hyperpolarising effect of GABA mediated by $GABA_A$Rs. In immature neurons, NKCC1 is responsible for the intracellular accumulation of Cl^-, depolarising the chloride reversal potential with respect to the membrane potential of the cell, thus leading to Cl^- efflux and depolarisation upon channel opening (Rivera et al., 2005).

Finally, the AIS itself possesses signal-processing capability based on the type and localisation of voltage-gated ion-channels and the influence of direct synaptic inputs (reviewed in Kole and Stuart, 2012). In cortical pyramidal neurons, for example, the inactivation of a subtype of K^+-channels at the AIS leads to a broadening of APs and thus an increase in transmitter release (Kole et al., 2007). Furthermore, dopaminergic inputs onto interneurons in the brainstem have been shown to selectively inhibit Ca^{2+}-channels at the AIS, thus modulating AP firing patterns (Bender et al., 2012).

The mechanisms that govern neuronal excitability are very robust, and at the same time, can undergo dynamic changes, in particular in response to endogenous neuromodulators, which result in a modification of neuronal output (Goldman et al., 2001).

5.1.2 GABAergic inhibition and cellular excitability

GABAergic interneurons comprise about 20% of cortical neurons and are an integral part of local neural networks, synapsing onto PCs as well as other interneurons, and shaping cortical output through feed-forward as well as feed-back inhibition (for a review, see Isaacson and Scanziani, 2011). GABAergic inhibition, through $GABA_A$Rs and $GABA_B$Rs, can impact on the excitability of a postsynaptic cell. $GABA_A$Rs are the main mediators of fast-acting inhibition, while postsynaptic $GABA_B$Rs provide a slower onset inhibitory conductance by coupling to K^+ channels (Dutar and Nicoll, 1988; Otis and Mody, 1992). The activation of $GABA_A$Rs reduces neuronal excitability by changing the membrane potential to approximate the Cl^- reversal potential, which in many mature neurons is usually hyperpolarised to the RMP. In addition, $GABA_A$Rs can decrease neuronal excitability by increasing the membrane conductance. In accordance with Ohm's law, an increase in membrane conductance leads to a decrease in input resistance and thus to a reduction in the amplitude of a concomitant PSP, a process known as "shunting inhibition" (reviewed in Mann and Paulsen, 2007; Staley and Mody, 1992). In most cases, this is probably the more dominant form of inhibition, since the Cl^- reversal potential and RMP tend to be quite close to each other, implying membrane potential shifts will generally be small.

GABA can initiate two forms of inhibition, phasic and tonic, which can have different effects on neuronal output (Farrant and Nusser, 2005). Phasic inhibition is spatially and temporally integrated to produce specific spike firing patterns, and, on a network level, synchronises the activity of pyramidal cells to modulate oscillations (Huntsman, 1999; Wang and Buzsaki, 1996). Furthermore, it can serve to increase the dynamic range through feed-forward inhibition (Pouille et al., 2009). Tonic inhibition, on the other hand, sets the threshold for neuronal excitability by increasing the membrane

conductance, thereby decreasing amplitude and increasing the temporal decay of PSPs. Consequently, this leads to a reduced likelihood for AP generation. Another function of tonic inhibition is gain control: in experiments using dynamic clamp, injection of typical excitatory conductance waveforms to mimic physiological input (compared to steady-step current injections), inhibitory tonic conductances reduced the slope of the input-output curve, i.e. the gain (Chance et al., 2002; Mitchell and Silver, 2003). In this situation, a reduced gain equates to a reduced increase in the response of a neuron to a given increase in synaptic input. It also means an increase in "resolution", i.e. the number of different inputs that can be distinguished becomes larger. On a network level, increasing gain by varying tonic inhibitory input can have a significant effect on network oscillations. Since they rely on recurrent excitation, decreasing the sensitivity to excitatory inputs in oscillatory networks can result in a reduction of feedback excitation (Chance et al., 2002).

In addition to the type of GABAergic inhibition, the impact on excitability can vary with the location of the inhibitory input (Cobb et al., 1995; Mann and Paulsen, 2007; Pouille et al., 2013). Somatic and axo-axonic connections formed by basket and Chandelier cells, respectively, can exert strong control over PC output (Pouille and Scanziani, 2001). Single dendritic inputs, on the other hand, may have less immediate impact on neuronal excitability, due to the decay in synaptic potentials along dendritic branches. Instead, these inputs appear to be involved in local dendritic computations and in modulating the impact of dendritic calcium spikes and AP back-propagation (Higley, 2014; Miles et al., 1996; Mody and Pearce, 2004).

Parallel to the difference in biophysical properties of distinct subcellular membrane compartments, $GABA_AR$ subtypes are differentially distributed throughout the cell (Nusser et al., 1996b, 2012), shaping the kinetic profiles of inhibitory inputs and thus allowing fine-tuning of cellular excitability. The $GABA_AR$ α2 subunit, for example, produces longer decay times in GABA synaptic currents compared to the more ubiquitous α1 subunit (Lavoie et al., 1997) and has been implicated in alterations to GABAergic inhibition in psychiatric disease (Engin et al., 2012; Rudolph and Möhler,

2014; Vollenweider et al., 2011). Given its relative enrichment at the AIS (Nusser et al., 1996b), it may play a significant role in shaping AP generation and controlling cortical PC excitability (Heistek et al., 2013).

Finally, while GABAergic transmission is mostly inhibitory, under certain circumstances the activation of $GABA_AR$s can instead lead to a net depolarisation (Stein and Nicoll, 2003). This is exemplified by the generation of "rebound" action potentials where an initial hyperpolarising potential is followed by a supra-threshold depolarisation. This is thought to be mediated through interaction of $GABA_AR$ activation with voltage-dependent conductances such as Ca^{2+} (Cobb et al., 1995; Mann and Paulsen, 2007). Another is due to a depolarising response to GABA itself, which is, as described above, dependent on the chloride electrochemical gradient across the membrane (Chavas and Marty, 2003; Rivera et al., 2005). Cases of excitatory GABAergic activity can be found in early neuronal development (Ben-Ari et al., 2012) and at the AIS (Gulledge and Stuart, 2003; Kole and Stuart, 2012). While this could potentially lead to an increase in excitability via GABAergic transmission, the concomitant increase in membrane conductance caused by GABA may still result in a net inhibitory effect, depending on the location and timing of excitatory inputs (Lamsa et al., 2000; Staley and Mody, 1992). Similarly, inhibitory GABAergic responses can have a net excitatory effect depending on their location and timing relative to excitatory inputs: In a study using extracellular and gramicidin-perforated patch recordings, Gulledge and Stuart (2003) found cortical GABAergic PSPs to be depolarising, but somatic GABAergic PSPs nevertheless had an inhibitory effect on temporally or spatially distant excitatory inputs, while the effect on coincident excitatory inputs was excitatory (Gulledge and Stuart, 2003). These observations further stress the importance of timing of PSPs and localisation of synaptic inputs in shaping synaptic integration and ultimately neuronal activity.

5.1.3 Objectives

The goal in this chapter was to investigate the importance of α2-$GABA_A$Rs on PC excitability in the mPFC. Due to their relative concentration at the AIS, these receptors, and the extent of any endogenous modulation, were hypothesised to be involved in regulating spike firing frequency. To test this, we used the neurosteroid-insensitive $\alpha2^{Q241M}$ mutant and compared the effects of THDOC on AP frequency between $\alpha2^{M/M}$ and $\alpha2^{WT}$ mice. In addition, the overall significance of changes in tonic and phasic inhibition for PC excitability was explored using a range of specific $GABA_A$R modulators.

5.2 Results

In chapter 4, the potential of exogenous application of the neurosteroid THDOC to modify synaptic inhibition in mPFC PCs was verified, revealing a significant contribution of α2-containing $GABA_A$Rs to phasic inhibition. Here we assessed, whether α2-$GABA_A$Rs are able to modulate cellular excitability. To this end, a current-clamp protocol was employed as described in Materials & Methods. In brief, PCs were identified morphologically as before and verified electrophysiologically based on their spiking pattern in response to a set of constant current injection steps (-200 to +200 pA in 20 pA increments, with a duration of 200 ms, see Materials & Methods). The firing frequency and the rheobase (the minimum depolarising current injection necessary to elicit an AP) of PCs varied between cells, with the rheobase ranging between 60-140 pA and frequency between 8-20 Hz. Under control conditions, PCs commonly displayed a hyperpolarising voltage 'sag' in response to hyperpolarising current injections and long after-hyperpolarisations as well as accommodation of AP frequency in response to supra-threshold current injections, as has been described previously (van Aerde and Feldmeyer, 2015). Only recordings from neurons with a stable membrane potential more negative than -60 mV were accepted for analysis. Excitability was initially assessed by depolarising neurons with a 1 s current-injection step above threshold (usually 200 pA, though the magnitude was adjusted based on the threshold of the first spike during the initial current step protocol, see Materials & Methods). After this, a 30 s recovery period was allowed between consecutive current-injection steps. AP frequency was measured as the average inter-event-interval (IEI) between spikes elicited by one current injection step, and this value was averaged over at least 5 consecutive recordings (i.e. a period of 2.5 min).

5.2.1 Neurosteroids affect PC excitability under conditions of high tonic GABA concentrations

Initially, the effect of THDOC alone on AP IEIs was assessed in layer II/III pyramidal neurons of $\alpha2^{WT}$ mice to reflect the conditions used for voltage-clamp experiments described in Chapter 4. We anticipated that, due to its enhancing effect on synaptic

inhibition, THDOC would reduce PC excitability, whereas a subsequent application of bicuculline should reverse this effect and increase excitability.

To this end, normalised IEIs for THDOC (300 nM) and bicuculline (20 µM) were compared to those measured in control aCSF (Figure 5.1 A & B – see Table 5.1 for absolute values). Despite the significant effect of 100 nM THDOC on sIPSC decay times (Table 4.1, Chapter 4), no significant reduction in PC firing rate was detected even with a higher concentration of 300 nM THDOC (Figure 5.1 A & B). While normalised IEIs in 300 nM THDOC were significantly reduced by bicuculline as would be expected ($P = 0.04$, paired t-test), they did not differ from control aCSF ($P = 0.27$, one-sample t-test vs null-effect of 1). Surprisingly, bicuculline did not result in the expected increase in firing rate, either ($P = 0.73$, one-sample t-test). One reason for this result is that the GABAergic tone might be too low in the slice preparation to affect excitability with the protocol used here. Therefore, in accord with previous work using these modulators (Jang et al., 2013), the concentration of THDOC was increased to 500 nM, and 5 µM GABA was added to the bath to increase the basal GABA 'tone' without adjusting GABA uptake (Figure 5.1 C & D, Table 5.1). Interestingly, under these conditions, neurons had a significantly faster basal firing rate (IEI = 76 ± 6 ms) compared to neurons stimulated in the absence of GABA (105 ± 7 ms, $P = 0.002$, unpaired t-test with Welch-correction). This was unexpected, given that GABA is inhibitory. Nevertheless, even under these conditions, application of bicuculline did not lead to a significant decrease in IEI compared to a preceding control period in aCSF (one-sample t-test vs null-effect of 1). However, it was sufficient to resolve a significant increase in the IEIs by THDOC compared to either bicuculline ($P = 0.0005$, paired t-test) or a mock application of aCSF ($P = 0.05$, one-tailed Mann-Whitney test).

The PC membrane potentials were monitored to determine if any shifts could underlie the effects of THDOC in GABA-supplemented slices on the IEIs. No effects on membrane potential were observed when applying 500 nM THDOC + 5 µM GABA or bicuculline to slices from either $\alpha2^{WT}$ or $\alpha2^{M/M}$ mice (Table 5.2). Although membrane potential appeared to be more depolarised in $\alpha2^{M/M}$ mice (-70.4 ± 2 mV in aCSF) compared to $\alpha2^{WT}$ (-73 ± 1.6 mV in aCSF), this difference was not statistically significant (unpaired t-

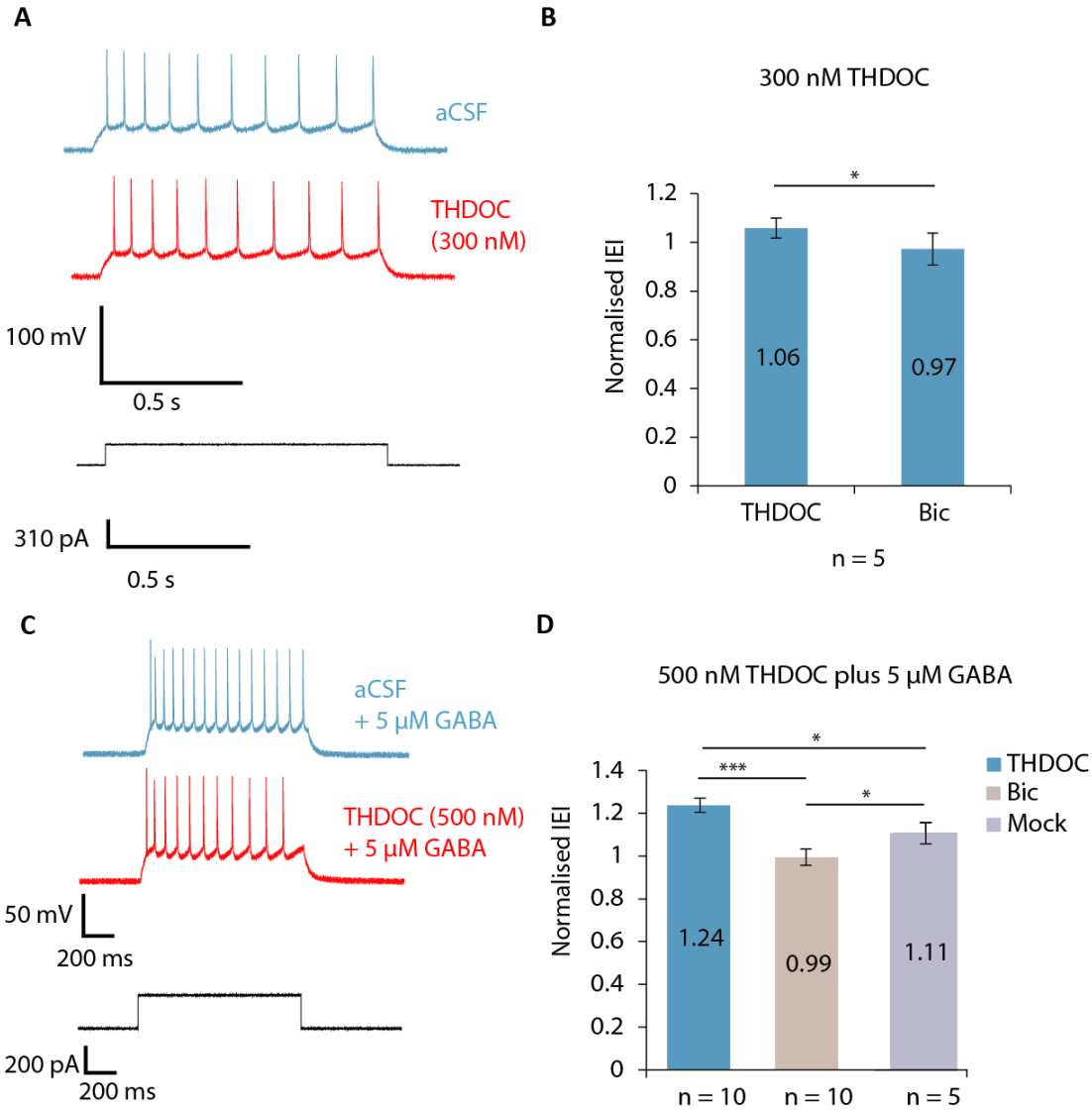

Figure 5.1 THDOC concentration and increasing basal inhibition on PC excitability
A. Representative traces showing the spike trains elicited in LII/III neurons by a 200 pA depolarising current injection step in the presence of aCSF or 300 nM THDOC, for wt slices of mPFC. **B** Excitability of PCs in the presence of THDOC (300 nM) or bicuculline (20 µM) presented as average IEIs normalised to a preceding control period in aCSF (= 1). * - $P < 0.05$, paired t-test. Neither of them is significantly different from the control period in aCSF (one-sample t-tests vs null-effect of 1). **C**. Representative traces showing the spike trains elicited in LII/III neurons by a 200 pA depolarising current injection step in the presence of aCSF or 500 nM THDOC, for wt slices of mPFC supplemented with 5 µM GABA in aCSF. **D.** Excitability of PCs in the presence of THDOC (500 nM) or bicuculline (20 µM; same cell as THDOC) or a mock application of aCSF in the presence of GABA (5 µM). IEIs were normalised to a preceding control period in aCSF. Kruskal Wallis test with subsequent pairwise comparisons: *** - $P < 0.001$, one-tailed Mann Whitney test. * - $P < 0.05$, paired t-test.

test, Table 5.2). As expected, the application of bicuculline significantly increased membrane resistance compared to aCSF in both genotypes (130.5 ± 22.8 MΩ in $\alpha2^{WT}$, P = 0.004, paired t-test and 116.5 ± 19.7 MΩ in $\alpha2^{M/M}$, P = 0.02, paired t-test). There was no difference in membrane resistance between the two genotypes (unpaired t-tests).

Treatment	IEI (ms) no GABA / 300 nM THDOC	IEI (ms) 5 µM GABA / 500 nM THDOC
aCSF	105 ± 7 (5)	76 ± 6 (11)$^{\#\#}$
THDOC	110 ± 4 (5)	109 ± 21 (11)$^{***\#}$
Bicuculline	100 ± 4 (5)	70 ± 4 (11)$^{\#\#\#}$

Table 5.1: The effect of different drugs, varying concentrations of THDOC and GABA on absolute IEIs for layer II/III $\alpha2^{WT}$ mPFC pyramidal neurons

PCs of acute mPFC slices were excited by suprathreshold current injections in the presence and absence of bath applied 5 µM GABA. IEIs of evoked spikes were measured for baseline conditions (aCSF with and without GABA), in the presence of THDOC (300 nM or 500 nM) or in the presence of bicuculline (20 µM). All values are shown as means ± SEM. Cell numbers are shown in parentheses. *** - P < 0.001, THDOC / bicuculline vs aCSF, paired t-test. # - P < 0.05, ## - P < 0.01, ### - P < 0.001, 5 µM GABA vs no GABA; unpaired t-test with Welch-correction.

Drugs and PC membrane parameters		$\alpha2^{WT}$	$\alpha2^{M/M}$
R_M [MΩ] n = 10 ($\alpha2^{WT}$) n = 9 ($\alpha2^{M/M}$)	**aCSF**	97.0 ± 16.4	92. 5 ± 12.4
	THDOC	105.5 ± 15.3	102.4 ± 19.4
	Bic	130.5 ± 22.8**	116.5 ± 19.7*
V_M [mV] n = 11 ($\alpha2^{WT}$) n = 11 ($\alpha2^{M/M}$)	**aCSF**	-73.0 ± 1.6	-70.4 ± 2.0
	THDOC	-73.7 ± 1.7	-70.8 ± 2.0
	Bic	-73.9 ± 1.7	-70.6 ± 2.2

Table 5.2: Effect of THDOC and bicuculline on membrane parameters in wild-type and mutant α2 mice.

Effect of 500 nM THDOC or 20 µM bicuculline (in the presence of 5 µM GABA) on input resistance (R_M) and membrane potential (V_M) in layer II/III pyramidal neurons of $\alpha2^{WT}$ and $\alpha2^{M/M}$ mPFC. **R_M:** There is a significant effect of bicuculline on R_M in both $\alpha2^{WT}$ (P = 0.004, paired t-test vs aCSF) and $\alpha2^{M/M}$ (P = 0.02, paired t-test vs aCSF). There is no difference in average R_M between genotypes (unpaired t-tests). **V_M:** There is no effect of either THDOC or bicuculline on V_M compared to aCSF in either genotype (paired t-tests). There is no difference in average V_M between genotypes (unpaired t-tests) ** - P < 0.01, * - P < 0.05, Bic / THDOC vs aCSF paired t-test.

5.2.2 Basal PC excitability and THDOC-mediated reduction in spiking across mPFC layers

Having ascertained the efficacy of 500 nM THDOC plus 5 µM GABA in modulating PC excitability in wt slices, we next investigated the effect of THDOC on spike firing in the $\alpha2^{M/M}$ mutant. The purpose of this was to examine if α2-$GABA_A$Rs were involved in mediating neurosteroid-effects on neuronal excitability. Furthermore, in light of the laminar variations in electrophysiological properties of PCs (van Aerde and Feldmeyer, 2015), recordings obtained from neurons of different laminar origin were compared.

Firstly, we compared the relative IEI changes in THDOC (500 nM) and GABA (5 µM), (Figure 5.2 A) using the standard constant current step protocol (see Materials & Methods). This revealed no significant differences in IEI between either genotype or the cortical layer (unpaired t-tests). While the absolute basal IEIs (Figure 5.2 B) showed a tendency towards increasing in layer V/VI in $\alpha2^{M/M}$, pairwise comparisons (unpaired t-test) did not detect a significant laminar difference in either genotype.

However, when comparing the input-output curves (number of spikes (N) evoked per step of injected current (I); (Figure 5.2 C1), there was a tendency towards increased excitability (i.e., a leftward shift of the input-output curve, which means APs are evoked with smaller current steps) in layers V/VI compared to layers II/III for $\alpha2^{WT}$, but not $\alpha2^{M/M}$ neurons. This apparently subtle difference appeared to increase after exposure of neurons to 500 nM THDOC (Figure 5.2 C2). Furthermore, the steady-state slopes (δN/δI) of the input-output relationship appeared steeper in layers II/III compared to V/VI in $\alpha2^{WT}$, but not in $\alpha2^{M/M}$ neurons (Figure 5.2 C1).

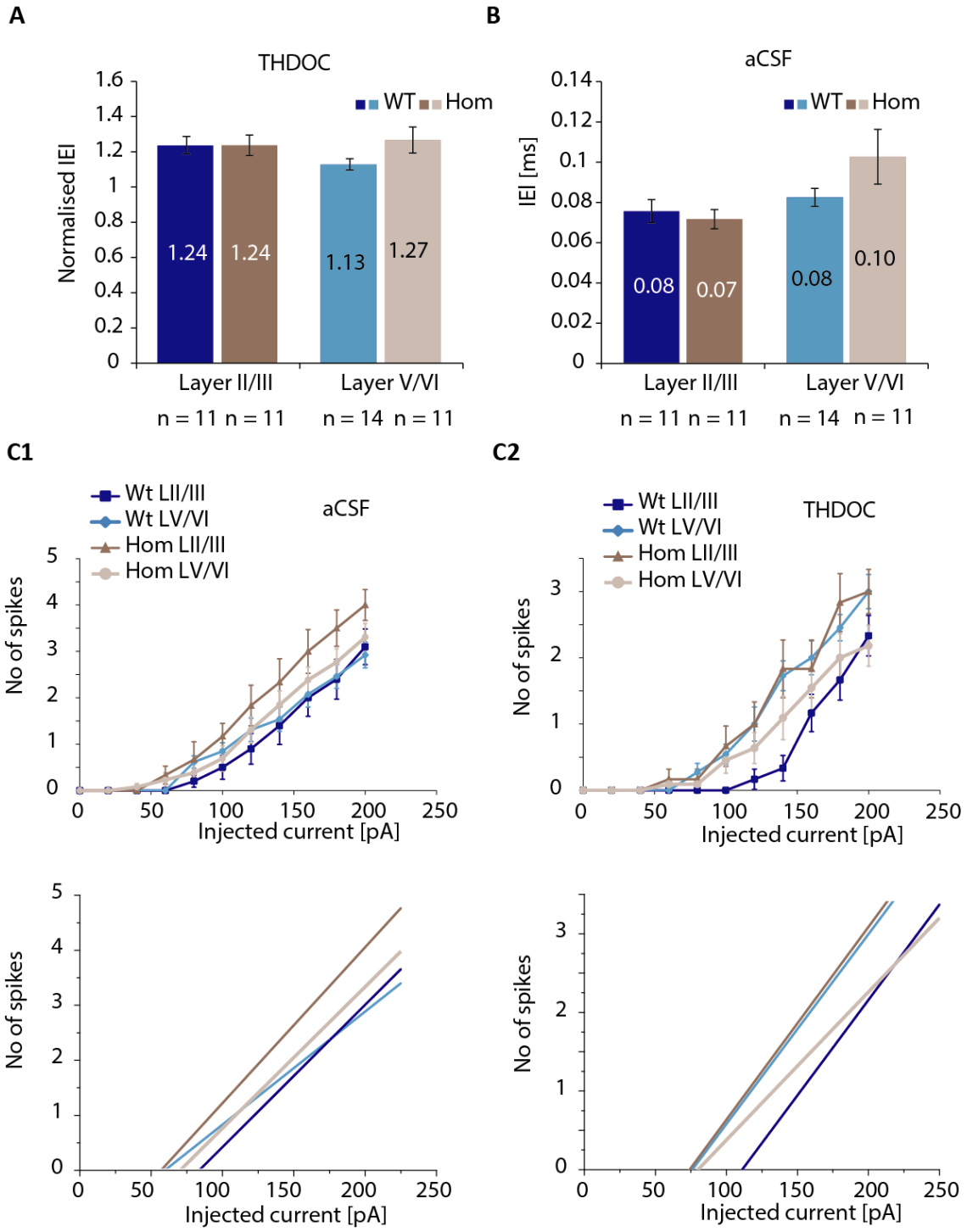

Figure 5.2 Effect of THDOC on neuronal excitability in different cortical layers and α2 genotypes

A. Effect of 500 nM THDOC and 5 µM GABA on IEIs (normalised to a control-period in aCSF = 1). Paired comparisons reveal no difference between layers or genotype (unpaired t-test). **B.** Baseline IEIs pairwise comparisons are not significantly different between $\alpha2^{M/M}$ and $\alpha2^{WT}$, or between layers of the same genotype (unpaired t-test). **C1 & C2.** Input-output curves generated from the average count of spikes elicited by incrementing (20 pA) current steps. Lower panels: Fits of the averaged curves above using linear regression. **C1.** Comparison of input-output curves in aCSF (+ 5 µM GABA) for different cortical layers and α2 genotypes. **C2.** Comparison of input-output curves in 500 nM THDOC (+ 5 µM GABA) for different cortical layers and α2 genotypes.

It would have been preferable to compare the threshold, slope, and maximum of sigmoid curve fitted data, but this was not possible, due to difficulties in maintaining AP firing under these conditions, which did not allow for application of sufficient numbers of current steps to reach saturation in the firing rate. Therefore, to compare curves, only the linear part of individual input-output curves was fitted using a linear regression equation. Due to the absence of firing in some cells (13 out of 55 cells, all of which were layer II/III cells) within the 200 pA current injection range, not all of the data could be fitted. As a consequence of using linear regression, the firing thresholds will be slightly underestimated.

Processing the data in this manner revealed a significant difference in basal firing threshold between cortical layers of $\alpha2^{WT}$ PCs (Figure 5.3 A, P = 0.01, Mann-Whitney test), with a firing threshold in layer II/III (97.4 ± 11.4 pA) twice that in layer V/VI (49.7 ± 8.3 pA), a distinction that was not observed with $\alpha2^{M/M}$ slices. In addition, the threshold for AP firing in layer II/III PCs of $\alpha2^{M/M}$ mice was significantly lower than its wild-type counterpart (52.0 ± 17.0 pA vs 97.4 ± 11.4 pA, P = 0.04, one-tailed t-test) and indicates an effect of the Q241M point mutation on intrinsic neuronal excitability in this layer.

Furthermore, there was a significant increase in firing threshold (i.e. a right-ward shift of input-output curves) in the presence of THDOC, as expected if THDOC is enhancing GABA inhibition (Figure 5.3 B, P = 0.002, Wilcoxon matched-pairs test). However, no differences in THDOC-mediated effects on input-output thresholds were observed between PCs of different laminar origin or between α2 genotypes (Figure 5.3 C), suggesting that the differences in basal thresholds did not stem from a lack of sensitivity to endogenous THDOC at α2 containing $GABA_A$Rs.

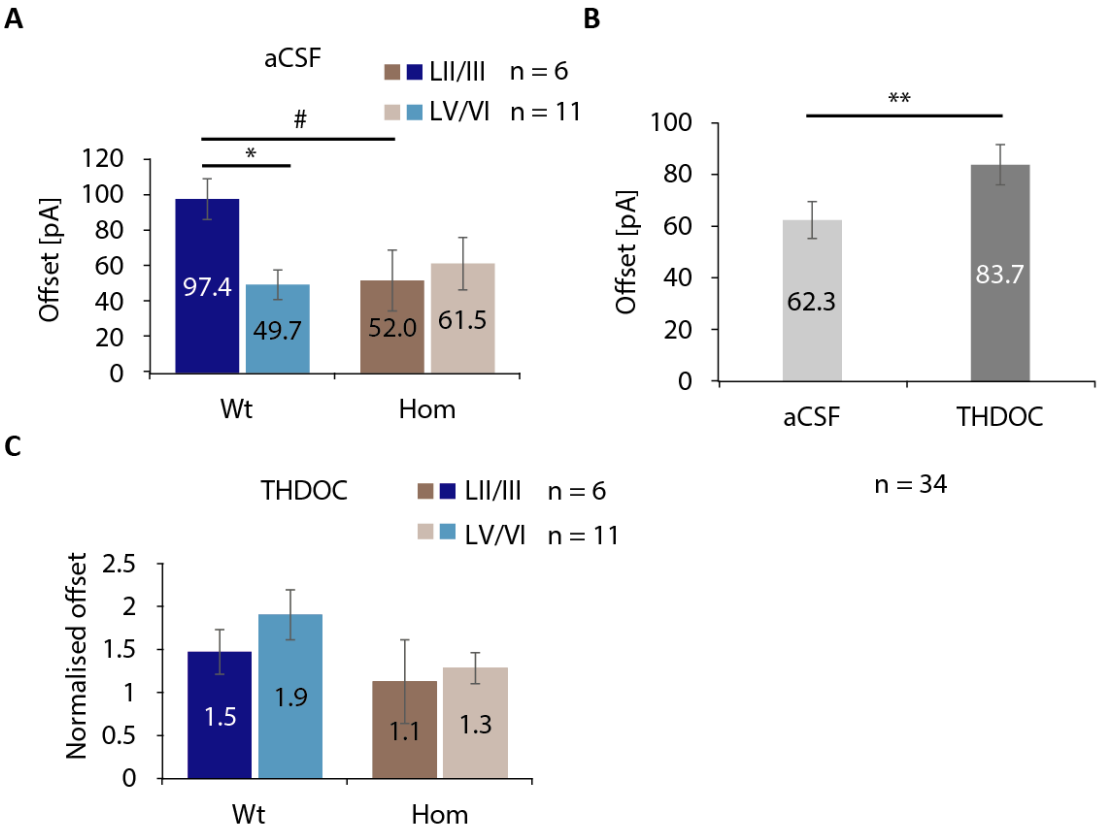

Figure 5.3: Effect of THDOC on input-output curve offsets
Input-output curve offsets were calculated by applying a linear regression fit to individual curves. To this end, only the linear part of the curves, i.e. the last 4-5 points, were used. Offsets were defined as the point of intersection for the fitted line with the x-axis. **A.** Comparison of baseline offsets in aCSF for $\alpha2^{M/M}$ and $\alpha2^{WT}$ pyramidal neurons from layers II/III and V/VI.* - $P < 0.05$, Mann-Whitney test. # - $P < 0.05$, single-tailed unpaired t-test. **B.** Combined offsets across both genotypes and layers compared between aCSF and after exposure to 500 nM THDOC. ** - $P < 0.01$, Wilcoxon matched pairs test. **C.** Comparison of offsets in THDOC normalised to aCSF for $\alpha2^{M/M}$ and $\alpha2^{WT}$ pyramidal neurons from layers II/III and V/VI. All recordings were carried out in the presence of 5 µM GABA.

When comparing input-output curve slopes (δN/δI), however, basal slopes were significantly smaller in layer V/VI (0.021 ± 0.001 spikes/pA) compared to layer II/III (0.030 ± 0.002 spikes/pA) for $\alpha2^{WT}$ PCs (Figure 5.4 A, P = 0.01, Mann-Whitney test), pointing to a smaller gain for neurons in layer V/VI. Interestingly, slopes were significantly larger in layer V/VI PCs of $\alpha2^{M/M}$ mice (Figure 5.4 A, 0.025 ± 0.002 spikes/pA) compared to their wild-type counterparts (P = 0.04, Mann-Whitney test), possibly reflecting a reduced effect of endogenous THDOC on inhibition. Furthermore, when comparing the combined slopes across layers between drug-treatments and genotypes (Figure 5.4 B), only $\alpha2^{M/M}$ showed a significantly reduced slope in THDOC (0.021 ± 0.002 spikes/pA)

compared to aCSF (0.026 ± 0.002 spikes/pA, P = 0.02, Wilcoxon matched-pairs test), which would reflect an increased ability of THDOC to potentiate GABA inhibition in the $\alpha2^{M/M}$ slices, but only in layer V/VI neurons. The relative effect of THDOC on slopes, however, was only significantly different between $\alpha2^{M/M}$ and $\alpha2^{WT}$ in layer V/VI (Figure 5.4 C, P = 0.05, unpaired t-test).

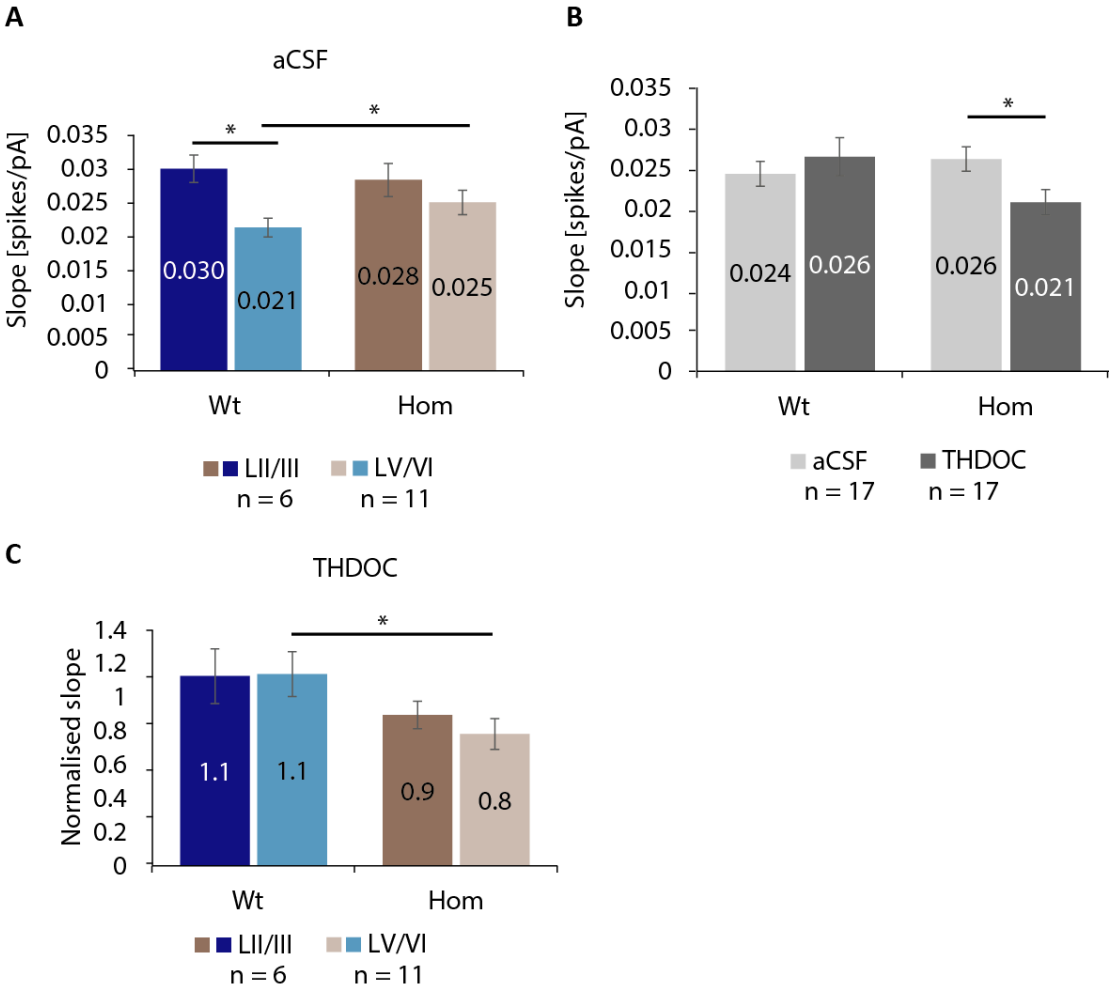

Figure 5.4: Effect of THDOC on input-output curve slopes
Input-output curve slopes were calculated by applying a linear regression fit to individual curves. Only the linear parts of the curves were used (last 4-5 points). **A.** Comparison of baseline slopes in aCSF for $\alpha2^{M/M}$ and $\alpha2^{WT}$ pyramidal neurons from layers II/III and V/VI.* - P < 0.05, Mann-Whitney test (one-tailed for $\alpha2^{M/M}$ vs $\alpha2^{WT}$). **B.** Combined slopes across both layer groups compared between drug treatments and genotypes. * - P < 0.05, Wilcoxon matched pairs test. **C.** Comparison of slopes in THDOC normalised to aCSF for $\alpha2^{M/M}$ and $\alpha2^{WT}$ pyramidal neurons from layers II/III and V/VI. * - P < 0.05, unpaired t-test. All recordings were carried out in the presence of 5 µM GABA.

In summary, these results indicate a difference in basal threshold and gain between layers of the mPFC as well as an effect of THDOC on firing frequency and threshold. Furthermore, introduction of the Q241M mutation appeared to have induced intrinsic changes in firing threshold in layer II/III and gain in layer V/VI. Interestingly, while neurosteroid-modulation of the threshold appears to be independent of genotype and layer, gain appears to be differentially affected in mutant layer V/VI, pointing to a role for α2 in mediating neurosteroid effects on gain, but not firing frequency and threshold (see Discussion).

Using 500 nM THDOC along with 5 µM GABA, however, might change the kinetic profile of sIPSCs, assessed in Chapter 4, or even lead to receptor desensitisation. To ascertain whether this higher concentration of THDOC, together with a GABA supplement, would still result in similar changes to sIPSC decay times between $\alpha2^{WT}$ mice and mutant $\alpha2^{M/M}$, voltage-clamp experiments were performed using the same conditions as those for the current-clamp experiments (Table 5.3). Both 100 nM and 500 nM THDOC plus 5 µM GABA prolonged sIPSC decay times to a greater extent in $\alpha2^{WT}$ pyramidal neurons compared to $\alpha2^{M/M}$ counterparts ($P = 0.02$ and $P = 0.04$, respectively, unpaired t-test). There was no significant difference between drug application on the increase in sIPSC decay time in either genotype ($P = 0.4$ for $\alpha2^{WT}$ and $P = 0.6$ for $\alpha2^{M/M}$, unpaired t-test) suggesting that 300 nM THDOC is saturating.

By contrast, tonic currents were differentially affected by the concentration of THDOC application and the presence or absence of GABA supplementation in both genotypes ($P = 0.003$ for $\alpha2^{WT}$ and $P = 0.01$ for $\alpha2^{M/M}$, unpaired t-test with Welch-correction), with larger tonic currents observed in 500 nM THDOC plus 5 µM GABA (Table 5.3) and no difference between genotypes (unpaired t-test).

It is worthwhile noting, however, that in the presence of 5 µM GABA, basal sIPSC frequency in $\alpha2^{WT}$ PCs (5.4 ± 0.9 Hz) was significantly lower compared to aCSF alone (10.4 ± 0.8 Hz, $P = 0.009$, unpaired t-test), while basal sIPSC decay times were significantly longer (Table 5.4, 10.6 ± 0.8 and 8.5 ± 0.3 ms, respectively, $P = 0.02$,

unpaired t-test). No differences in basal inhibitory sIPSC properties were present in $\alpha2^{M/M}$ (unpaired t-tests, Table 5.5). However, since the results assessing excitability were only compared between experiments carried out under the same conditions, and since we could show that the relative synaptic effects of THDOC had been unperturbed by the presence of GABA, the effects on basal sIPSC properties in elevated levels of GABA were considered to be insignificant for the assessment of neurosteroid-modulation of PC excitability.

Together, these results show that the recording conditions used have not affected THDOC-mediated effects on synaptic inhibition, despite the increase in tonic inhibition in both genotypes as well as lowered basal sIPSC frequency and prolonged basal decay times in wild-type PCs in the presence of 5 µM GABA.

Inhibitory GABA current properties in THDOC		$\alpha2^{WT}$	$\alpha2^{M/M}$
Normalised decay times	**500 nM THDOC + 5µM GABA**	1.32 ± 0.06 (5)	1.11 ± 0.05 (6)*
	100 nM THDOC	1.27 ± 0.03 (8)	1.14 ± 0.02 (7)*
Tonic current [pA]	**500 nM THDOC + 5µM GABA**	46.1 ± 10.1 (8)$^{\#\#}$	49.8 ± 10.3 (6)$^{\#}$
	100 nM THDOC	8.8 ± 1.9 (8)	10.6 ± 3.6 (6)

Table 5.3: Effect of THDOC concentration and GABA supplementation on sIPSC decay times and tonic currents

Comparison of sIPSC decay times (top; normalised to values in aCSF) and tonic currents (bottom; absolute shifts in holding current) in response to either 500 nM THDOC + 5 µM GABA or 100 nM THDOC alone, between $\alpha2^{WT}$ and $\alpha2^{M/M}$ slices in layer V/VI PCs. Cell numbers are shown in parentheses. * - $P < 0.05$ for $\alpha2^{M/M}$ vs $\alpha2^{WT}$, unpaired t-test. ## - $P < 0.01$, # - $P < 0.05$ for 500 nM THDOC vs 100 nM THDOC, unpaired t-test with Welch-correction.

$\alpha2^{WT}$ basal inhibitory GABA current properties	aCSF (13)	+ 5 µM GABA (5)
Frequency [Hz]	10.4 ± 0.9	5.4 ± 0.8**
Peak amplitude [pA]	-25.8 ± 2.7	-26.5 ± 1.0
Decay time [ms]	8.5 ± 0.3	10.6 ± 0.8*
Rise time [ms]	0.64 ± 0.02	0.68 ± 0.06

Table 5.4: Effect of supplementing aCSF with 5 µM GABA on basal sIPSC properties and frequency in $\alpha2^{WT}$ layer V/VI PCs
Comparison of basal sIPSC parameters in control aCSF or aCSF supplemented with 5 µM GABA. Recordings were acquired from separate cohorts of layer V/VI PCs of $\alpha2^{WT}$ mice. Cell numbers are shown in parentheses. * - $P < 0.05$, unpaired t-test. . ** - $P < 0.01$, unpaired t-test.

$\alpha2^{M/M}$ basal inhibitory GABA current properties	aCSF (9)	+ 5µM GABA (6)
Frequency [Hz]	9.2 ± 1.3	7.6 ± 1.3
Peak amplitude [pA]	-27.5 ± 0.7	-28.3 ± 2.1
Decay time [ms]	9.2 ± 0.4	10 ± 0.6
Rise time [ms]	0.59 ± 0.02	0.78 ± 0.08

Table 5.5: Effect of supplementing aCSF with 5 µM GABA on basal sIPSC properties and frequency in layer $\alpha2^{M/M}$ V/VI PCs
Comparison of basal sIPSC parameters in control aCSF or aCSF supplemented with 5 µM GABA. Recordings were acquired from separate cohorts of layer V/VI PCs of $\alpha2^{M/M}$ mice. Cell numbers are shown in parentheses.

In summary, we verified that the differences in sIPSC decay time prolongation between α2 genotypes were unaffected by increasing the concentration of applied THDOC and GABA. The results indicate a difference in basal excitability between layers of the mPFC, shown by the tendency for smaller offsets and smaller gains in layers V/VI. THDOC increased spike thresholds as expected but there was no differential effect on excitability between the cell layers or an effect of genotype, with the exception of a tendency to differentially modulate gains in $\alpha2^{M/M}$ compared to $\alpha2^{WT}$ animals. This could potentially indicate a role for α2-$GABA_A$Rs in modulating neuronal gain rather than firing

threshold. However, in layer II/III, the threshold for AP firing in $\alpha2^{M/M}$ slices was lower compared to the wild-type counterpart and this indicates a likely effect of the Q241M point mutation on intrinsic neuronal excitability.

5.2.3 Targeting GABA-mediated inhibition at PCs using a 5-HT_{2C} agonist

The lack of clear genotype-specificity in THDOC-mediated reduction of PC excitability questioned the importance of α2-$GABA_A$Rs in neurosteroid modulation of neuronal spike output in these cells. However, one possible confound could be that by bath-applying GABA to the slice, multiple $GABA_A$ receptor sub-populations might be activated and thus specific inputs onto the AIS, which would potentially be relevant in regulating AP generation under physiological conditions, might be masked. To address this potential problem, we sought alternative means to physiologically increase GABAergic transmission at this particular inhibitory synapse, as shown in Figure 5.5.

Serotonin type 2C (5-HT_{2C}) receptors are a member of the serotonin 7-transmembrane-spanning family of GPCRs (see Berg et al., 2008 for a review). They are mainly found postsynaptically, where they activate PLC, leading to neuronal depolarisation and increased spike firing (Stanford et al., 2005). In the rat mPFC, 5-HT_{2C}Rs are found to be enriched in PV-positive interneurons (Liu et al., 2007). A subgroup of these are the Chandelier cells, which preferentially form synaptic connections onto the AIS (Somogyi, 1977). Since activation of 5-HT_{2C}Rs leads to depolarisation of the cell, an enhanced activity of Chandelier cells and a concomitant increase in GABA release onto the AIS has previously been suggested (Liu et al., 2007). Hence, the selective 5-HT_{2C}R agonist, Ro-60-0175, was used to increase GABA release at AIS synapses, to specifically activate α2-containing $GABA_A$Rs and probe the extent of their contribution towards neurosteroid modulation of neuronal excitability.

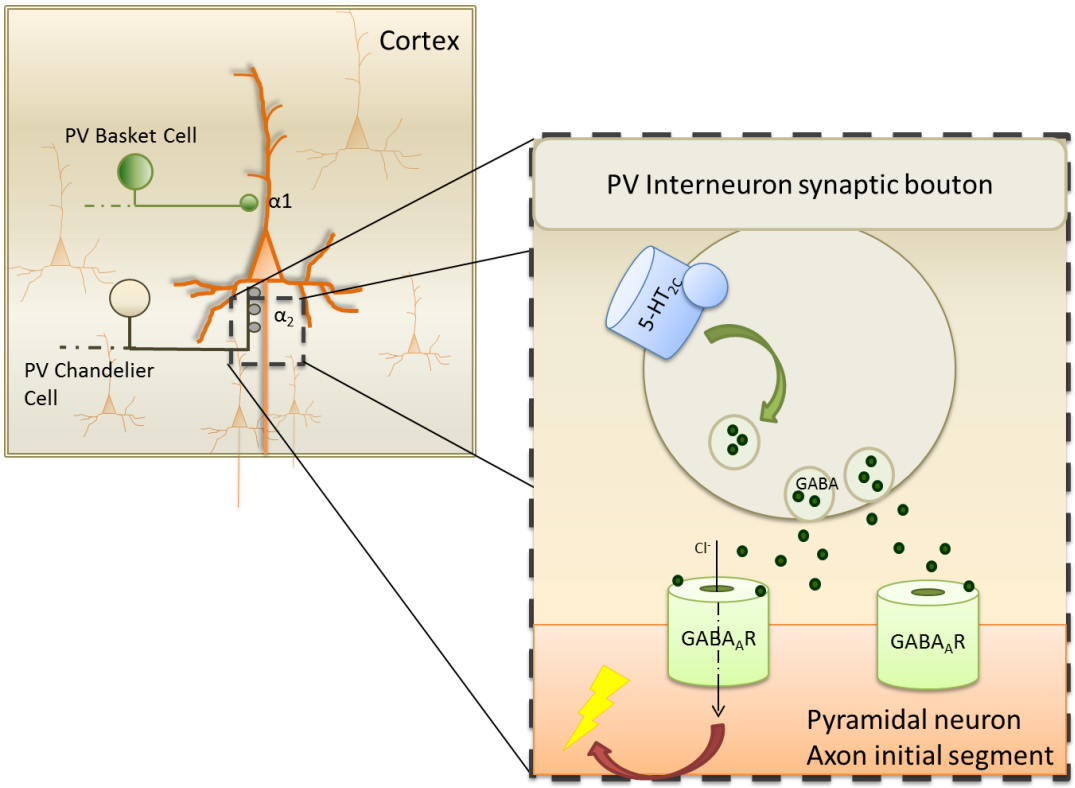

Figure 5.5 Increasing GABA release at mPFC axo-axonic synapses by 5-HT$_{2C}$ receptors
Model of a cortical pyramidal neuron receiving (peri)somatic and axonic inputs from two different types of PV interneurons: basket cells and Chandelier cells, respectively (there are other types of interneurons synapsing onto PCs, which are omitted for simplicity; for a review, see Druga, 2009). While somatic and perisomatic phasic inhibition in PCs is thought to be mostly mediated by α1-GABA$_A$Rs (Nusser et al., 1996b), which is the most prolific GABA$_A$R subtype (Möhler, 2002), the AIS is relatively enriched in α2-GABA$_A$Rs (Nusser et al., 1996b), positioning them in a central location for modulating PC output. Shown on the right is a model of an axo-axonic synapse, demonstrating how activation of 5-HT$_{2C}$ receptors might affect PC excitability. In the mPFC, 5-HT$_{2C}$ receptors are mostly found on PV interneurons in layers V/VI (Liu et al., 2007) where they are excitatory (Stanford et al., 2005). An increase in interneuron excitation should augment GABA release and theoretically reduce excitability of the postsynaptic PC.

To this end, 500 nM Ro-60-0175 was bath-applied after a period of recording sIPSCs under baseline conditions (in control aCSF). As a control, the same recording procedure was undertaken in the presence of the selective 5-HT$_{2C}$R antagonist, SB 242084 (250 nM). These concentrations were chosen to be 5x the EC$_{50}$ for Ro-60-175 as an agonist, and 20x the IC$_{50}$ for antagonism, at 5-HT$_{2C}$Rs (Alexander et al., 2011).

The effects of Ro-60-0175 (500 nM) on inhibitory synaptic inputs onto PCs in layer II/III and layer V/VI in α2^{WT}, as well as in layer VI/VI for α2$^{M/M}$ were examined (Figure 5.6 A &

B). The application of Ro-60-0175 increased sIPSC frequency by ~ 50% in layer V/VI pyramidal neurons only, regardless of the α2 subunit genotype ($P < 0.001$, pairwise comparisons with Bonferroni correction). The effect was apparent after 5 min and saturated within 10 - 15 min. It is noteworthy, however, that 3 out 13 cells did not respond to treatment with Ro-60-0175. Those cells were nonetheless included in the analysis.

Co-applying the 5-HT_{2C} receptor antagonist, SB 242084 (250 nM), prevented the increase in sIPSC frequency by Ro-60-0175, which was therefore most likely 5-HT_{2C} receptor-mediated. No significant changes in sIPSC frequency were observed with SB 242084 in layer II/III, in line with the low expression of 5-HT_{2C} receptors in this region (Liu et al., 2007).

Having found a method to specifically increase GABA release for perisomatic and axo-axonic inputs, we applied this method to test for variations in THDOC-mediated reduction of PC excitability between $\alpha2^{WT}$ and $\alpha2^{M/M}$ slices by measuring the action potential IEIs (Figure 5.6 C). Co-applying Ro-60-0175 and THDOC (500 nM) increased the IEI (normalised to values obtained in aCSF) when compared to just bicuculline (20 µM) alone in $\alpha2^{WT}$ slices ($P = 0.01$, paired t-test). In addition, significant genotypic differences in IEIs were evident in Ro-60-0175, and in Ro-60-0175 with THDOC (Figure 5.6 C, $P = 0.03$, $P = 0.04$, respectively, one-tailed unpaired t-test), comparing between $\alpha2^{WT}$ and $\alpha2^{M/M}$ slices. However, these treatments did not produce changes in the IEIs that were different from aCSF alone (one-sample t-test vs a null-effect of 1; Figure 5.6 C).
Moreover, co-applying THDOC with Ro-60-0175 did not significantly change the PC firing rate any further compared to Ro-60-0175 alone, in either genotype (paired t-test), though bicuculline could reverse the reduced excitability in Ro-60-0175 and THDOC but only in $\alpha2^{WT}$ slices.

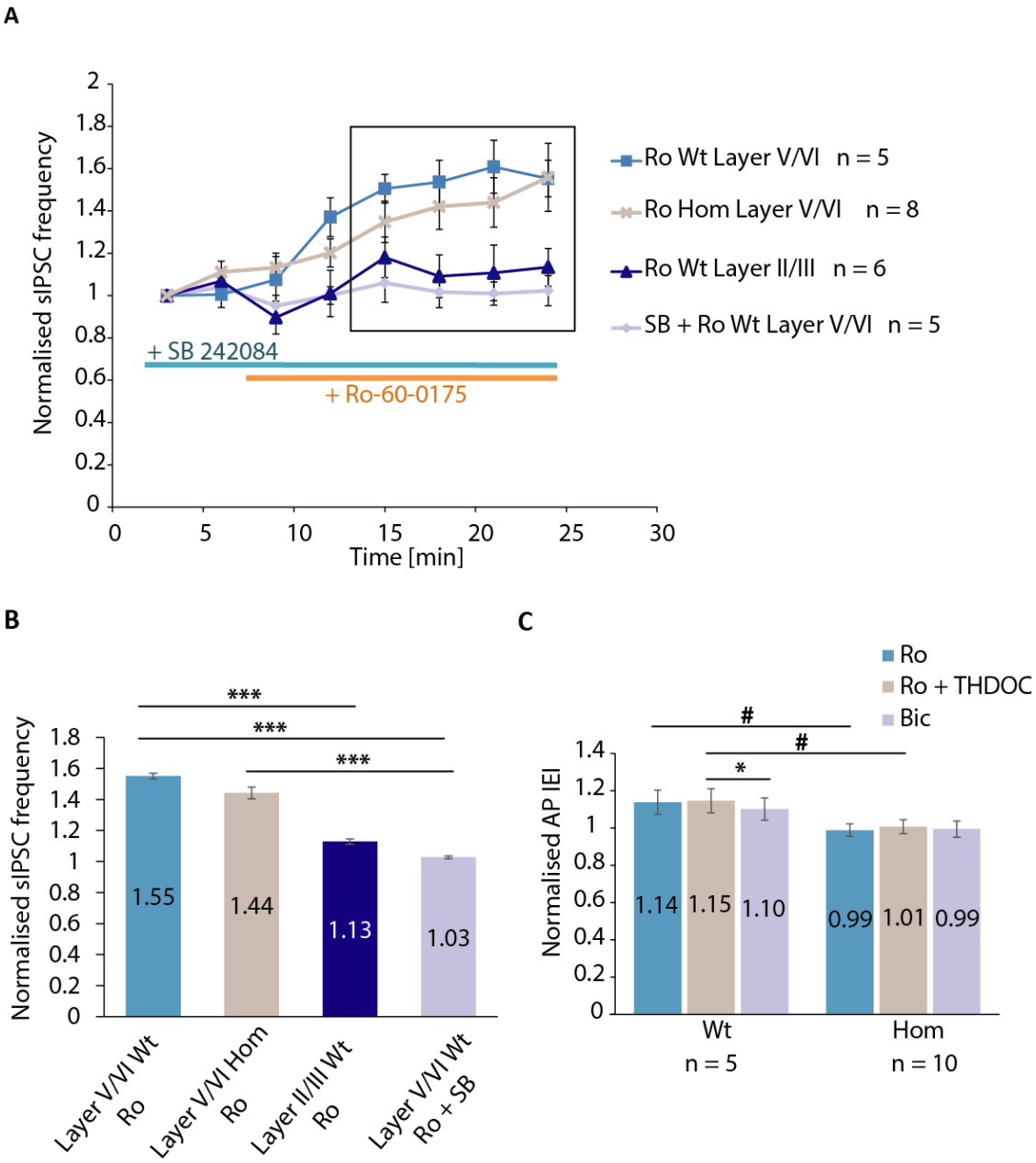

Figure 5.6 Effect of 5-HT$_{2C}$ receptor activation and inhibition on sIPSC frequency and PC excitability

A. Average sIPSC frequencies (normalised to the average frequency at the beginning of the recording) over the course of a 25 min recording in either aCSF or the 5-HT$_{2C}$ receptor agonist Ro-60-0175 (500 nM) with or without co-application of the specific antagonist, SB 242084 (250 nM). Ro-60-0175 (500 nM) was applied after recording baseline frequencies for 6 min. **B.** Normalised frequencies shown in A averaged over 12 min after the onset of drug effect (4 time-points between 12-24 min, box in A). *** = P < 0.001, Bonferroni corrected multiple comparisons of selected pairs. **C.** Comparison of average spike IEI (normalised to a control period in aCSF) between $\alpha2^{WT}$ and $\alpha2^{M/M}$ layer V/VI PCs in the presence of Ro-60-0175 (500 nM), Ro-60-0157 + THDOC (500 nM) or bicuculline (20 µM). * - P < 0.05, paired t-test. # - P < 0.05, unpaired one-tailed t-test.

The observed difference in excitability between $\alpha2^{WT}$ and $\alpha2^{M/M}$ in the presence of Ro-60-0175 is interesting, since neurons in either genotype both responded with a similar increase in presynaptic GABA release (inferred by the changes in sIPSC frequency; Figure 5.6 A). Since 5-HT_{2C}Rs have also been found on mPFC PCs (Liu et al., 2007), this points to a possible postsynaptic effect of Ro-60-0175, which may have been affected by introducing the Q241M mutation. Comparing membrane potential and input resistance confirms a potential postsynaptic action of Ro-60-0175 (Table 5.6): While both R_M and V_M were unaffected by Ro-60-0175 in $\alpha2^{WT}$ layer V/VI PCs, R_M increased (from 137 ± 10 MΩ to 161 ± 17 MΩ, P = 0.04, paired t-test) and V_M depolarised significantly in response to Ro-60-0175 in $\alpha2^{M/M}$ (from -67.2 ± 1.6 mV to -66.6 ± 1.5 mV, P = 0.02, paired t-test).

Hence, at least with regard to a possible role of α2-$GABA_A$Rs in modulating neurosteroid-effects on PC excitability, we could not find supporting evidence using our $\alpha2^{M/M}$ knock-in mouse model. However, the effects mediated by α2-$GABA_A$Rs may be masked by the postsynaptic effects of 5-HT_{2C} receptor activation (see Discussion).

Drug effect on cellular parameters		$\alpha2^{WT}$ (7)	$\alpha2^{M/M}$ (9)
R_M [MΩ]	**aCSF**	182 ± 17	137 ± 10$^{\#}$
	Ro-60-0175	209 ± 19	161 ± 17*
	Ro-60-0175 THDOC	204 ± 25	167 ± 17*
	Bic	179 ± 21	169 ± 17*
V_M [mV]	**aCSF**	-67.0 ± 1.2	-67.2 ± 1.6
	Ro-60-0175	-67.0 ± 0.8	-66.6 ± 1.5 *
	Ro-60-0175 THDOC	-66.9 ± 1.0	-65.9 ± 1.6 *
	Bic	-67.8 ± 1.2	-66.1 ± 1.7

Table 5.6: Effect of a 5-HT_{2C}R agonist and THDOC on Layer V/VI pyramidal cell membrane parameters

Effects of 500 nM Ro-60-0175; 500 nM Ro-60-0175 and 500 nM THDOC; or 20 µM bicuculline (all in the presence of 5 µM GABA) on input resistance (**R_M**) and membrane potential (**V_M**) in layer V/VI pyramidal neurons of $\alpha2^{WT}$ and $\alpha2^{M/M}$ mPFC neurons. # - P < 0.05, $\alpha2^{WT}$ vs $\alpha2^{M/M}$, unpaired t-test; * - P < 0.05, paired t-test vs aCSF.

5.2.4 Can tonic or phasic GABA inhibition modulate excitability of mPFC neurons?

The previous experiments raised the question, whether the single step current injection protocol is suitable for detecting a change in neuronal excitability caused by the manipulation of synaptic inhibition. The following observations are important: First, concentrations of THDOC, which have a clear prolongation effect on sIPSC decay times, did not change evoked AP firing; second, using higher concentrations of THDOC (300 – 500 nM) in conjunction with 5 µM GABA, led to increased tonic GABA currents without changing the effect of THDOC on sIPSC decays (Table 5.3), but caused a reduction in cell excitability; third, increasing a more focused synaptic release of GABA via 5-HT_{2C}R activation had no discernible effect on AP firing (Figure 5.6). Fourth, it is possible that synaptic and tonic inhibition are playing quite distinct roles in controlling cell excitability.

Consequently, we wanted to explore other means of specifically manipulating GABAergic synaptic and tonic inhibition and test their effects on PC firing rate using our current injection protocol. To simplify this study to regions where the most profound effects had so far been seen, only $\alpha2^{WT}$ layer V/VI neurons were used for comparison.

Initially, pentobarbitone (PB), a barbiturate acting as a non-selective positive modulator of $GABA_A$Rs (Sieghart, 1995), was bath-applied to mPFC slices (Figure 5.7). PB (25 µM) increased the holding current (Figure 5.7 A), reflected by the increased tonic current revealed by 20 µM bicuculline (Figure 5.7 B & C, P = 0.0002, unpaired t-test). In addition, PB also increased the decay times (Figure 5.7 D; P < 0.0001, paired t-test) and the peak amplitude of sIPSCs (P = 0.01, paired t-test). Consequently, similar to 500 nM THDOC and 5 µM GABA, PB increased tonic as well as synaptic inhibition and would therefore be expected to reduce PC excitability. Indeed, when comparing the application of PB to either bicuculline (P = 0.03, one-tailed paired t-test) or a null effect of 1 for the normalised IEI (P = 0.02, one-sample two-tailed t-test), PB significantly reduced PC firing (Figure 5.8).

Thus by modulating both tonic and synaptic inhibition with a barbiturate, we were able to resolve changes to PC excitability, though pentobarbitone is a very efficacious $GABA_A$ receptor modulator.

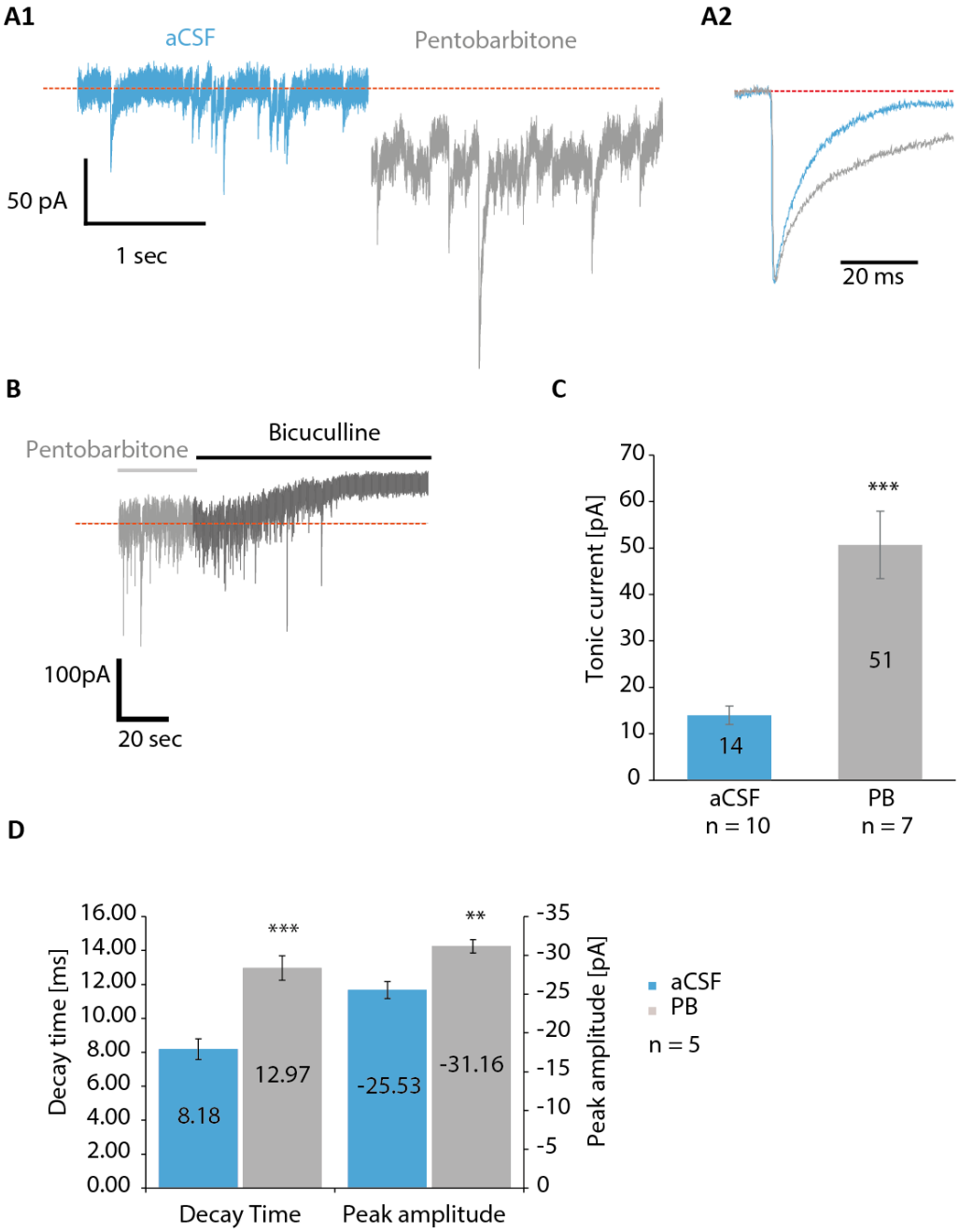

Figure 5.7: Effect of Pentobarbitone on phasic and tonic GABA inhibition in layer V/VI mPFC pyramidal neurons

A1. Representative current trace displaying the change in holding current and sIPSC amplitude and decay time after application of 25 µM PB. **A2.** Average peak-scaled sIPSC before and after application of pentobarbitone. **B.** Representative shift in holding current observed when applying 20 µM bicuculline to the bath after exposure to PB. **C.** Comparison of tonic GABA currents in aCSF and in 25 µM PB (recorded from different cohorts of neurons). Tonic current is significantly increased by PB. *** - $P < 0.001$, unpaired t-test. **D.** Effect of PB on sIPSC decay time and peak amplitude compared to aCSF determined in the same cells. ** - $P < 0.01$, *** - $P < 0.001$, paired t-test.

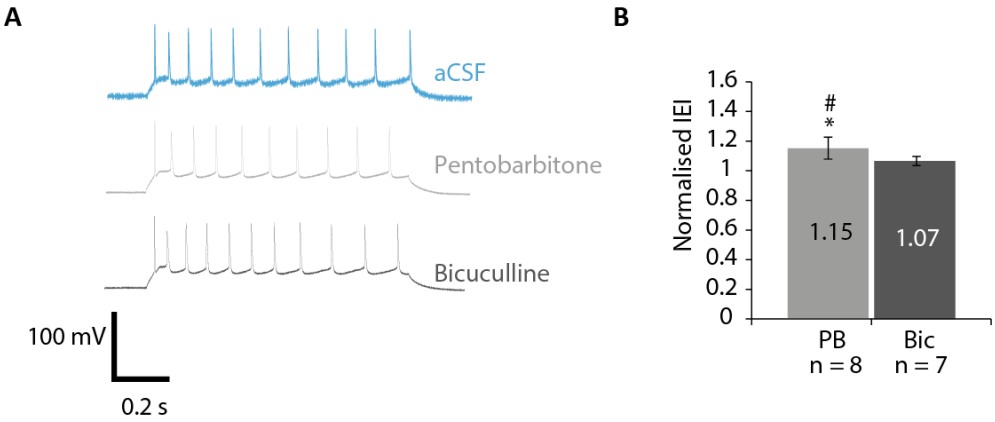

Figure 5.8: Pentobarbitone reduces the firing rate in layer V/VI mPFC pyramidal neurons
A. Representative traces of APs elicited by a 1 s long 200 pA injected current step in aCSF , 25 µM PB or 20 µM bicuculline. **B.** Average IEI (normalised to that determined in aCSF) in PB or bicuculline (20 µM). # - P < 0.05, PB vs null-effect of 1 (one-sample t-test); * - P < 0.05, PB vs Bic (paired t-test).

As an alternative test, the effect of the less efficacious diazepam (1 µM), a positive modulator selective for α1/2/3/5βγ2-$GABA_A$Rs (Korpi et al., 2002), was also explored (Figure 5.9). This is quite a high concentration for a benzodiazepine to modulate $GABA_A$ receptors and at this level only a significant increase in the sIPSC decay times (P = 0.03, paired t-test), as well as frequency (P = 0.04, paired t-test) was observed (Figure 5.9 D). Diazepam appeared to increase the holding current (possibly by potentiating extrasynaptic γ2-containing $GABA_A$Rs; (Figure 5.9 A), resulting in a larger tonic current (revealed by 20 µM bicuculline; Figure 5.9 B), however, this was not significant (P = 0.4, unpaired t-test; Figure 5.9 C). Hence, diazepam likely exerts a stronger effect on synaptic rather than tonic inhibition.

Interestingly, when cell excitability was assessed by evoking spikes in the presence of 1 µM diazepam (Figure 5.10), there appeared to be no significant effect on the firing rate compared to either bicuculline (P = 0.31, paired t-test) or a preceding control period (P = 0.2515, one-sample t-test vs null-effect of 1). Thus, a reduction in PC excitability caused by an increase in synaptic inhibition following potentiation by diazepam is not apparent. The main difference between pentobarbitone and diazepam treatments is the large tonic current elicited by the barbiturate, and this may be important since only pentobarbitone reduced cell excitability. We therefore next addressed whether tonic inhibition was playing a more significant role in cell excitability when using a current-step protocol.

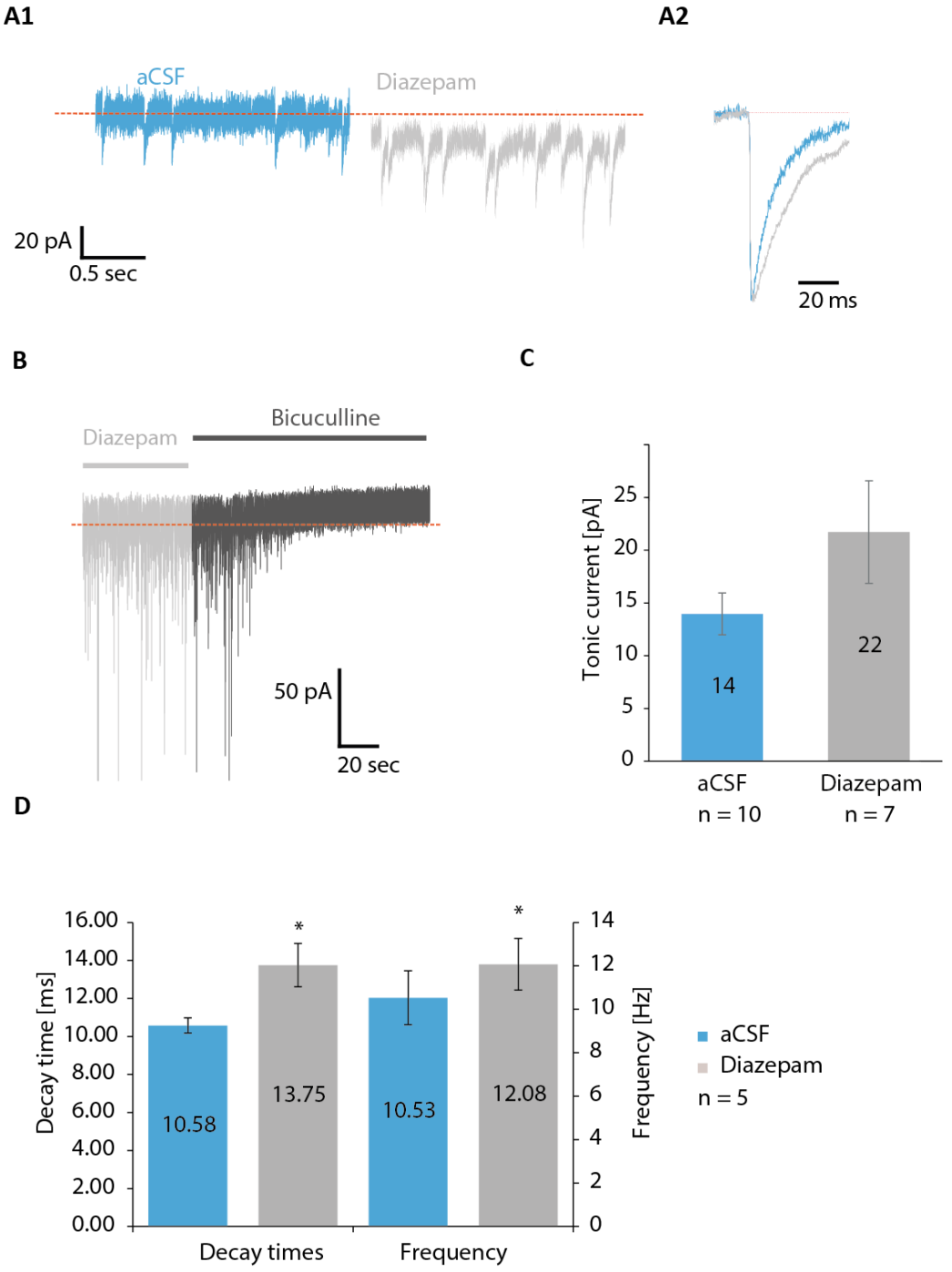

Figure 5.9: Effect of diazepam on pyramidal cell phasic and tonic GABA inhibition
A1. Representative current trace displaying the change in holding current (orange dotted line) and prolonged sIPSCs after application of 1 µM diazepam. **A2.** Average peak-scaled sIPSC before and after application of diazepam. **B.** Representative shift in the holding current observed when applying 20 µM bicuculline after exposure to diazepam. **C.** Comparison of tonic currents revealed by bicuculline (20 µM) in aCSF and diazepam (recorded from different cohorts of neurons). Tonic current was not significantly different in diazepam (unpaired t-test). **D.** Effect of diazepam on sIPSC decay time and frequency. * - $P < 0.05$, paired t-test.

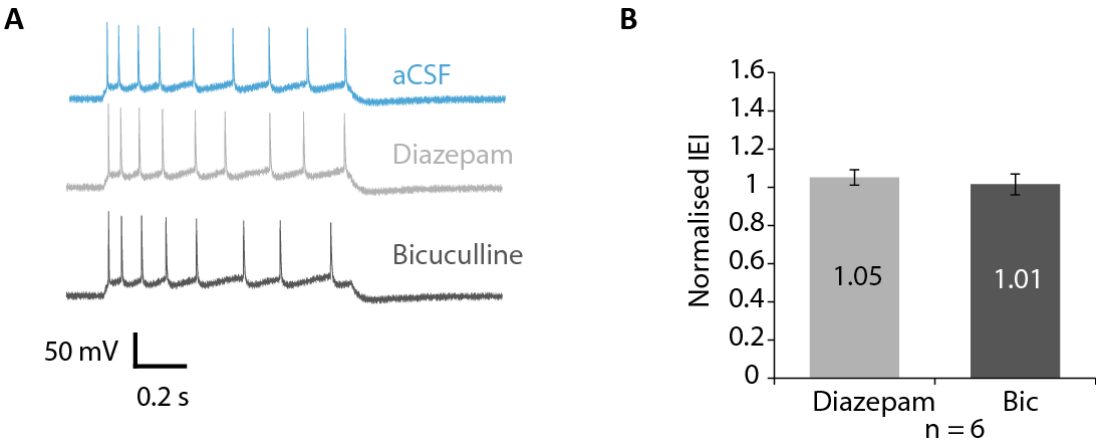

Figure 5.10: Effect of diazepam on PC excitability
A. Representative traces of APs elicited by a 1 s long 200 pA injected current step in aCSF, 1 µM diazepam or 20 µM bicuculline. **B.** Average IEI (normalised to that determined in aCSF) in diazepam (1 µM) or bicuculline (20 µM). There was no significant difference in PC excitability between diazepam and Bic (paired t-test) or between diazepam and a null-effect of 1 for the normalised IEI (one-sample t-test).

To address this question, the δ subunit $GABA_AR$-selective agonist THIP (1 µM, Brown et al., 2002) was used to specifically enhance tonic inhibition (see Figure 4.5 in chapter 4), which would be expected to rely substantially on extrasynaptic $GABA_ARs$ composed of αβδ subunits. Examining cell excitability by evoking spikes with current injection revealed that THIP significantly prolonged the IEIs when compared to bicuculline (Figure 5.11; P = 0.02, paired t-test) or when compared to a preceding control period (P = 0.02, one-sample t-test vs null-effect of 1). At this concentration, 1 µM THIP is selective for αβδ receptors (Krogsgaard-Larsen et al., 2004; Mortensen et al., 2010) and thus this effect is most likely caused by increased tonic inhibition mediated by THIP, since analysis of the phasic effects of 1 µM THIP (in standard aCSF supplemented with 2 mM KA) revealed no differences in sIPSC kinetics compared to a preceding control period in aCSF (Table 5.7). There was a reduction in sIPSC frequency (7.3 ± 1.2 Hz in aCSF compared to 5.1 ± 0.9 Hz in THIP, P = 0.02, paired t-test), which might stem from a reduction in presynaptic interneuron activity caused by the augmented tonic inhibition. This reduction in frequency, however, would presumably lead to increased PC firing rate and therefore, at most, reduce the effect of a THIP-mediated decrease in PC excitability.

In conclusion, by using the three modulators, changes to synaptic inhibition in the form of altered sIPSC decays and/or altered sIPSC amplitudes are not having effects on cell excitability that we can detect. By contrast, using the same methods, potentiating tonic inhibition does result in reduced cell excitability using two independent modulators, one possessing selectivity for extrasynaptic δ subunit-containing $GABA_A$ receptors.

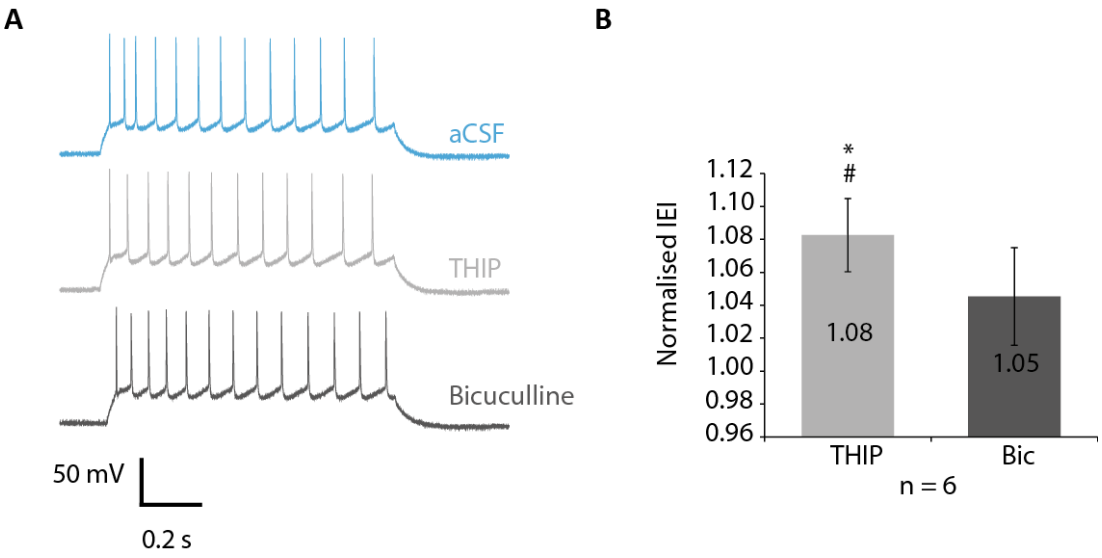

Figure 5.11: Effect of THIP on PC excitability
A. Representative traces of APs elicited by a 1 s long 200 pA injected current step in aCSF, 1 µM THIP or 20 µM bicuculline. **B.** Average IEI (normalised to aCSF) in THIP (1 µM) or bicuculline (20 µM). # - P < 0.05, THIP vs 1 (one-sample t-test); * - P < 0.05, THIP vs Bic (paired t-test).

sIPSC parameters	aCSF	THIP
Frequency [Hz]	7.3 ± 1.2	5.1 ± 0.9*
Peak amplitude [pA]	-21.8 ± 1.2	-22.1 ± 2.3
Decay time [ms]	8.8 ± 0.5	9.7 ± 1.0
Rise time [ms]	0.77 ± 0.06	0.97 ± 0.11

Table 5.7: Effect of THIP on sIPSC parameters
Table presenting the effects of 1 µM THIP on sIPSC parameters. Recordings were obtained from layer V/VI pyramidal neurons of acute mPFC slices in standard aCSF supplemented with 2 mM KA. N = 6 cells. * - P < 0.05, paired t-test.

5.3 Discussion

In the previous chapter we explored the basic characteristics of GABAergic inhibition in mPFC pyramidal neurons. We discovered that there was a stronger effect of the neurosteroid THDOC on inhibition of PCs in layers V/VI, as well as a significant contribution of α2-$GABA_A$Rs to phasic inhibition in both, layers II/III and layers V/VI. The objective in this chapter was to explore whether endogenous neurosteroid modulation of PC excitability via α2-$GABA_A$Rs could be resolved by ablating α2-mediated neurosteroid sensitivity in $\alpha2^{M/M}$ mice.

5.3.1 Selection of a single-step protocol over input-output curves

In the present study, a current-clamp protocol using single current step injections above the threshold for AP firing was applied and IEIs were measured to assess neuronal excitability (see Materials & Methods section). Normally, using a current-step protocol applying brief consecutive pulses of increasing amplitude would explore a wider range of electrophysiological properties, such as rheobase, gain (slope of the input-output curve) and the presence of hyperpolarisation sags and after-hyperpolarising rebound spikes. Although this was initially attempted, it proved difficult to implement. Due to the need to apply multiple drug applications with sometimes long equilibration periods (up to 10 min for Ro-60-0175), cells had to be repeatedly stimulated for up to 30 min. Most neurons showed “fatigue” after several of current injection trains, i.e. they reduced their firing rate and, in some cases, even ceased firing altogether.

This effect may have been caused by dialysis of the cell with the patch-electrode solution. Removing intracellular Ca^{2+} and increasing the concentration of the Ca^{2+} chelator EGTA helped to maintain AP firing over the course of the experiment, but a gradual decline in AP frequency was still evident.

Applying a single suprathreshold current step with a duration of 1 s, repeated at an interval of 30 s, produced consistent firing in most neurons and the IEI proved to be the parameter with the highest sensitivity to drug treatment. Therefore, this method was

used to investigate neuronal excitability. To allow a determination of the firing threshold and to differentiate between responses to stimuli of different strengths (i.e. neuronal gain), a brief current step protocol involving a series of 20 pA, 200 ms long steps was employed at the beginning of each recording and after equilibration of each drug to determine the rheobase and to obtain an input-output curve. As it was difficult to achieve saturation in spike firing, it was not possible to fit the input-output curves with a sigmoidal function. Nevertheless, measures of spike threshold and the slope of the relationship were obtained by linear regression.

Of course using current injections for examining cell excitability, in relation to the influence of specific inputs, is not meant to replicate neuronal excitation in a physiological context. The experimental stimulation delivers a depolarising current, which is independent of other inhibitory or excitatory inputs. Whereas, in a physiological network, the timing and location of different inputs and their integration are crucial for shaping neuronal firing and in regulating network oscillations (Isaacson and Scanziani, 2011; Miles et al., 1996; Pouille et al., 2013). Applying extracellular or loose cell-attached recording methods to circumvent the use of current-injection was unsuccessful due to the lack of intrinsic activity inherent in PCs of acute mPFC slices. This necessitated the use of direct current injections which are a well-established method for assessing drug effects on cellular excitability as demonstrated by their use with PB, diazepam and THIP for example, and so was considered a valid method of assessing excitability and the influence of α2-$GABA_A$Rs.

5.3.2 THDOC decreases PC excitability when basal GABA levels are elevated

The present study showed a significant effect of THDOC on sIPSC decay times of mouse mPFC PCs. Given the significance of GABAergic inputs in modulating cortical excitability (Isaacson and Scanziani, 2011), we hypothesised that THDOC, by potentiating $GABA_AR$ function and thus synaptic inhibition, should reduce PC excitability. However, similar to a previous study conducted in the rat visual cortex (Jang et al., 2013), we did not observe an effect of THDOC on PC excitability using concentrations of 100 nM or 300 nM. The study by Jang and colleagues did, however, detect an effect of 500 nM THDOC on both

tonic currents and PC excitability in a layer- and cell-type specific manner. Therefore, we increased the concentration of THDOC to 500 nM. However, for THDOC to potentiate, $GABA_AR$ receptors need to be activated by GABA and it was possible that extracellular concentrations of GABA may be significantly reduced in acute slices due to washout. We hypothesised that the GABAergic tone in the slice might therefore be too low to produce a significant change in conductance in response to THDOC or bicuculline. For this reason, 5 µM GABA was added to the bath, a concentration which had previously been used to increase tonic currents in cortical neurons (Glykys et al., 2008; Jang et al., 2013). At the cell membrane level, such a concentration is likely to be much lower than 5 µM due to the presence of GABA uptake mechanisms and could possibly resemble physiological GABA concentrations *in vivo* (Glykys and Mody, 2006). Similarly, endogenous neurosteroids have been shown to reach levels of around 20 nM in response to stress (Purdy et al., 1991) and can range up to 100 nM during pregnancy (Paul and Purdy, 1992). Therefore, 500 nM THDOC is a higher concentration than can be expected to occur physiologically and is close to threshold for directly activating $GABA_ARs$ (Callachan et al., 1987) though these agents will also distribute freely into cell membranes and intracellular structures, thus significantly limiting the free concentration that is able to bind to $GABA_ARs$ (Chisari et al., 2010b).

However, in the present study we found a similar increase in decay times when comparing 500 nM plus 5 µM GABA (32% increase) and 100 nM THDOC alone (27% increase) in layer V/VI pyramidal neurons, without affecting other sIPSC parameters. The difference in sIPSC decay prolongation by THDOC, previously described between genotypes, was also unaffected by the altered drug concentrations. Tonic currents, however, were 5-6 fold larger in the higher concentrations of THDOC and elevated GABA in both genotypes. This suggests that the altered experimental conditions have a comparable effect on synaptic inhibition, but significantly increase tonic inhibition.

Under these conditions, THDOC did produce a significant reduction in pyramidal cell excitability (Figure 5.1), showing that neurosteroids influence PC firing and thus shape PC output in the mPFC. Since we are dictating the chloride reversal potential (-66 mV)

to be slightly depolarised compared to the resting membrane (-70 to -73 mV) potential through the intracellular solution, the net effect of $GABA_AR$ activation on membrane potential would be presumed to be depolarising. However, our results show no effect of $GABA_AR$ activation on membrane potential (Table 5.2). Hence, the reduction in pyramidal cell firing observed here is most likely due to shunting inhibition.

5.3.3 Basal PC gain and THDOC modulation of excitability across cell layers and genotypes

Judging from the input output relationships (Figure 5.2), there appears to be a difference in the slopes and thresholds between layers II/III and V/VI of wild-type PCs under basal conditions, with lower thresholds and shallower slopes associated with cells in layers V/VI. Since the slope of the input-output curve corresponds to the neuronal gain, this might indicate a smaller gain for PCs in the layers V/VI, which increases their dynamic range for integrating signals compared to cells from the layers II/III. This could be indicative of a stronger requirement to produce distinctive outputs in layer V/VI, which is in line with their suggested role as the main output layer projecting to other cortical as well as subcortical areas (Shepherd, 2009). Similarly, the higher threshold observed in layer II/III neurons equates to a reduced excitability compared to layer V/VI, which is congruent with the alleged role of layer II/III as the main recipient of afferents from the thalamus and other brain areas (Shepherd, 2009) and hence a requirement to select only salient, strong inputs. Interestingly, in the presence of THDOC, the relative increase in threshold is similar across cortical layers and α2 genotypes, suggesting that α2-$GABA_ARs$ do not play a pivotal role in neurosteroid-modulation of mPFC excitability. However, THDOC does appear to increase the gradient of the input-output slopes in $\alpha2^{WT}$ cells and decrease similar slopes in $\alpha2^{M/M}$ cells (although this effect was only significant in $\alpha2^{M/M}$ cells), while a laminar difference in basal slopes is only present in $\alpha2^{WT}$ slices. These observations could point to a potential role for α2-$GABA_ARs$ in modulating neurosteroid-induced gain changes. Since we and others have found that α2-$GABA_ARs$ are enriched at the AIS (Nusser et al., 1996b) and since there is evidence for excitatory GABAergic transmission at the AIS (Kole and Stuart, 2012; Stein and Nicoll, 2003), THDOC might lead to an increase in excitation through α2-$GABA_ARs$ at the AIS.

Due to the ablation of this potential excitatory action of THDOC in $\alpha2^{M/M}$ slices, the remaining inhibitory effect of THDOC acting through other non-AIS located $GABA_A$Rs could explain the reduction in slope observed. However, these values were obtained from a linear regression of input-output relationships, so would need corroboration.

Furthermore, there was no difference in changes to IEIs caused by THDOC between different cortical layers or α2 genotypes. The lack of laminar difference is surprising, since THDOC was shown to have a stronger effect on synaptic decay times in the layers V/VI (see chapter 4). If the reduction in excitability was being mediated by phasic inhibition, then we would have expected to see a stronger reduction in excitability in the inner layers. However, as mentioned later, our current step protocol only detected excitability changes associated with changes in tonic conductance, which are elevated in 500 nM THDOC plus 5 µM GABA and do not vary across mPFC layers or α2 genotypes. As PC excitability was similar between genotypes, an involvement of α2-$GABA_A$R in modulating PC firing frequency seems less likely.

5.3.4 Activating 5-HT_{2C} receptors increases GABAergic release in mPFC but does not affect PC excitability

To selectively facilitate GABA release at Chandelier-PC synapses, and thus unmask the effect of incoming inhibition directly to the AIS, we turned to 5-HT_{2C} receptors. Previous studies have shown that 5-HT_{2C} receptors are expressed in PV interneurons present in the inner layers of mPFC (Liu et al., 2007) and that 5-HT_{2C} receptor activation can both increase and decrease GABAergic transmission. For example, whereas activation of 5-HT_{2C} receptors leads to an increase of GABAergic release in SN (Burke et al., 2014; Invernizzi et al., 2007) and increased mIPSC frequency in VTA dopaminergic neurons (Theile et al., 2009), activation in the NAcc inhibits potassium-stimulated GABA-release (Kasper et al., 2014). Since 5-HT_{2C} receptors are expressed on a variety of cells, however, their net effect depends on the particular interaction of neurons within the network investigated (Berg et al., 2008), which may at least in part explain the differences observed in those studies.

Here, we noted a 50% increase in GABA-induced activity on layer V/VI PCs in response to 5-HT_{2C} receptor activation (Figure 5.5), in accord with the predominant expression of these receptors on PV-interneurons in the mPFC and their crucial role in regulating PC firing. In particular in the case of Chandelier cells, we were expecting to see an influence of 5-HT_{2C} receptor activation on PC firing in response to our depolarising current injection. While it is debated whether Chandelier cells exert an excitatory or inhibitory effect over PC excitability (Woodruff et al., 2010), the main effect in the present study should be a shunting inhibition, since the chloride reversal potential was set close to the resting membrane potential. Nevertheless, despite the increase in sIPSC amplitude observed, 5-HT_{2C} receptor activation had no effect on spike IEIs, either alone or in conjunction with THDOC, compared to aCSF. This observation therefore does not strongly support a role for α2-$GABA_A$Rs in mediating neurosteroid-induced changes in excitability. However, previous studies have observed both excitatory and inhibitory effects of 5-HT_{2C} receptor activation, despite an overall increase in extracellular GABA concentration (Invernizzi et al., 2007). In line with this, sIPSC frequencies in the present study, while increased on average, were unaffected by 5-HT_{2C} receptor activation in some cells (3/13 cells). Due to the complex connectivity in the mPFC, the net response of an individual PC is determined by the interplay of both PCs and interneurons participating in the local circuit. To complicate matters further, 5-HT_{2C} receptors are also present on PCs themselves, albeit to a lesser extent than PV interneurons (Liu et al., 2007), where they could potentially increase excitability directly, significantly counteracting any presynaptic increase in inhibitory transmission. Indeed, we did find evidence for a postsynaptic effect of 5-HT_{2C} receptor activation on PC membrane potential and input resistance.

Therefore, while these results fail to show a contribution of α2-$GABA_A$Rs towards neurosteroid-mediated changes in excitability, they also cannot completely discount a role for α2-$GABA_A$Rs in modulating excitability *in vivo*.

Interestingly, it was notable that the IEIs after 5-HT_{2C}R activation in $\alpha2^{WT}$ slices were longer than those measured in $\alpha2^{M/M}$ slices in layer V/VI, which presented itself as a

reduced effect on excitability in the mutant compared to the wild-type. An explanation for this difference could be due to the previously described differential effects of activation of Chandelier cells (Woodruff et al., 2011). This study found that Chandelier cells could be excitatory or inhibitory depending on the postsynaptic membrane potential, being excitatory on cells held at the resting membrane potential and inhibitory on cells held at a membrane potential depolarised beyond E_{Cl}. Furthermore, difficulties in assessing effects of 5-HT_{2C} receptor agonism could lie in the non-GABAergic effects of 5-HT_{2C} receptor agonists. For example, in the spinal cord, Ro-60-0175, the 5-HT_{2C}R agonist used here has been shown to increase NMDA-mediated depolarisation (Bigford et al., 2012) and this could have been altered in the mutant model used in this study.

5.3.5 Increases in tonic GABA inhibition reduce PC excitability

As changes to synaptic inhibition had seemingly little effect on PC excitability, we used a number of modulators that are known to affect synaptic and extrasynaptic $GABA_AR$ activity, to assess whether changes in synaptic inhibition have any influence on spike intervals. Firstly, using 100 nM THDOC alone, which affected sIPSC decay times (i.e. synaptic inhibition), but not tonic inhibition, we were unable to alter PC firing. However, applying 5 µM GABA and increasing THDOC to 500 nM, which increased tonic currents 5-6 fold, but did not further prolong sIPSC decay times, did reduce PC excitability. Secondly, we detected no laminar difference in PC excitability in response to THDOC despite our previous evidence for an increased synaptic effect of THDOC in layer V/VI cells. Thirdly, the 5-HT_{2C} receptor agonist, Ro-60-0175 (which increased sIPSC frequency in layer V/VI PCs), did not influence spike IEIs. Fourthly, pentobarbitone, which robustly increased sIPSC amplitudes, prolonged their decay times and increased tonic currents, significantly reduced PC excitability. Fifthly, diazepam, which increased sIPSC frequency and prolonged sIPSC decay times, though not as efficaciously as pentobarbitone, had a negligible effect on tonic currents, and did not affect PC excitability. Finally, the δ-$GABA_AR$ selective agonist, THIP, used at 1 µM, enhanced tonic inhibition (as demonstrated in chapter 4) without affecting postsynaptic phasic inhibition and significantly reduced PC excitability. Both the effect on tonic inhibition and reduction in

excitability were more pronounced when a non-selective concentration of 5 µM THIP was used [data not shown].

Together, these data strongly suggest that the current step protocol used here is sufficiently sensitive to detect changes in GABAergic inhibition, and the effects of $GABA_AR$ modulators on cell excitability. The sensitivity of the protocol has alluded to an effect of tonic rather than phasic inhibition in modulating PC firing. The observed effects support a strong role of tonic GABAergic inhibition in modulating mPFC output and thus mPFC function, with its dysregulation possibly being important in psychiatric disease. Consistent with this, previous research has reported a schizophrenia-like phenotype in a mouse-model which elevates basal GABAergic tone in PFC (Yu et al., 2013), and a more recent study has found an increase in tonic GABAergic inhibition in response to neurosteroids in the amygdala, suggestive of a role in anxiety (Romo-Parra et al., 2015).

5.4 Conclusions

1. Under conditions of elevated extracellular GABA, THDOC reduces mPFC pyramidal cell AP firing frequency in $\alpha2^{WT}$ and $\alpha2^{M/M}$ neurons.

2. Baseline excitability and changes in excitability (measured as IEIs) mediated by THDOC are independent of α2-containing $GABA_A$Rs and of the mPFC cell layer.

3. Basal spike firing threshold (measured as input-output curve offset) varies across mPFC layers, but increased thresholds mediated by the neurosteroid THDOC are independent of the mPFC layer and $GABA_A$R α2 genotype.

4. Basal neuronal gain in the mPFC is larger in layers II/III in $\alpha2^{WT}$ only. THDOC differentially modulates the gain depending on α2 genotype. This points towards a potential role for α2-$GABA_A$Rs in mediating neurosteroid effects on gain but not on threshold or excitability of mPFC PCs.

5. The 5-HT_{2C} receptor agonist Ro-60-0175 increases GABAergic release onto layer V/VI pyramidal neurons without affecting excitability.

6. If co-applied with Ro-60-0175, THDOC (500 nM) does not alter spiking frequency compared to Ro-60-0175 alone, but IEIs are significantly longer in the presence of Ro-60-0175 in $\alpha2^{WT}$ compared to $\alpha2^{M/M}$ mice, possibly resulting from a postsynaptic effect of 5-HT_{2C} receptors. There is no evidence supporting a contribution of α2-$GABA_A$R towards the regulation of PC firing frequency by neurosteroids at the AIS.

7. Using our current step protocol, increases in tonic GABAergic inhibition have a stronger effect over PC firing rates than increases in synaptic inhibition, as demonstrated by the effects of PB, THIP and THDOC plus GABA. These modulators significantly increase tonic inhibition and reduce cell excitability. Moreover, the lack of an effect on cell spike firing when applying THDOC alone, Ro-60-0175 or diazepam to modulate just phasic GABAergic transmission, supports a significant role for tonic currents in regulating PC excitability.

6 General discussion

6.1 Modulation of prefrontal cortical inhibition

GABAergic inhibition can be modulated by a variety of endogenous compounds (neurosteroids, endocannabinoids, dopamine etc.) as well as by pharmacological agents (barbiturates, benzodiazepines, anaesthetics etc.). Given the important role of GABAergic inhibition for effective CNS function, and given the specific distribution and pharmacological properties of different $GABA_AR$ subtypes (Pirker et al., 2000; Sieghart, 1995), understanding how these subtypes are modulated in a physiological context can help in the design of novel drugs with a more targeted, narrow functional profile. Since the mPFC serves a central role in executive function and receives modulatory afferents from a number of central brain regions involved in motivation, reward, learning and emotion (Hoover and Vertes, 2007), it is important to study the effects of some of those neuromodulators and endogenous neurosteroids on prefrontal GABAergic inhibition, which was the motivation behind this thesis.

6.1.1 Activation of D4 receptors has no apparent functional effect on postsynaptic $GABA_ARs$

Previous studies had assessed the effect of activating D4 receptors on GABAergic inhibition in the PFC and found a reduction in synaptic inhibition via a downregulation of surface postsynaptic $GABA_ARs$ (Graziane et al., 2009; Wang et al., 2002). The aim of the present study was to identify whether these effects were mediated via specific $GABA_AR$ isoforms, given their preference for specific presynaptic inputs and their distinct subcellular distribution (Klausberger et al., 2002; Nusser et al., 1996b). Using a primary cortical culture, we found a global reduction in α2-$GABA_AR$ cell surface expression after exposure to the D4 agonist PD168077. Furthermore, we observed an upregulation of α2-$GABA_ARs$ in the presence of the D4 antagonist L-745,870, revealing a potential constitutive activity of D4 receptors in cultured neurons. However, there were no significant differences in the D4 receptor mediated effect between subcellular

compartments (AIS, dendrites and soma), suggesting that there are no preferred dopaminergic input sites for these cultured neurons. This may stem from a lack of dopaminergic afferents in this culture system, since an interaction between presynaptic terminals and postsynaptic sites can trigger receptor accumulation, as has previously been shown for $GABA_ARs$ (Jacob et al., 2005) as well as glutamate receptors (Broadie, 1994; Featherstone et al., 2002; Mi et al., 2002; Rao et al., 2000). However, the previous studies reporting an effect of DA on $GABA_ARs$ also used similar PFC cultures (Graziane et al., 2009). Nevertheless, the use of a VTA-PFC co-culture system may prove useful in this context by providing dopaminergic inputs to pyramidal neurons *in vitro*.

Contrary to the previous studies, we were unable to find any functional effects of D4 receptor activation on postsynaptic inhibition in either cultures or acute slice preparations of the PFC. While we cannot conclusively explain why this might be, it seems reasonable to propose that the causes lie in methodological variations, especially given the complexity of the dopaminergic system and resulting inconsistency between different studies (reviewed in Seamans and Yang, 2004).

6.1.2 Neurosteroids modulate GABAergic inhibition in the mPFC

Neurosteroids are potent endogenous allosteric modulators of $GABA_ARs$ and are involved in a range of physiological (stress response, oestrous cycle, etc) as well as pathophysiological processes (anxiety, depression, etc). Previous work from our group had used a Q241M knock-in mouse model, which expresses neurosteroid-insensitive $GABA_AR$ α2 subunits, to probe the potential anxiolytic and antidepressant function of neurosteroid-modulation at α2-$GABA_ARs$ (Durkin, 2012). In the present study we assessed the contribution of α2-$GABA_ARs$ to synaptic and tonic inhibition within different layers of the mPFC, and investigated the potential for endogenous neurosteroid-modulation via α2-$GABA_ARs$ in this brain region.

We found a significant contribution of α2-$GABA_ARs$ towards synaptic inhibition across the mPFC. In line with its distinctive laminar distribution, the α2-$GABA_AR$ component of neurosteroid-modulation of synaptic sIPSCs was larger in layers II/III, where the α2

subunit is more strongly expressed (Pirker et al., 2000; Sieghart and Sperk, 2002; Wisden et al., 1992), than in layer V/VI. This was supported by the discovery of an endogenous neurosteroid tone at α2-$GABA_A$Rs in layer II/III only, which, in addition to varying α2 subunit levels, may be mediated by differences in endogenous neurosteroid levels across cortical layers. Interestingly, while a previous study using combined *in situ* hybridisation and immunohistochemistry labelling showed increased presence of 3α-HSD and 5α-reductase in layer II/III of the somatosensory cortex (Agís-Balboa et al., 2006), a later study by the same group suggested similar levels of 3α-HSD across layers in frontal cortex and higher levels of 5α-reductase in layer V/VI (Agís-Balboa et al., 2007). However, the magnitude of enzymatic labelling does not necessarily allow conclusions about the levels of protein expression (their end-product). Hence, in the absence of any studies investigating cortical neurosteroid levels, our findings provide new evidence for a differential distribution of neurosteroids within the mPFC.

Furthermore, we resolved a larger exogenous neurosteroid-mediated enhancement of sIPSC duration in layer V/VI compared to layer II/III. This is in accord with the regional distribution of $GABA_A$R isoforms (Pirker et al., 2000; Sieghart and Sperk, 2002; Wisden et al., 1992) and expression of subtypes with higher neurosteroid-sensitivity, such as α3-$GABA_A$Rs, which show greater expression in layer V/VI and higher sensitivity to exogenous neurosteroids (Belelli et al., 2002).

Lastly, despite the distinct distribution of $GABA_A$R subunits contributing to extrasynaptic receptors across mPFC layers (Pirker et al., 2000; Sieghart and Sperk, 2002; Wisden et al., 1992), we did not observe laminar differences in the magnitude of GABA-mediated tonic currents in the mPFC. If, despite the presence of different isoforms of extrasynaptic $GABA_A$Rs, the observed tonic current under baseline conditions is the same across mPFC layers, then instead of mediating different absolute tonic currents, these receptors may play a role in differentially *modulating* tonic current under certain physiological or pharmacologically-induced situations. For example, δ-$GABA_A$Rs, which are more strongly expressed in layers II/III compared to α5-$GABA_A$Rs, are more sensitive to neurosteroids, but insensitive to benzodiazepines; while α5-$GABA_A$Rs are more strongly

expressed in layers V/VI, and are sensitive to benzodiazepines, with GABA being a high efficacy agonist (Sieghart, 1995). Hence, despite the absence of laminar differences in baseline tonic inhibition, it may still be differentially modulated depending on the cortical layer.

6.2 Effect of modulating different forms of GABAergic inhibition on PC excitability

6.2.1 Activating 5-HT_{2C}Rs increases GABAergic release onto PCs

Given the preferred localisation of α2-$GABA_A$Rs to the AIS, they are in a strong position to modulate PC firing and hence, cortical network activity (Nusser et al., 1996b; Veres et al., 2014). We therefore assessed the contribution of α2-$GABA_A$R mediated synaptic inhibition towards PC excitability using a single-step current injection protocol. In order to increase synaptic release of GABA onto the pyramidal neuron AIS, we used the 5-HT_{2C}R-agonist, Ro-60-0175, to stimulate 5-HT_{2C}Rs on presynaptic PV-positive interneurons in the mPFC (Liu et al., 2007). Moreover, 5-HT_{2C}R agonists have previously been shown to increase extracellular GABA (Abi-Saab et al., 1999; Invernizzi et al., 2007). However, it is important to note that the effect on GABA levels appears to be dependent on brain region, since a different study in the NAcc found a decrease in GABA levels upon 5-HT_{2C}R-activation (Kasper et al., 2014).

Targeting serotonergic receptors revealed some novel findings showing a Ro 60-0175-mediated increase in GABA presynaptic release onto mPFC PCs. This increase was completely blocked by a 5-HT_{2C}R-antagonist, which is compelling evidence for a 5-HT_{2C}R–mediated effect. This effect on GABA release was only manifest in layers V/VI, in accord with the laminar distribution of this receptor subtype (Liu et al., 2007). Given the important role of fast-spiking PV-positive interneurons in shaping PC output, and given their prolific axonal extensions contacting a large number of PCs, these results suggest a strong modulatory role for serotonergic inputs in regulating networks of pyramidal neurons (Puig and Gulledge, 2011). This may in turn affect the activity of other subcortical regions contacted by the mPFC, such as the VTA. Interestingly, previous studies found a serotonin-mediated increase in PC excitability and a concomitant

increase in excitatory transmission from the mPFC to the VTA via 5-HT_{2A}R expressing PCs (Bortolozzi et al., 2005; Puig et al., 2003). This could counteract the decrease in excitability of PCs via 5-HT_{2C}R-expressing interneurons, as shown here, and the net effect of serotonin would therefore depend on the balance of its excitatory and inhibitory actions. Since it has been shown in monkey brain that most serotonergic inputs onto PFC contact interneurons, the inhibitory pathway may be more favoured (Smiley and Goldman-Rakic, 1996). Changes in cortical serotonin levels and associated receptor activity may therefore have wide-ranging implications for prefrontal top-down control in pathways involved in reward, learning and planning. Such a key modulatory function of serotonin is in agreement with its central role in the treatment of neuropsychiatric conditions, such as depression.

6.2.2 The influence of tonic and phasic inhibition on mPFC pyramidal cell output

Despite the observed increase in GABAergic transmission onto PCs in the presence of Ro 60-0175, we could not detect a specific contribution of α2-$GABA_A$Rs to the reduction in PC excitability caused by applying the neurosteroid THDOC, although it may play a role in modulating neuronal gain. In addition, measuring IEIs using a current injection protocol to quantify neuronal excitability, we could not detect any significant changes to PC excitability mediated by phasic inhibition alone. In a series of experiments using relatively-selective $GABA_A$R modulators which increased or inhibited either tonic or phasic inhibition, or a combination of both, we discovered that while we were able to resolve changes in PC excitability when tonic inhibition, or a combination of tonic and phasic inhibition, were manipulated, we did not observe changes in excitability due to modulation of synaptic inhibition alone. This suggested a more important role for tonic inhibition in modulating mPFC pyramidal cell activity than previously thought.

However, an alternative possibility is that the method used to gauge PC excitability may be less sensitive to changes in phasic compared to tonic inhibition, since it is not expected to replicate the precise and complex computational integration, which dictates PC activity in an *in vivo* physiological context. Furthermore, it is usual when recording GABA inhibition to set the internal chloride concentration high. This will change the size and direction of currents flowing across the membrane upon $GABA_A$R

activation, though synaptic inhibition should also be more prolonged, thus having a greater effect (Houston et al., 2009). Nevertheless, whether internal Cl^- levels are important could be solved by using gramicidin-perforated patch recordings, which would allow recording under near physiological internal Cl^- concentrations. Furthermore, in order to specifically target synaptic inhibition, conducting paired recordings from fluorophore-labelled (GFP) Chandelier cells and PCs, to assess the effect of direct Chandelier excitation on PC spike firing, would be helpful. In a similar manner, a previous study has used paired perforated-patch as well as cell-attached recordings to study the effect of GFP-labelled Chandelier neurons in the somatosensory cortex (Woodruff et al., 2009) and found both depolarising as well as hyperpolarising effects of GABA that are dependent on the postsynaptic membrane potential (Woodruff et al., 2011). Therefore the physiological situation with regard to the effectors of synaptic inhibition may not be easily predictable. In conjunction with neurosteroids in our mouse model, paired recordings could be another powerful method to assess the contribution of α2-$GABA_A$Rs towards PC excitability.

Overall, we did find a significant contribution of GABA tonic inhibition towards PC excitability in the mPFC. The strength of this effect on excitability appeared to be similar across different mPFC layers and was proportionate to the magnitude of the tonic current. We also found that in layer V/VI PCs, changes in excitability involved, at least to some extent, δ subunit $GABA_A$Rs. Together, these results point to an important role for tonic inhibition via αβδ $GABA_A$Rs in shaping mPFC output, which may be linked to the emerging implication that dysfunctional tonic inhibition is an important component of some neuropsychiatric disorders (Brickley and Mody, 2012).

6.3 Future directions

6.3.1 Differences in $GABA_A$R modulation in mPFC subregions or between classes of interneurons

While the focus of the present study has been to assess modulation of GABAergic inhibition in mPFC PCs, this perspective could be widened to include the role of the

different classes of GABAergic interneurons in future experiments. Given their multifaceted nature (Druga, 2009; Markram et al., 2004), with more than 10 different types of interneurons synapsing onto subsets of other interneurons or PCs, often restricted to their own layer or cortical column, a detailed analysis and classification of distinctive modulation of different types of interneurons would be an ambitious project beyond the scope of this thesis. It may be worthwhile to focus initially on one group of interneurons of particular interest, the Chandelier cells. They have received an increasing amount of attention due to their prominent role at the AIS and have been associated with deficits in network oscillations which are a characteristic of schizophrenia (Lewis, 2011). A challenge will be the unequivocal identification of interneuron cell types. While a lot of evidence has accrued over the years to allow categorisation of interneurons based on a number of features, to date no reliable single marker exists. Instead, one would have to employ a combination of morphological, electrophysiological and biochemical markers for identification purposes. The use of a transgenic mouse-lines selectively expressing GFP in PV-positive interneurons could help in this endeavour (Meyer et al., 2002).

6.3.2 Modulation of GABAergic inhibition by the serotonergic system

Besides dopamine, serotonin is another major neuromodulator in the CNS. It is involved in the regulation of mood, impulse control and cognition and can increase the release of several neurotransmitters as well as alter the neurotransmitter response postsynaptically (Celada et al., 2013). Given the density of its innervation, the serotoninergic system is thought to play a crucial role in modulating PFC function. The main serotonergic afferents to the mPFC originate from the DRN and are mostly uniformly spread across the mPFC (Hoover and Vertes, 2007). There is significant interaction between the serotonergic and GABAergic system (Yan, 2002). For example, $GABA_A$Rs have been shown to be involved in stress-mediated down-regulation of 5-HT in the hippocampus by 5-HT_{2C}Rs (Martin et al., 2014), and, as mentioned previously and shown in the present study, activation of 5-HT_{2C}Rs can lead to changes in GABA levels depending on the brain region (Abi-Saab et al., 1999; Invernizzi et al., 2007; Kasper et al., 2014). Previous research has shown direct interactions between 5-HT receptor

activation and postsynaptic $GABA_AR$s. Activation of 5-HT_{2A}Rs in the rat cerebral cortex was shown to induce a significant enhancement of interneuron and PC sIPSC frequency and amplitude (Zhou and Hablitz, 1999b), while activation of 5-HT_{2C}R was shown to reduce $GABA_AR$ current when both receptors were co-expressed in *Xenopus* oocytes (Huidobro-Toro et al., 1996). In line with these results, a later study showed a decrease in sIPSCs of PFC pyramidal neurons after exposure to 5-HT, most likely mediated by phosphorylation of $GABA_AR$ γ2 subunits via PKC (Feng et al., 2001).

Together these results show an important role for the serotoninergic system in modulating PFC function, some of which may be mediated via changes in GABAergic transmission. The molecular mechanisms underlying serotonergic modulation of $GABA_AR$s, however, are so far not fully understood, nor are the roles of different receptor subtypes in this interaction known. In line with the present study, future experiments could therefore assess the effect of different 5-HT receptor ligands on PC GABAergic transmission as well as the potential effects on $GABA_AR$ isoform localisation.

6.4 Concluding remarks

The mPFC is a vital part of processes involved in reward, action-planning and cognitive control. Its complex network of inhibitory and excitatory circuits is tightly regulated to produce network oscillations in association with normal neural circuit function. The modulation of pyramidal neuron firing, the main output neurons of the mPFC, is orchestrated by a network of interneurons whose temporally and spatially differentiated inhibitory inputs shape network activity. The aim of the present study was to elucidate the modulation of the main inhibitory neurotransmitter receptors, $GABA_AR$s, by dopamine and neurosteroids and assess the downstream effects of changes in GABAergic transmission on PC firing.

Contrary to previous research (Graziane et al., 2009; Wang et al., 2002), we did not find a significant effect of dopaminergic activity via D4 receptors on $GABA_AR$-mediated postsynaptic currents. We did, however, observe a reduction in presynaptic GABA release in acute slices as well as an overall increase in α2-$GABA_AR$ surface expression in

cultured pyramidal-shaped neurons exposed to a D4 receptor agonist. This may mimic pathophysiological changes associated with schizophrenia (Beneyto et al., 2011; Lewis, 2011).

We have also demonstrated a significant contribution of α2-$GABA_A$Rs towards synaptic inhibition in pyramidal neurons of the mPFC. This $GABA_A$R isoform was of particular interest due to their preferred localisation at the AIS (Nusser et al., 1996b) and their involvement in neural circuits associated with anxiety (Löw et al., 2000). Their contribution to cortical pyramidal cell inhibition exhibited laminar variation, being more influential in layers II/III, in agreement with higher expression of $GABA_A$R α2 subunits in this area (Pirker et al., 2000; Sieghart and Sperk, 2002; Wisden et al., 1992). We also uncovered the presence of an endogenous neurosteroid tone in layers II/III, while pyramidal neurons of the deeper layers V/VI respond more strongly to exogenously-applied THDOC, suggesting a difference in neurosteroid sensitivity of the $GABA_A$ receptor population in the respective cortical layers.

Lastly, while we could not resolve a specific contribution of α2-$GABA_A$Rs towards neurosteroid-mediated changes in PC excitability, we were able to resolve an effect of tonic inhibition on PC excitability, and also provide evidence for a novel selective increase in presynaptic GABA-release, onto PCs, in response to 5-HT_{2C}R activation.

In summary, this study underlines the complexity of prefrontal GABAergic inhibition by demonstrating differential effects of specific agonists of physiologically relevant neuromodulatory pathways, which are dependent on the $GABA_A$R subtype and also on the cortical layer.

7 References

Abi-Saab, W.M., Bubser, M., Roth, R.H., and Deutch, A.Y. (1999). 5-HT_2 receptor regulation of extracellular GABA levels in the prefrontal cortex. Neuropsychopharmacology *20*, 92–96.

Abramian, A.M., Comenencia-Ortiz, E., Modgil, A., Vien, T.N., Nakamura, Y., Moore, Y.E., Maguire, J.L., Terunuma, M., Davies, P.A., and Moss, S.J. (2014). Neurosteroids promote phosphorylation and membrane insertion of extrasynaptic $GABA_A$ receptors. Proc. Natl. Acad. Sci. U. S. A. *111*, 7132–7137.

Acosta-García, J., Hernández-Chan, N., Paz-Bermúdez, F., Sierra, A., Erlij, D., Aceves, J., and Florán, B. (2009). D4 and D1 dopamine receptors modulate [3H] GABA release in the substantia nigra pars reticulata of the rat. Neuropharmacology *57*, 725–730.

Adams, J.M., Thomas, P., and Smart, T.G. (2015). Modulation of neurosteroid potentiation by protein kinases at synaptic- and extrasynaptic-type $GABA_A$ receptors. Neuropharmacology *88*, 63–73.

Van Aerde, K.I., and Feldmeyer, D. (2015). Morphological and physiological characterization of pyramidal neuron subtypes in rat medial prefrontal cortex. Cereb. Cortex *25*, 788–805.

Agís-Balboa, R.C., Pinna, G., Zhubi, A., Maloku, E., Veldic, M., Costa, E., and Guidotti, A. (2006). Characterization of brain neurons that express enzymes mediating neurosteroid biosynthesis. Proc. Natl. Acad. Sci. U. S. A. *103*, 14602–14607.

Agís-Balboa, R.C., Pinna, G., Pibiri, F., Kadriu, B., Costa, E., and Guidotti, A. (2007). Down-regulation of neurosteroid biosynthesis in corticolimbic circuits mediates social isolation-induced behavior in mice. Proc. Natl. Acad. Sci. U. S. A. *104*, 18736–18741.

Akk, G., and Steinbach, J.H. (2000). Activation and block of recombinant $GABA_A$ receptors by pentobarbitone: a single-channel study. Br. J. Pharmacol. *130*, 249–258.

Alexander, S.P.H., Mathie, A., and Peters, J.A. (2011). Guide to Receptors and Channels (GRAC), 5th edition. Br. J. Pharmacol. *164*, S1–S2.

Ali, A.B., and Thomson, A.M. (2008). Synaptic α5 Subunit–Containing $GABA_A$ Receptors Mediate IPSPs Elicited by Dendrite-Preferring Cells in Rat Neocortex. Cereb. Cortex *18*, 1260–1271.

Amatrudo, J.M., Weaver, C.M., Crimins, J.L., Hof, P.R., Rosene, D.L., and Luebke, J.I. (2012). Influence of highly distinctive structural properties on the excitability of pyramidal neurons in monkey visual and prefrontal cortices. J. Neurosci. *32*, 13644–13660.

Andersson, R., Johnston, A., and Fisahn, A. (2012). Dopamine D4 receptor activation increases hippocampal γ-oscillations by enhancing synchronization of fast-spiking interneurons. PLoS One *7*, e40906.

Arancibia-Cárcamo, I.L., and Kittler, J.T. (2009). Regulation of $GABA_A$ receptor membrane trafficking and synaptic localization. Pharmacol. Ther. *123*, 17–31.

Arancibia-Cárcamo, I.L., Yuen, E.Y., Muir, J., Lumb, M.J., Michels, G., Saliba, R.S., Smart, T.G., Yan, Z., Kittler, J.T., and Moss, S.J. (2009). Ubiquitin-dependent lysosomal targeting of GABAA receptors regulates neuronal inhibition. Proc. Natl. Acad. Sci. U. S. A. *106*, 17552–17557.

Ariano, M.A., Wang, J., Noblett, K.L., Larson, E.R., and Sibley, D.R. (1997). Cellular distribution of the rat D4 dopamine receptor protein in the CNS using anti-receptor antisera. Brain Res. *752*, 26–34.

Armstrong, C., and Soltesz, I. (2011). Basket cell dichotomy in microcircuit function. J. Physiol. *590*, 683–694.

Arnsten, A.F.T. (2007). Catecholamine and second messenger influences on prefrontal cortical networks of "representational knowledge": a rational bridge between genetics and the symptoms of mental illness. Cereb. Cortex *17 Suppl 1*, i6–i15.

Arnsten, A.F.T. (2009). Stress signalling pathways that impair prefrontal cortex structure and function. Nat. Rev. Neurosci. *10*, 410–422.

Arnsten, A.F.T. (2011). Prefrontal cortical network connections: key site of vulnerability in stress and schizophrenia. Int. J. Dev. Neurosci. *29*, 215–223.

Arnsten, A.F.T., Wang, M.J., and Paspalas, C.D. (2012). Neuromodulation of Thought: Flexibilities and Vulnerabilities in Prefrontal Cortical Network Synapses. Neuron *76*, 223–239.

Arnsten, A.F.T., Wang, M., and Paspalas, C.D. (2015). Dopamine's Actions in Primate Prefrontal Cortex: Challenges for Treating Cognitive Disorders. Pharmacol. Rev. *67*, 681–696.

Aron, A.R., Robbins, T.W., and Poldrack, R.A. (2014). Inhibition and the right inferior frontal cortex: one decade on. Trends Cogn. Sci. *18*, 177–185.

Atack, J.R., Maubach, K.A., Wafford, K.A., O'Connor, D., Rodrigues, A.D., Evans, D.C., Tattersall, F.D., Chambers, M.S., MacLeod, A.M., Eng, W.-S., et al. (2009). In vitro and in vivo properties of 3-tert-butyl-7-(5-methylisoxazol-3-yl)-2-(1-methyl-1H-1,2,4-triazol-5-ylmethoxy)-pyrazolo[1,5-d]-[1,2,4]triazine (MRK-016), a $GABA_A$ receptor α5 subtype-selective inverse agonist. J. Pharmacol. Exp. Ther. *331*, 470–484.

Azdad, K., Piet, R., Poulain, D.A., and Oliet, S.H.R. (2003). Dopamine D4 receptor-mediated presynaptic inhibition of GABAergic transmission in the rat supraoptic nucleus. J. Neurophysiol. *90*, 559–565.

Baimbridge, K.G., Celio, M.R., and Rogers, J.H. (1992). Calcium-binding proteins in the nervous system. Trends Neurosci. *15*, 303–308.

Barnes, E.M. (1996). Use-dependent regulation of $GABA_A$ receptors. Int. Rev. Neurobiol. *39*, 53–76.

Barral, S., Beltramo, R., Salio, C., Aimar, P., Lossi, L., and Merighi, A. (2014). Phosphorylation of histone H2AX in the mouse brain from development to senescence. Int. J. Mol. Sci. *15*, 1554–1573.

Bauer, E.P., Paz, R., and Paré, D. (2007). Γ oscillations coordinate amygdalo-rhinal interactions during learning. J. Neurosci. *27*, 9369–9379.

Beckstead, M.J., Grandy, D.K., Wickman, K., and Williams, J.T. (2004). Vesicular dopamine release elicits an inhibitory postsynaptic current in midbrain dopamine neurons. Neuron *42*, 939–946.

Béïque, J.-C., Imad, M., Mladenovic, L., Gingrich, J.A., and Andrade, R. (2007). Mechanism of the 5-HT_{2A} receptor-mediated facilitation of synaptic activity in prefrontal cortex. Proc. Natl. Acad. Sci. U. S. A. *104*, 9870–9875.

Belelli, D., and Herd, M.B. (2003). The contraceptive agent Provera enhances $GABA_A$ receptor-mediated inhibitory neurotransmission in the rat hippocampus: evidence for endogenous neurosteroids? J. Neurosci. *23*, 10013–10020.

Belelli, D., and Lambert, J.J. (2005). Neurosteroids: endogenous regulators of the $GABA_A$ receptor. Nat. Rev. Neurosci. *6*, 565–575.

Belelli, D., Casula, A., Ling, A., and Lambert, J.J. (2002). The influence of subunit composition on the interaction of neurosteroids with $GABA_A$ receptors. Neuropharmacology *43*, 651–661.

Ben-Ari, Y., Khalilov, I., Kahle, K.T., and Cherubini, E. (2012). The GABA Excitatory/Inhibitory Shift in Brain Maturation and Neurological Disorders. Neurosci. *18*, 467–486.

Bender, K.J., Uebele, V.N., Renger, J.J., and Trussell, L.O. (2012). Control of firing patterns through modulation of axon initial segment T-type calcium channels. J. Physiol. *590*, 109–118.

Benes, F.M., and Berretta, S. (2001). GABAergic interneurons: implications for understanding schizophrenia and bipolar disorder. Neuropsychopharmacology *25*, 1–27.

Beneyto, M., Abbott, A., Hashimoto, T., and Lewis, D.A. (2011). Lamina-Specific Alterations in Cortical $GABA_A$ Receptor Subunit Expression in Schizophrenia. Cereb. Cortex *21*, 999–1011.

Berg, K.A., Clarke, W.P., Cunningham, K.A., and Spampinato, U. (2008). Fine-tuning 5-HT_{2C} receptor function in the brain: molecular and functional implications. Neuropharmacology *55*, 969–976.

Bergman, J., and Rheingold, C.G. (2015). Dopamine D4 Receptor Antagonists for the Treatment of Cocaine Use Disorders. CNS Neurol. Disord. Drug Targets *14*, 707–715.

Berkowitz, R.L., Coplan, J.D., Reddy, D.P., and Gorman, J.M. (2007). The human dimension: how the prefrontal cortex modulates the subcortical fear response. Rev. Neurosci. *18*, 191–207.

Bertram, S., Cherubino, F., Bossi, E., Castagna, M., and Peres, A. (2011). GABA reverse transport by the neuronal cotransporter GAT1: influence of internal chloride depletion. Am. J. Physiol. Cell Physiol. *301*, C1064–C1073.

Bettler, B. (2004). Molecular Structure and Physiological Functions of $GABA_B$ Receptors. Physiol. Rev. *84*, 835–867.

Biagini, G., Panuccio, G., and Avoli, M. (2010). Neurosteroids and epilepsy. Curr. Opin. Neurol. *23*, 170–176.

Bianchi, M.T., and Macdonald, R.L. (2003). Neurosteroids shift partial agonist activation of $GABA_A$ receptor channels from low- to high-efficacy gating patterns. J. Neurosci. *23*, 10934–10943.

Bigford, G.E., Chaudhry, N.S., Keane, R.W., and Holohean, A.M. (2012). 5-HT_{2C} receptors form a protein complex with N-methyl-D-aspartate GluN2A subunits and activate phosphorylation of Src protein to modulate motoneuronal depolarization. J. Biol. Chem. *287*, 11049–11059.

Bormann, J., Hamill, O.P., and Sakmann, B. (1987). Mechanism of anion permeation through channels gated by glycine and GABA in mouse cultured spinal neurones. J. Physiol. *385*, 243–286.

Bortolozzi, A., Díaz-Mataix, L., Scorza, M.C., Celada, P., and Artigas, F. (2005). The activation of 5-HT receptors in prefrontal cortex enhances dopaminergic activity. J. Neurochem. *95*, 1597–1607.

Bowery, N.G. (1993). $GABA_B$ receptor pharmacology. Annu. Rev. Pharmacol. Toxicol. *33*, 109–147.

Branco, T., and Häusser, M. (2011). Synaptic integration gradients in single cortical pyramidal cell dendrites. Neuron *69*, 885–892.

Brandon, N., Jovanovic, J., and Moss, S. (2002). Multiple roles of protein kinases in the modulation of $GABA_A$ receptor function and cell surface expression. Pharmacol. Ther. *94*, 113–122.

Brandon, N.J., Delmas, P., Kittler, J.T., McDonald, B.J., Sieghart, W., Brown, D.A., Smart, T.G., and Moss, S.J. (2000). $GABA_A$ receptor phosphorylation and functional modulation in cortical neurons by a protein kinase C-dependent pathway. J. Biol. Chem. *275*, 38856–38862.

Brickley, S.G., and Mody, I. (2012). Extrasynaptic $GABA_A$ receptors: their function in the CNS and implications for disease. Neuron *73*, 23–34.

Brickley, S.G., Cull-Candy, S.G., and Farrant, M. (1996). Development of a tonic form of synaptic inhibition in rat cerebellar granule cells resulting from persistent activation of $GABA_A$ receptors. J. Physiol. *497 (Pt 3*, 753–759.

Brickley, S.G., Cull-Candy, S.G., and Farrant, M. (1999). Single-channel properties of synaptic and extrasynaptic $GABA_A$ receptors suggest differential targeting of receptor subtypes. J. Neurosci. *19*, 2960–2973.

Brickley, S.G., Farrant, M., Swanson, G.T., and Cull-Candy, S.G. (2001). CNQX increases GABA-mediated synaptic transmission in the cerebellum by an AMPA/kainate receptor-independent mechanism. Neuropharmacology *41*, 730–736.

Bright, D.P., and Smart, T.G. (2013). Methods for recording and measuring tonic $GABA_A$ receptor-mediated inhibition. Front. Neural Circuits *7*, 193.

Bright, D.P., Renzi, M., Bartram, J., McGee, T.P., MacKenzie, G., Hosie, A.M., Farrant, M., and Brickley, S.G. (2011). Profound desensitization by ambient GABA limits activation of δ-containing $GABA_A$ receptors during spillover. J. Neurosci. *31*, 753–763.

Broadie, K.S. (1994). Synaptogenesis in Drosophila: coupling genetics and electrophysiology. J. Physiol. Paris *88*, 123–139.

Brown, N., Kerby, J., Bonnert, T.P., Whiting, P.J., and Wafford, K.A. (2002). Pharmacological characterization of a novel cell line expressing human α4β3δ $GABA_A$ receptors. Br. J. Pharmacol. *136*, 965–974.

Brozoski, T.J., Brown, R.M., Rosvold, H.E., and Goldman, P.S. (1979). Cognitive deficit caused by regional depletion of dopamine in prefrontal cortex of rhesus monkey. Science *205*, 929–932.

Brünig, I., Scotti, E., Sidler, C., and Fritschy, J.-M. (2002). Intact sorting, targeting, and clustering of $GABA_A$ receptor subtypes in hippocampal neurons in vitro. J. Comp. Neurol. *443*, 43–55.

Brunton, P.J., and Russell, J.A. (2008). Keeping oxytocin neurons under control during stress in pregnancy. Prog. Brain Res. *170*, 365–377.

Brunton, P.J., Russell, J.A., and Hirst, J.J. (2014). Allopregnanolone in the brain: protecting pregnancy and birth outcomes. Prog. Neurobiol. *113*, 106–136.

Burke, M. V, Nocjar, C., Sonneborn, A.J., McCreary, A.C., and Pehek, E.A. (2014). Striatal 5-HT_{2C} receptors decrease nigrostriatal dopamine release by increasing $GABA_A$ receptor tone in the substantia nigra. J. Neurochem. *131*, 432–443.

Buschman, T.J., and Miller, E.K. (2007). Top-down versus bottom-up control of attention in the prefrontal and posterior parietal cortices. Science *315*, 1860–1862.

Callachan, H., Cottrell, G.A., Hather, N.Y., Lambert, J.J., Nooney, J.M., and Peters, J.A. (1987). Modulation of the $GABA_A$ receptor by progesterone metabolites. Proc. R. Soc. London. Ser. B, Biol. Sci. *231*, 359–369.

Caraiscos, V.B., Elliott, E.M., You-Ten, K.E., Cheng, V.Y., Belelli, D., Newell, J.G., Jackson, M.F., Lambert, J.J., Rosahl, T.W., Wafford, K.A., et al. (2004). Tonic inhibition in mouse hippocampal CA1 pyramidal neurons is mediated by α5 subunit-containing $GABA_A$ receptors. Proc. Natl. Acad. Sci. U. S. A. *101*, 3662–3667.

Carr, D.B., and Sesack, S.R. (2000). Projections from the rat prefrontal cortex to the ventral tegmental area: target specificity in the synaptic associations with mesoaccumbens and mesocortical neurons. J. Neurosci. *20*, 3864–3873.

Castelli, M.P., Casti, A., Casu, A., Frau, R., Bortolato, M., Spiga, S., and Ennas, M.G. (2013). Regional distribution of 5α-reductase type 2 in the adult rat brain: an immunohistochemical analysis. Psychoneuroendocrinology *38*, 281–293.

Celada, P., Puig, M., and Artigas, F. (2013). Serotonin modulation of cortical neurons and networks. Front. Integr. Neurosci. *7*, 1–20.

Chalifoux, J.R., and Carter, A.G. (2011). $GABA_B$ receptor modulation of synaptic function. Curr. Opin. Neurobiol. *21*, 339–344.

Chambers, M.S., Atack, J.R., Carling, R.W., Collinson, N., Cook, S.M., Dawson, G.R., Ferris, P., Hobbs, S.C., O'connor, D., Marshall, G., et al. (2004). An orally bioavailable, functionally selective inverse agonist at the benzodiazepine site of $GABA_A$ α5 receptors with cognition enhancing properties. J. Med. Chem. *47*, 5829–5832.

Chance, F.S., Abbott, L.., and Reyes, A.D. (2002). Gain Modulation from Background Synaptic Input. Neuron *35*, 773–782.

Chavas, J., and Marty, A. (2003). Coexistence of Excitatory and Inhibitory GABA Synapses in the Cerebellar Interneuron Network. J. Neurosci. *23*, 2019–2031.

Chiara, D.C., Jayakar, S.S., Zhou, X., Zhang, X., Savechenkov, P.Y., Bruzik, K.S., Miller, K.W., and Cohen, J.B. (2013). Specificity of intersubunit general anesthetic-binding sites in the transmembrane domain of the human α1β3γ2 $GABA_A$ receptor. J. Biol. Chem. *288*, 19343–19357.

Di Chiara, G., and Imperato, A. (1988). Drugs abused by humans preferentially increase synaptic dopamine concentrations in the mesolimbic system of freely moving rats. Proc. Natl. Acad. Sci. U. S. A. *85*, 5274–5278.

Chisari, M., Shu, H.-J., Taylor, a, Steinbach, J.H., Zorumski, C.F., and Mennerick, S. (2010a). Structurally diverse amphiphiles exhibit biphasic modulation of $GABA_A$ receptors: similarities and differences with neurosteroid actions. Br. J. Pharmacol. *160*, 130–141.

Chisari, M., Eisenman, L.N., Covey, D.F., Mennerick, S., and Zorumski, C.F. (2010b). The sticky issue of neurosteroids and $GABA_A$ receptors. Trends Neurosci. *33*, 299–306.

Christian, C.A., Herbert, A.G., Holt, R.L., Peng, K., Sherwood, K.D., Pangratz-Fuehrer, S., Rudolph, U., and Huguenard, J.R. (2013). Endogenous positive allosteric modulation of $GABA_A$ receptors by diazepam binding inhibitor. Neuron 78, 1063–1074.

Cobb, S.R., Buhl, E.H., Halasy, K., Paulsen, O., and Somogyi, P. (1995). Synchronization of neuronal activity in hippocampus by individual GABAergic interneurons. Nature *378*, 75–78.

Comenencia-Ortiz, E., Moss, S.J., and Davies, P.A. (2014). Phosphorylation of $GABA_A$ receptors influences receptor trafficking and neurosteroid actions. Psychopharmacology *231*, 3453-65.

Cooper, E.J., Johnston, G.A., and Edwards, F.A. (1999). Effects of a naturally occurring neurosteroid on $GABA_A$ IPSCs during development in rat hippocampal or cerebellar slices. J. Physiol. *521 Pt 2*, 437–449.

Corey, J.L., Guastella, J., Davidson, N., and Lester, H.A. (1994). GABA uptake and release by a mammalian cell line stably expressing a cloned rat brain GABA transporter. Mol. Membr. Biol. *11*, 23–30.

Corpéchot, C., Collins, B.E., Carey, M.P., Tsouros, A., Robel, P., and Fry, J.P. (1997). Brain neurosteroids during the mouse oestrous cycle. Brain Res. *766*, 276–280.

Craig, A.M., and Kang, Y. (2007). Neurexin-neuroligin signaling in synapse development. Curr. Opin. Neurobiol. *17*, 43–52.

Crestani, F., Löw, K., Keist, R., Mandelli, M., Möhler, H., and Rudolph, U. (2001). Molecular targets for the myorelaxant action of diazepam. Mol. Pharmacol. *59*, 442–445.

Crestani, F., Keist, R., Fritschy, J.-M., Benke, D., Vogt, K., Prut, L., Blüthmann, H., Möhler, H., and Rudolph, U. (2002). Trace fear conditioning involves hippocampal α5 $GABA_A$ receptors. Proc. Natl. Acad. Sci. U. S. A. *99*, 8980–8985.

Curley, A.A., and Lewis, D.A. (2012). Cortical basket cell dysfunction in schizophrenia. J. Physiol. *590*, 715–724.

DeFelipe, J. (1997). Types of neurons, synaptic connections and chemical characteristics of cells immunoreactive for calbindin-D28K, parvalbumin and calretinin in the neocortex. J. Chem. Neuroanat. *14*, 1–19.

Defelipe, J., González-Albo, M.C., Del Río, M.R., and Elston, G.N. (1999). Distribution and patterns of connectivity of interneurons containing calbindin, calretinin, and parvalbumin in visual areas of the occipital and temporal lobes of the macaque monkey. J. Comp. Neurol. *412*, 515–526.

Dégenètais, E., Thierry, A.-M., Glowinski, J., and Gioanni, Y. (2002). Electrophysiological properties of pyramidal neurons in the rat prefrontal cortex: an in vivo intracellular recording study. Cereb. Cortex *12*, 1–16.

Dembrow, N., and Johnston, D. (2014). Subcircuit-specific neuromodulation in the prefrontal cortex. Front. Neural Circuits *8*, 54.

Dias, R., Sheppard, W.F.A., Fradley, R.L., Garrett, E.M., Stanley, J.L., Tye, S.J., Goodacre, S., Lincoln, R.J., Cook, S.M., Conley, R., et al. (2005). Evidence for a significant role of α3-containing $GABA_A$ receptors in mediating the anxiolytic effects of benzodiazepines. J. Neurosci. *25*, 10682–10688.

Dixon, C., Sah, P., Lynch, J.W., and Keramidas, A. (2014). $GABA_A$ receptor α- and γ- subunits shape synaptic currents via different mechanisms. J. Biol. Chem. 289, 5399-411

Dixon, C.I., Rosahl, T.W., and Stephens, D.N. (2008). Targeted deletion of the GABRA2 gene encoding α2-subunits of $GABA_A$ receptors facilitates performance of a conditioned emotional response, and abolishes anxiolytic effects of benzodiazepines and barbiturates. Pharmacol. Biochem. Behav. *90*, 1–8.

Dixon, C.I., Morris, H. V, Breen, G., Desrivieres, S., Jugurnauth, S., Steiner, R.C., Vallada, H., Guindalini, C., Laranjeira, R., Messas, G., et al. (2010). Cocaine effects on mouse incentive-learning and human addiction are linked to α2 subunit-containing $GABA_A$ receptors. Proc. Natl. Acad. Sci. U. S. A. *107*, 2289–2294.

Drasbek, K.R., and Jensen, K. (2006). THIP, a hypnotic and antinociceptive drug, enhances an extrasynaptic $GABA_A$ receptor-mediated conductance in mouse neocortex. Cereb. Cortex *16*, 1134–1141.

Druga, R. (2009). Neocortical Inhibitory System. Folia Biol(Praha) *217*, 201–217.

Dunning, D.D., Hoover, C.L., Soltesz, I., Smith, M.A., and O'Dowd, D.K. (1999). $GABA_A$ receptor-mediated miniature postsynaptic currents and α-subunit expression in developing cortical neurons. J. Neurophysiol. *82*, 3286–3297.

Durkin, E.J. (2012). Physiological roles of endogenous neurosteroids at α2 subunit-containing $GABA_A$ receptors. PhD Thesis, University College London.

Dutar, P., and Nicoll, R.A. (1988). A physiological role for $GABA_B$ receptors in the central nervous system. Nature *332*, 156–158.

Edenberg, H.J., Dick, D.M., Xuei, X., Tian, H., Almasy, L., Bauer, L.O., Crowe, R.R., Goate, A., Hesselbrock, V., Jones, K., et al. (2004). Variations in GABRA2, encoding the α2 subunit of the $GABA_A$ receptor, are associated with alcohol dependence and with brain oscillations. Am. J. Hum. Genet. *74*, 705–714.

Ehrlich, I., Humeau, Y., Grenier, F., Ciocchi, S., Herry, C., and Lüthi, A. (2009). Amygdala inhibitory circuits and the control of fear memory. Neuron *62*, 757–771.

Elliott, R. (2003). Executive functions and their disorders. Br. Med. Bull. *65*, 49–59.

Elmslie, K.S., and Yoshikami, D. (1985). Effects of kynurenate on root potentials evoked by synaptic activity and amino acids in the frog spinal cord. Brain Res. *330*, 265-272.

Engin, E., Liu, J., and Rudolph, U. (2012). α2-containing $GABA_A$ receptors: a target for the development of novel treatment strategies for CNS disorders. Pharmacol. Ther. *136*, 142–152.

Eser, D., Baghai, T.C., Schüle, C., Nothdurfter, C., and Rupprecht, R. (2008). Neuroactive steroids as endogenous modulators of anxiety. Curr. Pharm. Des. *14*, 3525–3533.

Essrich, C., Lorez, M., Benson, J.A., Fritschy, J.M., and Lüscher, B. (1998). Postsynaptic clustering of major $GABA_A$ receptor subtypes requires the γ2 subunit and gephyrin. Nat. Neurosci. *1*, 563–571.

Fáncsik, A., Linn, D.M., and Tasker, J.G. (2000). Neurosteroid modulation of GABA IPSCs is phosphorylation dependent. J. Neurosci. *20*, 3067–3075.

Fang, C., Deng, L., Keller, C.A., Fukata, M., Fukata, Y., Chen, G., and Lüscher, B. (2006). GODZ-mediated palmitoylation of $GABA_A$ receptors is required for normal assembly and function of GABAergic inhibitory synapses. J. Neurosci. *26*, 12758–12768.

Farrant, M., and Nusser, Z. (2005). Variations on an inhibitory theme: phasic and tonic activation of $GABA_A$ receptors. Nat. Rev. Neurosci. *6*, 215–229.

Farzampour, Z., Reimer, R.J., and Huguenard, J. (2015). Endozepines. Adv. Pharmacol. 72, 147–164.

Faulhaber, J., Steiger, A., and Lancel, M. (1997). The $GABA_A$ agonist THIP produces slow wave sleep and reduces spindling activity in NREM sleep in humans. Psychopharmacology. *130*, 285–291.

Fava, M., Asnis, G.M., Shrivastava, R.K., Lydiard, B., Bastani, B., Sheehan, D. V, and Roth, T. (2011a). Improved insomnia symptoms and sleep-related next-day functioning in patients with comorbid major depressive disorder and insomnia following concomitant zolpidem extended-release 12.5 mg and escitalopram treatment: a randomized controlled trial. J. Clin. Psychiatry *72*, 914–928.

Fava, M., Schaefer, K., Huang, H., Wilson, A., Iosifescu, D. V, Mischoulon, D., and Wessel, T.C. (2011b). A post hoc analysis of the effect of nightly administration of eszopiclone and a selective serotonin reuptake inhibitor in patients with insomnia and anxious depression. J. Clin. Psychiatry *72*, 473–479.

Featherstone, D.E., Rushton, E., and Broadie, K. (2002). Developmental regulation of glutamate receptor field size by nonvesicular glutamate release. Nat. Neurosci. *5*, 141–146.

Feng, H.-J., and Macdonald, R.L. (2004). Multiple actions of propofol on αβγ and αβδ $GABA_A$ receptors. Mol. Pharmacol. *66*, 1517–1524.

Feng, J., Cai, X., Zhao, J., and Yan, Z. (2001). Serotonin receptors modulate $GABA_A$ receptor channels through activation of anchored protein kinase C in prefrontal cortical neurons. J. Neurosci. *21*, 6502–6511.

Finn, D.A., and Gee, K.W. (1993). The influence of estrus cycle on neurosteroid potency at the γ-$GABA_A$ receptor complex. J. Pharmacol. Exp. Ther. *265*, 1374–1379.

Fiorelli, R., Rudolph, U., Straub, C.J., Feldon, J., and Yee, B.K. (2008). Affective and cognitive effects of global deletion of α3-containing $GABA_A$ receptors. Behav. Pharmacol. *19*, 582–596.

Fries, P. (2009). Neuronal γ-band synchronization as a fundamental process in cortical computation. Annu. Rev. Neurosci. *32*, 209–224.

Fritschy, J.M., and Möhler, H. (1995). $GABA_A$ receptor heterogeneity in the adult rat brain: differential regional and cellular distribution of seven major subunits. J. Comp. Neurol. *359*, 154–194.

Fuchs, C., Abitbol, K., Burden, J.J., Mercer, A., Brown, L., Iball, J., Anne Stephenson, F., Thomson, A.M., and Jovanovic, J.N. (2013). $GABA_A$ receptors can initiate the formation of functional inhibitory GABAergic synapses. Eur. J. Neurosci. *38*, 3146–3158.

Funahashi, S. (2001). Neuronal mechanisms of executive control by the prefrontal cortex. Neurosci. Res. *39*, 147–165.

Furth, K.E., Mastwal, S., Wang, K.H., Buonanno, A., and Vullhorst, D. (2013). Dopamine, cognitive function, and gamma oscillations: role of D4 receptors. Front. Cell. Neurosci. *7*, 102.

Gabbott, P.L., Dickie, B.G., Vaid, R.R., Headlam, A.J., and Bacon, S.J. (1997). Local-circuit neurones in the medial prefrontal cortex (areas 25, 32 and 24b) in the rat: morphology and quantitative distribution. J. Comp. Neurol. *377*, 465–499.

Gabbott, P.L.A., Warner, T.A., Jays, P.R.L., Salway, P., and Busby, S.J. (2005). Prefrontal cortex in the rat: projections to subcortical autonomic, motor, and limbic centers. J. Comp. Neurol. *492*, 145–177.

Gamo, N.J., and Arnsten, A.F.T. (2011). Molecular modulation of prefrontal cortex: rational development of treatments for psychiatric disorders. Behav. Neurosci. *125*, 282–296.

Gao, W.-J., and Goldman-Rakic, P.S. (2003). Selective modulation of excitatory and inhibitory microcircuits by dopamine. Proc. Natl. Acad. Sci. U. S. A. *100*, 2836–2841.

Gao, W.J., Krimer, L.S., and Goldman-Rakic, P.S. (2001). Presynaptic regulation of recurrent excitation by D1 receptors in prefrontal circuits. Proc. Natl. Acad. Sci. U. S. A. *98*, 295–300.

Gao, W.-J., Wang, Y., and Goldman-Rakic, P.S. (2003). Dopamine Modulation of Perisomatic and Peridendritic Inhibition in Prefrontal Cortex. J. Neurosci. *23*, 1622–1630.

Gasca-Martinez, D., Hernandez, A., Sierra, A., Valdiosera, R., Anaya-Martinez, V., Floran, B., Erlij, D., and Aceves, J. (2010). Dopamine inhibits GABA transmission from the globus pallidus to the thalamic reticular nucleus via presynaptic D4 receptors. Neuroscience *169*, 1672–1681.

Gingrich, K.J., Roberts, W.A., and Kass, R.S. (1995). Dependence of the $GABA_A$ receptor gating kinetics on the α-subunit isoform: implications for structure-function relations and synaptic transmission. J. Physiol. *489,* 529–543.

Girault, J.-A., and Greengard, P. (2004). The neurobiology of dopamine signaling. Arch. Neurol. *61*, 641–644.

Glase, S.A., Akunne, H.C., Georgic, L.M., Heffner, T.G., MacKenzie, R.G., Manley, P.J., Pugsley, T.A., and Wise, L.D. (1997). Substituted [(4-phenylpiperazinyl)-methyl]benzamides: selective dopamine D4 agonists. J. Med. Chem. 40, 1771–1772.

Glykys, J., and Mody, I. (2006). Hippocampal network hyperactivity after selective reduction of tonic inhibition in $GABA_A$ receptor α5 subunit-deficient mice. J. Neurophysiol. *95*, 2796–2807.

Glykys, J., Mann, E.O., and Mody, I. (2008). Which $GABA_A$ receptor subunits are necessary for tonic inhibition in the hippocampus? J. Neurosci. *28*, 1421–1426.

Goldman, M.S., Golowasch, J., Marder, E., and Abbott, L.F. (2001). Global Structure, Robustness, and Modulation of Neuronal Models. J. Neurosci. *21*, 5229–5238.

Goldman-Rakic, P.S. (1995). Cellular basis of working memory. Neuron *14*, 477–485.

Goldman-Rakic, P.S. (1996). The prefrontal landscape: implications of functional architecture for understanding human mentation and the central executive. Philos. Trans. R. Soc. Lond. B. Biol. Sci. *351*, 1445–1453.

Goldman-Rakic, P.S. (1999). The physiological approach: functional architecture of working memory and disordered cognition in schizophrenia. Biol. Psychiatry *46*, 650–661.

Goldman-Rakic, P.S. (2011). Circuitry of Primate Prefrontal Cortex and Regulation of Behavior by Representational Memory. Compr. Physiol. 373–417.

Goldman-Rakic, P.S., Leranth, C., Williams, S.M., Mons, N., and Geffard, M. (1989). Dopamine synaptic complex with pyramidal neurons in primate cerebral cortex. Proc. Natl. Acad. Sci. U. S. A. *86*, 9015–9019.

Goldstein, R.Z., and Volkow, N.D. (2002). Drug addiction and its underlying neurobiological basis: neuroimaging evidence for the involvement of the frontal cortex. Am. J. Psychiatry *159*, 1642–1652.

Goldstein, R.Z., and Volkow, N.D. (2011). Dysfunction of the prefrontal cortex in addiction: neuroimaging findings and clinical implications. Nat. Rev. Neurosci. *12*, 652–669.

Gorelova, N., Seamans, J.K., and Yang, C.R. (2002). Mechanisms of dopamine activation of fast-spiking interneurons that exert inhibition in rat prefrontal cortex. J. Neurophysiol. *88*, 3150–3166.

Govindaiah, G., Wang, T., Gillette, M.U., Crandall, S.R., and Cox, C.L. (2010). Regulation of inhibitory synapses by presynaptic D4 dopamine receptors in thalamus. J. Neurophysiol. *104*, 2757–2765.

Graf, E.R., Zhang, X., Jin, S.-X., Linhoff, M.W., and Craig, A.M. (2004). Neurexins induce differentiation of GABA and glutamate postsynaptic specializations via neuroligins. Cell *119*, 1013–1026.

Graziane, N.M., Yuen, E.Y., and Yan, Z. (2009). Dopamine D4 Receptors Regulate $GABA_A$ Receptor Trafficking via an Actin/Cofilin/Myosin-dependent Mechanism. J. Biol. Chem. *284*, 8329–8336.

Grobin, A.C., and Morrow, A.L. (2001). 3Alpha-hydroxy-5alpha-pregnan-20-one levels and $GABA_A$ receptor-mediated 36Cl(-) flux across development in rat cerebral cortex. Brain Res. Dev. Brain Res. *131*, 31–39.

Grobin, A.C., Heenan, E.J., Lieberman, J.A., Morrow, A.L., and Carolina, N. (2003). Perinatal Neurosteorid Levels Influence GABAergic Interneuron Localization in Adult Rat Prefrontal Cortex. J. Neurosci. *23*, 1832–1839.

Grobin, A.C., Gizerian, S., Lieberman, J.A., and Morrow, A.L. (2006). Perinatal allopregnanolone influences prefrontal cortex structure, connectivity and behavior in adult rats. Neuroscience *138*, 809–819.

Gulledge, A.T., and Stuart, G.J. (2003). Excitatory actions of GABA in the cortex. Neuron *37*, 299–309.

Gunn, B.G., Cunningham, L., Mitchell, S.G., Swinny, J.D., Lambert, J.J., and Belelli, D. (2015). $GABA_A$ receptor-acting neurosteroids: a role in the development and regulation of the stress response. Front. Neuroendocrinol. *36*, 28–48.

Haage, D., Druzin, M., and Johansson, S. (2002). Allopregnanolone modulates spontaneous GABA release via presynaptic Cl- permeability in rat preoptic nerve terminals. Brain Res. *958*, 405–413.

Haas, K.F., and Macdonald, R.L. (1999). $GABA_A$ receptor subunit γ2 and δ subtypes confer unique kinetic properties on recombinant $GABA_A$ receptor currents in mouse fibroblasts. J. Physiol. *514*, 27–45.

Hannan, S., Wilkins, M.E., Dehghani-Tafti, E., Thomas, P., Baddeley, S.M., and Smart, T.G. (2011). $GABA_B$ receptor internalization is regulated by the R2 subunit. J. Biol. Chem. *286*, 24324–24335.

Harney, S.C., Frenguelli, B.G., and Lambert, J.J. (2003). Phosphorylation influences neurosteroid modulation of synaptic $GABA_A$ receptors in rat CA1 and dentate gyrus neurones. Neuropharmacology *45*, 873–883.

Haughey, H.M., Ray, L.A., Finan, P., Villanueva, R., Niculescu, M., and Hutchison, K.E. (2008). Human $GABA_A$ receptor α2 gene moderates the acute effects of alcohol and brain mRNA expression. Genes. Brain. Behav. *7*, 447–454.

Heidbreder, C.A., and Groenewegen, H.J. (2003). The medial prefrontal cortex in the rat: evidence for a dorso-ventral distinction based upon functional and anatomical characteristics. Neurosci. Biobehav. Rev. *27*, 555–579.

Heistek, T.S., Ruiperez-Alonso, M., Timmerman, A.J., Brussaard, A.B., and Mansvelder, H.D. (2013). α2-containing $GABA_A$ receptors expressed in hippocampal region CA3 control fast network oscillations. J. Physiol. *591*, 845–858.

Higley, M.J. (2014). Localized GABAergic inhibition of dendritic Ca2+ signalling. Nat. Rev. Neurosci. *15*, 567–572.

Hines, R.M., Hines, D.J., Houston, C.M., Mukherjee, J., Haydon, P.G., Tretter, V., Smart, T.G., and Moss, S.J. (2013). Disrupting the clustering of $GABA_A$ receptor α2 subunits in the frontal cortex leads to reduced γ-power and cognitive deficits. Proc. Natl. Acad. Sci. U. S. A. *110*, 16628–16633.

Hoestgaard-Jensen, K., Dalby, N.O., Wolinsky, T.D., Murphey, C., Jones, K.A., Rottländer, M., Frederiksen, K., Watson, W.P., Jensen, K., and Ebert, B. (2010). Pharmacological characterization of a novel positive modulator at α4β3δ-containing extrasynaptic $GABA_A$ receptors. Neuropharmacology *58*, 702–711.

Hof, P.R., Glezer, I.I., Condé, F., Flagg, R.A., Rubin, M.B., Nimchinsky, E.A., and Vogt Weisenhorn, D.M. (1999). Cellular distribution of the calcium-binding proteins parvalbumin, calbindin, and calretinin in the neocortex of mammals: phylogenetic and developmental patterns. J. Chem. Neuroanat. *16*, 77–116.

Hoover, W.B., and Vertes, R.P. (2007). Anatomical analysis of afferent projections to the medial prefrontal cortex in the rat. Brain Struct. Funct. *212*, 149–179.

Hosie, A.M., Wilkins, M.E., da Silva, H.M. a, and Smart, T.G. (2006). Endogenous neurosteroids regulate $GABA_A$ receptors through two discrete transmembrane sites. Nature *444*, 486–489.

Hosie, A.M., Wilkins, M.E., and Smart, T.G. (2007). Neurosteroid binding sites on $GABA_A$ receptors. Pharmacol. Ther. *116*, 7–19.

Hosie, A.M., Clarke, L., Silva, H., Smart, T.G., and Da Silva, H. (2009). Conserved site for neurosteroid modulation of $GABA_A$ receptors. Neuropharmacology *56*, 149–154.

Houston, C.M., Bright, D.P., Sivilotti, L.G., Beato, M., and Smart, T.G. (2009). Intracellular chloride ions regulate the time course of GABA-mediated inhibitory synaptic transmission. J. Neurosci. *29*, 10416–10423.

Houston, C.M., McGee, T.P., Mackenzie, G., Troyano-Cuturi, K., Rodriguez, P.M., Kutsarova, E., Diamanti, E., Hosie, A.M., Franks, N.P., and Brickley, S.G. (2012). Are extrasynaptic $GABA_A$ receptors important targets for sedative/hypnotic drugs? J. Neurosci. *32*, 3887–3897.

Howarth, C., Gleeson, P., and Attwell, D. (2012). Updated energy budgets for neural computation in the neocortex and cerebellum. J. Cereb. Blood Flow Metab. *32*, 1222–1232.

Huidobro-Toro, J.P., Valenzuela, C.F., and Harris, R.A. (1996). Modulation of $GABA_A$ receptor function by G protein-coupled 5-HT_{2C} receptors. Neuropharmacology *35*, 1355–1363.

Huntsman, M.M. (1999). Reciprocal Inhibitory Connections and Network Synchrony in the Mammalian Thalamus. Science *283*, 541–543.

Hutcheon, B., Morley, P., and Poulter, M.O. (2000). Developmental change in $GABA_A$ receptor desensitization kinetics and its role in synapse function in rat cortical neurons. J. Physiol. *522*, 3-17.

Inoue, M., and Akaike, N. (1988). Blockade of GABA-gated chloride current in frog sensory neurons by picrotoxin. Neurosci. Res. *5*, 380–394.

Invernizzi, R.W., Pierucci, M., Calcagno, E., Di Giovanni, G., Di Matteo, V., Benigno, A., and Esposito, E. (2007). Selective activation of 5-HT_{2C} receptors stimulates GABA-ergic function in the rat substantia nigra pars reticulata: a combined in vivo electrophysiological and neurochemical study. Neuroscience *144*, 1523–1535.

Isaacson, J.S., and Scanziani, M. (2011). How inhibition shapes cortical activity. Neuron *72*, 231–243.

Jacob, T.C., Bogdanov, Y.D., Magnus, C., Saliba, R.S., Kittler, J.T., Haydon, P.G., and Moss, S.J. (2005). Gephyrin regulates the cell surface dynamics of synaptic $GABA_A$ receptors. J. Neurosci. *25*, 10469–10478.

Jacob, T.C., Moss, S.J., and Jurd, R. (2008). $GABA_A$ receptor trafficking and its role in the dynamic modulation of neuronal inhibition. Nat. Rev. Neurosci. *9*, 331–343.

Jacobson-Pick, S., Audet, M.C., McQuaid, R.J., Kalvapalle, R., and Anisman, H. (2012). Stressor exposure of male and female juvenile mice influences later responses to stressors: modulation of $GABA_A$ receptor subunit mRNA expression. Neuroscience *215*, 114–126.

Jang, H.-J., Cho, K.-H., Kim, M.-J., Yoon, S.H., and Rhie, D.-J. (2013). Layer- and cell-type-specific tonic GABAergic inhibition of pyramidal neurons in the rat visual cortex. Pflugers Arch. *465*, 1797–1810.

Jin, Z., Bhandage, A.K., Bazov, I., Kononenko, O., Bakalkin, G., Korpi, E.R., and Birnir, B. (2014). Expression of specific ionotropic glutamate and $GABA_A$ receptor subunits is decreased in central amygdala of alcoholics. Front. Cell. Neurosci. *8*, 288.

Kaila, K. (1994). Ionic basis of $GABA_A$ receptor channel function in the nervous system. Prog. Neurobiol. *42*, 489–537.

Kaila, K., Rydqvist, B., Pasternack, M., and Voipio, J. (1992). Inward current caused by sodium-dependent uptake of GABA in the crayfish stretch receptor neurone. J. Physiol. *453*, 627–645.

Kaneda, M., Farrant, M., and Cull-Candy, S.G. (1995). Whole-cell and single-channel currents activated by GABA and glycine in granule cells of the rat cerebellum. J. Physiol. *485*, 419–435.

Kang, Y., Zhang, X., Dobie, F., Wu, H., and Craig, A.M. (2008). Induction of GABAergic postsynaptic differentiation by α-neurexins. J. Biol. Chem. *283*, 2323–2334.

Kareken, D.A., Liang, T., Wetherill, L., Dzemidzic, M., Bragulat, V., Cox, C., Talavage, T., O'Connor, S.J., and Foroud, T. (2010). A polymorphism in GABRA2 is associated with the medial frontal response to alcohol cues in an fMRI study. Alcohol. Clin. Exp. Res. *34*, 2169–2178.

Kasper, J.M., Booth, R.G., and Peris, J. (2014). $5\text{-}HT_{2C}$ receptor agonists decrease potassium-stimulated GABA release in the nucleus accumbens. Synapse *69*, 78-85.

Kasugai, Y., Swinny, J.D., Roberts, J.D.B., Dalezios, Y., Fukazawa, Y., Sieghart, W., Shigemoto, R., and Somogyi, P. (2010). Quantitative localisation of synaptic and extrasynaptic $GABA_A$ receptor subunits on hippocampal pyramidal cells by freeze-fracture replica immunolabelling. Eur. J. Neurosci. *32*, 1868–1888.

Kawaguchi, Y. (1993). Groupings of nonpyramidal and pyramidal cells with specific physiological and morphological characteristics in rat frontal cortex. J. Neurophysiol. *69*, 416–431.

Keller, C.A., Yuan, X., Panzanelli, P., Martin, M.L., Alldred, M., Sassoè-Pognetto, M., and Lüscher, B. (2004). The γ2 subunit of $GABA_A$ receptors is a substrate for palmitoylation by GODZ. J. Neurosci. *24*, 5881–5891.

Kerti-Szigeti, K., Nusser, Z., and Eyre, M.D. (2014). Synaptic $GABA_A$ receptor clustering without the γ2 subunit. J. Neurosci. *34*, 10219–10233.

Kesner, R.P., and Churchwell, J.C. (2011). An analysis of rat prefrontal cortex in mediating executive function. Neurobiol. Learn. Mem. *96*, 417–431.

Kittler, J.T., and Moss, S.J. (2001). Neurotransmitter receptor trafficking and the regulation of synaptic strength. Traffic *2*, 437–448.

Kittler, J.T., and Moss, S.J. (2003). Modulation of $GABA_A$ receptor activity by phosphorylation and receptor trafficking: implications for the efficacy of synaptic inhibition. Curr. Opin. Neurobiol. *13*, 341–347.

Kittler, J.T., Delmas, P., Jovanovic, J.N., Brown, D.A., Smart, T.G., and Moss, S.J. (2000). Constitutive endocytosis of $GABA_A$ receptors by an association with the adaptin AP2 complex modulates inhibitory synaptic currents in hippocampal neurons. J. Neurosci. *20*, 7972–7977.

Kittler, J.T., Thomas, P., Tretter, V., Bogdanov, Y.D., Haucke, V., Smart, T.G., and Moss, S.J. (2004). Huntingtin-associated protein 1 regulates inhibitory synaptic transmission by modulating $GABA_A$ receptor membrane trafficking. Proc. Natl. Acad. Sci. U. S. A. *101*, 12736–12741.

Kittler, J.T., Chen, G., Honing, S., Bogdanov, Y., McAinsh, K., Arancibia-Carcamo, I.L., Jovanovic, J.N., Pangalos, M.N., Haucke, V., Yan, Z., et al. (2005). Phospho-dependent binding of the clathrin AP2 adaptor complex to $GABA_A$ receptors regulates the efficacy of inhibitory synaptic transmission. Proc. Natl. Acad. Sci. U. S. A. *102*, 14871–14876.

Kittler, J.T., Chen, G., Kukhtina, V., Vahedi-Faridi, A., Gu, Z., Tretter, V., Smith, K.R., McAinsh, K., Arancibia-Carcamo, I.L., Saenger, W., et al. (2008). Regulation of synaptic inhibition by phospho-dependent binding of the AP2 complex to a YECL motif in the $GABA_A$ receptor γ2 subunit. Proc. Natl. Acad. Sci. U. S. A. *105*, 3616–3621.

Klausberger, T., Roberts, J.D.B., and Somogyi, P. (2002). Cell Type- and Input-Specific Differences in the Number and Subtypes of Synaptic $GABA_A$ Receptors in the Hippocampus. J. Neurosci. *22*, 2513–2521.

Klausberger, T., Magill, P.J., Márton, L.F., Roberts, J.D.B., Cobden, P.M., Buzsáki, G., and Somogyi, P. (2003). Brain-state- and cell-type-specific firing of hippocampal interneurons in vivo. Nature *421*, 844–848.

Kobayashi, M., Hamada, T., Kogo, M., Yanagawa, Y., Obata, K., and Kang, Y. (2008). Developmental profile of $GABA_A$-mediated synaptic transmission in pyramidal cells of the somatosensory cortex. Eur. J. Neurosci. *28*, 849–861.

Koksma, J.-J., van Kesteren, R.E., Rosahl, T.W., Zwart, R., Smit, A.B., Lüddens, H., and Brussaard, A.B. (2003). Oxytocin regulates neurosteroid modulation of $GABA_A$ receptors in supraoptic nucleus around parturition. J. Neurosci. *23*, 788–797.

Kole, M.H.P., and Stuart, G.J. (2012). Signal processing in the axon initial segment. Neuron *73*, 235–247.

Kole, M.H.P., Letzkus, J.J., and Stuart, G.J. (2007). Axon initial segment Kv1 channels control axonal action potential waveform and synaptic efficacy. Neuron *55*, 633–647.

Kordeli, E., Lambert, S., and Bennett, V. (1995). AnkyrinG. A new ankyrin gene with neural-specific isoforms localized at the axonal initial segment and node of Ranvier. J. Biol. Chem. *270*, 2352–2359.

Korpi, E.R., Gründer, G., and Lüddens, H. (2002). Drug interactions at $GABA_A$ receptors. Prog. Neurobiol. *67*, 113–159.

Kraszewski, K., and Grantyn, R. (1992). Development of GABAergic connections in vitro: increasing efficacy of synaptic transmission is not accompanied by changes in miniature currents. J. Neurobiol. *23*, 766–781.

Krogsgaard-Larsen, P., Frølund, B., and Liljefors, T. (2002). Specific $GABA_A$ agonists and partial agonists. Chem. Rec. *2*, 419–430.

Krogsgaard-Larsen, P., Frølund, B., Liljefors, T., and Ebert, B. (2004). $GABA_A$ agonists and partial agonists: THIP (Gaboxadol) as a non-opioid analgesic and a novel type of hypnotic. Biochem. Pharmacol. *68*, 1573–1580.

Kulagowski, J.J., Broughton, H.B., Curtis, N.R., Mawer, I.M., Ridgill, M.P., Baker, R., Emms, F., Freedman, S.B., Marwood, R., Patel, S., et al. (1996). 3-((4-(4-Chlorophenyl)piperazin-1-yl)-methyl)-1H-pyrrolo-2,3-b-pyridine: an antagonist with high affinity and selectivity for the human dopamine D4 receptor. J. Med. Chem. *39*, 1941–1942.

Kumar, S., Fleming, R.L., and Morrow, A.L. (2004). Ethanol regulation of $GABA_A$ receptors: genomic and nongenomic mechanisms. Pharmacol. Ther. *101*, 211–226.

Kvitsiani, D., Ranade, S., Hangya, B., Taniguchi, H., Huang, J.Z., and Kepecs, A. (2013). Distinct behavioural and network correlates of two interneuron types in prefrontal cortex. Nature *498*, 363–366.

Lambert, J.J., Peters, J.A., Sturgess, N.C., and Hales, T.G. (1990). Steroid modulation of the $GABA_A$ receptor complex: electrophysiological studies. Ciba Found. Symp. *153*, 56–71; discussion 71–82.

Lambert, J.J., Belelli, D., Peden, D.R., Vardy, A.W., and Peters, J.A. (2003). Neurosteroid modulation of $GABA_A$ receptors. Prog. Neurobiol. *71*, 67–80.

Lambert, J.J., Cooper, M.A., Simmons, R.D.J., Weir, C.J., and Belelli, D. (2009). Neurosteroids: Endogenous allosteric modulators of $GABA_A$ receptors. Psychoneuroendocrinology *34*, S48–S58.

Lamsa, K., Palva, J.M., Ruusuvuori, E., Kaila, K., and Taira, T. (2000). Synaptic $GABA_A$ Activation Inhibits AMPA-Kainate Receptor-Mediated Bursting in the Newborn (P0-P2) Rat Hippocampus. J Neurophysiol *83*, 359–366.

Laurie, D.J., Seeburg, P.H., and Wisden, W. (1992a). The distribution of 13 $GABA_A$ receptor subunit mRNAs in the rat brain. II. Olfactory bulb and cerebellum. J. Neurosci. *12*, 1063–1076.

Laurie, D.J., Wisden, W., and Seeburg, P.H. (1992b). The distribution of thirteen $GABA_A$ receptor subunit mRNAs in the rat brain. III. Embryonic and postnatal development. J. Neurosci. *12*, 4151–4172.

Lavoie, A.M., Tingey, J.J., Harrison, N.L., Pritchett, D.B., and Twyman, R.E. (1997). Activation and deactivation rates of recombinant $GABA_A$ receptor channels are dependent on α-subunit isoform. Biophys. J. *73*, 2518–2526.

Lee, D., and Seo, H. (2007). Mechanisms of reinforcement learning and decision making in the primate dorsolateral prefrontal cortex. Ann. N. Y. Acad. Sci. *1104*, 108–122.

Lee, V., and Maguire, J. (2014). The impact of tonic $GABA_A$ receptor-mediated inhibition on neuronal excitability varies across brain region and cell type. Front. Neural Circuits *8*, 3.

Lee, A.T., Vogt, D., Rubenstein, J.L., and Sohal, V.S. (2014a). A class of GABAergic neurons in the prefrontal cortex sends long-range projections to the nucleus accumbens and elicits acute avoidance behavior. J. Neurosci. *34*, 11519–11525.

Lee, A.T., Gee, S.M., Vogt, D., Patel, T., Rubenstein, J.L., and Sohal, V.S. (2014b). Pyramidal neurons in prefrontal cortex receive subtype-specific forms of excitation and inhibition. Neuron *81*, 61–68.

Lee, S., Yoon, B.-E., Berglund, K., Oh, S.-J., Park, H., Shin, H.-S., Augustine, G.J., and Lee, C.J. (2010). Channel-mediated tonic GABA release from glia. Science *330*, 790–796.

Lefkowitz, R.J., Cotecchia, S., Samama, P., and Costa, T. (1993). Constitutive activity of receptors coupled to guanine nucleotide regulatory proteins. Trends Pharmacol. Sci. *14*, 303–307.

Lewis, D.A. (2011). The chandelier neuron in schizophrenia. Dev. Neurobiol. *71*, 118–127.

Lewis, D.A., and Gonzalez-Burgos, G. (2006). Pathophysiologically based treatment interventions in schizophrenia. Nat. Med. *12*, 1016–1022.

Li, D., Sham, P.C., Owen, M.J., and He, L. (2006). Meta-analysis shows significant association between dopamine system genes and attention deficit hyperactivity disorder (ADHD). Hum. Mol. Genet. *15*, 2276–2284.

Li, Y.-C., Wang, M.-J., and Gao, W.-J. (2012). Hyperdopaminergic modulation of inhibitory transmission is dependent on GSK-3β signaling-mediated trafficking of $GABA_A$ receptors. J. Neurochem. *122*, 308–320.

Lidow, M.S., Goldman-Rakic, P.S., Rakic, P., and Innis, R.B. (1989). Dopamine D2 receptors in the cerebral cortex: distribution and pharmacological characterization with [3H]raclopride. Proc. Natl. Acad. Sci. U. S. A. *86*, 6412–6416.

Little, J.P., and Carter, a. G. (2012). Subcellular synaptic connectivity of layer 2 pyramidal neurons in the medial prefrontal cortex. J. Neurosci. *32*, 12808–12819.

Liu, S., Bubar, M.J., Lanfranco, M.F., Hillman, G.R., and Cunningham, K. a (2007). 5-HT_{2C} receptor localization in GABA neurons of the rat medial prefrontal cortex: implications for understanding the neurobiology of addiction. Neuroscience *146*, 1677–1688.

Loebrich, S., Bähring, R., Katsuno, T., Tsukita, S., and Kneussel, M. (2006). Activated radixin is essential for $GABA_A$ receptor α5 subunit anchoring at the actin cytoskeleton. EMBO J. *25*, 987–999.

Löw, K., Crestani, F., Keist, R., Benke, D., Brünig, I., Benson, J.A., Fritschy, J.M., Rülicke, T., Bluethmann, H., Möhler, H., et al. (2000). Molecular and neuronal substrate for the selective attenuation of anxiety. Science *290*, 131–134.

Luchetti, S., Bossers, K., Van de Bilt, S., Agrapart, V., Morales, R.R., Frajese, G.V., and Swaab, D.F. (2011). Neurosteroid biosynthetic pathways changes in prefrontal cortex in Alzheimer's disease. Neurobiol. Aging *32*, 1964–1976.

Lukasiewicz, P.D., Eggers, E.D., Sagdullaev, B.T., and McCall, M.A. (2004). $GABA_C$ receptor-mediated inhibition in the retina. Vision Res. *44*, 3289–3296.

Lupien, S.J., Fiocco, A., Wan, N., Maheu, F., Lord, C., Schramek, T., and Tu, M.T. (2005). Stress hormones and human memory function across the lifespan. Psychoneuroendocrinology *30*, 225–242.

Luscher, B., Fuchs, T., and Kilpatrick, C.L. (2011). $GABA_A$ receptor trafficking-mediated plasticity of inhibitory synapses. Neuron *70*, 385–409.

Maccaferri, G., and McBain, C.J. (1996). The hyperpolarization-activated current (Ih) and its contribution to pacemaker activity in rat CA1 hippocampal stratum oriens-alveus interneurones. J. Physiol. *497*, 119–130.

Maguire, J., and Mody, I. (2007). Neurosteroid synthesis-mediated regulation of $GABA_A$ receptors: relevance to the ovarian cycle and stress. J. Neurosci. *27*, 2155–2162.

Maguire, J., and Mody, I. (2008). $GABA_AR$ plasticity during pregnancy: relevance to postpartum depression. Neuron *59*, 207–213.

Maguire, J.L., Stell, B.M., Rafizadeh, M., and Mody, I. (2005). Ovarian cycle-linked changes in $GABA_A$ receptors mediating tonic inhibition alter seizure susceptibility and anxiety. Nat. Neurosci. *8*, 797–804.

Major, G., Larkum, M.E., and Schiller, J. (2013). Active properties of neocortical pyramidal neuron dendrites. Annu. Rev. Neurosci. *36*, 1–24.

Malmberg, A., Mikaels, A., and Mohell, N. (1998). Agonist and Inverse Agonist Activity at the Dopamine D3 Receptor Measured by Guanosine 5'-[gamma -Thio]Triphosphate-[35S] Binding. J. Pharmacol. Exp. Ther. *285*, 119–126.

Mann, E.O., and Paulsen, O. (2007). Role of GABAergic inhibition in hippocampal network oscillations. Trends Neurosci. *30*, 343–349.

Markram, H., Toledo-Rodriguez, M., Wang, Y., Gupta, A., Silberberg, G., and Wu, C. (2004). Interneurons of the neocortical inhibitory system. Nat. Rev. Neurosci. *5*, 793–807.

Marlin, J.J., and Carter, A.G. (2014). $GABA_A$ receptor inhibition of local calcium signaling in spines and dendrites. J. Neurosci. *34*, 15898–15911.

Marowsky, A., and Vogt, K.E. (2014). δ-subunit-containing $GABA_A$ receptors mediate tonic inhibition in paracapsular cells of the mouse amygdala. Front. Neural Circuits *8*, 27.

Martin, C.B.P., Gassmann, M., Chevarin, C., Hamon, M., Rudolph, U., Bettler, B., Lanfumey, L., and Mongeau, R. (2014). Effect of genetic and pharmacological blockade of GABA receptors on the $5\text{-}HT_{2C}$ receptor function during stress. J. Neurochem. *131*, 566-72.

Marty, A., and Llano, I. (1995). Modulation of inhibitory synapses in the mammalian brain. Curr. Opin. Neurobiol. *5*, 335–341.

Marx, C.E., Trost, W.T., Shampine, L.J., Stevens, R.D., Hulette, C.M., Steffens, D.C., Ervin, J.F., Butterfield, M.I., Blazer, D.G., Massing, M.W., et al. (2006). The neurosteroid allopregnanolone is reduced in prefrontal cortex in Alzheimer's disease. Biol. Psychiatry *60*, 1287–1294.

Masana, M., Santana, N., Artigas, F., and Bortolozzi, A. (2012). Dopamine neurotransmission and atypical antipsychotics in prefrontal cortex: a critical review. Curr. Top. Med. Chem. *12*, 2357–2374.

McClellan, A.M., and Twyman, R.E. (1999). Receptor system response kinetics reveal functional subtypes of native murine and recombinant human $GABA_A$ receptors. J. Physiol. *515*, 711–727.

McDonald, B.J., Amato, A., Connolly, C.N., Benke, D., Moss, S.J., and Smart, T.G. (1998). Adjacent phosphorylation sites on $GABA_A$ receptor β subunits determine regulation by cAMP-dependent protein kinase. Nat. Neurosci. *1*, 23–28.

McKernan, R.M., Rosahl, T.W., Reynolds, D.S., Sur, C., Wafford, K.A., Atack, J.R., Farrar, S., Myers, J., Cook, G., Ferris, P., et al. (2000). Sedative but not anxiolytic properties of benzodiazepines are mediated by the $GABA_A$ receptor α1 subtype. Nat. Neurosci. *3*, 587–592.

Melcangi, R.C., Magnaghi, V., Galbiati, M., and Martini, L. (2001). Formation and effects of neuroactive steroids in the central and peripheral nervous system. Int. Rev. Neurobiol. *46*, 145–176.

Mellon, S.H., and Vaudry, H. (2001). Biosynthesis of neurosteroids and regulation of their synthesis. Int. Rev. Neurobiol. *46*, 33–78.

Meyer, A.H., Katona, I., Blatow, M., Rozov, A., and Monyer, H. (2002). In vivo labeling of parvalbumin-positive interneurons and analysis of electrical coupling in identified neurons. J. Neurosci. *22*, 7055–7064.

Meyer, G., Kirsch, J., Betz, H., and Langosch, D. (1995). Identification of a gephyrin binding motif on the glycine receptor β subunit. Neuron *15*, 563–572.

Mi, R., Tang, X., Sutter, R., Xu, D., Worley, P., and O'Brien, R.J. (2002). Differing mechanisms for glutamate receptor aggregation on dendritic spines and shafts in cultured hippocampal neurons. J. Neurosci. *22*, 7606–7616.

Michaeli, a, and Yaka, R. (2010). Dopamine inhibits $GABA_A$ currents in ventral tegmental area dopamine neurons via activation of presynaptic G-protein coupled inwardly-rectifying potassium channels. Neuroscience *165*, 1159–1169.

Miles, R., Tóth, K., Gulyás, A.I., Hájos, N., and Freund, T.F. (1996). Differences between Somatic and Dendritic Inhibition in the Hippocampus. Neuron *16*, 815–823.

Mitchell, S.J., and Silver, R.A. (2003). Shunting Inhibition Modulates Neuronal Gain during Synaptic Excitation. Neuron *38*, 433–445.

Mitchell, E. a, Herd, M.B., Gunn, B.G., Lambert, J.J., and Belelli, D. (2008). Neurosteroid modulation of $GABA_A$ receptors: molecular determinants and significance in health and disease. Neurochem. Int. *52*, 588–595.

Modirrousta, M., and Fellows, L.K. (2008). Dorsal medial prefrontal cortex plays a necessary role in rapid error prediction in humans. J. Neurosci. *28*, 14000–14005.

Mody, I. (2005). Aspects of the homeostaic plasticity of $GABA_A$ receptor-mediated inhibition. J. Physiol. *562*, 37–46.

Mody, I., and Maguire, J. (2011). The reciprocal regulation of stress hormones and $GABA_A$ receptors. Front. Cell. Neurosci. *6*, 4.

Mody, I., and Pearce, R. (2004). Diversity of inhibitory neurotransmission through $GABA_A$ receptors. Trends Neurosci. *27*, 569–575.

Möhler, H. (2002). A New Benzodiazepine Pharmacology. J. Pharmacol. Exp. Ther. *300*, 2–8.

Möhler, H., Knoflach, F., Paysan, J., and Motejlek, K. (1995). Heterogeneity of $GABA_A$-receptors: cell-specific expression, pharmacology, and regulation. Neurochemical *20*, 631-636.

Möhler, H. (2006a). $GABA_A$ receptors in central nervous system disease: anxiety, epilepsy, and insomnia. J. Recept. Signal Transduct. Res. *26*, 731–740.

Möhler, H. (2006b). $GABA_A$ receptor diversity and pharmacology. Cell Tissue Res. *326*, 505–516.

Möhler, H. (2012). The GABA system in anxiety and depression and its therapeutic potential. Neuropharmacology *62*, 42–53.

Möhler, H., Benke, D., Fritschy, J., and Benson, J. (2000). The benzodiazepine site of $GABA_A$ receptors (Lippincott Williams & Wilkins, Philadelphia).

Möhler, H., Fritschy, J.-M., Crestani, F., Hensch, T., and Rudolph, U. (2004). Specific $GABA_A$ circuits in brain development and therapy. Biochem. Pharmacol. *68*, 1685–1690.

Le Moine, C., and Gaspar, P. (1998). Subpopulations of cortical GABAergic interneurons differ by their expression of D1 and D2 dopamine receptor subtypes. Brain Res. Mol. Brain Res. *58*, 231–236.

Morris, H. V, Dawson, G.R., Reynolds, D.S., Atack, J.R., Rosahl, T.W., and Stephens, D.N. (2008). α2-containing $GABA_A$ receptors are involved in mediating stimulant effects of cocaine. Pharmacol. Biochem. Behav. *90*, 9–18.

Mortensen, M., and Smart, T.G. (2006). Extrasynaptic αβ subunit $GABA_A$ receptors on rat hippocampal pyramidal neurons. J. Physiol. *577*, 841–856.

Mortensen, M., Ebert, B., Wafford, K., and Smart, T.G. (2010). Distinct activities of GABA agonists at synaptic- and extrasynaptic-type $GABA_A$ receptors. J. Physiol. *588*, 1251–1268.

Mortensen, M., Patel, B., and Smart, T.G. (2011). GABA potency at $GABA_A$ receptors found in synaptic and extrasynaptic zones. Front. Cell. Neurosci. *6*, 1.

Moss, S.J., and Smart, T.G. (2001). Constructing inhibitory synapses. Nat. Rev. Neurosci. *2*, 240–250.

Mrzljak, L., Bergson, C., Pappy, M., Huff, R., Levenson, R., and Goldman-Rakic, P.S. (1996). Localization of dopamine D4 receptors in GABAergic neurons of the primate brain. Nature *381*, 245–248.

Muir, J., Arancibia-Carcamo, I.L., MacAskill, A.F., Smith, K.R., Griffin, L.D., and Kittler, J.T. (2010). NMDA receptors regulate $GABA_A$ receptor lateral mobility and clustering at inhibitory synapses through serine 327 on the γ2 subunit. Proc. Natl. Acad. Sci. U. S. A. *107*, 16679–16684.

Mukherjee, J., Kretschmannova, K., Gouzer, G., Maric, H.-M., Ramsden, S., Tretter, V., Harvey, K., Davies, P. a, Triller, A., Schindelin, H., et al. (2011). The residence time of $GABA_A$Rs at inhibitory synapses is determined by direct binding of the receptor α1 subunit to gephyrin. J. Neurosci. *31*, 14677–14687.

Nakazawa, K., Zsiros, V., Jiang, Z., Nakao, K., Kolata, S., Zhang, S., and Belforte, J.E. (2012). GABAergic interneuron origin of schizophrenia pathophysiology. Neuropharmacology *62*, 1574–1583.

Nakazawa, S., Nakamichi, K., Imai, H., and Ichihara, J. (2015). Effect of dopamine D4 receptor agonists on sleep architecture in rats. Prog. Neuropsychopharmacol. Biol. Psychiatry *63*, 6–13.

Newland, C.F., and Cull-Candy, S.G. (1992). On the mechanism of action of picrotoxin on GABA receptor channels in dissociated sympathetic neurones of the rat. J. Physiol. *447*, 191–213.

Nguyen, Q., Sapp, D.W., Van Ness, P.C., and Olsen, R.W. (1995). Modulation of $GABA_A$ receptor binding in human brain by neuroactive steroids: species and brain regional differences. Synapse *19*, 77–87.

Nicoll, A., Kim, H.G., and Connors, B.W. (1996). Laminar origins of inhibitory synaptic inputs to pyramidal neurons of the rat neocortex. J. Physiol. *497*, 109–117.

Nusser, Z., Sieghart, W., Stephenson, F.A., and Somogyi, P. (1996a). The α6 subunit of the $GABA_A$ receptor is concentrated in both inhibitory and excitatory synapses on cerebellar granule cells. J. Neurosci. *16*, 103–114.

Nusser, Z., Sieghart, W., Benke, D., Fritschy, J.M., and Somogyi, P. (1996b). Differential synaptic localization of two major $GABA_A$ receptor α subunits on hippocampal pyramidal cells. Proc. Natl. Acad. Sci. U. S. A. *93*, 11939–11944.

Nusser, Z., Sieghart, W., and Somogyi, P. (1998). Segregation of different $GABA_A$ receptors to synaptic and extrasynaptic membranes of cerebellar granule cells. J. Neurosci. *18*, 1693–1703.

Nusser, Z., Sheng, M., and Triller, A. (2012). Differential subcellular distribution of ion channels and the diversity of neuronal function. Curr. Opin. Neurobiol. *22*, 366–371.

Nutt, D.J., and Stahl, S.M. (2010). Searching for perfect sleep: the continuing evolution of $GABA_A$ receptor modulators as hypnotics. J. Psychopharmacol. *24*, 1601–1612.

Nyíri, G., Freund, T.F., and Somogyi, P. (2001). Input-dependent synaptic targeting of α2-subunit-containing $GABA_A$ receptors in synapses of hippocampal pyramidal cells of the rat. Eur. J. Neurosci. *13*, 428–442.

O'Donnell, P. (2010). Adolescent maturation of cortical dopamine. Neurotox. Res. *18*, 306–312.

Oak, J.N., Oldenhof, J., and Van Tol, H.H. (2000). The dopamine D4 receptor: one decade of research. Eur. J. Pharmacol. *405*, 303–327.

Olsen, R.W., and Sieghart, W. (2008). International Union of Pharmacology. LXX. Subtypes of $GABA_A$ Receptors: Classification on the Basis of Subunit Composition, Pharmacology, and Function. Update. Pharmacol. Rev. *60*, 243–260.

Olsen, R.W., and Sieghart, W. (2009). $GABA_A$ receptors: Subtypes provide diversity of function and pharmacology. Neuropharmacology *56*, 141–148.

Orozco-Cabal, L., Pollandt, S., Liu, J., Vergara, L., Shinnick-Gallagher, P., and Gallagher, J.P. (2006). A novel rat medial prefrontal cortical slice preparation to investigate synaptic transmission from amygdala to layer V prelimbic pyramidal neurons. J. Neurosci. Methods *151*, 148–158.

Otis, T.S., and Mody, I. (1992). Differential activation of $GABA_A$ and $GABA_B$ receptors by spontaneously released transmitter. J Neurophysiol *67*, 227–235.

Palmer, L.M. (2014). Dendritic integration in pyramidal neurons during network activity and disease. Brain Res. Bull. *103*, 2–10.

Palmer, L., Murayama, M., and Larkum, M. (2012). Inhibitory regulation of dendritic activity in vivo. Front. Neural Circuits *6*, 26.

Parent, M.A., Wang, L., Su, J., Netoff, T., and Yuan, L.-L. (2010). Identification of the hippocampal input to medial prefrontal cortex in vitro. Cereb. Cortex *20*, 393–403.

Paul, S.M., and Purdy, R.H. (1992). Neuroactive steroids. FASEB J. *6*, 2311–2322.

Paul, K., Cox, C., Pharmacology, D., Paul, K., and Cox, C. (2013). Age-dependent actions of dopamine on inhibitory synaptic transmission in superficial layers of mouse prefrontal cortex. J. Neurophysiol. *109*, 1323–1332.

Payne, J.A., Rivera, C., Voipio, J., and Kaila, K. (2003). Cation-chloride co-transporters in neuronal communication, development and trauma. Trends Neurosci. *26*, 199–206.

Paysan, J., and Fritschy, J.M. (1998). $GABA_A$-receptor subtypes in developing brain. Actors or spectators? Perspect. Dev. Neurobiol. *5*, 179–192.

Pesaran, B., Pezaris, J.S., Sahani, M., Mitra, P.P., and Andersen, R.A. (2002). Temporal structure in neuronal activity during working memory in macaque parietal cortex. Nat. Neurosci. *5*, 805–811.

Petrini, E.M., Ravasenga, T., Hausrat, T.J., Iurilli, G., Olcese, U., Racine, V., Sibarita, J.-B., Jacob, T.C., Moss, S.J., Benfenati, F., et al. (2014). Synaptic recruitment of gephyrin regulates surface $GABA_A$ receptor dynamics for the expression of inhibitory LTP. Nat. Commun. *5*, 3921.

Picton, A.J., and Fisher, J.L. (2007). Effect of the α subunit subtype on the macroscopic kinetic properties of recombinant $GABA_A$ receptors. Brain Res. *1165*, 40–49.

Pillai, G., Brown, N., McAllister, G., Milligan, G., and Seabrook, G. (1998). Human D2 and D4 dopamine receptors couple through βγ G-protein subunits to inwardly rectifying K+ channels (GIRK1) in a Xenopus oocyte expression system: selective antagonism by L-741,626 and L-745,870 respectively. Neuropharmacology *37*, 983–987.

Pirker, S., Schwarzer, C., Wieselthaler, A., Sieghart, W., and Sperk, G. (2000). $GABA_A$ receptors: immunocytochemical distribution of 13 subunits in the adult rat brain. Neuroscience *101*, 815–850.

Poisbeau, P., Feltz, P., and Schlichter, R. (1997). Modulation of $GABA_A$ receptor-mediated IPSCs by neuroactive steroids in a rat hypothalamo-hypophyseal coculture model. J. Physiol. *500*, 475–485.

Poisbeau, P., Patte-Mensah, C., Keller, A.F., Barrot, M., Breton, J.-D., Luis-Delgado, O.E., Freund-Mercier, M.J., Mensah-Nyagan, A.G., and Schlichter, R. (2005). Inflammatory pain upregulates spinal inhibition via endogenous neurosteroid production. J. Neurosci. *25*, 11768–11776.

Pouille, F., and Scanziani, M. (2001). Enforcement of temporal fidelity in pyramidal cells by somatic feed-forward inhibition. Science *293*, 1159–1163.

Pouille, F., Marin-Burgin, A., Adesnik, H., Atallah, B. V, and Scanziani, M. (2009). Input normalization by global feedforward inhibition expands cortical dynamic range. Nat. Neurosci. *12*, 1577–1585.

Pouille, F., Watkinson, O., Scanziani, M., and Trevelyan, A.J. (2013). The contribution of synaptic location to inhibitory gain control in pyramidal cells. Physiol. Rep. *1*, e00067.

Price, J.L., Carmichael, S.T., and Drevets, W.C. (1996). Networks related to the orbital and medial prefrontal cortex; a substrate for emotional behavior? Prog. Brain Res. *107*, 523–536.

Pritchett, D.B., Sontheimer, H., Shivers, B.D., Ymer, S., Kettenmann, H., Schofield, P.R., and Seeburg, P.H. (1989). Importance of a novel $GABA_A$ receptor subunit for benzodiazepine pharmacology. Nature *338*, 582–585.

Puig, M.V., and Gulledge, A.T. (2011). Serotonin and prefrontal cortex function: Neurons, networks, and circuits. Mol. Neurobiol. *44*, 449–464.

Puig, M.V., Celada, P., Díaz-Mataix, L., and Artigas, F. (2003). In vivo modulation of the activity of pyramidal neurons in the rat medial prefrontal cortex by $5\text{-}HT_{2A}$ receptors: relationship to thalamocortical afferents. Cereb. Cortex *13*, 870–882.

Purdy, R.H., Morrow, A.L., Moore, P.H., and Paul, S.M. (1991). Stress-induced elevations of $GABA_A$ receptor-active steroids in the rat brain. Proc. Natl. Acad. Sci. U. S. A. *88*, 4553–4557.

Quick, M.W., Hu, J., Wang, D., and Zhang, H.-Y. (2004). Regulation of a GABA transporter by reciprocal tyrosine and serine phosphorylation. J. Biol. Chem. *279*, 15961–15967.

Quirk, K., Blurton, P., Fletcher, S., Leeson, P., Tang, F., Mellilo, D., Ragan, C.I., and McKernan, R.M. (1996). [3H]L-655,708, a novel ligand selective for the benzodiazepine site of $GABA_A$ receptors which contain the α5 subunit. Neuropharmacology *35*, 1331–1335.

Rall, W. (1967). Distinguishing theoretical synaptic potentials computed for different soma-dendritic distributions of synaptic input. J. Neurophysiol. *30*, 1138–1168.

Rall, W. (2006). Theory of physiological properties of dendrites. Ann. N. Y. Acad. Sci. *96*, 1071–1092.

Rall, W., and Rinzel, J. (1973). Branch input resistance and steady attenuation for input to one branch of a dendritic neuron model. Biophys. J. *13*, 648–687.

Rao, A., Cha, E.M., and Craig, A.M. (2000). Mismatched appositions of presynaptic and postsynaptic components in isolated hippocampal neurons. J. Neurosci. *20*, 8344–8353.

Reddy, D.S., and Rogawski, M.A. (2012). Neurosteroids — endogenous regulators of seizure susceptibility and role in the treatment of epilepsy. In: Noebels JL, Avoli M, Rogawski MA, et al., editors. Jasper's basic mechanisms of the epilepsies. 4th edition. Bethesda (MD): National Center for Biotechnology Information (US).

Do Rego, J.L., Seong, J.Y., Burel, D., Leprince, J., Luu-The, V., Tsutsui, K., Tonon, M.-C., Pelletier, G., and Vaudry, H. (2009). Neurosteroid biosynthesis: enzymatic pathways and neuroendocrine regulation by neurotransmitters and neuropeptides. Front. Neuroendocrinol. *30*, 259–301.

Reith, C.A., and Sillar, K.T. (1997). Pre- and postsynaptic modulation of spinal GABAergic neurotransmission by the neurosteroid, 5 beta-pregnan-3 alpha-ol-20-one. Brain Res. *770*, 202–212.

Renner, M., Schweizer, C., Bannai, H., Triller, A., E, S., and Lévi, S. (2012). Diffusion barriers constrain receptors at synapses. PLoS One *7*, e43032.

Richerson, G.B. (2004). Looking for GABA in all the wrong places: the relevance of extrasynaptic $GABA_A$ receptors to epilepsy. Epilepsy Curr. *4*, 239–242.

Richerson, G.B., and Wu, Y. (2003). Dynamic equilibrium of neurotransmitter transporters: not just for reuptake anymore. J. Neurophysiol. *90*, 1363–1374.

Riga, D., Matos, M.R., Glas, A., Smit, A.B., Spijker, S., and Van den Oever, M.C. (2014). Optogenetic dissection of medial prefrontal cortex circuitry. Front. Syst. Neurosci. *8*, 230.

Van Rijnsoever, C., Täuber, M., Choulli, M.K., Keist, R., Rudolph, U., Möhler, H., Fritschy, J.M., and Crestani, F. (2004). Requirement of α5-$GABA_A$ receptors for the development of tolerance to the sedative action of diazepam in mice. J. Neurosci. *24*, 6785–6790.

Rivera, C., Voipio, J., and Kaila, K. (2005). Two developmental switches in GABAergic signalling: the K^+-Cl^-- cotransporter KCC2 and carbonic anhydrase CAVII. J. Physiol. *562*, 27–36.

Romo-Parra, H., Blaesse, P., Sosulina, L., and Pape, H.-C. (2015). Neurosteroids increase tonic GABAergic inhibition in the lateral section of the central amygdala in mice. J. Neurophysiol. *113*, 3421–3431.

Ropert, N., Miles, R., and Korn, H. (1990). Characteristics of miniature inhibitory postsynaptic currents in CA1 pyramidal neurones of rat hippocampus. J. Physiol. *428*, 707–722.

Rudolph, U., and Möhler, H. (2014). $GABA_A$ receptor subtypes: therapeutic potential in Down Syndrome, affective disorders, schizophrenia, and autism. Annu. Rev. Pharmacol. Toxicol. *54*, 483–507.

Rudolph, S., Tsai, M.-C., von Gersdorff, H., and Wadiche, J.I. (2015). The ubiquitous nature of multivesicular release. Trends Neurosci. *38*, 428–438.

Rudolph, U., Crestani, F., Benke, D., Brünig, I., Benson, J.A., Fritschy, J.M., Martin, J.R., Bluethmann, H., and Möhler, H. (1999). Benzodiazepine actions mediated by specific $GABA_A$ receptor subtypes. Nature *401*, 796–800.

Rupprecht, R., di Michele, F., Hermann, B., Ströhle, A., Lancel, M., Romeo, E., and Holsboer, F. (2001). Neuroactive steroids: molecular mechanisms of action and implications for neuropsychopharmacology. Brain Res. Brain Res. Rev. *37*, 59–67.

Rupprecht, R., Rammes, G., Eser, D., Baghai, T.C., Schüle, C., Nothdurfter, C., Troxler, T., Gentsch, C., Kalkman, H.O., Chaperon, F., et al. (2009). Translocator protein (18 kD) as target for anxiolytics without benzodiazepine-like side effects. Science *325*, 490–493.

Rupprecht, R., Papadopoulos, V., Rammes, G., Baghai, T.C., Fan, J., Akula, N., Groyer, G., Adams, D., and Schumacher, M. (2010). Translocator protein (18 kDa) (TSPO) as a therapeutic target for neurological and psychiatric disorders. Nat. Rev. Drug Discov. *9*, 971–988.

Ruxton, G.D. (2006). The unequal variance t-test is an underused alternative to Student's t-test and the Mann-Whitney U test. Behav. Ecol. *17*, 688–690.

Salin, P.A., and Prince, D.A. (1996). Spontaneous $GABA_A$ receptor-mediated inhibitory currents in adult rat somatosensory cortex. J. Neurophysiol. *75*, 1573–1588.

Salling, M.C., and Harrison, N. (2014). Strychnine-sensitive glycine receptors on pyramidal neurons in layers II/III of the mouse prefrontal cortex are tonically activated. J. Neurophysiol. *112*, 1169-78.

Sanna, E., Talani, G., Busonero, F., Pisu, M.G., Purdy, R.H., Serra, M., and Biggio, G. (2004). Brain steroidogenesis mediates ethanol modulation of $GABA_A$ receptor activity in rat hippocampus. J. Neurosci. *24*, 6521–6530.

Santana, N., Mengod, G., and Artigas, F. (2008). Quantitative analysis of the expression of dopamine D1 and D2 receptors in pyramidal and GABAergic neurons of the rat prefrontal cortex. Cereb. Cortex *19*, 849–860.

Sanyal, S., and Van Tol, H.H. (1997). Review the role of dopamine D4 receptors in schizophrenia and antipsychotic action. J. Psychiatr. Res. *31*, 219–232.

Sarkar, J., Wakefield, S., MacKenzie, G., Moss, S.J., and Maguire, J. (2011). Neurosteroidogenesis is required for the physiological response to stress: role of neurosteroid-sensitive $GABA_A$ Receptors. J. Neurosci. *31*, 18198–18210.

Saxena, N.C., and Macdonald, R.L. (1996). Properties of putative cerebellar $GABA_A$ receptor isoforms. Mol. Pharmacol. *49*, 567–579.

Schneider, C.A., Rasband, W.S., and Eliceiri, K.W. (2012). NIH Image to ImageJ: 25 years of image analysis. Nat. Methods *9*, 671–675.

Schüle, C., Nothdurfter, C., and Rupprecht, R. (2014). The role of allopregnanolone in depression and anxiety. Prog. Neurobiol. *113*, 79–87.

Schultz, W. (1997). Dopamine neurons and their role in reward mechanisms. Curr. Opin. Neurobiol. *7*, 191–197.

Scimemi, A. (2014). Structure, function, and plasticity of GABA transporters. Front. Cell. Neurosci. *8*, 161.

Scimemi, A., Semyanov, A., Sperk, G., Kullmann, D.M., and Walker, M.C. (2005). Multiple and plastic receptors mediate tonic $GABA_A$ receptor currents in the hippocampus. J. Neurosci. *25*, 10016–10024.

Seamans, J.K., and Yang, C.R. (2004). The principal features and mechanisms of dopamine modulation in the prefrontal cortex. Prog. Neurobiol. *74*, 1–58.

Seamans, J.K., Gorelova, N., Durstewitz, D., and Yang, C.R. (2001). Bidirectional dopamine modulation of GABAergic inhibition in prefrontal cortical pyramidal neurons. J. Neurosci. *21*, 3628–3638.

Sedelnikova, A., Erkkila, B.E., Harris, H., Zakharkin, S.O., and Weiss, D.S. (2006). Stoichiometry of a pore mutation that abolishes picrotoxin-mediated antagonism of the $GABA_A$ receptor. J. Physiol. *577*, 569–577.

Seeman, P., Guan, H.C., and Van Tol, H.H. (1993). Dopamine D4 receptors elevated in schizophrenia. Nature *365*, 441–445.

Semyanov, A., Walker, M.C., Kullmann, D.M., and Silver, R.A. (2004). Tonically active $GABA_A$ receptors: modulating gain and maintaining the tone. Trends Neurosci. *27*, 262–269.

Serra, M., Pisu, M.G., Littera, M., Papi, G., Sanna, E., Tuveri, F., Usala, L., Purdy, R.H., and Biggio, G. (2000). Social isolation-induced decreases in both the abundance of neuroactive steroids and $GABA_A$ receptor function in rat brain. J. Neurochem. *75*, 732–740.

Sezgin, M. (2004). Survey over image thresholding techniques and quantitative performance evaluation. J. Electron. Imaging *13*, 146-168.

Shen, H., Gong, Q.H., Aoki, C., Yuan, M., Ruderman, Y., Dattilo, M., Williams, K., and Smith, S.S. (2007). Reversal of neurosteroid effects at $\alpha4\beta2\delta$ $GABA_A$ receptors triggers anxiety at puberty. Nat. Neurosci. *10*, 469–477.

Shepherd, G.M.G. (2009). Intracortical cartography in an agranular area. Front. Neurosci. *3*, 337–343.

Sheskin, D.J. (2007). Handbook of parametric and nonparametric statistical procedures. Third Edition (Chapman and Hall/CRC).

Sieghart, W. (1995). Structure and pharmacology of $GABA_A$ receptor subtypes. Pharmacol. Rev. *47*, 181–234.

Sieghart, W. (2015). Allosteric modulation of $GABA_A$ receptors via multiple drug-binding sites. Adv. Pharmacol. *72*, 53–96.

Sieghart, W., and Sperk, G. (2002). Subunit composition, distribution and function of $GABA_A$ receptor subtypes. Curr. Top. Med. Chem. *2*, 795–816.

Sigel, E., and Buhr, A. (1997). The benzodiazepine binding site of $GABA_A$ receptors. Trends Pharmacol. Sci. *18*, 425–429.

Sivilotti, L., and Nistri, A. (1991). GABA receptor mechanisms in the central nervous system. Prog. Neurobiol. *36*, 35–92.

Skilbeck, K.J., Johnston, G.A.R., and Hinton, T. (2010). Stress and GABA receptors. J. Neurochem. *112*, 1115–1130.

Smart, T.G. (1997). Regulation of excitatory and inhibitory neurotransmitter-gated ion channels by protein phosphorylation. Curr. Opin. Neurobiol. *7*, 358–367.

Smart, T.G., and Constanti, A. (1986). Studies on the mechanism of action of picrotoxinin and other convulsants at the crustacean muscle GABA receptor. Proc. R. Soc. London. Ser. B, Biol. Sci. *227*, 191–216.

Smart, T. G., & Paoletti, P. (2012). Synaptic neurotransmitter-gated receptors. Cold Spring Harbor Perspectives in Biology *4*, a009662.

Smiley, J.F., and Goldman-Rakic, P.S. (1996). Serotonergic axons in monkey prefrontal cerebral cortex synapse predominantly on interneurons as demonstrated by serial section electron microscopy. J. Comp. Neurol. *367*, 431–443.

Smith, K.S., and Rudolph, U. (2012). Anxiety and depression: Mouse genetics and pharmacological approaches to the role of $GABA_A$ receptor subtypes. Neuropharmacology *62*, 54–62.

Smith, K.R., Muir, J., Rao, Y., Browarski, M., Gruenig, M.C., Sheehan, D.F., Haucke, V., and Kittler, J.T. (2012). Stabilization of $GABA_A$ receptors at endocytic zones is mediated by an AP2 binding motif within the $GABA_A$ receptor β3 subunit. J. Neurosci. *32*, 2485–2498.

Somogyi, P. (1977). A specific “axo-axonal” interneuron in the visual cortex of the rat. Brain Res. *136*, 345–350.

Sperk, G., Schwarzer, C., Tsunashima, K., Fuchs, K., and Sieghart, W. (1997). $GABA_A$ receptor subunits in the rat hippocampus I: immunocytochemical distribution of 13 subunits. Neuroscience *80*, 987–1000.

Staley, K.J., and Mody, I. (1992). Shunting of excitatory input to dentate gyrus granule cells by a depolarizing $GABA_A$ receptor-mediated postsynaptic conductance. J. Neurophysiol. *68*, 197–212.

Stan, A.D., and Lewis, D.A. (2012). Altered cortical GABA neurotransmission in schizophrenia: insights into novel therapeutic strategies. Curr. Pharm. Biotechnol. *13*, 1557–1562.

Stanford, I.M., Kantaria, M.A., Chahal, H.S., Loucif, K.C., and Wilson, C.L. (2005). 5-Hydroxytryptamine induced excitation and inhibition in the subthalamic nucleus: action at 5-HT_{2C}, 5-HT_4 and 5-HT_{1A} receptors. Neuropharmacology *49*, 1228–1234.

Stein, V., and Nicoll, R.A. (2003). GABA generates excitement. Neuron *37*, 375–378.

Stell, B.M., Brickley, S.G., Tang, C.Y., Farrant, M., and Mody, I. (2003). Neuroactive steroids reduce neuronal excitability by selectively enhancing tonic inhibition mediated by δ subunit-containing $GABA_A$ receptors. Proc. Natl. Acad. Sci. U. S. A. *100*, 14439–14444.

Sternberg (1983). Biomedical image processing. Computer (Long. Beach. Calif). *16*, 22–34.

Strange, P.G. (1999). Agonism and inverse agonism at dopamine D2-like receptors. Clin. Exp. Pharmacol. Physiol. Suppl. *26*, S3–S9.

Ströhle, A., Pasini, A., Romeo, E., Hermann, B., Spalletta, G., di Michele, F., Holsboer, F., and Rupprecht, R. (2000). Fluoxetine decreases concentrations of 3α,5α-tetrahydrodeoxycorticosterone (THDOC) in major depression. J. Psychiatr. Res. *34*, 183–186.

Strous, R.D., Maayan, R., and Weizman, A. (2006). The relevance of neurosteroids to clinical psychiatry: from the laboratory to the bedside. Eur. Neuropsychopharmacol. *16*, 155–169.

Succol, F., Fiumelli, H., Benfenati, F., Cancedda, L., and Barberis, A. (2012). Intracellular chloride concentration influences the $GABA_A$ receptor subunit composition. Nat. Commun. *3*, 738.

Szabadics, J., Varga, C., Molnár, G., Oláh, S., Barzó, P., and Tamás, G. (2006). Excitatory effect of GABAergic axo-axonic cells in cortical microcircuits. Science *311*, 233–235.

Tarazi, F.I., and Baldessarini, R.J. (2000). Comparative postnatal development of dopamine D1, D2 and D4 receptors in rat forebrain. Int. J. Dev. Neurosci. *18*, 29–37.

Tarazi, F.I., Zhang, K., and Baldessarini, R.J. (2004). Dopamine D4 receptors: beyond schizophrenia. J. Recept. Signal Transduct. Res. *24*, 131–147.

Tasker, J. (2000). Coregulation of ion channels by neurosteroids and phosphorylation. Sci. STKE *2000(59)*:1.

Theile, J.W., Morikawa, H., Gonzales, R.A., and Morrisett, R.A. (2009). Ethanol potentiation of GABA release onto ventral tegmental area dopamine neurons. J. Pharmacol. Exp. Ther. *329*, 625–633.

Thomas, P., and Smart, T.G. (2005). HEK293 cell line: a vehicle for the expression of recombinant proteins. J. Pharmacol. Toxicol. Methods *51*, 187–200.

Thomas, P., Mortensen, M., Hosie, A.M., and Smart, T.G. (2005). Dynamic mobility of functional $GABA_A$ receptors at inhibitory synapses. Nat. Neurosci. *8*, 889–897.

Thompson, S.A., Whiting, P.J., and Wafford, K.A. (1996). Barbiturate interactions at the human $GABA_A$ receptor: dependence on receptor subunit combination. Br. J. Pharmacol. *117*, 521–527.

Thomson, A.M., and Jovanovic, J.N. (2010). Mechanisms underlying synapse-specific clustering of $GABA_A$ receptors. Eur. J. Neurosci. *31*, 2193–2203.

Thomson, A.M., Bannister, A.P., Hughes, D.I., and Pawelzik, H. (2000). Differential sensitivity to Zolpidem of IPSPs activated by morphologically identified CA1 interneurons in slices of rat hippocampus. Eur. J. Neurosci. *12*, 425–436.

Van Tol, H.H., Bunzow, J.R., Guan, H.C., Sunahara, R.K., Seeman, P., Niznik, H.B., and Civelli, O. (1991). Cloning of the gene for a human dopamine D4 receptor with high affinity for the antipsychotic clozapine. Nature *350*, 610–614.

Torres, J.M., and Ortega, E. (2003). Precise quantitation of 5α-reductase type 1 mRNA by RT-PCR in rat liver and its positive regulation by testosterone and dihydrotestosterone. Biochem. Biophys. Res. Commun. *308*, 469–473.

Tretter, E.V. (2008). $GABA_A$ receptor dynamics and constructing GABAergic synapses. Front. Mol. Neurosci. *1*, 7.

Tretter, V., Jacob, T.C., Mukherjee, J., Fritschy, J.-M., Pangalos, M.N., and Moss, S.J. (2008). The clustering of $GABA_A$ receptor subtypes at inhibitory synapses is facilitated via the direct binding of receptor α2 subunits to gephyrin. J. Neurosci. *28*, 1356–1365.

Tretter, V., Kerschner, B., Milenkovic, I., Ramsden, S.L., Ramerstorfer, J., Saiepour, L., Maric, H.-M., Moss, S.J., Schindelin, H., Harvey, R.J., et al. (2011). Molecular basis of the $GABA_A$ receptor α3 subunit interaction with the clustering protein gephyrin. J. Biol. Chem. *286*, 37702–37711.

Tretter, V., Mukherjee, J., Maric, H.-M., Schindelin, H., Sieghart, W., and Moss, S.J. (2012). Gephyrin, the enigmatic organizer at GABAergic synapses. Front. Cell. Neurosci. *6*, 23.

Tritsch, N.X., and Sabatini, B.L. (2012). Dopaminergic modulation of synaptic transmission in cortex and striatum. Neuron *76*, 33–50.

Tseng, K.-Y., and O'Donnell, P. (2007). Dopamine modulation of prefrontal cortical interneurons changes during adolescence. Cereb. Cortex *17*, 1235–1240.

Tseng, P., Donnell, Tseng, K.Y., and O'Donnell, P. (2007). D2 dopamine receptors recruit a GABA component for their attenuation of excitatory synaptic transmission in the adult rat prefrontal cortex. Synapse *61*, 843–850.

Twelvetrees, A.E., Yuen, E.Y., Arancibia-Carcamo, I.L., MacAskill, A.F., Rostaing, P., Lumb, M.J., Humbert, S., Triller, A., Saudou, F., Yan, Z., et al. (2010). Delivery of $GABA_A$Rs to synapses is mediated by HAP1-KIF5 and disrupted by mutant huntingtin. Neuron *65*, 53–65.

Ueno, S., Bracamontes, J., Zorumski, C., Weiss, D.S., and Steinbach, J.H. (1997). Bicuculline and Gabazine Are Allosteric Inhibitors of Channel Opening of the $GABA_A$ Receptor. J. Neurosci. *17*, 625–634.

Uylings, H.B.M., Groenewegen, H.J., and Kolb, B. (2003). Do rats have a prefrontal cortex? Behav. Brain Res. *146*, 3–17.

Veres, J.M., Nagy, G.A., Vereczki, V.K., Andrasi, T., and Hajos, N. (2014). Strategically positioned inhibitory synapses of axo-axonic cells potently control principal neuron spiking in the Basolateral Amygdala. J. Neurosci. *34*, 16194–16206.

Vithlani, M., Terunuma, M., and Moss, S.J. (2011). The dynamic modulation of $GABA_A$ receptor trafficking and its role in regulating the plasticity of inhibitory synapses. Physiol. Rev. *91*, 1009–1022.

Volk, D.W., and Lewis, D.A. (2005). GABA targets for the treatment of cognitive dysfunction in schizophrenia. Curr. Neuropharmacol. *3*, 45–62.

Volk, D.W., Pierri, J.N., Fritschy, J.-M., Auh, S., Sampson, A.R., and Lewis, D.A. (2002). Reciprocal alterations in pre- and postsynaptic inhibitory markers at chandelier cell inputs to pyramidal neurons in schizophrenia. Cereb. Cortex *12*, 1063–1070.

Vollenweider, I., Smith, K.S., Keist, R., and Rudolph, U. (2011). Antidepressant-like properties of α2-containing $GABA_A$ receptors. Behav. Brain Res. *217*, 77–80.

Wafford, K.A., and Ebert, B. (2006). Gaboxadol - a new awakening in sleep. Curr. Opin. Pharmacol. *6*, 30–36.

Wamsley, J.K., Alburges, M.E., McQuade, R.D., and Hunt, M. (1992). CNS distribution of D1 receptors: use of a new specific D1 receptor antagonist, [3H]SCH39166. Neurochem. Int. *20 Suppl*, 123S – 128S.

Wang, M. (2011). Neurosteroids and $GABA_A$ receptor function. Front. Endocrinol. *2*, 44.

Wang, X.-J., and Buzsaki, G. (1996). γ-Oscillation by synaptic inhibition in a hippocampal interneuronal network model. J. Neurosci. *16*, 6402–6413.

Wang, H., Bedford, F.K., Brandon, N.J., Moss, S.J., and Olsen, R.W. (1999). $GABA_A$-receptor-associated protein links GABAA receptors and the cytoskeleton. Nature *397*, 69–72.

Wang, X., Zhong, P., and Yan, Z. (2002). Dopamine D4 receptors modulate GABAergic signaling in pyramidal neurons of prefrontal cortex. J. Neurosci. *22*, 9185–9193.

Wang, Y., Markram, H., Goodman, P.H., Berger, T.K., Ma, J., and Goldman-Rakic, P.S. (2006). Heterogeneity in the pyramidal network of the medial prefrontal cortex. Nat. Neurosci. *9*, 534–542.

Wei, W., Zhang, N., Peng, Z., Houser, C.R., and Mody, I. (2003). Perisynaptic localization of δ subunit-containing $GABA_A$ receptors and their activation by GABA spillover in the mouse dentate gyrus. J. Neurosci. *23*, 10650–10661.

Weitlauf, C., and Woodward, J.J. (2008). Ethanol selectively attenuates NMDAR-mediated synaptic transmission in the prefrontal cortex. Alcohol. Clin. Exp. Res. *32*, 690–698.

Whiting, P.J., McKernan, R.M., and Wafford, K.A. (1995). Structure and pharmacology of vertebrate $GABA_A$ receptor subtypes. Int. Rev. Neurobiol. *38*, 95–138.

Whittington, M.A., and Traub, R.D. (2003). Interneuron diversity series: inhibitory interneurons and network oscillations in vitro. Trends Neurosci. *26*, 676–682.

Wieland, H.A., Lüddens, H., and Seeburg, P.H. (1992). A single histidine in $GABA_A$ receptors is essential for benzodiazepine agonist binding. J. Biol. Chem. *267*, 1426–1429.

Wisden, W., Laurie, D.J., Monyer, H., and Seeburg, P.H. (1992). The distribution of 13 $GABA_A$ receptor subunit mRNAs in the rat brain. I. Telencephalon, diencephalon, mesencephalon. J. Neurosci. *12*, 1040–1062.

Wisden, W., Cope, D., Klausberger, T., Hauer, B., Sinkkonen, S.T., Tretter, V., Lujan, R., Jones, A., Korpi, E.R., Mody, I., et al. (2002). Ectopic expression of the $GABA_A$ receptor α6 subunit in hippocampal pyramidal neurons produces extrasynaptic receptors and an increased tonic inhibition. Neuropharmacology *43*, 530–549.

Woodruff, A., Xu, Q., Anderson, S.A., and Yuste, R. (2009). Depolarizing effect of neocortical chandelier neurons. Front. Neural Circuits *3*, 15.

Woodruff, A.R., Anderson, S.A., and Yuste, R. (2010). The enigmatic function of chandelier cells. Front. Neurosci. *4*, 201.

Woodruff, A.R., McGarry, L.M., Vogels, T.P., Inan, M., Anderson, S.A., and Yuste, R. (2011). State-dependent function of neocortical chandelier cells. J. Neurosci. *31*, 17872–17886.

Yagüe, J., Cavaccini, A., Errington, A., Crunelli, V., and Giovanni, G. (2013). Dopaminergic modulation of tonic but not phasic $GABA_A$-receptor-mediated current in the ventrobasal thalamus of Wistar and GAERS rats. Exp. Neurol. *247*, 1–7.

Yamada, J., Furukawa, T., Ueno, S., Yamamoto, S., and Fukuda, A. (2007). Molecular basis for the $GABA_A$ receptor-mediated tonic inhibition in rat somatosensory cortex. Cereb. Cortex *17*, 1782–1787.

Yan, Z. (2002). Regulation of GABAergic inhibition by serotonin signaling in prefrontal cortex: molecular mechanisms and functional implications. Mol. Neurobiol. *26*, 203–216.

Yang, C.R., Seamans, J.K., and Gorelova, N. (1999). Developing a neuronal model for the pathophysiology of schizophrenia based on the nature of electrophysiological actions of dopamine in the prefrontal cortex. Neuropsychopharmacology *21*, 161–194.

Ye, Z., McGee, T.P., Houston, C.M., and Brickley, S.G. (2013). The contribution of δ subunit-containing $GABA_A$ receptors to phasic and tonic conductance changes in cerebellum, thalamus and neocortex. Front. Neural Circuits *7*, 203.

Yee, B.K., Keist, R., von Boehmer, L., Studer, R., Benke, D., Hagenbuch, N., Dong, Y., Malenka, R.C., Fritschy, J.-M., Bluethmann, H., et al. (2005). A schizophrenia-related sensorimotor deficit links α3-containing $GABA_A$ receptors to a dopamine hyperfunction. Proc. Natl. Acad. Sci. U. S. A. *102*, 17154–17159.

Yeung, J.Y.T. (2003). Tonically activated $GABA_A$ receptors in hippocampal neurons are high-affinity, low-conductance sensors for extracellular GABA. Mol. Pharmacol. *63*, 2–8.

Yu, Z., Fang, Q., Xiao, X., Wang, Y.-Z., Cai, Y.-Q., Cao, H., Hu, G., Chen, Z., Fei, J., Gong, N., et al. (2013). GABA Transporter-1 deficiency confers schizophrenia-like behavioral phenotypes. PLoS One *8*, e69883.

Yuan, X., Yao, J., Norris, D., Tran, D.D., Bram, R.J., Chen, G., and Luscher, B. (2008). Calcium-modulating cyclophilin ligand regulates membrane trafficking of postsynaptic $GABA_A$ receptors. Mol. Cell. Neurosci. *38*, 277–289.

Zeilhofer, H.U., Möhler, H., and Di Lio, A. (2009). GABAergic analgesia: new insights from mutant mice and subtype-selective agonists. Trends Pharmacol. Sci. *30*, 397–402.

Zhang, C., Atasoy, D., Araç, D., Yang, X., Fucillo, M. V, Robison, A.J., Ko, J., Brunger, A.T., and Südhof, T.C. (2010). Neurexins physically and functionally interact with $GABA_A$ receptors. Neuron *66*, 403–416.

Zhang, K., Grady, C.J., Tsapakis, E.M., Andersen, S.L., Tarazi, F.I., and Baldessarini, R.J. (2004). Regulation of working memory by dopamine D4 receptor in rats. Neuropsychopharmacology *29*, 1648–1655.

Zhong, P., and Yan, Z. (2014). Distinct physiological effects of dopamine D4 receptors on prefrontal cortical pyramidal neurons and fast-spiking interneurons. Cereb. Cortex. pii: bhu190.

Zhou, F.M., and Hablitz, J.J. (1999a). Dopamine modulation of membrane and synaptic properties of interneurons in rat cerebral cortex. J. Neurophysiol. *81*, 967–976.

Zhou, F.M., and Hablitz, J.J. (1999b). Activation of serotonin receptors modulates synaptic transmission in rat cerebral cortex. J. Neurophysiol. *82*, 2989–2999.